Physics Library
QC
1
.P5812
v.56
no.6

THE PHYSICAL REVIEW

VOLUME 56 | Second Series | NUMBER 6

SEPTEMBER 15, 1939

Published for the

AMERICAN PHYSICAL SOCIETY

by the

AMERICAN INSTITUTE OF PHYSICS

Incorporated

LANCASTER, PA., AND NEW YORK, N. Y.

UNIVERSITY OF MICHIGAN LIBRARIES

THE PHYSICAL REVIEW

A journal of experimental and theoretical physics established by E. L. Nichols in 1893

Published by the American Institute of Physics for the

American Physical Society

OFFICERS

President

JOHN T. TATE
University of Minnesota
Minneapolis, Minnesota

Vice President

JOHN ZELENY
Yale University
New Haven, Connecticut

Secretary

W. L. SEVERINGHAUS
Columbia University
New York, New York

Treasurer

G. B. PEGRAM
Columbia University
New York, New York

Local Secretary for the Pacific Coast

PAUL KIRKPATRICK
Stanford University
California

Editor

JOHN T. TATE
University of Minnesota
Minneapolis, Minnesota

BOARD OF EDITORS

JOHN T. TATE, *Editor* J. W. BUCHTA, *Assistant Editor*

Associate Editors

K. T. BAINBRIDGE	A. L. HUGHES	W. BLEAKNEY
H. P. ROBERTSON	T. H. JOHNSON	G. BREIT
H. B. WAHLIN	F. A. JENKINS	D. M. DENNISON

Manuscripts for publication should be submitted to John T. Tate, University of Minnesota, Minneapolis, Minnesota.

Proof and all correspondence concerning papers in the process of publication, should be addressed to the Publications Manager, American Institute of Physics, 175 Fifth Avenue, New York, New York.

Subscription Price

United States and Possessions and Canada $15.00
Foreign $16.50

Back Numbers

Complete set: Series 2,[1] Vol. 1, 1913–Vol. 54, 1938—$390.00
Yearly rate: $16.50
Single copies: $1.50 each prior to July, 1929; $.75 each after July, 1929.

Subscriptions and orders for back numbers should be addressed to Prince and Lemon Streets, Lancaster, Pennsylvania, or to the American Institute of Physics, 175 Fifth Avenue, New York, New York.

Advertising is not accepted for the *Physical Review* but attention is called to the *Review of Scientific Instruments* and the *Journal of Applied Physics*, companion publications of the Institute, and media through which the field of physics can be reached most effectively. Rates and other information will be furnished on request.

Changes of address and complaints of failure to receive the *Physical Review* in the case of members of the American Physical Society, should be addressed to the Treasurer; in the case of other subscribers, to the Publications Manager. New copies can be sent free in response to complaints of non-delivery only if notice of non-delivery is received within three months of date of issue.

[1] For Series 1 inquire of Physics Department, Cornell University, Ithaca, N. Y.

The Physical Review is published semi-monthly at Prince and Lemon Streets, Lancaster, Pennsylvania.

Entered at the Post Office at Lancaster, Pennsylvania, as second class matter.

Acceptance for mailing at special rate of postage provided for in section 1103, Act of October 3, 1917, authorized September 6, 1921.

Physics
Physics-LSA
Johnson
Replace

THE
PHYSICAL REVIEW

A Journal of Experimental and Theoretical Physics Established by E. L. Nichols in 1893

VOL. 56, NO. 6 SEPTEMBER 15, 1939 SECOND SERIES

Seasonal Cosmic-Ray Effects at Sea Level

R. A. MILLIKAN, H. V. NEHER AND D. O. SMITH
California Institute of Technology, Pasadena, California

(Received July 17, 1939)

By sending a Neher self-recording electroscope in a 10-cm lead shield repeatedly on a slow Norwegian steamer over the route Vancouver–Los Angeles, around South America and return to Los Angeles and Vancouver, we find (1) as heretofore an equatorial dip measured from Los Angeles of seven percent on the western side of South America, eight percent on the eastern side; (2) no measurable seasonal effect, or winter-summer differences, at all in the voyage from Los Angeles to the Straits of Magellan; (3) as heretofore constancy in cosmic-ray intensity in summer and fall, within the limits of uncertainty imposed by fluctuations estimated at not over one percent, on the voyage between Los Angeles and Vancouver; (4) but in winter and spring an increase of as much as two or three percent between Los Angeles and Vancouver. This is interpreted as the atmospheric-temperature effect earlier studied by Hess, Compton, and their respective collaborators.

ALTHOUGH prior to 1934 many of us had reported slight changes in cosmic-ray intensities as a function of temperature,[1] most of these were *positive* in sign and were, at least in part, due, as Bowen and Millikan[2] had found early in 1931, to lack of saturation in pressure electroscopes. However, in 1933 Hess[3] and his collaborators, with the entire elimination of this sort of cause, reported a small but apparently consistent *negative* variation of cosmic-ray intensities "with the temperature of the outer air," that is, for example, a greater intensity by as much as 1.2 percent in winter than in summer, though both the temperature of the electroscope and the barometer remained unchanged. These observers worked on the Hafelekar in Austria, altitude 2300 m, mag. lat. 48.4 N. They used a Steinke cosmic-ray meter shielded with 10 cm of lead. Basing their results on seasonal, rather than daily changes, they reported the coefficient of change $\alpha = -0.047$ percent deg.$^{-1}$ C, and later -0.091 percent deg.$^{-1}$ C.

Also, in 1936 Barnóthy and Forró[4] at Budapest got similarly, with the aid of counters rather than electroscopes, negative coefficient $\alpha = -0.38 \pm 0.05$ percent deg.$^{-1}$ C.

These results, though agreeing in sign, were widely divergent in magnitude, and furthermore we at Pasadena had never found any variation at all of this kind, though we had made careful diurnal, as well as monthly, studies on the constancy of the cosmic rays, and though the

[1] See R. A. Millikan, Phys. Rev. **36**, 1595 (1930) and **39**, 397 (1932); G. Hoffmann, Zeits. f. Physik **69**, 259 (1931); W. Messerschmidt, Zeits. f. Physik **78**, 668 (1932); J. Clay, Proc. Roy. Akad. Amsterdam **23**, 711 (1930).

[2] R. A. Millikan and I. S. Bowen, Nature **128**, 582 (1931); also R. A. Millikan, Phys. Rev. **39**, 397 (1932). Compton, Bennett and Stearns (see Phys. Rev. **39**, 873 (1932)) independently reached the same conclusion.

[3] Hess, Graziader and Steinmauer, Berliner Ber. **22**, 521, 672 (1933); also Wiener Ber. IIa, **143**, 313 (1934); **144**, 53 (1935).

[4] J. Barnóthy and M. Forró, Zeits. f. Physik **100**, 732 (1936).

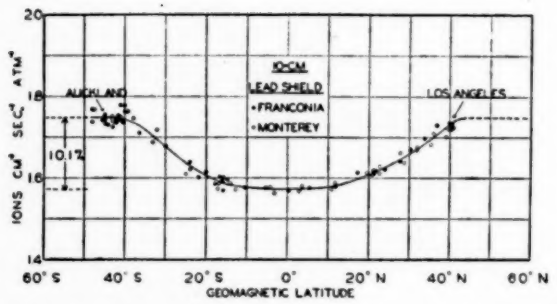

FIG. 1. The two trips here, made seven months apart (mid-summer and mid-winter), show the consistency found on going over the same route at different seasons.

large differences existing in Southern California between the day and night temperatures might well have brought to light a diurnal effect of this type if it existed.

More recently Compton and Turner[5] in sending a recording electroscope repeatedly on a ship plying between Vancouver and Sydney have reported that the increase in sea-level intensities in going from the equator to either Vancouver or Sydney is two or three percent greater in winter than in summer. They have interpreted these differences in terms of the aforesaid "atmospheric-temperature" effect.

The purpose of the present paper is to report upon the bearing upon this effect of the world-wide studies with shielded electroscopes (10 cm lead) of Millikan and Neher on sea-level cosmic-ray intensities.

[5] A. H. Compton and R. N. Turner, Phys. Rev. **52**, 799 (1937); also see A. H. Compton, J. Frank. Inst. **227**, 607 (1939).

The earliest pertinent data[6] taken after the development of precision high pressure electroscopes was obtained in July, August and September in Pasadena and in Churchill, Manitoba, when Millikan reported that as a result of week-long studies at both points with the same sensitive pressure electroscope kept at essentially the same mean temperature in both localities he found no change at all between these two points that could amount to as much as one percent. The precision of the reading was much greater than this, but the observed fluctuations were so large as to make it seem unsafe to claim any greater certainty than this.

To check these results as carefully as possible, in September 1932 Millikan and Neher took continuous readings on two different instruments during a five-day ocean voyage between Vancouver and Los Angeles, with the results shown in Table I. We summarized these results in the statement that within the limits of uncertainty of our readings there was no difference in cosmic-ray intensities of more than a percent between the latitudes of Vancouver and Los Angeles.

Again, in December of 1932 and January of 1933 we obtained a mean change of seven percent in sending an electroscope shielded with 10 cm of lead twice between Los Angeles and Mollendo, and in the following winter a 7.1 percent equatorial dip in sending a self-recording instrument on the *Valero III* from Los Angeles to the Galapagos Islands and return. These two trips were made in about the same season and

[6] R. A. Millikan, Phys. Rev. **36**, 1595 (1930).

TABLE I. *Five-day study of sea-level variations of cosmic-ray intensities between Victoria, B.C. and Los Angeles.**

ELECTROSCOPE NO. 1—UNSHIELDED (IONS CC PER SEC.)				ELECTROSCOPE NO. 2—SHIELDED (11 CM PB)			
	LAT.	4-HOUR MEANS	12-HOUR MEANS	LAT.	LONG	MAG. LAT.	12-HOUR MEANS
In Seattle Harbor	47.5	39.58	39.58*	47.5	122 W.	53.5 N.	24.60
In and near Victoria	48.4	39.45	39.45	48.3	123 W.	54.3 N.	24.71
At Sea	47.22	39.53	39.53	46.5	124 W.	52.5 N.	24.65
At Sea	44.4	39.67	39.67	44.0	124 W.	50.0 N.	24.78
At Sea	41.6	39.69	39.69	41.0	124 W.	47.0 N.	24.49
At Sea	39.0	39.34	39.33	37.5	122 W.	43.5 N.	24.79†
In San Francisco Harbor	—	39.82	39.82	36.0	122 W.	42.0 N.	24.57
In San Francisco Harbor	—	39.61	39.61	34.0	119 W.	40.6 N.	24.45†
At Sea	36.85	39.65	39.65			Mean	24.63
At Sea	34.8	39.63	39.65				
		Mean 39.60					

* 8-hour average. † 9-hour average.

are reported for comparison with our new observations, though in themselves they have no bearing on a seasonal effect.

Again, however, in the summer of 1933 and in the winter of 1934, just six months later when a seasonal difference might have appeared, we sent recording instruments on the *Monterey* of the Matson line and the *Franconia* of the Cunard line between Los Angeles and Sydney without bringing to light any seasonal difference at all, as can be seen from Fig. 1, again reproduced here. Indeed, up to the year 1938, neither in our own observing at Pasadena nor in our dozen voyages, had we obtained any definite evidence of seasonal effects, though it is true that most of the voyaging had been done south of magnetic latitude 41°. Further, when our instruments had gone north of magnetic latitude 45° it had been in *summer*.

In March, 1938, however, in order to settle some uncertainties that had been raised as to the precision of our measurements off the coast of South America, and to test for seasonal effects between Los Angeles and Vancouver, we placed still another shielded self-recording instrument on the Norwegian ship *Hoyanger* under Captain Fladmark, which voyages slowly—speed under 10 knots—from Vancouver south to Los Angeles, then all around South America and back to Vancouver, stopping frequently for periods of some days, or even a week, in different ports. The slow speed and the frequent stops of this ship make it particularly well adapted to getting a series of good mean values in the different latitudes traversed.

As appears from Figs. 2 and 3, the results of two voyages made five months apart show no seasonal effect either at Los Angeles or anywhere between there and the Straits of Magellan, though at certain points (e.g. at 20°) the two curves show differences as high as 0.6 percent. This is no larger, however, than the fluctuations in the 4–8-day means taken in port in the same season, indeed, on successive weeks. (See right side of Figs. 2 and 3.) Also, the readings made in late September between Los Angeles and Vancouver check nicely our 1930 and 1932 findings in that they show no changes in intensities between these points. Also, Fig. 2 shows that in these voyages, as in all our preceding ones, there is a seven-percent equatorial dip in going south to the equator from the plateau off the California coast. Also, in this voyage the edge of the plateau is again located, at least in this part of the world, fairly sharply at 41° mag. lat. Also, the dissymmetry brought to light in our preceding voyages between the northern and southern hemispheres is again marked in this one. Finally, as in our preceding reports, so here again we find, though the data shown in the figures do

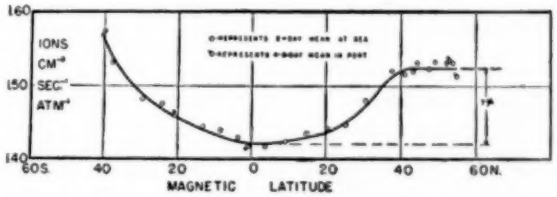

FIG. 2. Cosmic-ray measurements on steamer *Hoyanger*, Vancouver to Cape Horn, September 23rd to November 18, 1938.

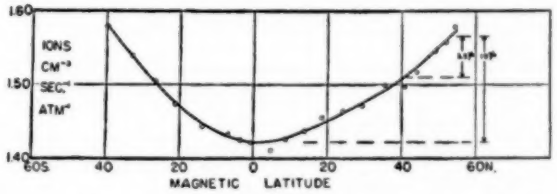

FIG. 3. Cosmic-ray measurements on steamer *Hoyanger*, Vancouver to Cape Horn, May 1st to June 19, 1938.

not cover this point, that the equatorial dip off the east coast of South America rises to eight percent instead of the seven percent found on the west coast.

In marked opposition to these findings, Fig. 3, however, shows a 3.5 percent change between Los Angeles and Vancouver. The fact that the Los Angeles reading remains nearly fixed and the Vancouver reading alone shows the seasonal change proves, if any further proof is needed, that *the change is not due to a magnetic cause*. A change dependent on temperature of the portion of the atmosphere through which the rays come seems the only possible interpretation to put upon these effects, as our predecessors have already concluded.

In Fig. 4 are given the results of three distinct voyages from Los Angeles to Vancouver and return. The voyage made in February and March shows only a two-percent rise between Los Angeles and Vancouver, while that made in

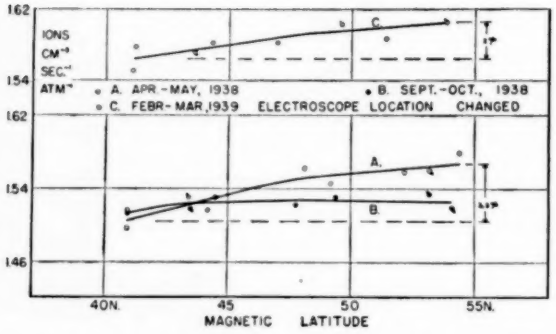

FIG. 4. Cosmic-ray measurements of three distinct voyages from Los Angeles to Vancouver and return.

May shows 3.5-percent change. That the larger change in the Vancouver intensity is found as late as May, instead of in February and March, is a little surprising and may mean that magnetic storms were then adding their effects to the seasonal change, though such a lag in a temperature effect after the astronomical mid-winter season is after all rather in keeping with other climatic lags in this area.

The conclusions that we draw from all of our own readings thus far are, then, (1) that there is no seasonal sea-level effect brought to light by our own readings at Los Angeles, or any point south of there down to the Straits of Magellan, that is of a sufficient magnitude to stand out above the fluctuations observable at the different localities traversed in these voyages; and (2) that between Los Angeles and Vancouver, however, there is a very definite increase in sea-level cosmic-ray intensity of at least two percent in winter that does not appear in summer.

These results are in essential agreement, so far as they go, with the results reported and discussed both by Compton and by Forbush.[7] The latter, by analyzing the data obtained by the Carnegie Institution's cosmic-ray meters running continuously at its stations at Cheltenham (near Washington, mag. lat. 50.1° N.), Teoloyucan (near Mexico City, mag. lat. 29.7° N.), Christchurch (New Zealand, mag. lat. 48.0° S.), and Huancayo (Peru, mag. lat. 0.6° S.), finds no seasonal effect (in his words, "no twelve-month wave") at Huancayo, which is in the equatorial belt. He finds a "twelve-month wave" at Cheltenham amounting to 1.6 percent of the normal cosmic-ray intensity and having the maximum in mid-January. He also finds such a wave at Christchurch (mag. lat. 48.0° S.) having an amplitude of 0.8 percent of the total intensity, its maximum occurring near the end of July (corresponding to the end of January in the Northern Hemisphere). He comments, also, on such a wave at Hafelekar (mag. lat. 48.0° S.) of amplitude 1.9 percent. This may be compared with the smaller of the winter-summer differences found at Seattle. Only in the case of this twelve-month wave of amplitude 1.0 percent at Teoloyucan are Forbush's results apparently somewhat out of line with ours in that, so far as these measurements go, we bring to light no seasonal change at Los Angeles (mag. lat. 41 N.) and none at Cape Horn (mag. lat. 42° S.), both of which are farther from the magnetic equator than is Teoloyucan. The high altitude of Teoloyucan may be the cause of this difference. In a succeeding paper we report upon an attempt to detect the effect of altitude on the seasonal changes.

[7] S. E. Forbush, Phys. Rev. **54**, 975 (1938).

New Evidence for a Change with Time of the Total Energy Brought into the Earth by Cosmic Rays

R. A. MILLIKAN AND H. V. NEHER
California Institute of Technology, Pasadena, California

(Received July 17, 1939)

In attempting to find a seasonal or winter-summer difference between the integrated value of the cosmic-ray ionization from sea level up to the top of the atmosphere at Omaha we obtain much too large a difference to be interpreted as an "atmospheric-temperature," or seasonal effect, at all. By comparison with Forbush's world-wide cosmic-ray changes we find in our results new evidence for a change with time in the total energy brought into the earth by cosmic rays.

PRACTICALLY all the work which we have thus far undertaken for the sake of determining the total or integrated ionization within a self-recording electroscope as it is carried from sea level up to a height 98 percent of the way to the top of the atmosphere has been done in mid-summer, i.e., between July and October. So far as we know, no one had ever attempted to determine such depth-ionization curves in mid-winter. This seemed to us an important point to investigate.

Accordingly, in the week before Christmas, 1938, we went to Omaha (Nebraska) where we already had made successful flights in warm summer weather and succeeded in that week in making four successful flights in cold winter weather. There is contained in Table I, columns *A* and *B*, the mean ionization currents as a function of altitude, h (measured in meters of water from the top, 10 meters therefore corresponding to sea level), both for the mean of the five flights made in Omaha in September, 1937 and for the mean of the four flights made there in December, 1938. The measuring electroscopes were in large part the same ones in both sets of flights, or when different electroscopes were used they were made essentially identical by identity in structure and careful calibration, so that the readings should be strictly comparable.

A comparison of the readings in the two

TABLE I. *Comparison of Incoming Cosmic-Ray Energies at Different Times.*

h	*A* Omaha Sept. 1937	*B* Omaha Dec. 1938	Percent Increase	*C* Saskatoon Aug. 1937	*D* Bismarck July 1938	Percent Difference
0.2	328	344	5	355	370	3.8
0.3	337	356	5.5	359	375	3.8
0.4	333	361	8.3	361	375	3.8
0.6	326	358	9.7	347	364	4.7
0.8	310	336	8.1	329	346	
1.0	290	314	8.3	308	323	4.4
1.2	267	288	7.8	280	296	5.3
1.4	242	259	7.1	252	268	5.2
1.6	217	235	7.3	225	239	5.8
1.8	195	210	7.5	202	214	5.7
2.0	173	192	11	180	190	5.3
2.25	150	167	11.3	156	159	2.0
2.5	128	146	13.8	134	133	0
2.75	110	127	15.4	115	111	−4
3.0	94	110	17.0	97	93	−4
3.5	69	80	16	68	66	−3
4.0	49	57	16.5	51	48	−6
4.5	35	41	17	36	39	+7
5.0	26	29	12	25	26	+2
5.5	20	23	15	18	17	−5
6.0	16	18	12	13	13	0
7.0	11	12	9	10	7	

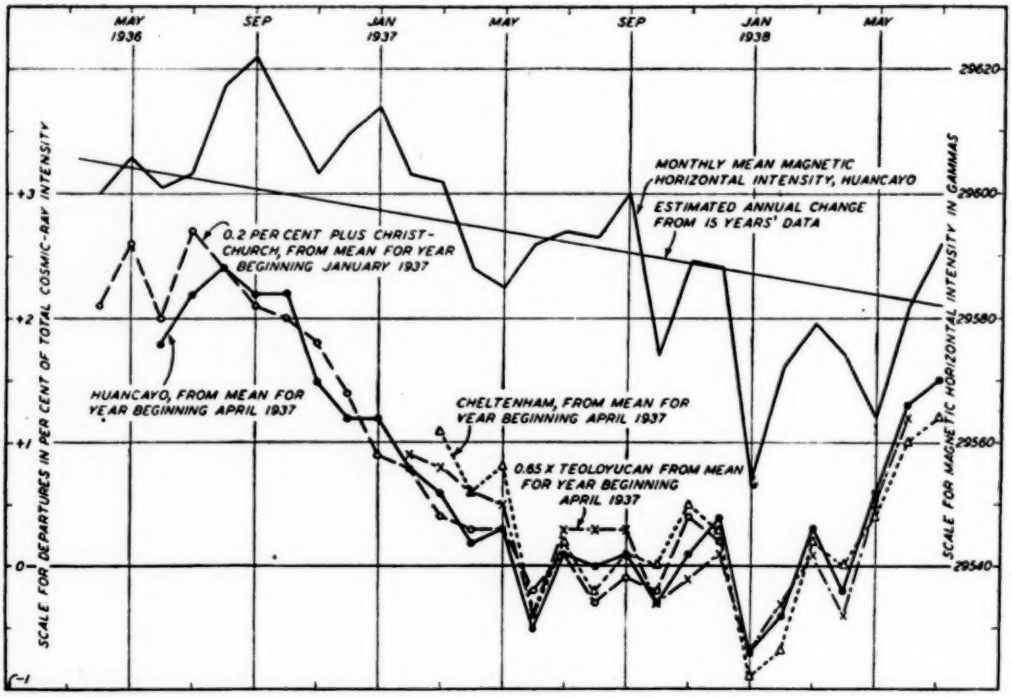

FIG. 1. Reproduction of the curve by Forbush (reference 5) for the world-wide changes in cosmic-ray intensities between April, 1936, and July, 1938.

columns *A* and *B* shows that our winter readings are indeed everywhere very markedly higher than our summer readings. Not only is that true, but it is also true that the total area underneath the depth ionization curve corresponding to our winter readings at Omaha is some 9.7 percent greater than the area underneath the corresponding summer curve in September, 1937.

This result is particularly significant, for it means that since the total incoming energy must ultimately manifest itself in the ionization of the atmosphere, the actual *entering* cosmic-ray energy was greater in December, 1938, than in September, 1937. *This result cannot, then, be interpreted as an "atmospheric-temperature effect" at all.* For any such pure atmospheric-temperature effect, when integrated over the full depth of the atmosphere, must come out independent of temperature, or of season. It can only affect the *distribution* of ionization with altitude, not its total amount.[1]

Although, then, the atmospheric-temperature effect which we studied in the foregoing paper may be involved in, and modify the relation of, the percentage differences shown in the fourth column of the accompanying table, it is wholly inadequate to explain what we have here observed in our attempt to study *seasonal* effects at all altitudes up to the top of the atmosphere. Blackett[2] on the basis of a theory developed by Euler and Heisenberg[3] has suggested an explanation of the pure atmospheric-temperature effect which is intriguing[4] and which we hope that further study will ultimately justify, but we must seek entirely different explanations of the

[1] This conclusion could only be doubted if the extreme assumption were made that an appreciable portion of the incoming energy, instead of appearing ultimately in the form of ionization, did not appear at all but became lost or carried away somehow in unobservable form, by neutrinos, for example. This hypothesis would destroy the most stable basis upon which all theoretical physics rests. We therefore prefer not to make it.

[2] P. M. S. Blackett, Phys. Rev. **54**, 973 (1938).

[3] H. Euler and W. Heisenberg, Ergeb. d. Exak. Nat. (1938).

[4] This theory is essentially that the mesotrons formed in the upper atmosphere by incoming cosmic-ray electrons (or photons) have a radioactive lifetime comparable with the time they require to traverse the atmosphere. This traversal time is less in winter, when the atmosphere is contracted (less deep), than in summer, when it is expanded. More mesotrons, therefore, get down to sea level in winter than in summer and produce there more ionization.

results brought to light in the accompanying table. *They constitute direct evidence that the incoming cosmic rays are variable in intensity, not necessarily seasonally but at least as some sort of a function of time.*

However, this is not the first time that such evidence has been brought to light. For Forbush[5] in his paper entitled "On World-Wide Changes in Cosmic-Ray Intensity" has deducted the seasonal effect, or the "12-month wave," as he calls it, from the data obtained by continuous recording instruments which the Carnegie Institution of Washington is keeping running at Cheltenham (U. S.), mag. lat. 50.1° N., Teoloyucan (Mexico), mag. lat. 29.7° N., Christchurch (New Zealand), mag. lat. 48.0° S., and Huancayo (Peru), mag. lat. 0.6° S., and obtained finally in his Fig. 15,* a figure which we reproduce here for convenience of reference, a curve which gives "the world-wide changes" in cosmic-ray intensities between April, 1936, and July, 1938. This curve shows that between September, 1937, and July, 1938, the intensity of cosmic rays increased the world over as measured in these instruments on the earth's surface by about 1.5 percent. Forbush's curve is not carried up to the time of our observations in December, 1938, but the curve had been moving up rapidly from January, 1938, to July, 1938, and Dr. Forbush informs us that it continued to rise for some months thereafter, so that our result, indicating a considerable increase in the incoming rays between September, 1937, and December, 1938, is at least qualitatively in accord with the Forbush curve.

But the data found in columns *C* and *D* of the accompanying table give still better opportunity for comparison with this curve. For as columns *C* and *D* show clearly, the total cosmic-ray energy coming in at Saskatoon (mag. lat. 60° N.) in August, 1937, is smaller than that coming in at Bismarck (mag. lat. 56° N.) at the end of June and beginning of July, 1938. Since, however, Saskatoon is four degrees farther north than Bismarck, and on the plateau or polar cap of constant cosmic-ray intensities which begins at very high altitudes at about mag. lat. 56°, it should in no case show a *lower* value of the incoming cosmic rays than is found at Bismarck, unless between the observation dates there had been an increase in the total energy of the cosmic rays entering the atmosphere. But *the Forbush curve shows that there was what he calls a "world-wide" increase of about 1.5 percent in the cosmic-ray intensity between these two dates as measured on the earth's surface,* so that at least qualitatively the data both of columns *A* and *B* and those of columns *C* and *D* of the accompanying table are in accord with the predictions of the Forbush curve.

The net result, then, of this preliminary attempt to find a seasonal or atmospheric temperature effect at very high altitudes is *to bring forward new evidence for a change with time of the total energy brought into the earth by cosmic rays which is large enough to mask completely any possible seasonal effect.*

[5] S. E. Forbush, Phys. Rev. **54**, 975 (1938).
* Reference 5, page 986.

On the Production of the Hard Component of the Cosmic Radiation

I. The Photon Hypothesis*

L. W. NORDHEIM AND M. H. HEBB
Duke University, Durham, North Carolina

(Received July 5, 1939)

The number of quanta (and electrons) of energy k within dk times their range in units of radiation theory (photon lengths) produced in matter by a primary electron of energy E is calculated from the theory of showers to be $Z(k)dk=\alpha(E/k^2)dk$, where $\alpha=0.57$ for quanta and 0.44 for electrons. With the help of the known energy distribution of the electrons coming from the outside, the energy distribution of photon lengths in the higher atmosphere is obtained. A comparison with the number and energy distribution of mesons (obtained from data near sea level and underground) leads to the following consequences of the hypothesis that the mesons are created by photons. The production process must be of moderate multiplicity and its cross section must increase from about 1/100 of the cross section for pair production by photons in air at moderate energy (7 to 10 Bev) to about 1/10 at higher energy (over 18 Bev). These high cross sections required for the production of energetic mesons seem to imply correspondingly large cross sections for absorption and constitute a serious difficulty for the understanding of their great penetrating power.

1. THE SECONDARY NATURE OF THE HARD COMPONENT

IT can hardly be doubted that the mesons forming the hard component of the cosmic radiation do not come from outside but are created within the atmosphere itself by primaries of a different nature. This follows at once if the instability of the mesons is admitted and the evidence on this point now seems quite convincing.[1] A comparison of the energy distribution of the mesons and of their observed geomagnetic effect with the energies necessary to reach points of various geomagnetic latitudes leads to the same conclusion.[2] A direct proof of the production of mesons in higher strata of the atmosphere has been recently obtained by Schein and Wilson.[3] Interesting indirect evidence for the production of mesons is provided by the new observations of S. A. Korff[4] who finds a high concentration of neutrons in the upper atmosphere. Any meson production process should according to Yukawa's theory be accompanied by fairly large recoils of nuclear particles and should therefore constitute an effective neutron source. With respect to the nature of the primaries and the details of the production mechanism, however, no satisfactory experimental evidence is yet available.

The theory of mesons as developed by Yukawa[5] and others in its present form can be applied only in a qualitative way, as it is not yet possible to treat high energy phenomena satisfactorily owing to divergence difficulties. One might use this theory, however, to obtain a classification of possible processes. Among them are the production of mesons by a kind of photoelectric effect and their production by protons in analogy to the emission of quanta by electrons.[6]

Most authors seem to be inclined to the opinion that the hard component is created by the soft component as the simplest possible assumption. We have therefore investigated the consequences of this hypothesis by comparing all

* A preliminary report of this paper was given at the Washington Meeting of the American Physical Society, Phys. Rev. **55**, 1111 (1939).

[1] See for example H. Euler and W. Heisenberg, Ergebn. d. exact. Naturwiss. **17**, 1 (1938).

[2] L. W. Nordheim, Phys. Rev. **53**, 694 (1938). In this paper an attempt was made to account for the behavior of the hard component by assuming that the primaries are of the same nature as the secondaries they produce. This hypothesis is, of course, not compatible with the supposed instability of the mesons, and further it would lead to the conclusion that every primary has to be accompanied by a large number (of order 10) of slow secondaries even at great depths in contradiction to recent experiments, reference 21.

[3] M. Schein and V. C. Wilson, Phys. Rev. **54**, 304 (1938).

[4] S. A. Korff, Phys. Rev. **56**, 210(A) (1939).

[5] H. Yukawa and others, I–IV, Proc. Phys. Math. Soc. Japan **17**, 58 (1935); **19**, 1084 (1937); **20**, 319, 720 (1938). H. Fröhlich, W. Heitler and N. Kemmer, Proc. Roy. Soc. **A166**, 154 (1938).

[6] W. Heitler, Proc. Roy. Soc. **A166**, 529 (1938), L. W. Nordheim and G. Nordheim, Phys. Rev. **54**, 254 (1938), M. Kobayasi and T. Okayama, Proc. Phys. Math. Soc. Japan **21**, 1 (1939).

available data regarding the number and energy distribution of electrons, photons* and mesons. It is possible to arrive in this way at a rather complete description of the features of the production process. It has to be of moderate multiplicity (i.e., a single photon has to be converted into more than one but not too many mesons in one single act) and the cross section for this conversion but not the multiplicity must increase with energy reaching values of the order $\frac{1}{10}$ of the cross section for pair production in air at energies of some 10 Bev.

This latter result leads, however, to a serious difficulty for the photon hypothesis. From general principles one has to conclude that the inverse of the production process should have a cross section of the same order of magnitude as the direct process; this means, as will be discussed in Section 5, that a high efficiency of production has as a consequence also a high rate of absorption or, at least, a rapid rate of degradation of energy. It is then hardly possible to account for the high penetrating power and hardening of the cosmic radiation at greater depths underground.[7] Though it might not be absolutely impossible to circumvent this difficulty, it seems that this could be effected only by rather artificial means. A discussion of alternative hypotheses regarding the origin of the hard component is given in the following paper.

2. The Number of Photons Produced by One Primary Electron

When a primary electron of energy E enters the atmosphere it starts at once to build up a shower, i.e., it multiplies into many electrons and photons of correspondingly lower energy. As long as the cross section for meson production is small compared to the cross section for radiative processes, the former effect will not disturb the course of the shower. The quantity which determines the rate of meson production will then be the total number of photons per energy interval dk multiplied with the average range, i.e.,

$$Z_\gamma(k)dk = dk\int N_\gamma(k, x)dx,$$

where $N_\gamma(k, x)$ is the distribution function for quanta of energy k as a function of depth x. The number of mesons of energy ϵ produced by the primary electron will then be

$$F(\epsilon) = \int Z_\gamma(k)\sigma(k, \epsilon)dk,$$

where $\sigma(k, \epsilon)$ is the cross section for creating one meson ϵ by a quantum k.

This quantity $Z_\gamma(k)$ can be obtained from the theory of showers[8] in the following way. Let $N_e(k, x)$ be the distribution function for particles (electrons and positrons) corresponding to the distribution $N_\gamma(k, x)$ of photons. At $x=0$ there is one particle of energy E and no photons so that we have $N_e(k, 0)=\delta(E-k)$ and $N_\gamma(k, 0)=0$. We introduce the moments

$$\begin{aligned} n_e(s, x) &= \int_0^E dk(k/E)^s N_e(k, x), \\ n_\gamma(s, x) &= \int_0^E dk(k/E)^s N_\gamma(k, x). \end{aligned} \tag{1}$$

Then if x is measured in units of the shower theory, n_e and n_γ satisfy[9]

$$\begin{aligned} \frac{d}{dx}n_e(s, x) &= -A(s)n_e(s, x) + B(s)n_\gamma(s, x) \\ \frac{d}{dx}n_\gamma(s, x) &= C(s)n_e(s, x) - Dn_\gamma(s, x), \end{aligned} \tag{2}$$

* We shall always speak of photons and not electrons as the part of the soft component which is effective for the meson production, as this is suggested by Yukawa's theory. As we shall see later the assumption that electrons are the active agent or that both electrons and photons contribute, would lead to practically the same results as the photon hypothesis.

[7] This difficulty was pointed out by L. W. Nordheim, J. Frank. Inst. **226**, 575 (1938), but the state of affairs can now be much more precisely shown.

[8] J. F. Carlson and J. R. Oppenheimer, Phys. Rev. **51**, 220 (1937); H. J. Bhabha and W. Heitler, Proc. Roy. Soc. **A159**, 432 (1937); L. Landau and G. Rumer, Proc. Roy. Soc. **A166**, 213 (1938); D. Iwanenko and A. Sokolow, Phys. Rev. **53**, 910 (1938).

[9] L. Landau and G. Rumer, reference 8, Eq. (17). Our $N_e(k, x)$, $N_\gamma(k, x)$ are the same as their $\Pi(E, t)$, $\Gamma(E, t)$ and n_e, n_γ differ only by a factor from Π_s, Γ_s.

where

$$A(s)=\frac{4}{3}[\psi(s+1)+\gamma]-\frac{s(5s+7)}{6(s+1)(s+2)},$$
$$B(s)=\frac{2}{3}\cdot\frac{3s^2+11s+14}{(s+1)(s+2)(s+3)},$$
$$C(s)=\frac{3s^2+7s+8}{3s(s+1)(s+2)}, \tag{3}$$
$$D=7/9$$

with $\psi(s+1)=(d/ds)\log\Gamma(s+1)$ and γ equal to Euler's constant. Eqs. (2), (3) are derived with the exact expressions at high energies for the cross sections for pair production and radiation by electrons. They do not include, however, the loss of energy due to ionization nor the Compton effect. This omission is of no importance for our application since in the production of mesons by quanta we are concerned only with high energies where these two effects are negligible.

If we integrate $n_e(k, x)$, $n_\gamma(k, x)$ over x, letting

$$z_e(s)=\int_0^\infty dx n_e(s, x), \quad z_\gamma(s)=\int_0^\infty dx n_\gamma(s, x), \tag{4}$$

we find from (2)

$$n_e(s, \infty)-n_e(s, 0)=-A(s)z_e(s)+B(s)z_\gamma(s),$$
$$n_\gamma(s, \infty)-n_\gamma(s, 0)=C(s)z_e(s)-Dz_\gamma(s).$$

The initial conditions on N_e, N_γ, with the definitions (1) and for $s>1$ lead to

$$n_e(s, 0)=1, \quad n_e(s, \infty)=0,$$
$$n_\gamma(s, 0)=0, \quad n_\gamma(s, \infty)=0,$$

so that we have

$$-A(s)z_e(s)+B(s)z_\gamma(s)=-1,$$
$$C(s)z_e(s)-Dz_\gamma(s)=0.$$

Hence

$$z_e(s)=D/[A(s)D-B(s)C(s)],$$
$$z_\gamma(s)=C(s)/[A(s)D-B(s)C(s)]. \tag{5}$$

Now inversion of the Laplace-Mellin[10] transformation (1) gives with the help of (4)

$$Z_e(k)=\int_0^\infty dx N_e(k, x)=\frac{1}{2\pi ik}\int_{\delta-i\infty}^{\delta+i\infty} ds(E/k)^s z_e(s),$$
$$Z_\gamma(k)=\int_0^\infty dx N_\gamma(k, x)=\frac{1}{2\pi ik}\int_{\delta-i\infty}^{\delta+i\infty} ds(E/k)^s z_\gamma(s). \tag{6}$$

The contour is a line running parallel to the imaginary axis and passing to the right of $s=1$, corresponding to the condition on Eqs. (5). Both $z_e(s)$ and $z_\gamma(s)$ have simple poles at this point. Since we are primarily interested in $Z_\gamma(k)$ we consider it in some detail. In addition to the pole at $s=1$, $z_\gamma(s)$ has simple poles on the real axis[11] in the intervals between $s=-2$, -3, $-4\cdots$. We can evaluate the integral by deforming the contour to the left and finding the residues of the integrand at each of these poles. Thus if the residue of $z_\gamma(s)$ at $s=1$ is R_1 and the residues at the points $s=-a_n$ $(n<a_{-n}<n+1$, $n\geq 2)$ are R_{-n}, then

$$Z_\gamma(k)=(1/k)\{(E/k)R_1+(k/E)^{a-2}R_{-2}+(k/E)^{a-3}R_{-3}+\cdots\}. \tag{7}$$

One easily finds that $R_1=0.57$, $R_{-2}\simeq 0.06$, $a_{-2}\simeq 2.6$. The second term is therefore smaller than the first by a factor $(0.06/0.57)(k/E)^{3.6}$ and for our purposes it is sufficient to write

$$Z_\gamma(k)=0.57E/k^2. \tag{8}$$

The case for electrons is essentially the same, only the residues are different. Corresponding to Eq. (8) we have

$$Z_e(k)=0.44E/k^2. \tag{9}$$

The formulas (8), (9) will break down in the immediate neighborhood of the point $k=E$. One can show that the function $Z_\gamma(k)$ actually goes to zero at this point but with a vertical tangent, so that the error committed in using (8) right up to this point will be quite insignificant.

[10] Courant and Hilbert, *Methoden der Mathematischen Physik I* (Springer, second edition, 1930), p. 87. The results (6) can be obtained in a slightly different manner by integrating the Laplace-Mellin integrals for N_e and N_γ. The order of the integrations is interchanged and the integration over x performed first.

[11] There seem to be no poles off the real axis. We made a numerical search for such poles in the vicinity of $s=1$. The presence of poles off the real axis would not influence the result greatly. They would introduce oscillatory terms into (7) which would not be expected with the smooth dependence on energy of the cross sections for pair production and radiation.

TABLE I. *Energy flux.*

ENERGY INTERVAL BEV	FLUX BEV CM^{-2} SEC.$^{-1}$
1–3	0.11
3–7	0.44
7–18	0.87
>18	0.94

3. THE TOTAL NUMBER OF QUANTA IN THE ATMOSPHERE

The number of photon lengths as produced by one primary electron of energy E was determined in Section 2 as

$$Z(E, k)dk = 0.57Edk/k^2, \quad k \lesssim E \qquad (10)$$

where the length is measured in the units of radiation theory, i.e., for air 0.39 m water equivalent or about 1/25 of the whole atmosphere. The corresponding electron distribution is obtained simply by multiplying (10) with 7/9 giving a numerical factor of 0.44 (electrons and photons together give a factor very nearly one.) Except for this insignificant difference in the numerical factor it will make no difference whether the photons or electrons or both are held responsible for the meson production.

To obtain the total number of photon lengths in the cosmic radiation we have to integrate $Z(E, k)$ over the distribution of the primary electrons. This distribution has been obtained with sufficient accuracy by Bowen, Millikan and Neher[12] by integrating the ionization *versus* depth curves over depth at various geomagnetic latitudes. Their result is reproduced in Table I showing the total energy per second and cm^2 brought in at various energy intervals. The greater part of this intensity must consist of electrons and positrons only, as shown by the good agreement between the soft intensity in the higher atmosphere as calculated from the above primary distribution and as actually observed.[13] The tolerance for an extra nonelectronic component would depend on the accuracy of the shower theory which we believe to be within about 30 percent, an uncertainty which is irrelevant for our purpose. Also our present discussion is based explicitly on the hypothesis that the hard component is generated by the soft one so that no other primaries than electrons are considered.

Regarding the distribution in the high energy tail (>18 Bev) (i.e., not influenced by the geomagnetic field) no absolutely definite statements can be made. It seems, however, fairly certain that it actually consists of electrons and not of photons of lower energies. This is shown by the shift of the maximum and slower decrease at increasing depth of the cosmic-ray intensity at the equator as compared to the difference between the curves for higher latitudes. The actual shape of the absorption curve suggests a power law,[14] $E^{-(s+1)}dE$ with s between 1 and 2 and most probably about 1.8. This law also agrees well with the observed number of multiplicative showers

The above distribution refers to the total incoming radiation with all around incidence. To convert the flux $S(E)$ corresponding to this condition into the number of rays $j(E)$ coming in per unit solid angle we have the obvious relation (θ = angle to vertical)

$$S(E) = Ej(E)\int_0^{2\pi} d\varphi \int_0^{\pi/2} \cos^2\theta \sin\theta d\theta = \frac{2\pi}{3} Ej(E), \qquad (11)$$

$$j(E) = \frac{3}{2\pi} \cdot \frac{S(E)}{E}.$$

To obtain convenient formulas we note that the flux per energy interval in the range from 3 to 18 Bev is nearly constant. If we make this approximation and assume a power law for higher energies the absolute number of ionizing primary electrons per unit solid angle and cm^{-2} sec.$^{-1}$ will be

$$\left.\begin{aligned} j(E)dE &= 0.042dE/E, \quad 3 < E < 18 \\ &= 0.0014(s-1)(18/E)^{s+1}dE \\ &= 3.6dE/E^{2.8} \end{aligned}\right\} 18 < E \qquad (12)$$

with E in Bev, $s = 1.8$. This distribution shows of

[12] I. S. Bowen, R. A. Millikan and H. V. Neher, Phys. Rev. **53**, 855 (1938).

[13] L. W. Nordheim, reference 7; R. Serber, Phys. Rev. **54**, 317 (1938).

[14] L. W. Nordheim, Phys. Rev. **51**, 1110 (1937), W. Heitler, Proc. Roy. Soc. **A161**, 261 (1937), H. Euler and W. Heisenberg, reference 1.

course a slight discontinuity and a change of slope at $E=18$.

For the absolute number of photon lengths $X(k)=\int Z(E, k)j(E)dE$ also per unit solid angle, cm^{-2}, $sec.^{-1}$ and Bev energy range, one finds from (10) and (12):

(a) due to primaries over 18 Bev (field insensitive)

$$\begin{aligned} X_a(k)dk &= 2.65dk/k^{2.8}, \quad k>18 \\ &= 0.27dk/k^2. \quad k<18 \end{aligned} \tag{13a}$$

(b) field sensitive part due to all primaries between E and 18 Bev.

$$\begin{aligned} X_b(E, k)dk &= (0.43-0.024E)dk/k^2, \\ &\qquad k<E<18 \\ &= (0.43-0.024k)dk/k^2. \\ &\qquad E<k<18 \end{aligned} \tag{13b}$$

The sum of X_a+X_b gives the total number of photon lengths as a function of the minimum energy E which itself is determined by the geomagnetic latitude. The field sensitive part is represented by X_b alone. All this distribution will be found near the intensity maximum of the cosmic radiation in the atmosphere at about 1 m H_2O equivalent, and it will introduce no appreciable error, if for the discussion of meson production, we assume that it is entirely concentrated there.

4. Comparison with the Number of Mesons

Unfortunately not much is known regarding the number, energy distribution, and geomagnetic effect of the hard component in the upper atmosphere. Near sea level and underground, however, more complete data are available. It seems safe to extrapolate from sea level upwards, as the mesons seem to exhibit fairly definitely a range type absorption, as shown by the comparison of energy distribution and absorption measurements. Furthermore they apparently do not multiply to a great extent once they have been created.[15]

The total number of cosmic rays per unit solid angle cm^{-2} $sec.^{-1}$ near the vertical[16] is at sea level about $j=0.015$. The number of hard rays is about 70 percent of this, i.e., $j=0.0105$. The geomagnetic effect for the hard component is of the order 12 to 15 percent, i.e., about $j=0.009$ rays must have been produced by primaries of an energy greater than ~ 18 Bev. The total number of the latter as determined from (12) is 0.011 which means that there is nearly one meson at sea level per primary high energy electron.

The energy distribution of the mesons has been studied by Anderson and Neddermeyer and by Blackett.[17] The chief result of these measurements is, that the individual energies of the mesons, though large, are comparatively small compared to the energies of the primaries to which they are due in the last instance (as shown by the geomagnetic effect). The average energy at sea level is about 3 or 4 Bev. It has been remarked by Blackett that the total energy carried by the mesons at sea level is about 1/20 of the total incoming energy or about $\frac{1}{10}$ of the energy incoming at the equator, while the number of rays there is of the same order of magnitude as the number of incoming rays.

This low average energy of the mesons leads to an important conclusion. From (13a) and (13b) one finds that the field-sensitive part of the cosmic radiation produces more quanta of energy below 6 or 7 Bev than the high energy part.[18] The total energy loss by a meson in the atmosphere from ionization is around 2 Bev, i.e., mesons created with 7 Bev will arrive at sea level with around 5 Bev. The fraction of mesons over 5 Bev at sea level is about 20 percent only (in Blackett's series 169 out of 829). If, therefore, the mesons were created by photons of the same energy, i.e., the photon energy transferred to a single meson, the geomagnetic effect would be of the order of 40 to 50 percent instead of 15 percent. Therefore mesons of a given energy below 7 Bev must have been created by photons of considerably higher energy. The most reasonable interpretation of

[15] A production of low energy meson secondaries for which there is some evidence and an additional real absorption by production of showers (compare Euler and Heisenberg, reference 1) will make no appreciable difference in the following comparison as long as the cross sections for these processes are as small as they seem to be, or as long as these effects are restricted to low energies.

[16] T. H. Johnson, Rev. Mod. Phys. **10**, 208 (1938).

[17] C. D. Anderson and S. Neddermeyer, Int. Conf. Nuclear Physics, London, 1934; P. M. S. Blackett, Proc. Roy. Soc. **A159**, 1 (1937).

[18] This result is independent of any finer details of the primary distribution, as according to (10) the number of quanta k is proportional simply to the total energy brought in by electrons of energy higher than k.

this fact is that a photon divides its energy over several mesons, i.e., it produces them in multiples so that each meson receives only a fraction of the primary energy. The alternative hypothesis that a photon gives only a fraction of its energy to single mesons while continuing to exist with reduced energy seems less likely from the point of view of Yukawa's theory and would require correspondingly higher cross sections for the production process.

More detailed information regarding this behavior can be obtained from the analysis of the geomagnetic effect by Compton and Turner.[19] Primaries below 7 or 8 Bev give only an insignificant contribution to the cosmic radiation at sea level. As only 2 Bev are required by a meson to traverse the atmosphere the above threshold can be explained by assuming a multiplicity of 3 or 4 in the average.

We can also estimate the absolute value of the cross section for meson production. According to Compton and Turner the contribution of primaries between 7.5 and 15 Bev is about 1.3 percent per Bev energy range, i.e., in absolute numbers for the hard radiation $0.013\times0.011 \leqq 1.5\times10^{-4}$ ray per unit solid angle cm^{-2} $sec.^{-1}$. From (10) and (12) we calculate on the other hand for the total number of photon lengths with energies larger than k_0 created by electrons of energy less than E_0

$$Q(E_0, k_0)=\int_{k_0}^{E_0}dE\int_{k_0}^{E}dkZ(E,k)j(E)$$

$$=0.024\left(\frac{E_0}{k_0}-1-\log\frac{E_0}{k_0}\right)$$

and therefore for the number produced per Bev energy interval

$$\frac{dQ(E_0,k_0)}{dE_0}=0.024\left(\frac{1}{k_0}-\frac{1}{E_0}\right). \tag{14}$$

If the minimum energy for a meson to reach sea level is ϵ Bev and the multiplicity of the production process r, then $k_0=\epsilon r$ and the probability that a photon is converted into r mesons in one unit length (39 cm H_2O) is

$$w(k)=\frac{1.5\times10^{-4}}{0.024r[(1/\epsilon r)-(1/E_0)]}, \tag{15}$$

which is not quite a constant but nearly so in the region of 8 to 15 Bev and of the order of magnitude 1.2×10^{-2} for $\epsilon\backsimeq2$ Bev. Thus the cross section has to be of the order 1/80 to 1/50 of the cross section for pair production of quanta in air, or ~0.5 to 1×10^{-27} cm^2 per nuclear particle. This estimate is, of course, rather rough and could be refined only with a more accurate knowledge regarding the laws of distribution of the energy of the photon over the mesons produced, but it should give a fair idea of the order of magnitude. The latter seems to be entirely reasonable from the point of view of Yukawa's theory.

The situation is, however, rather different for mesons of very high energy. An estimate of their number and distribution can be made from the absorption measurements underground,[20] if we assume that they lose energy only by ionization (or more generally that they show a specific energy loss independent of energy). If we then extrapolate backwards to the top of the atmosphere we obtain a lower limit for the number of mesons there since one would have to have a larger number to start with in case there were any additional mechanisms for absorption or degradation of energy.

If the energy distribution of mesons at the place of their generation is $M(E)dE$ then the total intensity at depth x is

$$I(x)=\int_0^\infty M(E+\beta x)dE=\int_{\beta x}^\infty M(E)dE,$$

where β is the specific energy loss. The observed x^{-s} law for the absorption ($s=1.8$ between 30 and 300 m H_2O, $s=2.4$ between 300 and ~1000 m H_2) results then from

$$M(E)dE=(C/E^{s+1})dE,$$
$$I(x)=C/s(\beta x)^s. \quad s=1.8 \tag{16}$$

To determine the constant C we notice from the data of Wilson[20] that the intensity at 50 m below

[19] A. H. Compton and R. N. Turner, Phys. Rev. **52**, 799 (1937). The authors are indebted to Professor Compton for the following remark in the text.

[20] V. C. Wilson, Phys. Rev. **53**, 337 (1938); P. H. Clay, A. van Gemert and J. Clay, Physica **6**, 184 (1939).

sea level, i.e., 60 m H_2O below the top of the atmosphere is 0.073 of the intensity of 0.015 at sea level. Of this around 80 percent are mesons. Taking $\beta=0.2$ Bev per m H_2O we obtain

$$\begin{aligned} M(E)dE &= 0.14dE/E^{2.8}, \quad 6<E<60 \\ &= 1.6dE/E^{3.4}. \quad 60<E \end{aligned} \tag{17}$$

In case a different value for β is assumed the first line has to be multiplied by $(\beta/0.2)^{1.8}$ with a corresponding change in the second line.

The most important feature to be deduced from the absorption measurements is the very high penetrating power of fast mesons which corresponds to a distribution extending to very high energies. That the charged particles themselves are responsible for carrying the cosmic radiation underground has been proved by the measurements of Nielsen and Morgan and of Wilson[21] which show that the true absorption coefficient as measured by absorbing material between counters is actually as small as demanded by the power absorption law.

Comparing now the meson distribution (17) with the primary electron distribution (12) and the photon distribution (13a) we find that we have for every 26 primary electrons or every 19 photon lengths one meson of the *same* energy. If we again make the assumption that the production process is a multiple process of average multiplicity r and that the photon energy is in the average about equally distributed over the r mesons created, we obtain for the probability of such a process in one unit length

$$w(k)=\frac{0.14}{2.65}[r(k)]^{s-1}=\frac{1}{19}r^{0.8}. \tag{18}$$

With $r\backsimeq 3$ this is $0.13\backsimeq\frac{1}{8}$. If the multiplicity varies with energy the cross section has to change correspondingly. As a general result we find that the cross sections at these high energies are considerably greater than at lower energies, namely by about a factor 10, if the multiplicity of ~ 3 is conserved.

The same result regarding the efficiency of high energy quanta in producing mesons follows also from a comparison of the energy carried downward by mesons, with the total energy coming in at the equator. It follows also from the total number of photon lengths compared to the total number of mesons.

5. Difficulties of the Photon Hypothesis

We have arrived at a well-defined picture of the meson production on the photon hypothesis. There are, however, two serious objections which have to be considered in detail. From a comparison between the geomagnetic latitude and east-west asymmetry effect Johnson[22] concluded that the field-sensitive part of the cosmic radiation near sea level must be due practically entirely to positive primaries. In his new asymmetry measurements at high altitudes near the equator he found, on the other hand, that the east-west effect is rather small near the intensity maximum in the upper atmosphere. As at this location the soft component predominates[23] by far, Johnson concluded that the hard rays near sea level must be due to primaries different from electrons. There seems to be, however, a possibility of getting around this argument. The minimum energies for positives to be able to reach the equator under an angle of 60° to the vertical in the east and west directions are very far apart, *viz.*, around 32 and 11 Bev (Stoermer's limits) while the latitude effect at greater depths is determined in the main by the radiation which comes in near the vertical and is due to a much smaller energy range for the primaries. The above mentioned behavior might possibly be explained therefore by assuming that there is a large excess of positive primaries in a fairly narrow energy band near the threshold for the vertical of 15 to 18 Bev which is compensated partly or entirely by negative primaries still within the energy limits for the east-west effect.

The other difficulty is of a more intrinsic nature. The production process discussed here consists in the conversion of a photon into one or more mesons upon collision with an atomic

[21] W. M. Nielsen and K. Z. Morgan, Phys. Rev. **54**, 245 (1938); V. C. Wilson, Phys. Rev. **53**, 908 (1938).

[22] T. H. Johnson, reference 16, p. 232; T. H. Johnson and J. G. Barry, Phys. Rev. **55**, 503 (1939).

[23] The multiplication in the region of maximum intensity of a primary electron in air is of the order 1 for every Bev energy, i.e., near the equator of the order 30 (average energy for the electrons coming in at the equator). Any noticeable east-west effect observed there can then only be due either to the electrons themselves or to a radiation which also multiplies considerably in 1–2 m H_2O.

nucleus. Necessarily then the inverse processes must also be possible, i.e., processes in which the same number of photons and mesons are involved and only one meson and the photon exchange their role in initiating the process. In the case of a single process, namely the production of one meson by one photon, the inverse process is simply the one of reversed direction; in case of multiple production the inverse process is the creation by one meson of a photon and several other mesons, which all share the available energy. Such a process means either a complete absorption for the single process or for the multiple process an appreciable energy loss and degradation of the initial energy. Furthermore, as long as all individual energies are large compared to the rest energies of the involved "particles" (photons and mesons) the cross section for the inverse processes should be of the same order of magnitude as the direct processes, and in particular should show the same asymptotic behavior at high energies. This relationship between direct and inverse processes is well illustrated by the example of the normal radiative processes of electrons. The production of mesons is the analog of the pair production by quanta. The inverse process is the radiation by electrons, which, as is well known, is similarly effective in dissipating their energy as the absorption of quanta by pair production.

To the high efficiency of the production process at high energies then must also correspond a considerable rate of energy dissipation for the meson. From the value 1/19 for the probability of one process per unit length (from (18) and the assumption of single processes which is actually too favorable), one would have an average free path of around 19 times the unit length or 7 m H_2O or an absorption coefficient of 0.0011 g^{-1} cm^2. The observed integral absorption coefficient for the hard component (which includes the loss of particles by normal stopping in addition to any true absorption) is at sea level 0.0006 g^{-1} cm^2, which is already lower than the expected one, and at 100 m H_2O is as low as 1.8×10^{-4} (calculated from the power law $x^{-1.8}$ for the absorption). The discrepancy is actually more serious than would appear from the above figures. Even if one did accept the last low value (1.8×10^{-4}) which would mean a reduction of the absorption cross section by a factor 8 to 10, it would mean that one would have to increase the number of mesons created with energies sufficient to reach a depth of 100 m, by a factor e, so that the ratio of production to absorption cross section would have to be of the order 30, going to still higher values at still lower depths. The difficulty coming from the inverse processes is in fact already of a grossly qualitative nature, as the apparent constancy of the production cross section at high energies (following from the asymptotic behavior of the meson distribution as shown by the absorption underground) is incompatible with the continuous hardening of the hard component when going to greater depths, i.e., to higher energies.

It might not be absolutely impossible to overcome this difficulty by varying the primary distribution or introducing numerical factors or the like, or by inventing a mechanism which excludes the inverse processes. The situation seems, however, to be such that the burden of proof lies now on the opposite side. That is, the feasibility of the photon hypothesis (or at least the assumption of the exclusive photonic origin of the hard component) has to be demonstrated before it can be accepted.

It seems important, therefore, to discuss other possibilities, a preliminary survey of which will be presented in the following paper.

On the Production of the Hard Component of the Cosmic Radiation

II. Protons or Neutral Particles as Primaries

L. W. NORDHEIM
Duke University, Durham, North Carolina

(Received July 5, 1939)

The general requirements for understanding the hardening of the cosmic radiation underground together with a terrestrial origin of the hard component are discussed. It is shown that the hypotheses of photons or protons as primaries for mesons lead to the consequence that the inversion of the production processes (i.e., absorption of mesons by production of photons or protons accompanied by multiplication of the mesons) must have cross sections smaller by a factor of order 10 compared to the production processes. As a possibility to avoid this difference, the hypothesis of neutral mesons as additional primaries is discussed.

1. GENERAL REQUIREMENTS FOR EXPLAINING THE ORIGIN OF THE HARD COMPONENT

ONE of the principal problems which has to be solved in accounting for the terrestrial origin of the hard component of the cosmic radiation is the simultaneous explanation of the following two facts. Firstly, the occurence of penetrating particles of very high energy (100 Bev and over) and secondly the enormous penetrating power and the hardening of the hard component underground. That this hardening is actually due to the behavior of the ionizing particles themselves is shown by the near equality of the absorption by matter brought between or above the counters of a telescope.[1]

In the preceding paper[2] (quoted henceforth as I) it has been pointed out that the possibility of creating an energetic meson leads by necessity to a mechanism of absorption by the inversion of the production process. Roughly speaking one would expect that a particle will have a range only of the order of magnitude of the free path of the primary with regard to the production process. Any acceptable hypothesis regarding the terrestrial origin of the mesons has therefore to satisfy the condition that the production mechanism does not entail too strong an absorption or multiplication at the same time.

It was shown in (I) that it would be somewhat difficult to account for the mesons with photons (or electrons) as sole primaries. For these the meson production would be in competition with the normal radiative processes and would be crowded out, unless uncomfortably large production cross sections were assumed at high energies.

If we admit other primaries than photons, we have unfortunately much less information to go on since both the initial distribution of such incoming primaries as well as the laws of production of secondaries are unknown. A discussion of this subject has therefore to be of a very preliminary nature, and one can only try to account qualitatively for the most typical features of cosmic-ray effects. However, some general conclusions seem possible.

The hardening of the cosmic radiation underground can hardly be explained otherwise than by ascribing a larger average range to rays of higher energy. Therefore, in case the rays responsible for the hardening suffer, in addition to an energy loss independent of energy, a discontinuous absorption, the absorption coefficient has to decrease for an increasing energy; and the same must be true for the production cross section. In such a picture the meson production would have to extend over a considerable depth range, the more energetic primaries being effective at greater depths. We shall see in the next section, that it is possible to account for a power absorption law and a hardening in this way, even if it is assumed that in the primary process mesons of all energies

[1] W. M. Nielsen and K. Z. Morgan, Phys. Rev. **54**, 245 (1938); V. C. Wilson, Phys. Rev. **53**, 908 (1938). Though these measurements have been made only down to a depth of 60 m H_2O equivalent, the smooth continuation of the absorption curve to considerably greater depths leads to the expectation that also the hardening of the individual rays will continue downwards.

[2] L. W. Nordheim and H. M. Hebb, Phys. Rev. **56**, 494 (1939).

from the primary energy down to very low energies are produced.

It remains, however, difficult to explain the equality of absorption with an absorber between or above the counters of a cosmic-ray telescope, which equality means that the number of particles produced in the absorber is much less than the number which is actually absorbed. It is quite possible to make the ratio between both absorption coefficients a constant. In order to have a ratio near unity, however, the average range either of the primaries or of the secondaries has to be much larger than that of the others for the same energy. In the first case (the range of the primaries is the longer) the absorption will in the main be determined by the primaries, in the second case it will be determined by secondaries.

We shall illustrate these points in Section 2 on a simple model. As has already been emphasized, the details of this model should not be taken too literally. In the remaining sections we shall then attempt to give a discussion of the most plausible mechanisms for the production of mesons.

2. On the Mechanism of the Hardening of the Cosmic Radiation

We suppose that there are two kinds of particles, the primaries, whose distribution as function of their energy E and of depth below the top of the atmosphere is $P(E, x)$, and the secondaries (mesons) with a distribution function $S(k, x)$, where k is the energy of the mesons. We assume furthermore a probability $\phi(E, k)dk$, that a primary E creates a secondary in the interval dk per unit path where ϕ is supposed to decrease with increasing E. The number of mesons produced in a layer dx is then

$$R(k, x)dx = dx\int_k^\infty P(E, x)\phi(E, k)dE. \quad (1)$$

As the absorption of the mesons seems to be well represented as a range absorption, we assume for them a linear law of energy loss. The equation determining the distribution function $S(k, x)$ is then

$$\partial S(k, x)/\partial x = \beta\partial S/\partial k + R(k, x), \quad (2)$$

which is solved for the boundary condition $S(k, 0) = 0$, i.e., no incoming mesons, by

$$S(k, x) = \int_0^x R(k+\beta z\,;\, x-z)dz. \quad (3)$$

Here β is the specific energy loss assumed to be independent of energy. The total number of mesons with an energy $>k_0$ at depth x will be then

$$S(x) = \int_{k_0}^\infty S(k, x)dk = \int_0^x dz\int_{\beta z+k_0}^\infty R(k; x-z)dk, \quad (4)$$

i.e., all mesons created with an energy $k > k_0+\beta z$ at a distance z above the place of observation can reach x. The true absorption is determined by the number of mesons which actually stick in a layer dx, i.e., those which are created at z with a k between $k_0+\beta z$ and $k_0+\beta z+\beta dx$. It is then

$$A(x)dx = dx\int_0^x R(k_0+\beta z;\, x-z)dz = dx\beta S(k_0, x), \quad (5)$$

where k_0 is the sticking energy, i.e., the energy at which the meson can be considered as absorbed. It will be of the order of the rest energy. The total change of S with depth, the number $G(x)$ of generated mesons and the number $A(x)$ of absorbed mesons are connected by the relation

$$\frac{dS(x)}{dx} = \int_{k_0}^\infty R(k, x)dx - \beta S(k, x) = G(x) - A(x). \quad (6)$$

These formulas will remain approximately correct even if we assume, in addition to a linear energy loss β_0, a true absorption with an absorption coefficient $\kappa = \beta_1/k$, i.e., inversely proportional to the energy, as such an absorption will make the average range again proportional to the initial energy; the constant β will stand then for the sum $\beta = \beta_0+\beta_1$.

For the primaries we similarly assume a linear energy loss and a true absorption, which latter will be due, in first instance, to the production of

the mesons. We neglect the reproduction[3] of primaries by secondaries. The equation for $P(E, x)$ will then be

$$\frac{\partial P(E, x)}{\partial x}=\beta\frac{\partial P(E, x)}{\partial x}-\kappa(E)P(E, x), \quad (7)$$

where $\kappa(E)$ is the absorption coefficient. The solution of this equation in terms of the initial distribution $P(E, 0)$ is

$$P(E, x)=P(E+\beta x; 0) \times\exp\left[-\int_0^x \kappa(E+\beta z)dz\right]. \quad (8)$$

If we neglect the ionization loss β this reduces to

$$P(E, x)=P(E, 0)\exp\left[-\kappa(E)x\right]. \quad (8a)$$

We give two examples of the application of these formulas. In the first one it is assumed that a primary of energy E can create r secondaries of energy $k=E/r$ with a probability α/E. The latter quantity also gives the absorption coefficient for the primaries. For the initial distribution we take a power law

$$Z(E, 0)=C/E^{s+1},$$
$$Z(E, x)=\frac{C}{E^s}\cdot e^{-\alpha x/E} \quad (9)$$

and we specify for simplicity $s=2$, which makes all necessary integrations elementary ones. We then obtain the following results for a depth such that $k_0<\alpha x$ and $k_0<\beta x$. The number of particles created per unit layer becomes

$$R(k, x)=\frac{\alpha C}{r^2k^4}\exp\left[-\frac{\alpha}{r}\frac{x}{k}\right], \quad (10a)$$

the total number of primaries and secondaries

$$P(x)=\frac{C}{(\alpha x)^2}; \quad S(x)=\frac{C}{(\alpha x)^2}\left[\frac{1}{2r}\left(\frac{\alpha}{\beta}\right)^2+\frac{\alpha}{\beta}\right] \quad (10b)$$

and the number of secondaries generated and absorbed per unit layer

$$G(x)=\frac{C}{(\alpha x)^2}\frac{2}{x};$$
$$A(x)=\frac{C}{(\alpha x)^2}\cdot\frac{2}{x}\left[r+\frac{\alpha}{\beta}+\frac{1}{2r}\left(\frac{\alpha}{\beta}\right)^2\right]. \quad (10c)$$

We see that the features previously discussed are well verified. We have a power law for both the primary and the secondary intensity and a hardening as shown by a more rapid decrease of $G(x)$ and $A(x)$ with depth than the total intensity. Also the ratio A/G is constant, which leads to a constant ratio between the absorption coefficient with matter between or above counters. In order to make the latter ratio of the order unity one has either to make the secondary intensity very small compared to the primary one, i.e., $\alpha\ll\beta$, or one has to make the secondaries much less absorbable than the primaries, i.e., $G\ll A$, $\alpha\gg\beta$. In either case the absorption coefficient for matter between counters will approach the over-all value $2/x$ corresponding to the power law. From the inversion argument, however, a near equality of α and β would be expected.

As the second example we take a case where the energies of the secondaries produced are continuously distributed with preference to lower energies. To obtain formulas which can be handled easily we choose for the cross section and primary distribution

$$\phi(E, k)dk=\frac{\alpha}{\lg(E/k_0)}\frac{dk}{Ek}; \quad k>k_0, \quad (11a)$$

$$Z(E, 0)=(C/E^3)\lg(E/k_0). \quad (11b)$$

The expression (11a) gives again a total absorption coefficient $\kappa(E)=\alpha/E$ and we obtain for the number of mesons generated at x

$$R(k, x)=\frac{1}{k}\int_k^\infty\frac{\alpha C}{E^4}e^{-\alpha x/E}dE$$
$$=\frac{\alpha C}{k(\alpha x)^3}\left[2-e^{\alpha x/k}\left\{2+\frac{2\alpha x}{k}+\left(\frac{\alpha x}{k}\right)^2\right\}\right]. \quad (12)$$

For the further integration we approximate this by the asymptotic expressions for large and

[3] The consideration of this effect would lead to an integral equation similar to the one used in the theory of showers. The neglect of the reproduction is here less serious than in the shower theory as the cross sections decrease with increasing energy.

small $\alpha x/k$

$$R(k,x)=\begin{cases}\dfrac{2\alpha C}{k(\alpha x)^3} & \text{for } k\leqslant \alpha x,\\[2ex] \dfrac{\alpha C}{3k^4} & \text{for } k>\alpha x.\end{cases} \tag{12a}$$

The remaining integrations are then elementary (with some attention to the integration limits) and give the result

$$P(x)=\frac{C}{(\alpha x)^2}\lg\frac{\alpha x}{3k_0};$$
$$S(x)=\frac{C}{(\alpha x)^2}\left\{\frac{\alpha}{\beta}\cdot\frac{13}{6}+\left(\frac{\alpha}{\beta}\right)^2\frac{2}{3}\right\}; \tag{13a}$$
$$G(x)=\frac{C}{(\alpha x)^2}\cdot\frac{2}{x}\left[\lg\frac{\alpha x}{k_0}+\frac{1}{18}\right];$$
$$A(x)=G(x)+\frac{2}{x}S(x). \tag{13b}$$

These results are very similar to those of the first example, and the same remarks apply.

It is also possible to admit only primaries with an energy larger than a critical energy E_0, in order to take the geomagnetic effect into account. We quote only one result for later discussion. In the second example, the geomagnetic effect will be small for $\alpha x>E_0$ as then the missing primaries of lower energy will be ineffective. For smaller depths the ratio of the number of primaries to secondaries will become

$$\frac{P(x)}{S(x)}=\frac{3E_0\lg(E_0/k_0)}{2\alpha x[\lg(E_0/\beta x)+(4/3)]},\quad \alpha x<E_0,$$

i.e., the number of secondaries remains smaller than the number of primaries for any choice of the constants.

3. The Proton Hypothesis

The most natural choice of primaries other than electrons consists, of course, in the admission of protons, a hypothesis which has already been discussed occasionally in connection with the hard component before the discovery of the meson.[4] It has been advocated strongly by Johnson[5] for reason of the east-west effect as discussed in I. Also a mechanism for the production of mesons by protons follows quite naturally from Yukawa's theory.[6] It seems, however, to be rather unlikely that protons could be made entirely responsible for all of the hard component. The smallness of the geomagnetic effect demands that protons of an energy below the critical energy at the equator are either comparatively small in number, or else so highly absorbable (through the process of meson production) that their effect near sea level remains small. It is rather certain, furthermore, that only a minor fraction of the penetrating rays at sea level can be protons. This follows from the near equality of the numbers of positives and negatives, the failure to find slow protons,[7] and the considerable number of energetic electron secondaries, produced in direct collisions.[8] The percentage of protons according to these observations can hardly be as large as 20 percent, but might be considerably less. It is then necessary to assume that a single proton of an energy above the geomagnetic threshold at the equator, produces quite a large number of mesons which come down to sea level.[9] The free path of a proton of 15 to 20 Bev energy therefore must be considerably less than one atmosphere. The application of the models discussed in Section 2 leads to results in keeping with the general argument above. In order to make the geomagnetic effect small and the number of secondaries large, the constant α in the absorption coefficient $\kappa=\alpha/E$ for the protons has to be made so large that $\alpha x>E_0$. With $E_0\sim 17$ Bev (threshold energy for protons at the equator) and $x=10$ m H_2O one obtains $\alpha>1.7$ Bev/m H_2O. This would correspond to a cross section of $0.3\times10^{-25}(10^9\text{ ev}/E)$

[4] A. H. Compton and H. Bethe, Nature **134**, 734 (1934); L. W. Nordheim, Annales Inst. Poincaré (1936).
[5] T. H. Johnson, J. Frank. Inst. **227**, 37 (1939); T. H. Johnson and J. G. Barry, Phys. Rev. **55**, 504 (1939).
[6] L. W. Nordheim and G. Nordheim, Phys. Rev. **54**, 254 (1938).
[7] C. G. Montgomery, D. D. Montgomery, W. E. Ramsey and W. F. G. Swann, Phys. Rev. **50**, 403 (1936).
[8] J. I. Hopkins, W. M. Nielsen and L. W. Nordheim, Phys. Rev. **55**, 233 (A) (1939).
[9] The same conclusion follows from the argument in *I* that only a small fraction of the field-insensitive primaries can be protons while the number of hard rays at sea level is nearly equal to the total number of all field-insensitive primaries.

per nuclear particle. It is then again difficult to see how a meson of 15 to 20 Bev energy could have a range of perhaps 50 to 100 m H_2O as seems to follow from Blackett's and Clay's[10] comparison of the energy spectrum of the mesons and their absorption underground. The range of the mesons would have to be made greater than the range of protons of the same energy by a factor of order 10. In addition, special assumptions for protons of smaller energies would have to be made (i.e., that they either are very small in number or can produce only mesons of rather low energy), but the situation is better than for the photon hypothesis since the discrepancy does not increase with depth.

It seems difficult, otherwise, to decide between the two hypotheses. The cross sections have to be of the same order of magnitude in both cases. For protons, however, the competition of the meson production process with the radiative processes is absent, and therefore a smaller number of primaries would be required. As practically all of the protonic energy would be given over to mesons, the protons would have to bring in only about 10 percent of the total cosmic-ray energy, an amount which is certainly compatible with our knowledge regarding the multiplication of the primary distribution (compare I).

The assumption of a combined photonic and protonic origin of the mesons would not improve the situation very much. If we assume that the cross section for photons of high energies are of the same order as those for medium energies (7 to 18 Bev) as determined in I, then we can account only for 10 to 20 percent of all the mesons at sea level and the situation regarding the protonic part is not much changed.

4. Neutral Particles as Primaries to the Hard Component

The seriousness of the inversion difficulty might be a matter for debate. It seems, however, that one is justified to go to some length to avoid it. It will evidently remain as long as charged particles are assumed as primaries for the mesons, since the geomagnetic effect makes it necessary that primaries above 18 Bev are the most effective ones. It is suggestive, therefore, to attempt to make a neutral primary radiation responsible for at least part of the hard component. It is probably more than a coincidence that the recent theories of nuclear forces, based on Yukawa's ideas, lead quite naturally to a suitable primary of this kind and a production mechanism for charged particles.

In the theories of nuclear forces the mesons appear as the carrier particles associated with the nuclear force field. The exchange nature of the nuclear forces is then connected with the fact that the mesons are charged. However, the apparent equality of the forces between protons and protons, and between neutrons and protons makes it necessary to assume[11] the additonal existence of neutral particles of properties otherwise similar to those of charged mesons. The process of producing charged mesons by neutral ones is simply a generalized scattering process. The Compton effect and other scattering of light can be described as the absorption of a photon by an electron and the immediate re-emission of another photon. Analogously, the scattering of a meson consists in its absorption by a nuclear particle (proton or neutron) and again a re-emission. If now the interaction between a nuclear particle and a meson is independent of the charge of the latter, then the scattering cross sections for processes with conservation of charge and with change of charge will be the same. These scattering processes are really the simplest processes involving mesons and nuclei and should be at least as probable as the meson production by photons or protons. The usefulness of an uncharged meson to explain certain cosmic-ray effects and the possibility of change of charge has already been pointed out by Arley and Heitler[12] who proposed the name "neutretto" for the uncharged mesons. We tentatively suggest the neutretto as a possible primary of the cosmic radiation.[13]

[10] P. M. S. Blackett, Proc. Roy. Soc. **A159**, 1 (1937); P. H. Clay, A. van Gemert and J. Clay, Physica **6**, 184 (1939).

[11] N. Kemmer, Proc. Camb. Phil. Soc. **34**, 354 (1938); H. Yukawa and others, Proc. Math. Phys. Soc. Japan **20**, 720 (1938); H. A. Bethe, Phys. Rev. **55**, 1130(A) (1939).

[12] N. Arley and W. Heitler, Nature **142**, 158 (1938).

[13] It should be mentioned that energetic neutrons could be taken equally well as primaries. The objection against this hypothesis is, however, that neutrons are probably not stable but β-radioactive.

There seems to be no inherent difficulty with regard to this hypothesis. It is, of course, necessary to admit that part of the cosmic-ray mesons are produced by field-sensitive primaries, i.e., electrons (photons) or protons, but the cross section can then be made much smaller, particularly at high energies. The theory leads, furthermore, to the expectation that all the processes mentioned are actually possible and that they have cross sections which are not too different. The occurence of more than one mode of production is therefore quite likely.

Furthermore it seems to be no harder to account for the ultimate origin of the neutrettos than for that of any other kind of cosmic-ray particles. Under conditions which make the production of mesons possible, a mixture of charged and uncharged ones would always be expected. They might then possibly be accelerated by electric fields in the charged state and then suffer a change of charge. Of the mesons which finally escape, the charged ones will decay spontaneously into electrons and neutrinos while the neutrettos remain stable until they collide with matter, as when falling on the surface of the earth.

The neutretto hypothesis evidently could serve to explain the large number of mesons of comparatively low energies which are not influenced by the geomagnetic field. It has to be remarked, however, that one difficulty still remains with this hypothesis, and that is the problem to account for the near equality of the absorption coefficients with matter between and above counters. It would be entirely removed, if the absorption of the neutral mesons were slightly stronger than that for charged mesons. It appears from the second model of Section 2 (which has been chosen with reference to the neutretto hypothesis, as (11a) is similar to the formula for the Compton scattering) that a factor 2 or 3 (i.e., $\alpha \sim 3\beta$) would be sufficient. It would be, of course, premature to base any definite conclusions on such considerations.[14]

Summarizing our whole discussion it appears that a final answer to the question of meson production cannot be given at the present time. We hope, at least, to have clarified the problems which have to be solved. We wish to repeat that there is no absolute objection against either the photon or the proton hypothesis or a combination of the two. If the present data on the number and distribution of primaries and mesons and the penetrating power of mesons are correct, one has to admit, however, that the probabilities for the inverse of the production processes have to be smaller by a factor of order 10 to 100 compared to the latter, and this for the *same* energies of primaries and mesons. If one wishes to avoid this factor, a way out might be offered by the assumption of neutral mesons as primaries.

---

[14] It might be mentioned, however, that in Bethe's form of the theory of nuclear forces (compare reference 11) the interaction of neutrettos with nuclei is assumed to be much larger than the one of charged mesons and nuclei, and this would make the scattering of a neutretto without change of charge more probable than a conversion process.

β-Decay and Spin of Light Nuclei[1]

B. O. GRÖNBLOM
Cornell University, Ithaca, New York

(Received May 12, 1939)

The β-decay of the nuclei He^6, Be^7, N^{13}, O^{15} and F^{17} is investigated from a point of view of the Gamow-Teller modification of the Fermi-theory. It is assumed that the lowest state of each nucleus forms a spin-multiplet. The various transition probabilities are given as functions of the total angular momentum I of the various states of the nuclei. An accurate knowledge of the β-spectrum would lead to a definite prediction of the spins of the nuclei. For the time-constant in the β-theory a value of $3 \cdot 10^3$ sec. is obtained as compared to the previous value of $11 \cdot 10^3$ sec.

AN investigation of the shape of the β-spectrum of the light nuclei[2] seems to lead to a better agreement with the original theory of Fermi than with the modified theory of Uhlenbeck and Konopinski.[3] The observed asymmetry of the electron spectrum is assumed to be due to the fact that the β-decay leads to several states of the final nucleus, from which a transition to the ground state with the emission of γ-rays occurs. In fact such a γ-radiation has been observed by Richardson,[4] who by the process $N^{13} \rightarrow C^{13} + \beta^+ + \nu_0$ found a γ-radiation of the energy 285 ± 15 kev with an intensity of 0.8 quanta per disintegration. This figure has lately been corrected by Richardson[5] and Lyman[6] who found the figures 0.4 and 0.25 quanta per decay for the intensity, the energy remaining unchanged by 280 kev. It seems thus to be proved that the decay leads to two states of C^{13}, the ground state and an excited state, with an energy difference of 280 kev, though the ratio between the transition probabilities is only inaccurately known.[7]

The small energy difference predicts (considering that the regarded nucleus is light) that the levels most probably are levels of the same multiplet. The same can be concluded from the processes $O^{15} \rightarrow N^{15} + \beta^+ + \nu_0$ (energy difference $= 500$ kev), $F^{17} \rightarrow O^{17} + \beta^+ + \nu_0 (+900$ kev) and $Be^7 \rightarrow Li^7 - \beta^- + \nu_0$ where a K electron is captured into two states with an energy difference of 550 kev, whereas in the other processes, investigated by Bethe, Hoyle and Peierls ($B^{12} \rightarrow C^{12} + \beta^+ + \nu_0$, $F^{20} \rightarrow Ne^{20} + \beta^+ + \nu_0$) the large energy to be expected of the γ-rays (5 and 2 Mev, respectively) seems to predict two entirely different states.

The original theory of Fermi for the interaction between the heavy particles and the field of the light particles would not yield any transitions between states of different spins. A direct evidence that such transitions can occur is however given by the large probability of the process $He^6 \rightarrow Li^6 + \beta^+ + \nu_0$, which is probably a $^1S - {}^3S$ transition.[8] We will therefore use the spin-dependent modification of the Fermi theory as given by Gamow and Teller,[9, 10] using for the Hamiltonian of the interaction the expression

$$H = g(Q\sigma^H \psi^* \sigma^L \varphi + Q^* \sigma^{H*} \psi \sigma^{L*} \varphi^*), \qquad (1)$$

where g is the normal Fermi constant, σ^H and σ^L are the Pauli spin-operators, acting on the heavy and light particles, respectively. Q is an operator, which converts a neutron into a proton, Q^* is the inverse operator. ψ and φ are wave functions for the electron and the neutrino, respectively, taken as plane waves. The relativistic theory is here used only for the light particles.

This gives for the transition probability per time-unit the expression:[11]

[1] The subject of this paper was first presented at the Washington Meeting, 1939.
[2] H. A. Bethe, F. Hoyle and R. Peierls, Nature **143**, 200 (1939).
[3] E. J. Konopinski and G. E. Uhlenbeck, Phys. Rev. **48**, 107 (1935).
[4] J. R. Richardson, Phys. Rev. **53**, 610 (1936).
[5] J. R. Richardson, Phys. Rev. **55**, 609 (1939).
[6] E. Lyman, Washington Meeting, 1939.
[7] S. Kikuchi, Y. Watase, J. Itoh, E. Takeda, S. Yamaguchi, Proc. Phys. Math. Soc. of Japan **21**, 41 (1939).
[8] M. Goldhaber, unpublished.
[9] G. Gamow and E. Teller, Phys. Rev. **49**, 895 (1936).
[10] The fact that the transition $Be^7 \rightarrow Li^7$ speaks in favor of the Gamow-Teller theory has already been pointed out by G. Breit and J. Knipp, Phys. Rev. **54**, 652 (1938).
[11] H. A. Bethe and R. F. Bacher, Rev. Mod. Phys. **8**, 193 (1936). (Integrating over ϵ in the formula 210 according to the formula 213 on the page 193.)

$$w=\frac{1}{\tau_0}f(W)|G|^2. \quad (2)$$

τ_0 is here the decay-constant, and $f(W)$ is given as:

$$f(W)=(W^2-1)^{\frac{1}{2}}\left(\frac{W^4}{30}-\frac{3}{20}W^2-\frac{2}{15}\right)+\frac{W}{4}\log\left[W+(W^2-1)^{\frac{1}{2}}\right], \quad (3)$$

W being the energy including the rest mass of the electron, in units of mc^2. (The original Fermi theory leads to the same expression.) A graphic representation of the function $f(W)$ is given in Fig. 1. One has

$$|G|^2=\frac{1}{3}\left\{\left|\int u_n^*\sigma_x v_m d\tau\right|^2+\left|\int u_n^*\sigma_y v_m d\tau\right|^2+\left|\int u_n^*\sigma_z v_m d\tau\right|^2\right\}, \quad (4)$$

where u_n and v_m are the wave functions of the heavy particle. We will make the assumption that u_n and v_m approximately belong to the same set of orthogonal functions. This assumption seems to be justified because the Hamiltonians, corresponding to the systems of functions denoted by u and v, respectively, differ only by a Coulomb term, and thus the neglected effect is only one of the second order in the Coulomb energy.

$$He^6\rightarrow Li^6+\beta^++\nu_0.$$

The β-spectrum has lately been measured by Bjerge and Brostrøm.[12] The half-lifetime has been found to be 0.8 ± 0.1 sec., the upper limit of the spectrum was found at 3.5 Mev. If we write the wave function of the initial state of He^6 in the form:

$$\psi=n(1)n(2)\cdot\frac{\alpha(1)\beta(2)-\alpha(2)\beta(1)}{2^{\frac{1}{2}}}u_{\text{space}}$$

and apply on this function the operator $Q_1\sigma_{z1}+Q_2\sigma_{z2}$ (corresponding to the fact that we have two terms like (1) in the complete interaction,

[12] T. Bjerge and K. J. Brostrøm, Det. Kgl. Danske Videnskabernes Med. **16**, no. 8 (1938).

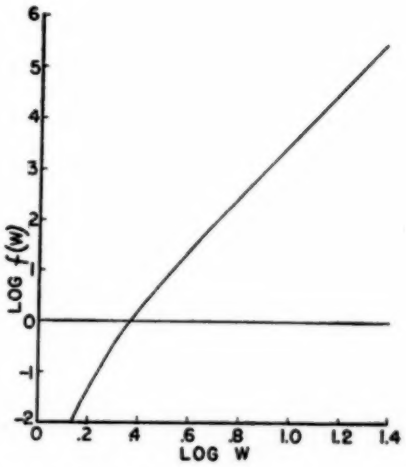

FIG. 1. Value of $f(W)$ *vs.* log W (Eq. (3)).

one for particle 1 and one for particle 2), we obtain:

$$2^{\frac{1}{2}}\cdot\frac{n(1)p(2)-n(2)p(1)}{2^{\frac{1}{2}}}\cdot\frac{\alpha(1)\beta(2)+\alpha(2)\beta(1)}{2^{\frac{1}{2}}}u_{\text{space}}=2^{\frac{1}{2}}\varphi_{\text{charge}}\chi_{\text{spin}}u_{\text{space}}.$$

This yields[13] $|G|^2=2$.

Taking for W the value $W=7.9$ and for the half-lifetime the value 0.8 sec. we thus obtain for the decay constant the value $\tau_0=2.2\cdot10^3$ sec.

$$Be^7\rightarrow Li^7-\beta^-+\nu_0.$$

This process means a capture of a K electron. The final nucleus Li^7 has an excited level at 450 kev. The K-electron capture leading to this state has been observed by means of the γ-rays emitted in the subsequent transition of Li^7 from the excited state to the ground state. From the intensity of these γ-rays as compared to the number of neutrons emitted in the original formation of Be^7 it has been concluded that roughly 10 percent lead to the excited state of Li^7. The total energy involved in the K-electron capture can best be obtained from the threshold of the reaction $Li^7+H^1\rightarrow Be^7+n^1$.[14] This threshold has been observed by Hill and Valley[15] to be 1.75 Mev. Subtracting 0.75 Mev

[13] Compare, however, G. Breit and J. Knipp, reference 10.

[14] R. B. Roberts, N. P. Heydenburg and G. L. Locher, Phys. Rev. **53**, 1016 (1938). L. H. Rumbaugh, R. B. Roberts and L. R. Hafstad, Phys. Rev. **54**, 657 (1938).

[15] J. E. Hill and G. E. Valley, New York Meeting, 1939.

from the difference between neutron and proton we find 1.00 Mev for the energy of the neutrino emitted when the K-electron capture leads to the ground state of Li^7. When the transition leads to the excited state the neutrino energy will accordingly be 0.55 Mev.—The observed half-lifetime of Be^7 is 43 days.[16]

The probability per time unit of an electron capture is:[17]

$$w=(\pi^2\epsilon^2\rho/\tau_0)(\hbar/mc)^3|G|^2. \tag{5}$$

ϵ means the energy of the outgoing neutrino, ρ is the density of the two K electrons in the nucleus:

$$\rho=2Z_{eff}^3/\pi a_0^3 \quad (a_0=\text{Bohr radius}). \tag{6}$$

The ground state of Be^7 is in the Hartree model given as a $^2P_{3/2}$ state,[18] which is in agreement with the experiments.[19] We shall here, as well as with the other nuclei, consider the ground state of the formed nucleus to be the same as for the initial nucleus, which is equivalent to the assumption that the splitting is not magnetic, but is due to the Thomas force.[20] The excited state involved in the process is assumed to be a $^2P_{1/2}$ state.

If we write the Pauli eigenfunctions for the hole in the p shell in the form:[21]

$$u_{nl,\ j=l+1/2,\ m}=\frac{1}{(2l+1)^{\frac{1}{2}}}\begin{pmatrix} k_1 Y_{l,\ m-1/2}(\vartheta,\varphi) \\ -k_2 Y_{l,\ m+1/2}(\vartheta,\varphi)\end{pmatrix}R_{nl}(r),$$

$$u_{nl,\ j=l-1/2,\ m}=\frac{1}{(2l+1)^{\frac{1}{2}}}\begin{pmatrix} k_2 Y_{l,\ m-1/2}(\vartheta,\varphi) \\ k_1 Y_{l,\ m+1/2}(\vartheta,\varphi)\end{pmatrix}R_{nl}(r), \tag{7}$$

where $k_1=(l+m+\frac{1}{2})^{\frac{1}{2}}$, $k_2=(l-m+\frac{1}{2})^{\frac{1}{2}}$ we obtain (averaging over m in the initial state and summing over m in the final state):

$$\begin{aligned}
|G(^2P_{3/2}\rightarrow{}^2P_{3/2})|^2&=\tfrac{1}{4}\sum_{m=-3/2}^{m=+3/2}|k_1^2-k_2^2|^2=5/9\\
|G(^2P_{3/2}\rightarrow{}^2P_{1/2})|^2&=\tfrac{1}{4}\sum_{m=-1/2}^{m=+1/2}|k_1k_2|^2=4/9\\
|G(^2P_{1/2}\rightarrow{}^2P_{1/2})|^2&=\tfrac{1}{2}\sum_{m=-1/2}^{m=+1/2}|k_1^2-k_2^2|^2=1/9\\
|G(^2P_{1/2}\rightarrow{}^2P_{3/2})|^2&=\tfrac{1}{2}\sum_{m=-1/2}^{m=+1/2}|k_1k_2|^2=8/9.
\end{aligned} \tag{8}$$

Using these figures for the matrix element and the value 3.7 for Z_{eff}, we obtain as the result: 20 percent of the transitions lead to the excited state if the ground state is a $^2P_{3/2}$ state. 72 percent of the transitions lead to the excited state if the ground state is a $^2P_{1/2}$ state.

A comparison with the experimental figure thus predicts a $^2P_{3/2}$ state, in agreement with the known spin of Li^7.

For the decay constant we obtain the value $\tau_0=1.8\cdot10^3$ sec. If the spin of Be^7 were $\frac{1}{2}$, different from the spin of Li^7, the value would be $\tau_0=2.2\cdot10^3$ sec.

$$N^{13}\rightarrow C^{13}+\beta^++\nu_0.$$

The result of the investigation of this process by Richardson and Lyman has been already mentioned. The upper limit of the spectrum lies at 1.20 Mev[22] and the half-lifetime has been found to be 11 minutes. For the intensity of the γ-rays we choose the value found by Lyman from the analysis of his measurements of the β-spectrum, according to which 25 percent of the transitions should lead to the excited state. For the spin of C^{13} the Hartree model predicts the value $\frac{1}{2}$ whereas the α-particle model[23] leads to the value $\frac{3}{2}$. The spin of C^{13} has not been measured.* The calculation of the transition probabilities to the ground state and to the excited state could allow a decision between these values, but since the experimental figure has been subject to considerable change, our

[16] The figures for the half-lifetimes for Be^7, N^{13}, O^{15} and F^{17} are taken from H. A. Bethe and M. S. Livingston, Rev. Mod. Phys. **9**, 245 (1937).

[17] H. Yukawa and S. Sakata, Proc. Phys. Math. Soc. of Japan **17**, 465 (1935). C. Møller, Phys. Rev. **51**, 84 (1937).

[18] M. E. Rose and H. A. Bethe, Phys. Rev. **51**, 205 (1937).

[19] H. A. Bethe and R. F. Bacher, Rev. Mod. Phys. **8**, 215 (1936).

[20] D. R. Inglis, Phys. Rev. **50**, 783 (1936).

[21] H. A. Bethe, *Handbuch der Physik*, Vol. 24, No. 2 (Leipzig, 1933), p. 309.

[22] E. Lyman, Washington Meeting, 1939.

[23] L. R. Hafstad and E. Teller, Phys. Rev. **54**, 684 (1938). B. O. Grönblom and R. E. Marshak, Phys. Rev. **55**, 229 (1939). R. G. Sachs, Phys. Rev. **55**, 825 (1939).

* *Note added in proof.*—C. H. Townes, Stanford meeting, 1939, finds the value $\frac{1}{2}$ for the spin of C^{13} from measurements on the $C^{13}-C^{13}$ band spectrum.

conclusions should be taken with reservations. This is *a fortiori* true for the nuclei N^{15} and O^{17} where the observations could be still more uncertain.

Using the value 280 kev for the energy difference between the levels and the figures (8) for the matrix elements we obtain: 19 percent of the transitions lead to the excited state if the ground state is a $^2P_{3/2}$ state. 71 percent of the transitions lead to the excited state if the ground state is a $^2P_{1/2}$ state. Hence a spln $\frac{3}{2}$ for the ground state of C^{13} is favored.

For the decay constant we obtain the value $6.0\cdot10^3$ sec. if the spin of the ground state is $\frac{3}{2}$. If the spin of the ground state were $\frac{1}{2}$ the corresponding figure would be $3.2\cdot10^3$ sec.

$$O^{15}\rightarrow N^{15}+\beta^+ +\nu_0.$$

The β-spectrum of O^{15} is measured by Fowler, Delsasso and Lauritsen[24] and investigated from the point of view of the Fermi theory by Bethe, Hoyle and Peierls, who conclude that the transitions lead to two states with an energy difference of 500 kev, 40 percent of the transitions leading to the excited state. The observed half-lifetime is 126 sec. and the upper limit of the spectrum lies at 1.7 Mev. The value $\frac{1}{2}$ for the spin of the ground state of N^{15} was found by Wood and Dieke from the band spectrum of the N^{15} molecule.[25] This value was predicted by Rose and Bethe theoretically.

Using again the formulas (8) we obtain that 63 percent of the transitions should lead to the excited state. Under the false assumption that the ground state has the spin $\frac{3}{2}$ the corresponding figure would be 14 percent.

The value of the decay constant as deduced from this process is $\tau_0=2.1\cdot10^3$ sec.

$$F^{17}\rightarrow O^{17}+\beta^+ +\nu_0.$$

The half-life of F^{17} is 70 sec. The upper limit of the β-spectrum lies at 2.05 Mev. From the measurements of Fowler, Delsasso and Lauritsen, Bethe, Hoyle and Peierls found that the transition leads again to two states with an energy difference of about 900 kev. It is predicted that 60 percent of the transitions lead to the excited state.

As the p shell is completely filled with O^{16}, the ground state of F^{17} has to be either an $^2S_{1/2}$, a $^2D_{3/2}$ or a $^2D_{5/2}$ state. We will assume that the states involved are ^2D states.

For the matrix elements we obtain, again using the eigenfunctions (7):

$$\begin{aligned}
&|G(^2D_{5/2}\rightarrow{}^2D_{5/2})|^2=7/15\\
&|G(^2D_{5/2}\rightarrow{}^2D_{3/2})|^2=8/15\\
&|G(^2D_{3/2}\rightarrow{}^2D_{3/2})|^2=1/5\\
&|G(^2D_{3/2}\rightarrow{}^2D_{5/2})|^2=4/5.
\end{aligned}\tag{9}$$

If the ground state is a $^2D_{3/2}$ state, 29 percent of the transitions should lead to the excited state as against 5 percent if the ground state is a $^2D_{5/2}$ state. A comparison with the estimated figures of Bethe, Hoyle and Peierls thus decisively favors a spin $\frac{3}{2}$ for the ground state, though a considerable discrepancy still remains. Even a slight change in the predicted value of the γ-ray would change the figure noticeably. Another possibility is that the $^2S_{1/2}$ state is involved in the process, which could be taken as implied by the large energy difference between the levels. A decision can, however, be obtained only by more precise experiments. Even a direct determination of the spins of O^{17} as well as for C^{13}, would be very desirable. This process yields $\tau_0=2.5\cdot10^3$ sec.

Conclusions

An accurate knowledge of the shape of the β-spectrum of the light nuclei as well as of the energy and the intensity of the γ-rays emitted by the final nuclei would allow some more precise statements regarding the mechanism of the decay. This would even make possible a prediction of the spin of the nuclei involved.

For the decay constant we obtain values between $1.8\cdot10^3$ sec. and $6.0\cdot10^3$ sec. The probable value thus seems to lie around $3\cdot10^3$ sec. This is to be compared with the previous value of $11\cdot10^3$ sec. calculated as an upper limit from the process $N^{13}\rightarrow C^{13}+\beta^+ +\nu_0$ by Bethe and Critchfield.[26]

The author wishes to express his gratitude to Professor H. A. Bethe for the suggestion of this problem as well as for many helpful discussions.

[24] W. A. Fowler, L. A. Delsasso and C. C. Lauritsen, Phys. Rev. **49**, 569 (1936).
[25] R. H. Wood and G. H. Dieke, J. Chem. Phys. **6**, 908 (1938).
[26] H. A. Bethe and C. L. Critchfield, Phys. Rev. **54**, 248 (1938).

Short-Lived Radioactivities Induced in Fluorine, Sodium and Magnesium by High Energy Protons

M. G. WHITE, L. A. DELSASSO, J. G. FOX, AND E. C. CREUTZ
Palmer Physical Laboratory, Princeton University, Princeton, New Jersey

(Received July 20, 1939)

On the basis of simple theoretical considerations it is expected that short-lived positron emitters should be produced in fluorine, sodium, and magnesium under bombardment with 6-Mev protons. These activities have been found and ascribed to Ne^{19}, Mg^{23}, and $Al^{25, 26}$. Half-lives, positron spectra and threshold investigations have been made and found to compare very well with the theory. It is concluded that for isobars of the type $(n-p)=\pm 1$ the difference in binding energy is due solely to the effect of Coulomb forces up to at least mass number 25. The half-lives are found to depend on the inverse fifth power of the upper limit of the positron spectra in agreement with the theory.

I. INTRODUCTION

THE theoretical determination of nuclear binding energies is at present difficult because little is known about the exact character of the forces involved, and because of the many-body nature of the problem. By assuming equality of $n-n$ and $p-p$ interactions there results a great simplification in the calculations. In particular, for isobars formed by the interchange of all the protons and neutrons we are led to expect that almost[1] the entire difference in binding energy is due to Coulomb forces alone.[2] The assumption that neutrons and protons interact in the same way has been amply verified by recent binding energy calculations.[3] Several authors[4] have made binding energy calculations on this basis for isobars of the type ${}_4Be^7-{}_3Li^7$, ${}_5B^9-{}_4Be^9$, ${}_6C^{11}-{}_5B^{11}$, etc., which are characterized by $(n-p)=\pm 1$, i.e., the number of protons and neutrons differ by one. Positron emission by the heavier member of the pair then results in an interchange in the number of protons and neutrons, and the difference in binding energy may be attributed to Coulomb forces.

It is possible to calculate the classical electrostatic difference in energy if we make the simplifying assumption of a uniform distribution of charge throughout a volume which is proportional to the mass number. Barkas,[5] using Wigner's[6] formula, has determined the empirical value of the constant necessary to express the Coulomb energy as a function of the mass number. According to this work the Coulomb energy is given by $\Delta E=0.594(A-1)A^{-\frac{1}{3}}$ Mev where A is the mass number.

Comparison with experiment may be made by observing the upper limit of positron spectra of isobars of the above type, for the difference in binding energy is given by

$$\Delta E=E_{max}{}^{+}+2e+(n-H).$$

Here $E_{max}{}^{+}$ is the upper limit of the positron spectrum, and e, n, H are the masses of the electron, neutron and hydrogen atom, respectively. If positron emission always leads to an excited state it is of course necessary to add this excitation energy to $E_{max}{}^{+}$.

Data prior to this paper have been thoroughly examined by various authors[7] who concluded that up to F^{17} the agreement between theory and experiment is surprisingly good. However, Si^{27}, formed by $Mg^{24}(\alpha, n)Si^{27}$, has a reported upper limit which ranges from 2 to 2.7 Mev and the expected upper limit is nearly 3.4 Mev. Between F^{17} and Si^{27} there were no reported activities

[1] A small correction arises from the slightly higher kinetic energy of the particles in the lighter member of the isobaric pair.
[2] W. Heisenberg, Zeits. f. Physik **77**, 1 (1932).
[3] E. Feenberg and E. Wigner, Phys. Rev. **51**, 95 (1937); W. Barkas, Phys. Rev. **55**, 691 (1939).
[4] H. A. Bethe, Phys. Rev. **54**, 436 (1938); E. Feenberg and J. Knipp, Phys. Rev. **48**, 906 (1935); S. Share, Phys. Rev. **50**, 488 (1936); H. Brown and D. Inglis, Phys. Rev. **55**, 1182 (1939); W. A. Fowler, L. A. Delsasso and C. C. Lauritsen, Phys. Rev. **49**, 561 (1936).
[5] W. Barkas, Phys. Rev. **55**, 694 (1939).
[6] E. Wigner, Phys. Rev. **51**, 947 (1937).
[7] See references 3 and 4 in particular.

although Ne^{19}, Na^{21}, Mg^{23}, and Al^{25} should be easily formed by p, n reactions if the bombarding energy exceeds the reaction threshold.[8] It is clearly of importance to fill up this gap in order to determine where these simple and apparently reasonable considerations begin to break down, if indeed they do. Assuming the applicability of the electrostatic energy formula we are led to expect an upper limit of 2.20, 2.79, and 3.07 Mev for Ne^{19}, Mg^{23}, and Al^{25}, respectively.

Nordheim and Yost[9] first pointed out that the absolute magnitude of the half-life could be predicted on the basis of the Fermi theory of β-decay. If one assumes that the positron transition is between ground states it is found that the half-life varies as $(E_{max}{}^{+})^{-5}$. By extrapolation from F^{17}, O^{15}, N^{13}, C^{11} we expect the Ne^{19}, Mg^{23}, Al^{25} half-lives to be about 40, 12 and 8 sec., respectively. Wigner[10] has considered in detail the influence on the half-life of the possible transitions to excited states. He finds that for nuclei of this type the simple E^{-5} power dependence gives a fairly accurate representation of the data.

Production of these nuclei by $F^{19}(p, n)Ne^{19}$, $Na^{23}(p, n)Mg^{23}$, $Mg^{25}(p, n)Al^{25}$ reactions can take place only if the bombarding energy exceeds the value given by

$$E_p=(E_{max}{}^{+}+2e+n-H)\frac{(A+1)}{A},$$

where E_p is the bombarding energy, A is the atomic weight of the bombarded nucleus and the factor $(A+1)/A$ takes care of recoil. We have again assumed that $E_{max}{}^{+}$ corresponds to ground state transitions. The expected thresholds for these reactions are then 4.18, 4.78 and 5.06 Mev in the order given above. It is to be noted that threshold determinations give an independent measurement of the binding energy difference.[11]

We have looked for and found the expected activities. The remainder of this paper will be devoted to a discussion of the experimental data and their interpretation in the light of these considerations.

II. Experimental Procedure

Targets of compounds or pure elements were bombarded by protons with a maximum energy of 6.0 Mev and the resulting activity observed with a Lauritsen electroscope. Because of the short half-lives of the activities under investigation it was necessary to bombard outside the cyclotron so that targets could be quickly removed to the electroscope. An atmosphere of hydrogen surrounding the target was found important in order to avoid strong contamination activities arising from oxygen and nitrogen[12] in the air. To facilitate rapid measurements a moving tape chronograph was actuated by the observer as the fiber shadow moved across the divided scale. Observations could be started within 5 seconds after cessation of bombardment. Electroscope characteristics such as non-linearity, lack of saturation at high ion densities, and polarization of the amber insulating post were investigated and corrected for in the final results. With a standard uranium β-ray source it was found that 1.2×10^{4} disintegrations were required to produce a drift of one division.

Positron spectra and upper limits were secured by photographing tracks in a hydrogen-filled Wilson chamber situated in a magnetic field of 600 gauss constant to one percent over the chamber area. Although considerable care was exercised in measuring the field it is probably not accurate to better than one percent in absolute magnitude. Positrons entered the chamber through a 0.002″ copper window which formed part of a brass well let into the chamber top. In order to obtain several expansions per target bombardment, and still avoid an excess of tracks in the early expansions, a variable aperture lead slit was incorporated in the chamber well.

[8] Professor L. A. DuBridge has informed the authors that the Rochester group has produced a short period in sodium by proton bombardment.

[9] L. W. Nordheim and F. L. Yost, Phys. Rev. **51**, 942 (1937).

[10] E. Wigner, Phys. Rev. this issue.

[11] Even in the event that positron decay is always to an excited state the threshold determination provides a value of the binding energy difference. In view of the difficulty of securing gamma-ray energies the threshold measurement provides the most precise method of getting binding energy differences.

[12] Nitrogen has been investigated in this laboratory and found to yield a strong 20-min. C^{11} activity which is ascribed to $N^{14}(p, \alpha)C^{11}$. See W. Barkas, Phys. Rev. **56**, 287 (1939). This activity undoubtedly explains the 20-min. period earlier found in magnesium and reported by Ridenour, Delsasso, White and Sherr in Phys. Rev. **53**, 770 (1938).

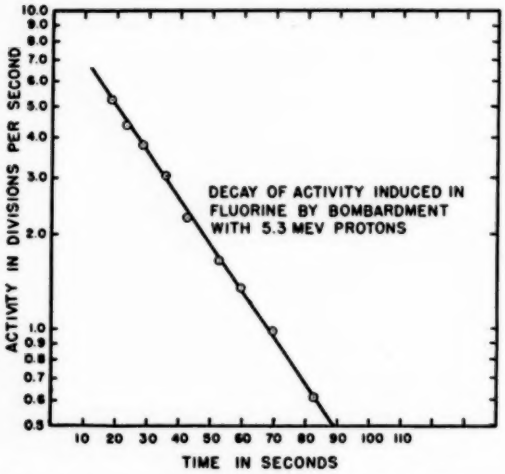
ACTIVITY IN DIVISIONS PER SECOND
DECAY OF ACTIVITY INDUCED IN FLUORINE BY BOMBARDMENT WITH 5.3 MEV PROTONS
TIME IN SECONDS

FIG. 1. Decay curve of Ne^{19}. Half-life 20.3 ± 0.5 sec.

Measurement of track curvature was carried out by the customary method of reprojection. Care was taken to exclude from the measurements all scattered tracks and tracks too short to permit accurate curvature determinations.

III. Activities Investigated

Ne^{19}

Half-life.—We have already briefly reported[13] on the production of Ne^{19} by proton bombardment of fluorine compounds. Targets were prepared by melting a layer of lead fluoride on a backing strip of tantalum; lead and tantalum having previously shown no appreciable activity under bombardment with protons of this energy. In Fig. 1 is shown a typical decay curve for the radioactive neon resulting from a 1-min. bombardment of PbF_2. There is apparently only a single period and the mean value of several runs was found to be 20.3 ± 0.5 sec.

Absorption measurements.—An attempt was made to secure the absorption curve of the emitted particles by using two electroscopes simultaneously. One electroscope was arranged to measure particles emerging from the back side of the target, and the other electroscope measured the activity from the front side after the particles had passed through a known thickness of aluminum. The ratio of these two observations at various absorber thicknesses is then a measure of the relative number of particles able to penetrate the aluminum absorbers. Since the first electroscope served merely as a monitor it was not necessary to know anything about the target thickness nor the stopping power of the tantalum. Complete decay curves were taken for every absorber and frequent checks were made on the relative efficiencies of the two electroscopes. Fig. 2 shows the resulting absorption curve, and though no precision is claimed it is clear that two conclusions may be drawn. First, that from Feather's[14] most recent mass-range expression the energy of the particles is about 2.3 Mev, and second, that there are no detectable gamma-rays except the annihilation radiation from the positrons. The latter conclusion may be inferred from the fact that after all the positrons were absorbed out there still remained a background of about 1.8 percent. This amount of residual ionization is interpreted as due to the positron annihilation radiation, for in the case of Zn^{63} about the same background was ob-

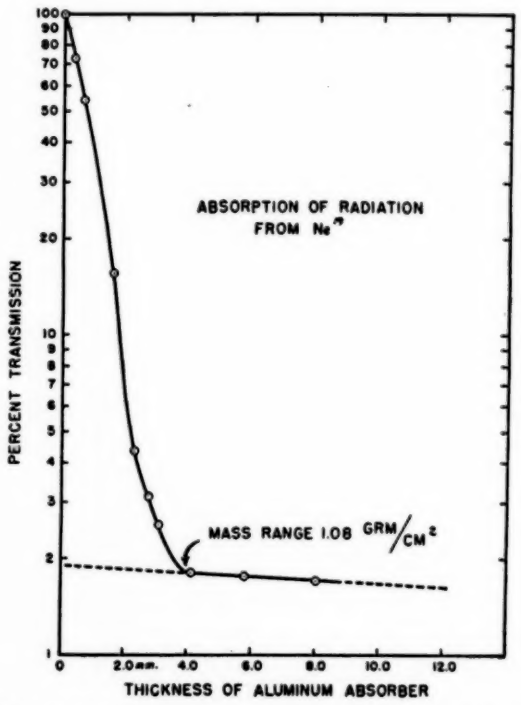

FIG. 2. Absorption curve of positrons and annihilation radiation from Ne^{19}. Upper limit of positrons as indicated by mass range is about 2.3 Mev.

[13] J. G. Fox, E. C. Creutz, M. G. White, L. A. Delsasso, Phys. Rev. **55**, 1106 (1939).

[14] N. Feather, Proc. Camb. Phil. Soc. **34**, 599 (1938).

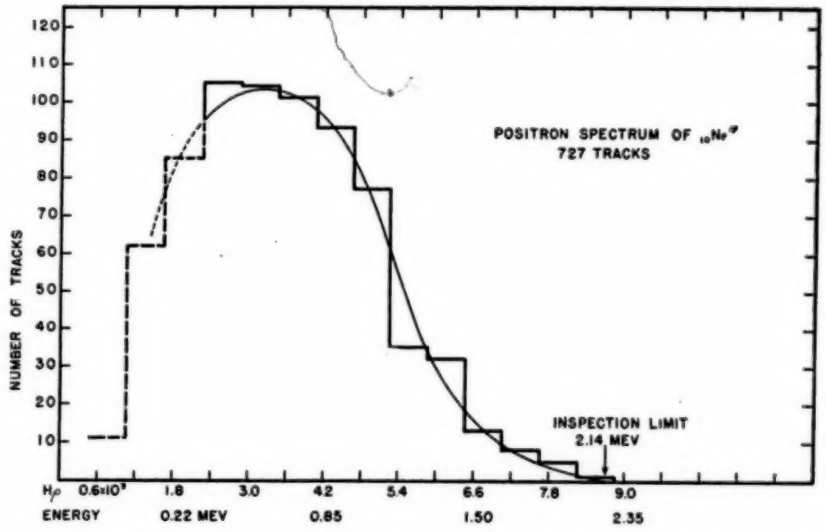
POSITRON SPECTRUM OF $_{10}Ne^{19}$
727 TRACKS
NUMBER OF TRACKS
INSPECTION LIMIT
2.14 MEV
Hρ 0.6×10³ 1.8 3.0 4.2 5.4 6.6 7.8 9.0
ENERGY 0.22 MEV 0.85 1.50 2.35

FIG. 3. Positron spectrum of Ne^{19}. Upper limit after foil correction is 2.20 Mev.

tained[15] and it was possible to show that the slope of the gamma-ray absorption curve corresponded to the expected annihilation energy. Obviously it is not possible to assert the complete absence of gamma-rays, but if *every* positron decayed to an excited state this would result in approximately 50 percent more background than that actually observed.

Positron spectrum.—Absorption measurements of electron energies are, in general, not reliable, for the degree of accuracy obtained depends on very careful observations near the endpoint where the intensity is low. Feather[14] has described a procedure for improving the determination of the mass range, but it was felt that more reliance could be placed in a cloud chamber investigation of the spectrum. We accordingly took about one thousand cloud chamber pictures with the resulting spectrum shown in Fig. 3. To reduce the chance of building up a long period contamination activity a large number of targets was employed. Although the shape of the spectrum is of considerable interest to the theory of β-decay we were chiefly concerned with the high energy end, and consequently the low energy portion was not accurately determined. Dotted lines indicate the regions of doubtful precision. By inspection the upper limit of the Ne^{19} spectrum was found to be 2.14 Mev, to which must be added 0.06 Mev lost in the copper window. The final upper limit of 2.20 Mev is thus seen to be in excellent accord with the expected value of 2.2 Mev.

In all this discussion we have assumed that the activity can only be ascribed to the production of Ne^{19}, for all other reactions involving the emission of heavy particles or gamma-rays lead either to stable isotopes or known activities of quite different periods.

Long periods in fluorine.—A one-hour bombardment of NaF with one microampere of 4.5-Mev protons gave weak 10-min. and 106-min. periods which are very probably contamination activities arising from traces of oxygen and carbon in the target. No attempt has been made to verify chemically this assumption.

Threshold determination.—Under ideal circumstances of a monochromatic proton beam and thin targets the measurement of the reaction threshold should provide a very accurate means of determining the difference in binding energy. However, the large spread in beam energy due to the cyclotron makes such an investigation difficult. A rough excitation curve was obtained by placing a PbF_2 target in the proton beam at various points along its path in air. After bombarding for a known time the target was removed and the activity measured with an electroscope. The curve of activity *versus* energy showed the steep rise characteristic of p, n

[15] L. A. Delsasso, L. N. Ridenour, R. Sherr and M. G. White, Phys. Rev. **55**, 113 (1939).

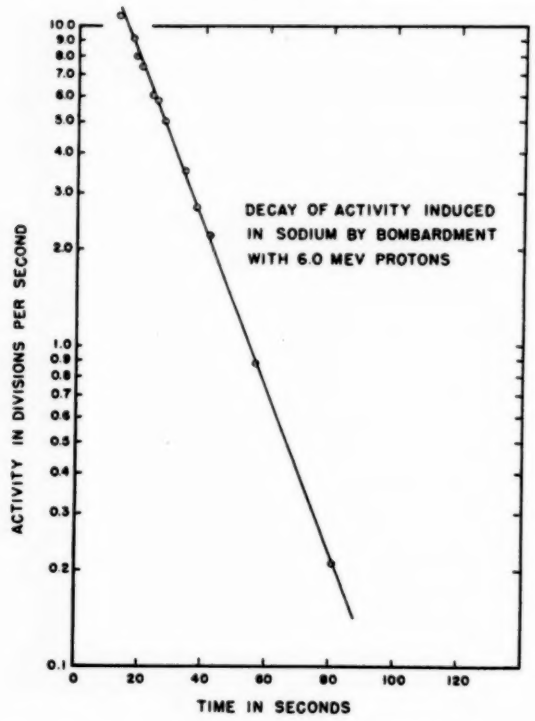
DECAY OF ACTIVITY INDUCED
IN SODIUM BY BOMBARDMENT
WITH 6.0 MEV PROTONS
ACTIVITY IN DIVISIONS PER SECOND
TIME IN SECONDS

FIG. 4. Decay curve of Mg^{23}. Half-life 11.6±0.3 sec.

reactions and the threshold was within ±0.25 Mev of the expected value of 4.18 Mev.

Mg^{23}

Half-life.—A short description of Mg^{23} was given at the Princeton meeting of the Physical Society.[16] Since that time more data have been collected and more accurate values for the upper limit and half-life obtained. Sodium, in the form of NaCl, was bombarded for one minute with 6.0-Mev protons. A characteristic decay curve is shown in Fig. 4. The half-life, as found by averaging several runs, is 11.6±0.5 sec. We assume that the activity indicates the production of Mg^{23}, for all other possible reactions lead either to stable isotopes or well-known long periods. In a separate experiment $PbCl_2$ was found to yield no short periods when bombarded under the same conditions as the NaCl.

Positron spectrum.—In order to obtain the spectrum it was necessary to make over one thousand bombardments. To minimize the building up of long period contamination activities the targets were carefully scraped before each fresh bombardment. In Fig. 5 is shown the resulting spectrum. An upper limit of 2.82 Mev was found after correcting for absorption in the copper window. This is seen to agree very well indeed with the expected value of 2.79 Mev. As in the case of Ne^{19} we were largely concerned with the upper limit and consequently little attention was paid to the lower part of the spectrum.

Gamma-rays.—It is important to investigate the possible presence of gamma-rays before

[16] E. C. Creutz, M. G. White, L. A. Delasso and J. G. Fox, Phys. Rev. **56**, 207(A) (1939).

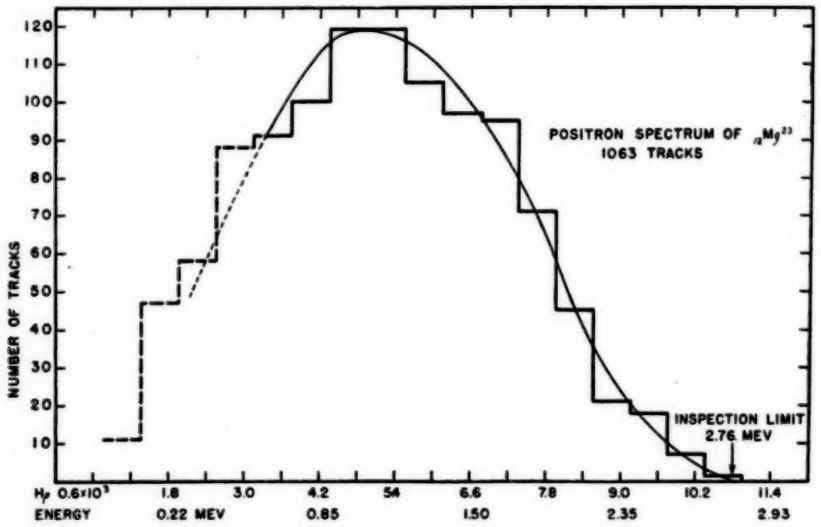

FIG. 5. Positron spectrum of Mg^{23}. Upper limit 2.82 Mev after foil correction.

assuming that the upper limit of the positron spectrum actually gives the difference in binding energy. A complete absorption curve would greatly aid in this decision, but unfortunately the short half-life makes such measurements difficult. We have accordingly limited the absorption measurements to just one thickness of absorber, the technique employed being the same as that described for Ne^{19}. When 1.25 cm of aluminum was interposed between target and electroscope the transmitted activity was found to be only 1.8 percent, from which we conclude, as in the case of Ne^{19}, that there are no detectable gamma-rays other than the annihilation radiation.

Threshold determination.—Difficulties attendant on securing the dependence of activity on bombarding energy have already been discussed for Ne^{19}. The shorter half-life of the radioactive magnesium makes such measurements even more troublesome; so the best that could be done was to insert aluminum foils in the path of the protons until no more activity was observed. We concluded that the activity disappeared at a proton energy within ± 0.3 Mev of the expected threshold of 4.78 Mev.

Long periods.—A search for long periods gave a negative result. We bombarded sodium metal in vacuum for 20 min. with 0.4 microampere of 5.5-Mev protons and found a fairly strong 20-min. activity. Further work with NaCl and nitrogen has convinced us that this period was due to $N^{14}(p, \alpha)C^{11}$ which arose from the nitrogen taken up by the sodium metal.

$Al^{25, 26}$

Half-life.—The study of Al^{25} which may be formed by the reaction $Mg^{25}(p, n)Al^{25}$ is complicated by the possibility of forming Al^{26} in the reaction $Mg^{26}(p, n)Al^{26}$. Frisch[17] was the first to report the production of Al^{26} by the reaction $Na^{23}(\alpha, n)Al^{26}$ and gave the half-life as 7 sec. Since sodium has but one isotope there is little doubt that his assignment is correct, especially in view of the detection of the emitted neutrons by Savel.[18] We have bombarded magnesium metal of commercial purity with 6.0-Mev protons and obtained the decay curve shown in Fig. 6. From the average of several runs we find the half-life to be 7.0 ± 0.5 sec. Although the decay curve seems to be simple, it cannot be determined whether two periods of nearly the same value are actually present, and it is impossible definitely to assign the activity.

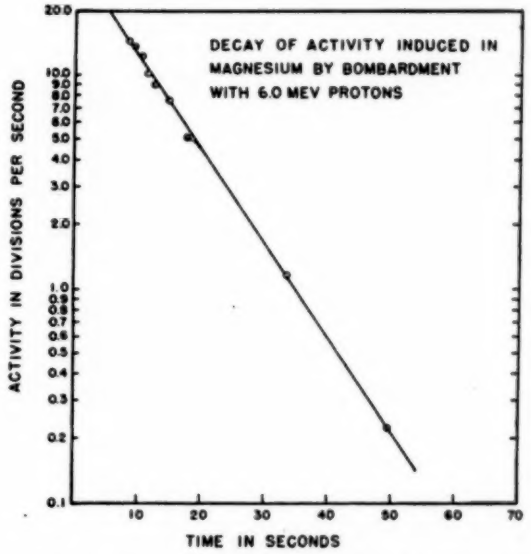

FIG. 6. Decay curve of activity induced in magnesium metal by 1-min. bombardment with protons of 6.0-Mev energy.

Positron spectrum.—Frisch[17] and Brandt,[19] using the absorption method, determined the upper limit of Al^{26} to be 1.8 and 1.5 Mev, respectively. As this value is far from the expected Al^{25} value of 3.07 Mev it was hoped that a study of the positron spectrum arising from our 7-sec. activity would help decide the question of isotope assignment. From Fig. 7 it is seen that the upper limit of the 7-sec. period induced by protons on magnesium is 2.99 Mev. This value compares very favorably with the expected Al^{25} upper limit of 3.07 Mev, and is in strong disagreement with the Al^{26} limit quoted above. Unfortunately little reliance is to be placed on absorption determinations; so we can not exclude the possibility that a large fraction of the spectrum near the upper end is due to Al^{26}. If one takes the absorption measurements at their face value it is clear that the high energy end of Fig. 7 can be ascribed to Al^{25}, and the low energy end to Al^{26}. Difficulties in measuring low energy positrons with a magnetic field adjusted for the high energy tail make uncertain any attempted

[17] O. Frisch, Nature **133**, 721 (1934).
[18] M. P. Savel, Comptes rendus **198**, 1404 (1934).
[19] H. Brandt, Zeits. f. Physik **108**, 726 (1938).

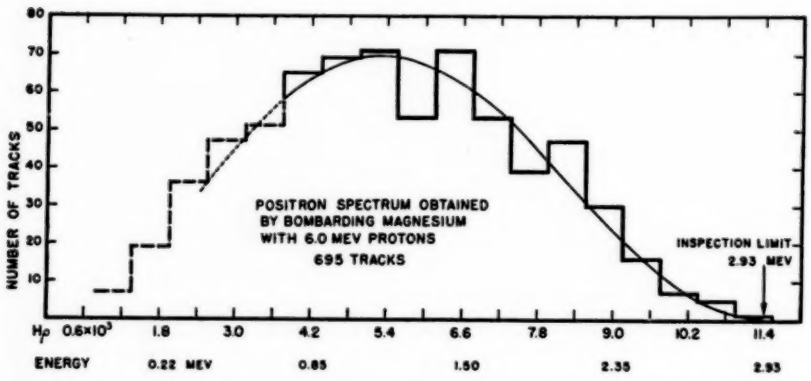

FIG. 7. Positron spectrum of activity induced in magnesium metal by 6.0-Mev protons. Upper limit after foil correction is 2.99 Mev.

resolution of the curve into two components. Nevertheless the shape of the curve does not indicate a decided preponderance of low energy positrons.

Threshold.—On theoretical grounds[3, 4] it is quite certain that the $Mg^{26}-Al^{26}$ binding energy difference is only a little less than that for $Mg^{25}-Al^{25}$, and there seems no reason to suppose that both activities are not present in the decay curve and in the spectrum. On the other hand, Al^{24} certainly cannot be formed at our energies from Mg^{24} if the threshold is actually 13 Mev as deduced from Barkas' table of computed masses. Actual threshold measurements indicate that there is no detectable activity below 5 Mev, in agreement with the expected Al^{25} threshold of about 4.5–5 Mev, and we must therefore conclude that the reported upper limit of Al^{26} is in error. Another alternative is to assume that Al^{26} always decays to an excited state about 1.2 Mev above the ground level. This would, however, not be in accord with the short half-life.

IV. DISCUSSION

Our measurements indicate that up to mass 23 and possibly even 25 the simple picture discussed at the beginning of this paper is able to account for the binding energy differences of isobars of the type $(n-p)=\pm 1$. Deviations might have been expected if shell structure plays an important role in determining the size of the nucleus, but apparently such effects are not important. The further conclusion may be drawn that there is no appreciable swelling of the nucleus because of Coulomb forces. The work also gives additional support to the hypothesis of equal $n-n$ and $p-p$ interactions.

From the half-life measurements and their comparison with the values as predicted on the basis of the Fermi theory it seems evident that in general for light elements the inverse fifth power dependence of half-life on energy gives a reasonably good description of the facts.

V. ACKNOWLEDGMENTS

It is a pleasure to thank Professor Wigner for pointing out the interest in this problem and for many discussions on the theoretical questions involved. The assistance of Dr. Barkas in making some of the measurements is also appreciated.

On Coupling Conditions in Light Nuclei and the Lifetimes of β-Radioactivities

E. P. WIGNER
Princeton University, Princeton, New Jersey

(Received July 19, 1939)

Two series of β-activities are considered. The first series involves nuclei in which the number n_p of protons exceeds the number n_n of neutrons by 1. The second series involves the nuclei for which $n_p = n_n$ is odd. Similarly two coupling conditions are considered: in approximation 1, the forces do not depend on either ordinary or isotopic spin. In approximation 2 only the independence of isotopic spin is assumed. Apart from these coupling conditions, no use is made of any special model. The lifetimes of the disintegrations of the first series can be calculated on the basis of either coupling condition if one adopts Fermi's original theory. The transitions of the second series are forbidden in this theory. If one adopts the modification of Fermi's theory which has been proposed by Gamow and Teller, one can calculate the lifetimes for both series assuming the validity of the first approximation but this cannot be done if only the validity of the second approximation is assumed. The discussion of the experimental data indicates that the 1st approximation applies quite well for the normal states of nuclei up to a mass of about 30.

1

NORDHEIM and Yost[1] were the first to point out that the absolute magnitude (not only the order of magnitude) of the lifetime of certain β-radioactive elements can be predicted on the basis of Fermi's theory.[2] The transitions they considered were between nuclei in which the number of protons and neutrons differed by ± 1.

The work of Nordheim and Yost was founded on the original formulation of Fermi's theory in which the spin does not change in allowed transitions. Gamow and Teller[3] have pointed out that Fermi's ideas allow another formulation in which the spin change is ± 1 or 0 for these transitions. Breit and Knipp[4] found evidence in the $Be^7 \rightarrow Li^7$ transformation confirming the selection rules of Gamow and Teller. Grönblom[5] considered the β-activities of He^6 and of the elements which were the subjects of Nordheim and Yost's investigation from this point of view. Using Hartree's approximation for the wave functions, he found in all these cases that the β-spectrum should be composite (excepting the case of He^6 where it should be simple). This was in agreement with the hypothesis put forward by Bethe, Hoyle and Peierls[6] who attempted to explain the deviation of the observed energy distribution of the β-rays from the distribution following from Fermi's theory by postulating a composite nature for all transitions in which the energy distribution has been observed so far. For the elements considered in Grönblom's work the intensity formulas derived here are identical with Grönblom's. It is shown, however, that the assumption of a spin independent Hamiltonian, and only this, is necessary for the validity of these formulas.

The experimental information already used by Nordheim and Yost, together with similar data on disintegrations involving elements in which the number of protons is odd and equal to the number of neutrons, will be used in the present paper to determine the amount of deviation from Russell-Saunders coupling and from the inaccuracy of wave functions obtained by using a symmetric Hamiltonian.[7] The former question has become particularly important lately for three reasons. First, the discovery of the quadripole moment of the deuteron[8] made it evident that, at least in this case, the deviation from Russell-Saunders coupling cannot be neglected. The work of Way[9] on the interpretation of magnetic and quadripole moments of heavy elements points strongly in the same direction.

[1] L. W. Nordheim and F. L. Yost, Phys. Rev. **51**, 943 (1937).
[2] E. Fermi, Zeits. f. Physik **60**, 320 (1934).
[3] G. Gamow and E. Teller, Phys. Rev. **49**, 895 (1936).
[4] G. Breit and J. K. Knipp, Phys. Rev. **54**, 652 (1938).
[5] B. O. Grönblom, Phys. Rev. **56**, 508 (1939).
[6] H. A. Bethe, F. Hoyle and R. Peierls, Nature **143**, 200 (1939). Kikuchi, Watase, Itoh, Takeda, Yamaguchi, Proc. Phys. Math. Soc. Japan **21**, 52 (1939). See also A. I. Alichanian and V. Berestezky, Phys. Rev. **55**, 978 (1939).
[7] G. Breit and E. Feenberg, Phys. Rev. **50**, 850 (1936).
[8] J. M. B. Kellogg, I. I. Rabi, N. F. Ramsey, Jr., and J. R. Zacharias, Phys. Rev. **55**, 318 (1939).
[9] K. Way, Phys. Rev. **55**, 963 (1939).

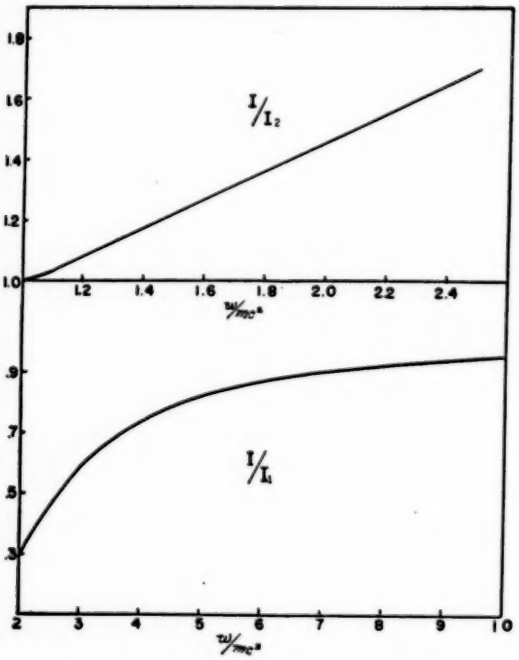

FIG. 1. Correction factors for the approximate formulas (2) for Fermi's function $I(w)$ of (1a).

Finally, the meson theory of nuclear forces[10] yields a Hamiltonian on the basis of which the Russell-Saunders coupling cannot be expected to be valid in nuclei. On the other hand, Barkas' work[11] shows that one can successfully systematize the mass defects of the lighter elements by using a picture on the basis of which one would expect the above-mentioned simple coupling conditions to be prevalent in these nuclei.

2

We shall use for our calculations the formalism[12] which has been employed before by Breit and Knipp.[4] The transition probability λ_{if} is given[13] in Fermi's theory by

$$\lambda_{if}=GI(w), \tag{1}$$

$$I(w)=(w^2-1)^{\frac{1}{2}}(w^4/30-3w^2/20-2/15) +\tfrac{1}{4}w\ln(w+(w^2-1)^{\frac{1}{2}}), \tag{1a}$$

where $w=1+\epsilon_l/mc^2$ with m the electronic mass and ϵ_l the upper limit of the energy of the emitted β-ray. One can represent (1a) for large and small w, respectively, by the formulas

$$I_1(w)=w^5/30, \tag{2}$$
$$I_2(w)=(16\sqrt{2}/105)(w-1)^{7/2}=0.215(w-1)^{3.5},$$

and the correction factors I/I_1 and I/I_2 are plotted in Fig. 1. The G is given, in Fermi's original theory by $G_0=g_0^2f_0$ where

$$f_0=|(\psi_f, \tfrac{1}{2}(\tau_{\eta 1}+\tau_{\eta 2}+\cdots+\tau_{\eta n})\psi_i)|^2. \tag{3a}$$

Here, g_0 is the interaction constant in Fermi's theory, ψ_i and ψ_f the wave functions of the disintegrating and product nuclei in the formalism using isotopic spin.[14] The $\tau_{\eta i}$ are the same operators as the $s_{\nu i}$, acting, however, on the isotopic spin coordinate τ_i instead of the ordinary spin coordinate σ_i. In the formulation of Gamow and Teller,[3] there are, in addition to G_0 three other terms of the character $g_1^2f_x$ where

$$f_x=|(\psi_f, \tfrac{1}{2}(\tau_{\eta 1}s_{x1}+\tau_{\eta 2}s_{x2}+\cdots +\tau_{\eta n}s_{xn})\psi_i)|^2. \tag{3b}$$

The G of (1) is then given by

$$G=g_0^2f_0+g_1^2f_1=g_0^2f_0+g_1^2(f_x+f_y+f_z). \tag{4}$$

The decay constant λ_i of the state ψ_i is, of course, $\Sigma_f\lambda_{if}$.

The form (1a) is characteristic for Fermi's theory.[15] In most of the following applications $I_1(w)$ could be substituted for $I(w)$ without greatly affecting the conclusions.

Clearly, (4) is only an approximate expression for G, valid, according to Fermi, if the dimension of the nucleus is very much smaller than the wave-length of the emitted β-particle and neutrino. If this is not the case, additional terms will enter, in analogy to the terms corresponding to the quadripole etc. radiation in ordinary light emission.[16] The three terms (3b) can be thought of as corresponding to polarizations of

[10] H. Fröhlich, W. Heitler and N. Kemmer, Proc. Roy. Soc. **A166**, 154 (1939). H. J. Bhabha, Proc. Roy. Soc. **A166**, 501 (1938). N. Kemmer, Proc. Camb. Phil. Soc. **34**, 354 (1938). H. A. Bethe, Phys. Rev. **55**, 1261 (1939).
[11] W. H. Barkas, Phys. Rev. **55**, 691 (1939).
[12] E. Wigner, Phys. Rev. **51**, 106, 947 (1937).
[13] Cf. reference 2 and E. J. Konopinski and G. E. Uhlenbeck, Phys. Rev. **48**, 7 (1935).
[14] W. Heisenberg, Zeits. f. Physik **77**, 1 (1932). J. H. Bartlett, Phys. Rev. **49**, 102 (1936). W. Elsasser, J. de phys. et rad. **7**, 312 (1936). B. Cassen and E. U. Condon, Phys. Rev. **50**, 846 (1936) and reference 12.
[15] G. E. Uhlenbeck and S. Goudsmit have shown that (1a) is the sum of statistical factors and has as simple a form as can be expected. For modifications of (1a), due to the Coulomb field, cf. reference 13.
[16] Cf. F. Hoyle, Proc. Roy. Soc. **A166**, 249 (1939).

the electron neutrino field in the X, Y and Z directions. The term (3a) would correspond to the emission of a scalar (longitudinal) wave.

It should be mentioned, perhaps, in this connection that the operators of (3a) and (3b) are both even and thus correspond to the β-particle and neutrino being emitted in the $^1S_0$ and $^3S_1$ states, respectively. Making use of a four-valued spin for the heavy particles, operators can be found, which—though not involving the space coordinates,—have an odd character and correspond to the electron-neutrino pair to be emitted in P states. In the case of such an interaction one would obtain in the approximation in which the nuclear dimension can be neglected only transitions from even to odd terms, and conversely. In the present theory one has, in the same approximation, only transitions without change of parity. Operators of the above-mentioned character would give no β-decay for a free neutron and the β-decay would, in general, depend on relativistic effects and on the part of the wave function which corresponds to negative kinetic energies.

3

We shall consider, first of all, the matrix elements (3a) and (3b) from the point of view of the "first approximation" of reference 12. In this approximation, the ordinary spin and isotopic spin variables play the same role which the spin variables play in the theory of atomic spectra, assuming Russell-Saunders coupling. The matrix elements (3a) and (3b) can be calculated under these conditions without making further special assumptions about the wave functions, just as, for instance, the Zeeman splitting can be calculated in the corresponding theory of atomic spectra. The operators

$$T_\eta = \tfrac{1}{2}(\tau_{\eta 1}+\tau_{\eta 2}+\cdots+\tau_{\eta n}) = \tfrac{1}{2}\sum_k \tau_{\eta k}, \quad (5a)$$

$$Y_{\eta x} = \tfrac{1}{2}\sum \tau_{\eta k} S_{xk}; \quad Y_{\eta y} = \tfrac{1}{2}\sum \tau_{nk} S_{yk}; \quad Y_{\eta z} = \tfrac{1}{2}\sum \tau_{\eta k} S_{zk}, \quad (5b)$$

are infinitesimal operators of rotation acting in the four-dimensional unitary space of the σ, τ just as the S_x, S_y, S_z were infinitesimal operators of rotation acting in the two-dimensional space of the σ alone. It follows from this, first of all, that only transitions between the "fine structure components" of a multiplet are "allowed," transitions between different multiplets always "forbidden," both for the Fermi and the Gamow-Teller matrix elements.

Since, in general, the initial state of a β-transition is the lowest state of that element, it is, according to Fig. 4, reference 12, the term of a multiplet which has the largest possible $T_\zeta = \frac{1}{2}(n_n - n_p)$ for that multiplet.[17] The reason for this is that the energy of a multiplet, in general, increases with increasing value of the largest T_ζ of that multiplet so that the lowest term of any element belongs to a multiplet, the largest T_ζ of which is as small as possible, i.e., equal to the T_ζ of the element in question. If the element makes a β-transition, T_ζ will change; if it increases (positron emission) the transition will naturally go to another multiplet. If T_ζ is decreased by the transition, this could lead to another component of the same multiplet —were it not that all other components have higher energies, the energy decreasing with increasing T_ζ within a multiplet on account of the Coulomb energy. These conditions are represented in Fig. 2, which is a partial reproduction of Fig. 4, reference 12. It follows from this that

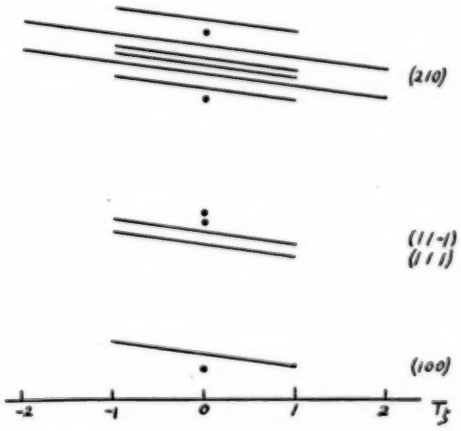

FIG. 2. The energy of a $(PP'P'')$ (numbers at right) multiplet increases with increasing P. The P is the highest T_ζ occurring in the multiplet. Within the multiplet the energy decreases with increasing T_ζ. Every multiplet is the lowest for $T_\zeta = P$ and $T_\zeta = -P$, only (100) is the lowest for all three T_ζ, *viz.* -1, 0, 1.

[17] The largest T_ζ of a multiplet is the P of the $(PP'P'')$ symbol of the multiplet. The $(PP'P'')$ symbol is defined in the papers of reference 12 where it is denoted by (STY). The term multiplet (without qualification) is used in the present paper for a $(PP'P'')$ "supermultiplet."

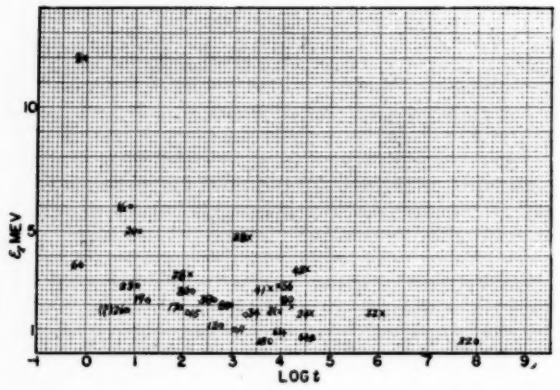

FIG. 3. Energy *vs.* $\log_{10}$ of lifetime for light nuclei. Small circles represent disintegrations considered in the present paper, + positron emitters, × electron emitters.

practically all β-transitions are "forbidden" transitions.

There are two exceptions to this: the lowest states of elements with negative T_z belong to multiplets the highest T_z of which is $|T_z|$. The elements $T_z=-\frac{1}{2}$ give the well-known series of positron emitters discussed already in reference 1. Second, the multiplet (100), occurring for nuclear masses of the form $4k+2$, is the lowest one both for the elements with $T_z=0$ and $T_z=\pm 1$. One will expect, therefore, "allowed" transitions for these elements. It is in agreement with this that for light elements only transitions involving elements of this character are on the first Sargent curve (Fig. 3). Several of the transitions occurring in heavier elements are, however, at any rate very near to this curve and we shall return to this point later.

In order to calculate the absolute value of expressions (3a) and (3b) it is simplest to calculate first

$$(\psi_i, T_\eta^2\psi_i)=\sum_f |(\psi_f, T_\eta\psi_i)|^2 \qquad (6a)$$

and

$$(\psi_i, (Y_{\eta x}^2+Y_{\eta y}^2+Y_{\eta z}^2)\psi_i = \sum_f |(\psi_f, Y_{\eta x}\psi_i)|^2+|(\psi_f, Y_{\eta y}\psi_i)|^2 + |(\psi_f, Y_{\eta z}\psi_i)|^2, \qquad (6b)$$

where f runs over all possible states. The expressions (6a), (6b) represent the sum of the G of one initial state with respect to all possible final states.

Since the T_η^2 etc. are infinitesimal operators of the unitary group of the σ, τ space, the expressions (6a) and (6b) will assume the same values for all ψ which belong to the same row of the same representation of this group. The representation of the unitary group depends only on the multiplet so that we can calculate (6a) and (6b) with a particularly simple example of that multiplet.[18] For the $(\frac{1}{2}, \frac{1}{2}, \frac{1}{2})$ multiplet we can choose a problem of one single particle. In this case $T_\eta^2=\frac{1}{4}\tau_\eta^2=\frac{1}{4}$ and similarly $Y_{\eta x}^2=Y_{\eta y}^2=Y_{\eta z}^2=\frac{1}{4}$. This holds for all wave functions of such a multiplet. Hence, in this case

$$(\psi_i, T_\eta^2\psi_i)=\tfrac{1}{4}, \qquad (7a)$$

$$(\psi_i, (Y_{\eta x}^2+Y_{\eta y}^2+Y_{\eta z}^2)\psi_i)=\tfrac{3}{4}. \qquad (7b)$$

For the multiplet $(\frac{1}{2}\frac{1}{2}-\frac{1}{2})$ which occurs for masses of the form $4k+3$ we can choose a three-particle problem in which all three particles are in equivalent s states. It follows then from the theory of holes[19] that Eq. (7a), (7b) remain valid for this multiplet also as the matrix elements for the states of the closed shell all vanish.

There are six states in the multiplet (100) and the corresponding representation of the four-dimensional unitary group is six-dimensional. The simplest example in this case contains two particles. Dropping the factor of the wave function which depends on the space coordinates, we can write for the six wave functions

$$\begin{aligned} &b_{-1}(\tau_1\tau_2)a(\sigma_1\sigma_2), \quad b_0(\tau_1\tau_2)a(\sigma_1\sigma_2), \quad b_1(\tau_1\tau_2)a(\sigma_1\sigma_2),\\ &\qquad a(\tau_1\tau_2)b_1(\sigma_1\sigma_2),\\ &\qquad a(\tau_1\tau_2)b_0(\sigma_1\sigma_2),\\ &\qquad a(\tau_1\tau_2)b_{-1}(\sigma_1\sigma_2). \end{aligned} \qquad (8)$$

Here $a(uv)$ is the wave function of the singlet state $a(u, v)=2^{-\frac{1}{2}}[(u-1)(v1)-(u1)(v-1)]$ and b_1, b_0, b_{-1} the three triplet wave functions

$$\begin{aligned} b_1(uv)&=(u1)(v1),\\ b_0(uv)&=2^{-\frac{1}{2}}[(u-1)(v1)+(u1)(v-1)],\\ b_{-1}(uv)&=(u-1)(v-1), \end{aligned}$$

where $(u-1)$ and $(u1)$ stand for δ_{u-1} and δ_{u1}, respectively. The arrangement of the wave func-

[18] Cf. E. Wigner, *Gruppentheorie* etc. (Braunschweig, 1931), p. 302.

[19] Cf. E. U. Condon and G. Shortley, *The Theory of Atomic Spectra* (Cambridge University Press, 1935), p. 284.

tions in (8) corresponds to Fig. 2. Calculating $(\psi, T_\eta^2\psi)$ for the six functions of (8), we obtain, respectively,

$$\begin{matrix} \frac{1}{2} & 1 & \frac{1}{2} \\ & 0 & \\ & 0 & \\ & 0 & \end{matrix} \qquad (9a)$$

The values of $(\psi, (Y_{\eta x}^2+Y_{\eta y}^2+Y_{\eta z}^2)\psi)$ are, in the same arrangement,

$$\begin{matrix} \frac{3}{2} & 0 & \frac{3}{2} \\ & 1 & \\ & 1 & \\ & 1 & \end{matrix} \qquad (9b)$$

It is easy now to calculate the expressions (3a), (3b) themselves by means of the ordinary theory of spectra, i.e., considering the τ as parameters. The operator T_η is a scalar-scalar operator (i.e., scalar in the space coordinates and also scalar in the ordinary spin coordinates). Hence, the selection rules are $\Delta J=0$, $\Delta L=0$, $\Delta S=0$, $\Delta m=0$. Thus only one matrix element is different from zero for any initial state in which the isotopic spin is as large as it can be for this multiplet. The square of this matrix element is $\frac{1}{4}$ in the case of the $(\frac{1}{2}\frac{1}{2}\pm\frac{1}{2})$ multiplet and $\frac{1}{2}$ in the case of the (100) multiplet. In both cases the matrix element is independent of the azimuthal quantum number. The β-spectra of the elements in which the number of protons differs by one from the number of neutrons becomes simple. Since the lowest state of the nuclei with $2k+1$ protons and $2k+1$ neutrons is assumed to be a triplet state, the β-transition between this state and the lowest state of the nucleus with $2k$ protons and $2k+2$ neutrons is forbidden because the latter is a singlet state. The allowed transitions with intensities are represented in Fig. 4(a) and 5(a) for the $(\frac{1}{2}\frac{1}{2}\pm\frac{1}{2})$ and the (100) multiplets, respectively.

On the other hand, the operators $T_{\eta x}$, $T_{\eta y}$, $T_{\eta z}$ form the components of a scalar-vector operator (scalar in space, vector in ordinary spin coordinates) and the intensities of the transitions from the different components of a spin multiplet to the different components of another spin multiplet can be computed by the well-known Hönl-Kronig intensity formulas.[20] Of course, the role of S and L has to be interchanged in these as the operator responsible for light emission is a vector in its dependence on space coordinates, while our operators are vectors in their dependence on (ordinary) spin coordinates. In case of the multiplet (100) the transitions from the $b_1(\tau_1\tau_2)a(\sigma_1\sigma_2)$ state all lead to the $a(\tau_1\tau_2)b(\sigma_1\sigma_2)$ states, none to the $b_0(\tau_1\tau_2)a(\sigma_1\sigma_2)$ states, as can be seen from the fact that according to (9b) the sum of the intensities of all transitions starting from or leading to $b_0(\tau_1\tau_2)a(\sigma_1\sigma_2)$ is zero. This allows the calculation of all intensities and these are represented in Figs. 4(b) and 5(b) and (c).

The results contained in Fig. 4(a) were given before by Breit and Knipp.

Before going over to the discussion of the "second" etc. approximation, it should be remarked that all terms of the multiplet (100), e.g., have the same energy in the "first approximation." Their splitting is due to forces which involve the ordinary and isotopic spin coordinates. The wave functions of the states with $J=L+1$ and $J=L-1$ are, for very small splitting, independent of the form of the forces involving the isotopic and ordinary spin coordinates, and this is the situation for all wave functions in case of S terms. The situation is, however, in general different for the two states with $J=L$. Fig. 5(b) and (c) is drawn in the

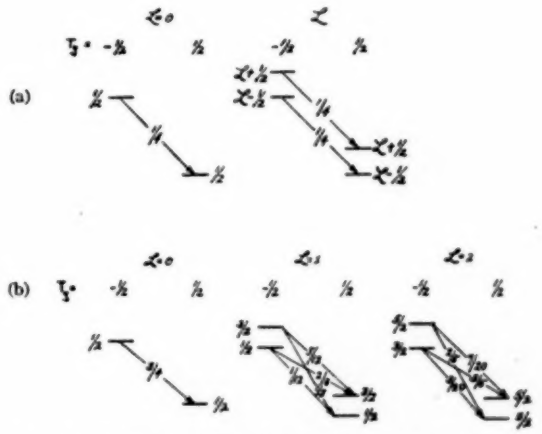

FIG. 4. (a) Value of f_0 of (3a) for multiplets $(\frac{1}{2}\frac{1}{2}\pm\frac{1}{2})$ i.e., for the stable states of elements in which the difference of the number of protons and neutrons is 1. The number at each level denotes the J value of that level. (b) Value of f_1 of (4), (3b) for the same elements. The arrangement of the levels is such that the lower J has the lower energy. This is purely arbitrary and the reverse arrangement occurs just as frequently as that used in the figure. Cf. Table II.

[20] Cf. reference 19, p. 241 or reference 18, p. 297.

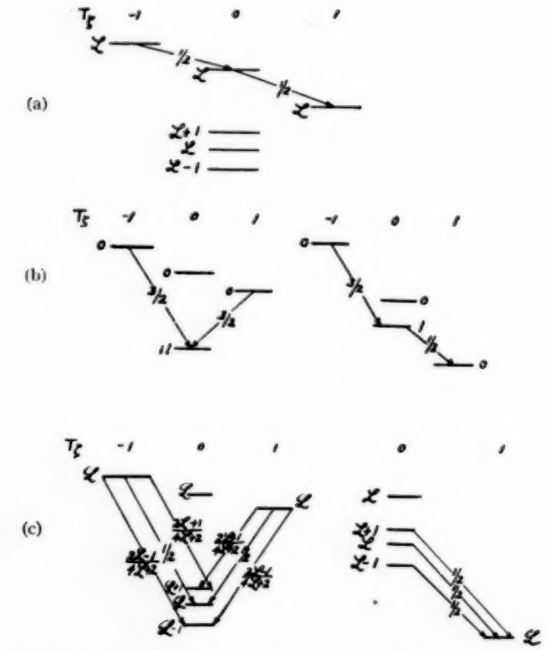

FIG. 5. (a) Allowed transitions and values of f_0 of (3*a*) for the multiplet (100). The transitions to and from the lowest state of elements with odd number of protons and neutrons is forbidden in the original theory of Fermi. (b) For S terms. Allowed transitions and values of f_1 of (3*b*) for the same elements. In the diagram at the left the odd-odd elements are the stable ones (Li^6, B^{10}, N^{14}). The diagram at the right represents the conditions at higher A where the odd-odd element ($T_\zeta=0$) is unstable. (c) For higher L. Values of f_1 of (3*b*) for the same elements as in (b), drawn, however, on the assumption that the lowest term is not an S term. The number at each level denotes the J value of that level. The arrangement of the levels is again arbitrary (cf. Fig. 4(b)). The $T_\zeta=-1$ part is omitted in the last diagram.

customary way which involves in this case the assumption that forces involving both ordinary and isotopic spin coordinates can be neglected when determining the splitting. This is, however, questionable and it is possible, therefore, that the two states with $J=L$ are actually linear combinations of triplet and singlet states.[21] The transition probabilities to these two states will be proportional to the amount of singlet wave function contained in them if Fermi's original formulation is adopted. It is proportional to the amount of triplet wave functions contained in them if the matrix elements of 5(b) are responsible for the transition.

[21] The L–S coupling is not a consequence of the first approximation, except in special cases. All terms have a definite L in this approximation but not necessarily a definite S, unless there is only one S for the corresponding element in the whole ($PP'P''$) multiplet. This is, according to the theory, always true for the lowest states (giving $S=0$ for even, $S=\frac{1}{2}$ for odd elements), with the exception mentioned in the text, *viz.* elements with odd number of protons and odd number of neutrons.

4

From the point of view of the "second approximation" (forces identical for protons and neutrons, depending, however, on ordinary spin) the matrix elements of T_η still can be calculated on the basis of general considerations[4] because T_η plays in this theory the same role which S_y plays in ordinary atomic theory. The result is, of course, the same as given in the previous section. On the other hand, the matrix elements of $Y_{\eta z}$ etc. cannot be calculated by assuming only approximation 2, and no regular relation between energy and lifetime could be expected if this operator determined the transition probabilities. In fact, the matrix elements connecting states of different multiplets would become as great as the matrix elements between states of a single multiplet. Since the sum of squares of the matrix elements between one state and all others is limited and there are very many of them, each single matrix element would become very much smaller than one would expect from the previous section. The same would hold for both operators T_η and $Y_{\eta z}$, etc., in the third and fourth approximation, i.e., if the forces affecting protons and those affecting neutrons were so different that no particular relations existed between the wave functions of isobars with different isotopic numbers. These relations are summarized in Table I. The column App. 1 is based upon the assumption that one obtains good wave functions even if one neglects all forces involving ordinary or isotopic spin coordinates, App. 2 that one can neglect only forces depending on isotopic spin coordinates. App. 3

TABLE I. *Dependence of transition probabilities under various conditions.*

		App. 1	App. 2	App. 3 or 4
$n_p-n_n=\pm1$	a	r	r	s
	b	r	s	s
$n_p-n_n=0,\ \pm2$	a	r	s	s
	b	r	s	s

refers to neglecting only ordinary spin forces and App. 4 that no such approximations are permissible. The letters a and b refer to the operators 5(a) and 5(b), the letter *r* means that the transition probabilities depend regularly on the energy, *s* means that the transition probabilities are small and their dependence on the disintegration energy shows no marked regularity.

5

Table II contains a summary of the experimental information on nuclei with a difference of one in the number of protons and neutrons ($((\frac{1}{2}\frac{1}{2}\pm\frac{1}{2})$ multiplet). The first column contains the atomic mass, the second the symbol of the lowest term, as assumed at present. The third contains in the first row the observed upper limit of the position spectrum in Mev, in the second row the calculated values for this quantity, assuming a Coulomb energy of[22] $\frac{1}{2}\times 2.35 n_p(n_p-1)A^{-\frac{1}{3}}$ mc². From this, two electron masses and the neutron-proton energy difference, i.e., 1.78 Mev, were subtracted in order to obtain the upper limit of the positron spectrum. One sees that the agreement is quite good, it is within 7 percent for the whole Coulomb energy. This shows that for the nuclei in question at any rate there is no appreciable blowing up by the electrostatic repulsion of the protons. The column I gives the values of I, given in (1a), calculated for both values of ϵ_l. The next column gives the observed half-life t in seconds, the following one 10^{-3} $It/\ln 2$ which should be a constant on assumption (3a) for the matrix element. The last column gives the product of the previous one and f_1 taken from Fig. 4(b), for the lowest state of both initial and final nucleus. This number should be a constant on assumption (3b) if there were only transitions to the lowest state of the final nucleus. Actually, a certain average of the last two columns should be taken,

TABLE II. *Summary of experimental information on nuclei with a difference of one in the number of protons and neutrons.*

A	TERM	ϵ_l	I	t	It/l	$It f_1/l$
7	$P_{\frac{1}{2}}$	<0.09		$3.72\cdot 10^6$		
		0.05?	7.10^{-5}?			
9	$P_{\frac{1}{2}}$					
		0.46?	0.21?			
11	$P_{\frac{1}{2}}$?	1.05	5.23	1230	9.3	3.90
		.87	2.49		4.45	1.85
13	$P_{\frac{1}{2}}$	1.21	9.30	630	8.45	3.50
		1.24	10.3		9.35	3.90
15	$P_{\frac{1}{2}}$	1.72	38.6	125	6.95	0.60
		1.58	28.6		5.15	0.43
17	$S_{\frac{1}{2}}$?	1.93	65.6	64?	6.05	4.55
		1.91	63.7		5.90	4.40
19	$S_{\frac{1}{2}}$	2.20	123	20.3	3.50	2.60
		2.23	123		3.60	2.70
21						
		2.49	198			
23		2.82	348	11.6	5.85	
		2.82	348		5.85	
25		2.99?				
		3.10	523			

$A=7$. Cf. reference 4. Hill and Valley, Phys. Rev. **55**, 678 (1939).
$A=11$. Bonner and Brubaker, Phys. Rev. **50**, 308 (1936).
$A=13$. Kikuchi, Watase, Itoh, Takeda, Yamaguchi reference 6. E. M. Lyman, Phys. Rev. **55**, 234 (1939).
$A=15$. Fowler, Delsasso and Lauritsen, Phys. Rev. **49**, 561 (1936).
$A=17$. Kurie, Richardson and Paxton, Phys. Rev. **49**, 368 (1936).
$A=19$, 23 and 25. White, Delsasso, Fox and Creutz, Phys. Rev., preceding paper.

as has been shown by Grönblom. The calculation has not been carried out for $A=7$ since K-capture plays an important role in this case.[4] The fluctuations of the last two columns are probably within the limits of experimental error as they are very sensitive to small errors in ϵ_l. The very small value of $It f_1/l$ for $A=15$ could be explained by assuming that the $^2P_{3/2}$ level is very near to the ground state $^2P_{1/2}$ in this case. Certainly, the figures of the last column do not increase strongly with increasing A as would be expected by assuming a breakdown of the underlying formulas for the larger A. The corresponding numbers, calculated for all transitions not considered in this paper (such as $F^{20}\rightarrow Ne^{20}$) are a hundred times greater. We must infer that *either* approximation 1 is valid for these elements, *or* Fermi's original matrix element (3a) is responsible for the major part of the decay constant and approximation 2 holds sufficiently well. In the latter case, most of the transitions would go from the lowest state of the parent element to the lowest state of the product nucleus.

We now go over to the nuclei with a mass number $A=4k+2$. The first three of these are

[22] The constant of this equation was assumed to be 2.4 in the second paper of reference 12 and 2.32 in reference 11. More accurate calculations on the Coulomb energy were made by E. Feenberg and J. Knipp, Phys. Rev. **48**, 906 (1935). S. Share, Phys. Rev. **50**, 488 (1936). E. Feenberg and E. Wigner, Phys. Rev. **51**, 95 (1937). H. A. Bethe, Phys. Rev. **54**, 436 (1938). H. Brown and D. Inglis, Phys. Rev. **55**, 1182 (1939). The fact that ϵ_l is given by the Coulomb energy alone was already pointed out by W. A. Fowler, L. A. Delsasso and C. C. Lauritsen, Phys. Rev. **49**, 561 (1936).

TABLE III. *Summary of experimental information about nuclei with mass number 4k+2.*

A		I	t	It/l	Itf_1/l
6	3.6	1000	0.8	1.15	1.75
10	?				
14	?				
18	0.55	0.43	6700	4.15	2.10
22	0.55	0.43	9.5×10^7	5.9×10^4	2.9×10^4
26	?		7		
30	2.6	241	170	59.2	29.5
34	2.6	240	1970	680	340
38	2.2	116	460	77	39

$A=6$. Bjerge and Broström, quoted from reference 5.
$A=18$. Snell, Phys. Rev. **51**, 142 (1937), DuBridge, Barnes and Buck, Phys. Rev. **51**, 995 (1937), Jasaki and Watanabe, Nature **141**, 787 (1938).
$A=22$. F. Oppenheimer and Tomlinson, Am. Phys. Soc. Stanford Meeting (1939).
$A=26$. The experiments on the limit of the β-ray spectrum widely disagree. If the values of R. O. Frisch (Nature **133**, 721 (1934)) or Brandt (Zeits. f. Physik **108**, 726 (1938)) of 1.8 or 1.5 Mev should prove correct the present considerations became untenable. Almost equal difficulties would be encountered if Magnan's value of 4.6 Mev (Comptes rendus **205**, 1147 (1937)) were correct.
$A=30$. The experiments greatly disagree in this case also. The value of Meye (Zeits. f. Physik **105**, 232 (1937)) appears most reliable at present.
$A=34$. Sagane, Phys. Rev. **50**, 1141 (1936).
$A=38$. Hurst and Walke, Phys. Rev. **51**, 1033 (1936), Ridenour and W. J. Henderson, Phys. Rev. **52**, 889 (1936).

electron emitters, the others positron emitters. Unfortunately, the experimental information, summarized in Table III, is much less conclusive than that for the odd elements.

Unlike the constancy of the It/l column of Table II, the constancy of the It/l column of Table III cannot be brought into connection with the validity of Fermi's original assumption (3a) since (3a) would give 0 for the probability of the β-disintegration of these elements.

Disregarding $A=22$ for the time being, Table III allows a decision to be made between the two alternatives left open at the consideration of Table II. Assuming only the validity of the second approximation it seems to be very difficult to account for the small values of Itf_1/l particularly for that of F^{18}. The short lifetime of Al^{26} points in the same direction. The energy of this disintegration must be much greater than the values given by Frisch and by Brandt. On the other hand, the calculated value for the difference of the Coulomb energies of Al^{26} and Mg^{26} is 4.85 Mev. This gives 3.05 for the disintegration energy of the state of Al^{26} which corresponds in the second approximation to the normal state of Mg^{26}. This state of Al^{26} is a singlet state and should lie above the normal state of Al^{26}. Hence $\epsilon_l \leq 3.05$ Mev in this case; $\epsilon_l=2.80$ Mev would give $Itf_1/l=1.75$. All this speaks strongly in favor of the assumption that the first approximation is valid for the normal states up to about $A\sim26$ and g_1 is at least of the same order of magnitude as g_0 and even allows Grönblom's assumption of $g_0=0$.

On the other hand, the increase of Itf_1/l beginning at about $A=30$ indicates that approximation 1 becomes inaccurate from this point on. The values of ϵ_l for the elements in question are not very well known but it is unlikely that they are in error by an amount sufficiently large to bring the last column down to about 2.3.

The case of $A=22$ remains puzzling on every interpretation. It does not appear reasonable to assume that approximation 1 gives a wave function which is contained in the correct one only with a coefficient of about $(1.7/2.9\times10^4)^{\frac{1}{2}}=0.007$. It is much more likely that the states of Na^{22} and Ne^{22} between which the β-transition is observed do not correspond to the same multiplet.

6

If the interpretation of the experimental data as given in the previous section is correct, one would expect that the distinction between allowed and forbidden β-transition becomes increasingly vague at about $A=30$. For a given ϵ_l, the lifetime of the allowed transitions should increase, that of the forbidden ones decrease and the matrix element for both should tend to some average value. When this condition is reached, only the selection rules for J and parity would remain valid ($\Delta J=\pm1$ or 0, no change in parity allowed). The breakdown of one set of selection rules while others remain intact is a familiar phenomenon in atomic spectra.

The test to which the approximation 1 is put by the investigation of the lifetimes of β-transitions is a very severe one. One must expect a breakdown of the formulas derived in Section 4 whenever two ($PP'P''$) multiplets overlap. Such an overlapping of two multiplets will not greatly influence the validity of the expressions for the energy which were used in references 11 and 12, because the multiplets will differ only in their azimuthal quantum numbers, not in their ($PP'P''$). If the spin dependent forces are not too strong, they will leave ($PP'P''$) and in most

cases even S (cf. reference 21) good quantum numbers while L and the grouping of states into multiplets will be more easily destroyed. If approximation 1 makes S a good quantum number it will remain a good quantum number in spite of small perturbations which already affect L. This picture suggests e.g. that the $^2P_{3/2}$ and $^2D_{3/2}$ parts are contained in the normal state of an element with $J=\frac{3}{2}$ to a much greater extent than, say, the $^4S_{3/2}$ part.

It may be worth while to note that according to the considerations presented here the following β-spectra should be simple: He^6, F^{18} and probably Al^{26}, and all elements of Table II in which the ground state is a ^2S state. This is very probable for $A=19$ since the magnetic moment of F^{19} is very nearly equal to the magnetic moment of the proton. These elements should offer a possibility for a simple test of the ideas of reference 6.

I wish to express my gratitude to Drs. M. G. White, L. A. Delsasso and W. H. Barkas for many helpful discussions, especially concerning the experimental material.

SEPTEMBER 15, 1939 PHYSICAL REVIEW VOLUME 56

On the Nuclear Magnetic Moments of the Isotopes of Rubidium and Chlorine*

P. KUSCH AND S. MILLMAN
Columbia University, New York, New York

(Received July 24, 1939)

The molecular beam, magnetic resonance method has been applied to the measurement of the nuclear gyromagnetic ratios of Rb^{87}, Rb^{85}, Cl^{37} and Cl^{35}. The g values are 1.820 ± 0.006, 0.536 ± 0.002, 0.454 ± 0.002 and 0.546 ± 0.002, respectively. The magnetic moments of Rb^{87} and Rb^{85}, obtained from the observed g values and the known nuclear spins, are 2.741 ± 0.009 and 1.345 ± 0.005, respectively. The substantial agreement of the moment ratio μ_{87}/μ_{85}, 2.038, found by this method, with that obtained from atomic beam measurements indicates that any contribution to h.f.s. by a form of interaction between electron and nucleus not electromagnetic in character is small. A nuclear moment of 1.365 ± 0.005 is obtained for Cl^{35} if one takes the band spectra spin value of 5/2 for this nucleus. No information concerning the spin of Cl^{37} is available.

INTRODUCTION

A BRIEF preliminary report[1] of the measurements, by the molecular beam, magnetic resonance method,[2] of the nuclear magnetic moments of the isotopes of rubidium and chlorine has already been published. It is the purpose of this paper to present the results in further detail.

The hyperfine structure of atomic energy states of the rubidium isotopes has been investigated both by spectroscopic methods[3] and by the method of atomic beams.[4] Both methods yield nuclear spins of 3/2 and 5/2 for Rb^{87} and Rb^{85}, respectively. Approximate values of the magnetic moments have been obtained from the h.f.s. of the ground state by use of the Goudsmit, Fermi-Segrè formula. In accordance with our experience with the other alkali nuclei,[2,5] the magnetic moments so calculated may be expected to differ by not more than 10 percent from the values of nuclear moments directly measured by the present method. The differences arise from the fact that exact wave functions for the alkali atoms are not known. On the basis of the assumption that hyperfine structure of atomic energy states is due solely to the magnetic interaction of the nuclear moment with the external electrons, the ratio of the nuclear moments of two isotopes of the same element can be obtained from the ratio of the observed

* Publication assisted by the Ernest Kempton Adams Fund for Physical Research of Columbia University.

[1] P. Kusch and S. Millman, Phys. Rev. **55**, 680 (1939).

[2] I. I. Rabi, S. Millman, P. Kusch and J. R. Zacharias, Phys. Rev. **55**, 526 (1939).

[3] H. Kopfermann, Zeits. f. Physik **83**, 417 (1933); D. A. Jackson, Proc. Roy. Soc. **A139**, 673 (1933).

[4] S. Millman and M. Fox, Phys. Rev. **50**, 220 (1936).

[5] P. Kusch, S. Millman and I. I. Rabi, Phys. Rev. **55**, 1176 (1939).

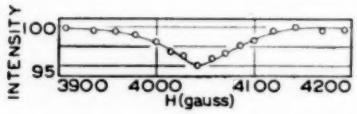

FIG. 1. Rb^{87} resonance curve in Rb_2, with a frequency of 5.604 megacycles per second and an oscillating current of 7 amp.

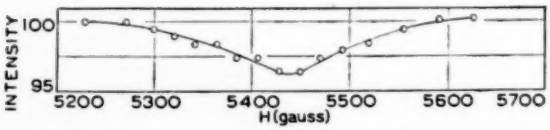

FIG. 2. Rb^{85} resonance curve in Rb_2, with a frequency of 2.230 megacycles and a current of 23 amp.

h.f.s. of a given atomic energy state without the use of the semi-empirical G.F.S. formula, since the electronic wave functions are the same for the two isotopes. This assumption can be subjected to an experimental test by comparing the moment ratio of two isotopes deduced from h.f.s. measurements with that directly measured by the molecular beam, magnetic resonance method. This question was discussed for the case of the lithium isotopes in an earlier paper.[2] In that case the ratio of moments as measured directly was known to a high degree of precision. The ratio of moments as determined from h.f.s.[6] was, however, subject to a considerable uncertainty, and the observed discrepancy of about 2 percent between the two ratios, although outside the experimental error, was not considered sufficiently great to give conclusive indication of a real physical effect. The ratio of the moments of the two isotopes of rubidium is known from h.f.s. data[4] to within 0.2 percent. A comparison of this ratio with one directly determined is of considerable interest, therefore, for testing the validity of the hypothesis that magnetic interactions alone account for observed h.f.s. patterns.

No measurements of the spins and nuclear magnetic moments of the chlorine isotopes are available from the work on the h.f.s. of chlorine. Because of his inability to observe h.f.s. for chlorine, Tolansky[7] concludes that the nuclear g values must be abnormally small. Elliot[8] has found the most probable value of the spin of Cl^{35} to be 5/2 from observations on the alternating intensities in band spectra. No information is available as to the spin of Cl^{37}.

EXPERIMENTAL

The apparatus and the experimental method of determining both the magnitude and the sign of the nuclear gyromagnetic ratios have been previously described.[2, 9] Rb_2 molecules were used in this work in a manner similar to that described[5] for the use of the molecules Na_2 and K_2 in the determination of the magnetic moments of Na^{23} and K^{39}. The principal difficulty in the observation of the resonance curves of rubidium arose from the limited intensity of the *molecular* beam. The molecular content of the beam was only about 0.6 percent. Raising the oven temperature served only to increase the *atomic* beam intensity and left the absolute *molecular* intensity practically unchanged. This occurred because of the greater dissociation that accompanies higher temperatures. The molecules LiCl and RbCl were used for the observation of the resonance minima of the chlorine isotopes.

RESULTS

The two resonance curves shown in Figs. 1 and 2 are typical of curves observed in Rb_2. The beam-intensity ordinate is plotted to a relatively small scale, reflecting the generally low intensities obtainable in these cases. The resonance minima give rise to the g values 1.820 ± 0.006 and 0.536 ± 0.002 in units of $e/2Mc$, when referred to the g of Li^7 which we take to be 2.167. These values are not exactly the same as those obtained from the oscillating frequencies and applied fields given in Figs. 1 and 2 because of the fact that for any one field direction the end effects of the oscillating field produce a shift in the minimum.[9] This error is eliminated from the final result by obtaining data for opposite field directions for a given oscillating frequency and averaging the two apparent g values so obtained. The principal factor limiting the precision of these g values was the difficulty of locating the minima of the resonance curves, which were broad and shallow. The signs of both g's and therefore the signs of the corresponding moments were found to be positive, verifying

[6] J. H. Manley and S. Millman, Phys. Rev. **51**, 19 (1936).
[7] S. Tolansky, Zeits. f. Physik **73**, 470 (1931); S. Tolansky, Zeits. f. Physik **74**, 336 (1932).
[8] A. Elliot, Proc. Roy. Soc. **A127**, 638 (1930).
[9] S. Millman, Phys. Rev. **55**, 628 (1939).

results obtained by other methods.[3, 10] The depths of the observed resonance curves were not sufficiently large to permit an assignment of the observed g values to the appropriate isotopes by comparing the known abundance of the isotopes with the relative depths of the curves. However, a comparison of the ratio of the observed g's, 3.397, with that accurately determined from atomic beam measurements[4] can lead to but one assignment, i.e., that the larger g is to be attributed to Rb^{87} and the smaller to Rb^{85}. The observed nuclear magnetic moments of Rb^{87} and Rb^{85} are then 2.730 ± 0.009 and 1.340 ± 0.005 nuclear magnetons. Since we are dealing with atoms of high atomic number we must apply a correction arising from the diamagnetism of the atom. The correction serves to increase the measured value of the magnetic moment. The contribution, $\bar{H}$, to the magnetic field at the nucleus by the electronic structure is given[5] in terms of the applied field, H, and the atomic number, Z, by $\bar{H}/H=0.32\times10^{-4}Z^{4/3}$. In the present case the correction is 0.4 percent. The corrected values of the moments of Rb^{87} and Rb^{85} are then 2.741 ± 0.009 and 1.345 ± 0.005 nuclear magnetons, respectively. The ratio μ_{87}/μ_{85} is 2.038. Errors in the individual moments, as referred to Li^7, because of gradual shifts in the apparent calibration constant of the homogeneous magnet, do not enter in the evaluation of the ratio of the moments since the resonance curves were obtained under identical experimental conditions. We estimate the precision of this ratio to be 0.5 percent.

It has not been possible to observe resonance curves for rubidium with either RbF or RbCl molecules. The depths of the resonance curves, even with Rb_2 molecules, were small. The factor which limits the depths of the resonance curves is not due to insufficient deflecting power of the inhomogeneous magnets since similar g's have, in many cases, produced deeper minima. The small depths probably arise from some sort of an interaction between the nuclear spin and the molecule. The specific nature of this interaction is not as yet understood. Variations in the depths of resonance minima, depending on the nature of the molecule in which the nucleus exists, have been found for other nuclei as well.[5]

Chlorine resonance minima were observed in the LiCl and the RbCl molecules. Figs. 3 and 4 show typical resonance curves. The observed g values are 0.454 ± 0.002 and 0.546 ± 0.002. The signs of these g's were found to be positive. The assignment of these g's to the appropriate isotopes may be made by comparing the observed depths of the resonance curves with the known ratio of the abundance of Cl^{35} to Cl^{37}, about 76 to 24. The ratio of the depth of the resonance curve of the larger g to that of the smaller g, when LiCl is loaded in the oven, is 3.4 and 3.1 for currents in the wires which produce the oscillating field of 20 and 10 amperes, respectively. At 20 amp. the depth of the resonance curve of the larger g was about 10 percent of the total beam intensity. The observed ratio of the depths of the resonance curves points strongly to the conclusion that the g value of 0.546 is to be assigned to Cl^{35}. An assignment on this basis, of course, assumes that any interaction which might affect the depth of the resonance curve is the same for the $LiCl^{35}$ and the $LiCl^{37}$ molecules. The fact that the widths of the resonance curves are about the same for both isotopes probably shows that these interactions are not markedly different for the two nuclei. A more cogent argument arises from a consideration of the observed depth, 10 percent, of the resonance curve of the larger g. If this is to be ascribed to Cl^{37} and if we assume that the molecules in the beam are LiCl, then 42 percent

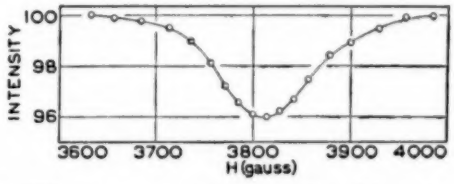

FIG. 3. Cl^{37} resonance curve in LiCl, with a frequency of 1.318 megacycles and a current of 40 amp.

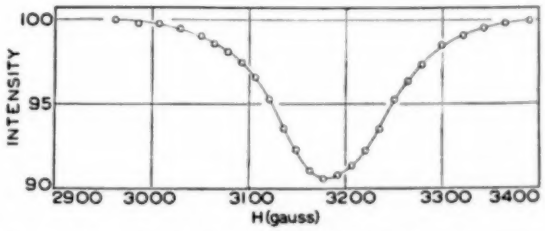

FIG. 4. Cl^{35} resonance curve in LiCl, with a frequency of 1.318 megacycles and a current of 20 amp.

[10] S. Millman and J. R. Zacharias, Phys. Rev. **51**, 1049 (1937).

of the molecules containing Cl^{37} have missed the detector because of reorientations in the transition field. This amount is much greater than can be expected to occur for a nucleus whose g is as small as 0.55. We have no knowledge, however, that the molecules in our beam are LiCl rather than $(LiCl)_n$ with $n \geq 2$. If $n=2$ then 42 percent of the molecules in the beam will contain Cl^{37}, and the assignment of the larger g to Cl^{37} would imply that 24 percent of the molecules in the beam have missed the detector due to reorientations. This fraction is also greater than can reasonably be expected, especially for a curve as broad as that in Fig. 3. It therefore seems quite certain that the g value of 0.546 is to be assigned to Cl^{35} and that of 0.454 to Cl^{37}. If we take the band spectra[8] value of 5/2 for the spin of Cl^{35} its moment is 1.365 ± 0.005 nuclear magnetons. It must be borne in mind, however, that determinations of spin from measurements of alternating intensities in band spectra are not decisive for spin values as large as 5/2. The correction due to diamagnetic susceptibility is less than 0.1 percent and can be neglected. Since the spin of Cl^{37} is not known its magnetic moment cannot be obtained from the observed g.

Discussion

Our values, 2.741 and 1.345, for the magnetic moments of Rb^{87} and Rb^{85}, respectively, are to be compared with 2.67 and 1.32, calculated from the h.f.s. of the ground state by the use of the G.F.S. formula.[11] It is seen that the results obtained from the G.F.S. formula are in good agreement with those obtained from our direct measurements. The value which we obtain for the ratio, 2.038 ± 0.010, is to be compared with the ratio obtained by Millman and Fox[4] from atomic beam measurements, 2.026 ± 0.004. The discrepancy of 0.6 percent lies within the limits of experimental error. Any contribution to the h.f.s. of an atomic energy state by a form of an interaction, not electromagnetic in character, between the nucleus and the electronic structure is certainly very small.

This research has been aided by a grant from the Research Corporation.

[11] The results given by Millman and Fox are slightly high because of an error in the use of the relativity correction factor, $(1-ds/dn)$, in the G.F.S. formula. The moments here given have been recalculated from their data.

SEPTEMBER 15, 1939 PHYSICAL REVIEW VOLUME 56

The Electron-Positron Field Theory of Nuclear Forces

EUGENE P. WIGNER
Princeton University, Princeton, New Jersey
AND
CHARLES L. CRITCHFIELD AND EDWARD TELLER
George Washington University, Washington, D. C.

(Received July 31, 1939)

A simple, spin-independent interaction is assumed between heavy particles (neutrons and protons) and electrons. Saturation of resulting forces between heavy particles is assured by choosing a bounded interaction. The change in energy of electrons in negative levels which is caused by the presence of a heavy particle is calculated. Certain general restrictions on the choice of interactions between electrons and heavy particles are discussed.

Introduction

1.

IT has been suggested[1] that nuclear forces are characterized by an exchange of electron-positron pairs between the interacting particles. This type of field theory was conceived of as a possible explanation of the equality of proton-proton and neutron-proton forces which became apparent from the results of scattering of protons

[1] G. Gamow and E. Teller, Phys. Rev. **51**, 289 (1937).

by protons.[2] An interaction between the heavy elementary particles which does not entail an exchange of charge or of spin, however, will not show the same kind of saturation which has been customarily assumed to exist between nuclear particles.

One species of saturation which may occur if neutrons and protons interact strongly with electrons and positrons in certain states has been investigated.[3] It was assumed that a single heavy particle attracts electrons of either spin if they occupy a particular spherical state which will be designated by ψ_A and repels electrons in the spherical state ψ_B. ψ_A and ψ_B are assumed to have the same space dependence, centered on the position of the heavy particle, and to differ only in the components of the four-valued spin of relativistic electron theory. The interaction is assumed to be strong enough so that it is permissible to say that in the zero-order approximation the lowest state of a single heavy particle system is that in which ψ_A states of both spins are filled and ψ_B states empty. Let the interaction energy per electron be $\pm\eta$, so that the energy in zero-approximation of a heavy particle at rest is -2η, neglecting the proper mass of the heavy particle. In first approximation one should add the average kinetic energy of the light particle field, E_{kin}. The perturbation method used is valid if $\eta \gg E_{\text{kin}}$. Interaction with electrons in states orthogonal to the ψ_A's and ψ_B's has been assumed to be zero.

Attraction between heavy particles which interact with electrons as assumed above was found to be a consequence of the change in average kinetic energy of the light particle field which was effected by bringing the heavy particles close together. In particular, disregarding the application of the exclusion principle to the heavy particles, N heavy particles located at the same point will be in the lowest state if the ψ_A states centered at that point are filled and the ψ_B states empty. The energy of this system in first approximation is $-2N\eta+E_{\text{kin}}$ as compared with $-2N\eta+NE_{\text{kin}}$ in case the N heavy particles are widely separated. It has also been shown that the interaction energy per particle, -2η, was independent of the configuration of heavy particles and could therefore be considered as part of the rest energy of the particles. The maximum attractive potential in a nucleus of N particles is thus $(N-1)E_{\text{kin}}$. A binding energy per particle which is independent of the number of other particles in heavy nuclei may then be obtained. The range of forces which is essentially the linear dimension of states ψ_A and ψ_B is known to be of the order of e^2/mc^2 so that $E_{\text{kin}} \sim ch/(e^2/mc^2) \sim 137mc^2$ in agreement with the order of magnitude of depths of potential wells found necessary to account for the stability of light nuclei.

2.

The present paper differs from the previous work (I) in two respects. First, the interaction between heavy particles and the light particle field has a different form. This change was introduced in order to assure that the interaction has the proper symmetry with respect to inversion. The consequences of the lack of invariance of the previously assumed interaction with respect to inversion are briefly discussed.

On the other hand, it will be assumed again that the heavy particle does not change its state as a consequence of the interaction with the electron-positron field so that we do not obtain spin-dependent forces. A modification of the theory leading to spin dependence will be discussed in a forthcoming paper.

Second, it is shown that saturation will appear for any value of the interaction constant, η. In fact, we shall see at once that the reason of the saturation is that the assumed interaction of a heavy particle with the light particle field has a lower bound (i.e., the characteristic values of the interaction operator do not extend to $-\infty$).

Let the interaction be $-\eta$ between the heavy particle and the light particles (electrons) in certain states, ψ_A, and let the interaction be $+\eta$ between the heavy particle and the light particles in certain other states, ψ_B, which are orthogonal to the ψ_A. Electrons in states orthogonal to both the ψ_A and the ψ_B shall not interact with the heavy particle. The lowest value of the

[2] M. Tuve, N. Heydenburg, L. Hafstad, Phys. Rev. **50**, 806 (1936) and **53**, 239 (1938); G. Breit, E. Condon, R. Present, Phys. Rev. **50**, 825 (1936).

[3] C. Critchfield and E. Teller, Phys. Rev. **53**, 812 (1938). This reference will be quoted throughout the remainder of the paper as I.

interaction energy will be obtained if all states ψ_A are filled and all states ψ_B empty. The total minimum of the interaction energy of a heavy particle with the light particle field will be -2η if there are two states ψ_A (and two states ψ_B). The total energy of the system will consist of three parts: the energy of the heavy particle, the above interaction energy and the increase of the kinetic energies of the electrons under the influence of the heavy particle. This last quantity is always positive as the sum of the kinetic energies of the electrons in the vacuum (when all levels with negative kinetic energy are filled, all levels with positive kinetic energy empty) is the absolute minimum which the value of the kinetic energy of the electrons can assume. The lowest possible value of the sum of these three energies will correspond to the observable mass M of a heavy particle.

The total energy of N heavy particles will also contain three parts. First the proper energy of the heavy particles, NM_pc^2, second the interaction energy between light and heavy particles and third the increase of kinetic energy for the light particles. As this last quantity is always positive, the total energy of N particles is always greater than $E_N > NM_pc^2 - 2N\eta$ as -2η is the absolute minimum of the interaction of a heavy particle with the electron field. Thus the total binding energy between N particles, $NMc^2 - E_N < N(M-M_p)c^2 + 2N\eta$, will be below a constant, $(M-M_p)c^2+2\eta$, times N, which will assure the saturation character of the assumed interaction for sufficiently large values of N for any η.

The assumption of a finite value for η appears necessary because a very large η would lead to a strong repulsion of heavy particles which are not at rest with respect to each other. One can see this in the following way. Naturally, the states ψ_A and ψ_B will depend on the position of the heavy particle and will be, in fact, centered around it. Let us assume now that all ψ_A are orthogonal to all ψ_B, also to those centered around a different heavy particle. This condition is fulfilled[3] if the spin parts of the ψ_A are perpendicular to the spin parts of the ψ_B. If this is true, the lowest value of the interaction energy of the electron field with a system of heavy particles will be assumed if both ψ_A of each heavy particle are occupied and both ψ_B of each heavy particle unoccupied. If η is very large, this will be a reasonable first approximation. The total energy Mc^2 of one heavy particle will then be in first approximation

$$Mc^2 = M_pc^2 - 2\eta + E_{1\ \mathrm{kin}},$$

where $E_{1\ \mathrm{kin}}$ is the lowest value of the increase of kinetic energy of the electrons, compatible with the condition that the ψ_A are occupied, the ψ_B unoccupied. Similarly, for N particles, the total energy becomes in first approximation

$$E_N = NM_pc^2 - 2N\eta + E_{N\ \mathrm{kin}},$$

where $E_{N\ \mathrm{kin}}$ is the lowest possible increase in the kinetic energy of the electrons which allows all $2N$ of the ψ_A to be occupied and all $2N$ of the ψ_B to be empty. The binding energy will be, therefore, in first approximation

$$NMc^2 - E_N = NE_{1\ \mathrm{kin}} - E_{N\ \mathrm{kin}}.$$

This can be easily obtained for a coincident position of the heavy particles: in this case all pairs of ψ_A are the same and all pairs of ψ_B also. Thus the kinetic energy $E_{N\ \mathrm{kin}} = E_{1\ \mathrm{kin}}$ and the total binding becomes for coincident heavy particles

$$NMc^2 - E_N = (N-1)E_{1\ \mathrm{kin}}.$$

The above consideration, which is a repetition of that in (I), assumes that the ψ_A are all orthogonal to all ψ_B. This cannot be true, however, since the states ψ_A, ψ_B, etc., are defined in the system of reference in which the corresponding heavy particle is at rest. If one of them is moving with a velocity v, the corresponding ψ_B states will not be orthogonal any more to the ψ_A states of a heavy particle at rest but will contain them with a coefficient of the order of magnitude v/c. Hence, it will be impossible to fill all the ψ_A states of the particle at rest and leave the ψ_B states of the moving particle empty. Thus, under these conditions, the interaction energy between light particle field and heavy particles will not be the sum of the interaction energies of the light particles with the heavy particles separately but will lie higher by an amount of the order of magnitude $\eta v^2/c^2$.

Although other, at present unpredictable, effects may arise from the difficulty connected with the simultaneous creation of pairs at finite

distances from the heavy particle, there is good reason for assuming that η is less than about 100 times greater than the kinetic energy of the electronic states ψ_A and ψ_B. Otherwise in nuclei with $v/c=1/10$ too strong repulsive forces may be obtained.

We wish to mention, finally, that we consider the mathematical formalism as the most permanent part of the present paper. It is possible that this can be taken over into a new theory the physical foundation of which is quite different.

Form of Interaction

In the earlier treatment of saturation of pair-emission forces (I) it was assumed for simplicity that a heavy particle created and annihilated pairs in spherically symmetrical states. A consequence of the Dirac theory of the electron is, however, that spherical states of negative kinetic energy and spherical states of positive kinetic energy have opposite transformation properties under inversion of the coordinate system. According to the hole theory of positrons the creation of an electron-positron pair in a spherically symmetrical state is interpreted as a transition of an electron from a spherical state of negative energy to one of positive energy. Since no change is assumed to take place in the heavy particle state during pair-emission or reabsorption it follows that the addition to the Hamiltonian representing the interaction between heavy particle and light particle field is odd under inversion. With an odd term in the Hamiltonian it would no longer be possible to have nuclear wave functions which are purely odd or purely even and the usual argument showing that nuclei cannot have permanent electric dipoles will break down. In fact, with an even Hamiltonian nuclear wave functions will be either odd or even; in both cases the charge distribution is even and no dipoles can result.

Nuclear electric dipoles would give ortho-para hydrogen and (or) deuterium conversions in the presence of a strong dipole gas at atmospheric pressure in about 10^{-4} seconds. Such conversions fail to take place even in a month. If an odd Hamiltonian is introduced new reasons should be found for the absence of dipoles in nuclei. In addition there seems to be no reason to abandon the postulate of the symmetry of elementary particles with respect to inversion.

It is known[4] that the sixteen linearly independent square matrices which can be formed as linear operators on the four-component electron spin can be represented as one scalar, four components of a polar vector, six components of an antisymmetric tensor, four components of a pseudovector and one pseudoscalar. Scalar additions to the Hamiltonian which refer to the spin-coordinates of two particles (heavy particle and electron) can therefore be constructed in five ways: *viz.*, as products of each of the five covariant operators associated with one particle with the corresponding contravariant operator of the other. Since we are at present interested only in those operators which, in nonrelativistic approximation, leave the heavy particle in the same state the only combinations of possible use are the scalar-scalar and vector-vector products. The vector-vector product would give the same attraction for electrons in positive states as for electrons in negative states and a strong interaction could not be assumed without attracting electrons to the heavy particle and changing the charge with which the heavy particle is associated in its lowest state. The scalar-scalar interaction will therefore be adopted.

We shall write the scalar-scalar interaction in accordance with the formulism of the quantization of the wave equation. Let $\psi_k(x)$ be the four-component operator of the electron state $\psi_k(x)$ and $\psi_k(x)^\dagger$ the adjoint operator. $\psi_k(x)$, $\psi_i(x')^\dagger$ then obey the commutation rules:

$$\begin{aligned}\psi_k(x)\psi_i(x')^\dagger+\psi_i(x')^\dagger\psi_k(x)&=\delta_{ik}\delta(x-x'),\\ \psi_k(x)\psi_i(x')+\psi_i(x')\psi_k(x)&=0.\end{aligned}\tag{1}$$

In the same way $\Psi_m(x)$ and $\Psi_m(x)^\dagger$ are operators associated with the heavy particle state. The interaction between a heavy particle located at the origin, $\Psi_m(0)$, and an electron in the state $\psi_k(x)$ may then be written:

$$J=\sum_{iklmn}-\eta\int dx\int dx'\rho_{mn}{}^3\rho_{ik}{}^3\Psi_m(0)^\dagger\Psi_n(0)\times\psi_i(x)^\dagger\psi_k(x')\delta(x)\delta(x')\tag{2}$$

[4] J. von Neumann, Zeits. f. Physik **48**, 868 (1928).

where the form of ρ_{mn}^3 and ρ_{ik}^3 is given by

$$\rho^3=\begin{Vmatrix}1&0&0&0\\0&1&0&0\\0&0&-1&0\\0&0&0&-1\end{Vmatrix}, \tag{2a}$$

referring to the four spin-states of the heavy particle in one case and of the light particle in the other, and η is a constant. For simplicity we restrict our attention to operators which do not change the state of the heavy particle in nonrelativistic approximation (neglecting the last two rows) so that the operator of the heavy particle may be considered to be equivalent to unity and will not be explicitly mentioned hereafter. It is further supposed, in order to avoid divergent interaction between heavy particles, that the δ-functions in (2) are replaced by spherically symmetrical functions of finite extent, $u(x)$, $u(x)^*$, and, in particular, of linear dimensions comparable to the electron radius, e^2/mc^2. Invariance under Lorentz transformation cannot be had for J when these assumptions are made and, in fact, it will be seen that this failure is just the usual one found in applying relativistic methods to the theory of interactions of elementary particles with fields. The proposed addition to the energy of a single electron is then

$$J=\sum_{ik}-\eta\int dx\int dx'\,\rho_{ik}{}^3\psi_i(x)^\dagger\psi_k(x')u(x)^*u(x'). \tag{3}$$

It will be convenient to have J expressed in momentum space, so the following transformations are used:

$$\begin{aligned}u(x)&=C\int e^{ipx}v(p)dp,\\ u(x)^*&=C\int e^{-ipx}v(p)^*dp,\\ \varphi_k(p)&=C\int e^{ipx}\psi_k(x)dx,\\ \varphi_k(p)^\dagger&=C\int e^{-ipx}\psi_k(x)^\dagger dx,\\ C&=(2\pi)^{-\frac{3}{2}}\hbar^{-\frac{3}{2}},\end{aligned} \tag{4}$$

and $v(p)$ will be assumed to be normalized so that

$$\int_0^\infty v(p)^2 4\pi p^2dp=1.$$

$$J=-\eta\sum_{ik}\int\int\rho_{ik}{}^3v(p)v(p')^*\varphi_i(p)^\dagger\varphi_k(p')dpdp'. \tag{5}$$

The whole Hamiltonian is obtained by adding to this the Hamiltonian corresponding to Dirac's wave equation of the electron in its quantized form. The whole Hamiltonian has, therefore, the form $\sum_{\kappa\lambda}H_{\kappa\lambda}\varphi_\kappa{}^\dagger\varphi_\lambda$ and is therefore equivalent[5] to the Hamiltonian of a system of electrons which do not interact with each other and the energy equation of which is in Schrödinger form

$$\begin{aligned}&-\sum_k[c\sum_l(\rho^l\sigma^l)_{ik}p^l+\rho_{ik}{}^3mc^2]\varphi_k(p)\\ &\quad-\eta v(p)\sum_k\rho_{ik}{}^3\int v(p')^*\varphi_k(p')dp'=E\varphi_i(p),\end{aligned} \tag{6}$$

where E is the proper value of the energy. We shall solve now this equation and determine its characteristic values and characteristic states. In the state of the whole system for which the total energy is lowest, all electron states defined by (6) will be occupied if the corresponding E is negative, and all electron states with a positive E will be unoccupied.

For the further work, we drop the subscripts on the ρ, σ and ψ and consider them as four-dimensional matrices and vectors, respectively. For $\eta=0$, one has the ordinary Dirac equation which can be transformed[6] by

$$\begin{aligned}T(p)=(T(p)^{-1})^\dagger&=[E_p+mc^2+ic\rho_2(\sigma,p)]\\ &\quad\times[2E_p(E_p+mc^2)]^{-\frac{1}{2}},\\ E_p&=(m^2c^4+c^2p^2)^{\frac{1}{2}},\end{aligned} \tag{7}$$

into $-\rho_3E_p$. One may hope, therefore, to obtain some simplification by transforming the whole Eq. (6) with $T(p)$. This corresponds to replacing $\varphi(p)$ by

$$\varphi'(p)=T(p)\varphi(p). \tag{8}$$

The transformed Eq. (6) becomes particularly

[5] P. Jordan and E. Wigner, Zeits. f. Physik **47**, 631 (1928).
[6] E. Fermi, Rev. Mod. Phys. **4**, 131 (1932).

simple if we restrict ourselves to high energy values $E_p > mc^2$. The $T(p)$ is then, if we neglect mc^2 in comparison with E_p,

$$T(p)=2^{-\frac{1}{2}}(1+i\rho_2(\sigma, p)/p),$$
$$T(p)^{-1}=2^{-\frac{1}{2}}(1-i\rho_2(\sigma, p)/p), \quad (9)$$

and we have, instead of (6),

$$(E-\rho_3 E_p)\varphi'(p)+\eta v(p)\int T(p)\rho_3 T(p')^{-1} \times v(p')^*\varphi'(p')dp'=0. \quad (10)$$

Solution of Proper-Value Problem

Equation (10) will now be used to determine the proper energies of electrons. It must be remembered that in this equation only the kinetic energy of the electron for $E_p \gg mc^2$ and the non-Coulomb interaction with the heavy particle is taken into account. One important term which has been neglected is the Coulomb interaction between electrons. Neglecting this interaction makes it possible to restrict ourselves to the one-electron problem. The effect of all the terms neglected may be expected to be of the general order of magnitude of mc^2.

The dependence of $v(p')$ on p' is spherically symmetrical. Only $\varphi'(p)$ functions which contain a spherically symmetrical part will give a nonvanishing integral in (10). Since angular momentum in the electron state will be conserved we need only to consider functions with $j=\frac{1}{2}$ which one can write in the form $S(p)+[(\sigma, p)/p]P(p)$. $S(p)$ and $P(p)$ are functions of the absolute value of p, i.e., spherically symmetrical also. Higher j values will vary with the angle as higher spherical harmonics. The nature of the space dependence of $\varphi'(p)$ is not changed by the transformation $T(p)$. Hence even after the transformation with T only the wave functions of the form $S(p)+[(\sigma, p)/p]P(p)$ need be considered. S and P have four components each, i.e., are four-dimensional vectors, and $[(\sigma, p)/p]P(p)$ has the angular dependence of a first spherical harmonic, transforming like a P_1 function. Integration over dp' is understood to mean integration over $dp_x'dp_y'dp_z'$, or in spherical coordinates over $p'^2dp'd\phi d(\cos\theta)$. The integral over an odd power of $(\sigma, p)/p$ will obviously be zero, whereas every even power of $(\sigma, p)/p$ is equivalent to unity.

Substituting for T and $\varphi'(p)$, the integral in (10) may be written in the form:

$$I=\tfrac{1}{2}\int \rho_3\left[1-i\rho_2\frac{(\sigma, p)}{p}\right]\left[1-i\rho_2\frac{(\sigma, p')}{p}\right]v(p')\left[S(p')+\frac{(\sigma, p')}{p}P(p')\right]p'^2\sin\theta d\theta d\phi dp'$$
$$=\tfrac{1}{2}\rho_3\left\{\left[1+\rho_1\rho_3\frac{(\sigma, p)}{p}\right]\xi_S+\left[\rho_1\rho_3-\frac{(\sigma, p)}{p}\right]\xi_P\right\}, \quad (11)$$

where $$\xi_S=4\pi\int S(p')v(p')^*p'^2dp', \quad \xi_P=4\pi\int P(p')v(p')^*p'^2dp'$$

and Eq. (10) becomes

$$0=(E-\rho_3 E_p)\left[S(p)+\frac{(\sigma, p)}{p}P(p)\right]+\tfrac{1}{2}\eta v(p)\rho_3\left\{\left[1+\rho_1\rho_3\frac{(\sigma, p)}{p}\right]\xi_S+\left[\rho_1\rho_3-\frac{(\sigma, p)}{p}\right]\xi_P\right\}. \quad (12)$$

Multiplying by $(E+\rho_3 E_p)/(E^2-E_p^2)$

$$S(p)+\frac{(\sigma, p)}{p}P(p)=-\tfrac{1}{2}\eta\frac{E\rho_3+E_p}{E^2-E_p^2}v(p)\left\{\left[1+\rho_1\rho_3\frac{(\sigma, p)}{p}\right]\xi_S+\left[\rho_1\rho_3-\frac{(\sigma, p)}{p}\right]\xi_P\right\}. \quad (13)$$

Multiply both sides by $4\pi v(p)^*p^2dp$ and integrate

$$\xi_S=-2\pi\eta\int_0^\infty\frac{E\rho_3+E_p}{E^2-E_p^2}|v(p)|^2p^2dp[\xi_S+\rho_1\rho_3\xi_P]$$

and by $4\pi v(p)^*(\sigma, p)p^2dp/p$

$$\xi_P = -2\pi\eta\int_0^\infty \frac{E\rho_3+E_p}{E^2-E_p^2}|v(p)|^2p^2dp[\rho_1\rho_3\xi_S-\xi_P].$$

Or, defining α and β as

$$\begin{aligned} \alpha &\equiv 2\pi\eta\int_0^\infty \frac{E|v(p)|^2p^2dp}{E^2-E_p^2}, & \beta &\equiv 2\pi\eta\int_0^\infty \frac{E_p|v(p)|^2p^2dp}{E^2-E_p^2}, \\ \xi_S &= -(\alpha\rho_3+\beta)(\xi_S+\rho_1\rho_3\xi_P), & \xi_P &= -(\alpha\rho_3+\beta)(\rho_1\rho_3\xi_S-\xi_P). \end{aligned} \tag{14}$$

The ξ's are, of course, four-component spinors in general but since the forces in the present theory are indifferent to spin orientation we shall consider only two components of ξ_S, $\xi_S{}^1$ and $\xi_S{}^2$. $\xi_S{}^1$ and $\xi_S{}^2$ are the first and third elements of the four-rowed form if the spin has one direction and they are the second and fourth elements for the opposite spin direction. Thus the formulae to be given will represent both spin orientations. Similarly we shall consider $\xi_P{}^1$ and $\xi_P{}^2$. The operator

$$\rho_3 = \begin{Vmatrix} 1 & 0 \\ 0 & -1 \end{Vmatrix}$$

will operate on these two-dimensional vectors. There are then two sets of equations:

$$\begin{aligned} \xi_S{}^1 &= -(\alpha+\beta)(\xi_S{}^1-\xi_P{}^2), & \xi_P{}^1 &= (\alpha+\beta)(\xi_S{}^2+\xi_P{}^1), \\ \xi_P{}^2 &= (\alpha-\beta)(\xi_S{}^1-\xi_P{}^2), & \xi_S{}^2 &= (\alpha-\beta)(\xi_S{}^2+\xi_P{}^1), \\ \begin{vmatrix} 1+\alpha+\beta & -\alpha-\beta \\ -\alpha+\beta & 1+\alpha-\beta \end{vmatrix} &= 0, & \begin{vmatrix} 1-\alpha-\beta & -\alpha-\beta \\ -\alpha+\beta & 1-\alpha+\beta \end{vmatrix} &= 0, \\ 1+2\alpha &= 0, & 1-2\alpha &= 0, \\ \alpha &= -\tfrac{1}{2}, & \alpha &= \tfrac{1}{2}, \\ \xi_P{}^2 &= -\frac{1+2\beta}{1-2\beta}\xi_S{}^1, & \xi_P{}^1 &= \frac{1+2\beta}{1-2\beta}\xi_S{}^2. \end{aligned} \tag{15}$$

The equation $\alpha=-\frac{1}{2}$ determines proper values, E, of the problem with proper functions which are composed of $S(p)$ functions of the type S^1 and $[(\sigma, p)/p]P(p)$ functions of the type P^2 (where the superscripts have the same meaning as for the ξ's in (15)). For $\alpha=\frac{1}{2}$ the proper functions are combinations of S^2 and P^1 functions.

It has been assumed that electron states of kinetic energy which is large compared with mc^2 are the only ones of interest in considering nuclear forces. In this approximation $E_p=cp$. We evaluate the integral for α by the following device. Let p be quantized in a region of length L. Then $p_n=\pi\hbar n/L$ and $E_n=na$, where $a=\pi\hbar c/L$. Under this assumption the integral is represented by a sum which, in case $\alpha=\frac{1}{2}$, is

$$\frac{1}{2\eta}=\sum_0^\infty \frac{2\pi Ev(p_n)^2p_n{}^2a}{c(E^2-c^2p_n{}^2)}, \quad \frac{1}{\eta}=\sum_0^\infty \frac{4\pi E^3v(E/c)^2a}{c^3(E^2-a^2n^2)}+\sum_0^\infty \frac{4\pi Ea}{c^3(E^2-a^2n^2)}[c^2p_n{}^2v(p_n)^2-E^2v(E/c)^2]. \tag{16}$$

The second sum may be replaced by an integral,

$$f(E)\equiv\int_0^\infty 4\pi\frac{p^2v(p)^2-(E^2/c^2)v(E/c)^2}{E^2-c^2p^2}Edp,$$

$$\frac{1}{\eta}=\sum_0^\infty \frac{4\pi E^3v(E/c)^2}{c^3a}\left[\frac{1}{E^2/a^2-n^2}\right]+f(E), \quad \frac{1}{\eta}-f(E)=\frac{4\pi E^3v(E/c)^2}{c^3a}\left[\frac{\pi a}{2E}\operatorname{cotg}\frac{\pi E}{a}-\frac{a^2}{2E^2}\right], \tag{17'}$$

whence as we increase L and diminish "a" toward zero we get:

$$\left[\frac{1}{\eta}-f(E)\right]\frac{1}{2\pi^2E^2v(E/c)^2}=\operatorname{cotg}\frac{\pi E}{a}. \tag{17}$$

Equation (17) can be considered as the secular equation for E. If $v(E/c)$ does not vanish for $E=na$ and $E=(n+1)a$ and does not change its sign in this region the right-hand side will go from $+\infty$ to $-\infty$ when E changes from na to $(n+1)a$. Thus there will be in general a root between na and $a(n+1)$. We write, therefore,[7]

$$E=E_n+ax=a(n+x),\quad 0\leq x\leq 1,\quad \operatorname{cotg}\pi E/a=\operatorname{cotg}(n+x)\pi=\operatorname{cotg}\pi x,$$

$$x=\frac{1}{\pi}\operatorname{arctg}\frac{2\pi^2E^2v(E/c)^2/c^3}{1/\eta-f(E)}. \tag{18}$$

If L has been chosen large enough the difference between E_n and E tends toward zero and we may use E_n instead of E in (18), thus obtaining an explicit expression for x. In the following treatment we shall, however, drop the index, n, as has been done in (18).

An identical procedure applied in the case $\alpha=-\frac{1}{2}$ leads to $E=E_n+ax'$ and

$$x'=\frac{1}{\pi}\operatorname{arctg}\frac{2\pi^2E^2v(E/c)^2/c^3}{-1/\eta-f(E)}. \tag{19}$$

The sum of $a(x+x')$ over all states of negative E of both spins will be the total change effected by the introduction of J in the energy of the lowest state of the system:

$$\Delta E=2\sum_{E<0}a(x+x'), \tag{20}$$

$$\Delta E=\frac{2}{\pi}\int_{-\infty}^{0}\operatorname{arctg}\frac{(4\pi^2/c^3)E^2v(E/c)^2f(E)}{1/\eta^2-f(E)^2+(4\pi^4/c^6)E^4v(E/c)^4}dE. \tag{21}$$

Discussion

Since $4\pi\int p^2v(p)^2dp=1$ and therefore $p^2v(p)^2$ decreases more strongly than p^{-1} for large p one finds that $f(E)$ decreases to zero as E^{-1} for large E. Neither $f(E)$ nor $E^2v(E/c)^2$ are infinite anywhere. If, therefore, η is very small the denominator of (21) is always positive and essentially equal to η^{-2}. Furthermore, η^2 times the numerator remains small and one finds $\Delta E\sim\eta^2$ in accordance with expectation for small perturbations.

On the other hand if η is large compared with the argument for maximum $v(E/c)$ the denominator will change sign as E varies from $-\infty$ to 0. It is required that perturbations of levels as $E\rightarrow-\infty$ become zero. Since $f(E)$ and with it the argument of the arctangent will be negative in this region the arctangent in (21) must lie in the fourth quadrant as the lower limit is approached. If E is large compared with the argument for maximum $v(E/c)$ but still smaller than η, both numerator and denominator will be negative. The arctangent then lies in the third quadrant because, as we have seen, for $|E|>|\eta|$ it lies in the fourth and at $|E|\leqq|\eta|$ the argument is infinite. Since in the regions for E that we are discussing here the argument always remains small except for a short range where $|E|\leqq|\eta|$ the arctangent will be approximately equal to $-\pi$ for $|E|<|\eta|$ and zero for $|E|>|\eta|$. Thus a rough value for ΔE is $(2/\pi)(-\pi|\eta|)=-2|\eta|$. The behavior of the integral in the region where $v(E/c)$ and $f(E)$ have their maxima will affect the value of ΔE only by amounts comparable to the argument of $v(E/c)$ and $f(E)$

[7] O. K. Rice, Phys. Rev. **33**, 748 (1929).

in the region of the maximum. This latter contribution will correspond to the main part of the change in average kinetic energy due to the presence of the strong interaction with the heavy particle. For large η it will become independent of η provided that the integral

$$\int_0^\infty \frac{E^2 v(E/c)^2}{f(E)} dE \leqq \int_0^\infty E^3 v(E/c)^2 dE$$

converges. This is also the condition for a finite kinetic energy in the state $v(E/c)$. We can thus write $\Delta E = -2(|\eta| - E_{\text{kin}})$, the factor 2 being a consequence of summing over the spins. If N heavy particles are located at the same point the total change in energy is found from (21) by replacing η by $N\eta$. For sufficiently large values of $|\eta|$, therefore, $\Delta E(N) \leqq -2N|\eta| + 2E_{\text{kin}}$ and the total attractive potential for the N particles is $2(N-1)E_{\text{kin}}$. Thus the type of saturation obtained in this case is essentially the same as that obtained in (I). That the terms depending on η alone are additive for any configuration of the heavy particles follows from our general arguments since proper states of the term proportional to η are also proper states of ρ_3 and thus the states belonging to positive and negative proper values are orthogonal regardless of the positions of the heavy particles. The arguments given in the beginning of this paper also show that saturation would be obtained for any value of η.

It is not necessary in the theory presented here to require the average kinetic energy in the state $v(p)$ to be finite, i.e.,

$$\int_0^\infty p^3 v(p)^2 dp$$

may diverge. As an example of the above calculation we take such a particular function. We assume $u(r) \sim (1/r) e^{-E_0 r/\hbar c}$.

$$v(p) = \frac{1}{\pi}\left(\frac{c}{E_0}\right)^{\frac{1}{2}} \frac{1}{1 + c^2 p^2 / E_0^2},$$

$$\int E^3 v(E/c)^2 dE = E_0 \int E^3 dE / (E_0^2 + E^2)^2$$

diverges but the evaluation of (21) becomes particularly simple. We obtain

$$f(E) = E(E^2 - E_0^2)/(E^2 + E_0^2)^2,$$

$$\Delta E = -\frac{4}{\pi} E_0 [G \arccos (1 - 2F^2) - F \operatorname{arccosh} (1 + 2G^2)],$$

$$F^2 = [(\eta^4 + 16 E_0^2 \eta^2)^{\frac{1}{2}} - \eta^2]/8E_0^2,$$

$$G^2 = [(\eta^4 + 16 E_0^2 \eta^2)^{\frac{1}{2}} + \eta^2]/8E_0^2,$$

and the arccos in ΔE is restricted by the boundary conditions to lie in the first and second quadrants.

For large values of η, one finds in first approximation:

$$\Delta E = -2\eta + \frac{8}{\pi} E_0 \log \frac{\eta}{E_0} + \frac{5}{2\pi} E_0,$$

$$N\Delta E - \Delta E(N) = (N-1) E_0 \left[\frac{8}{\pi} \log \frac{\eta}{E_0} + \frac{5}{2\pi}\right] - \frac{8}{\pi} E_0 \log N.$$

The binding potential per particle is therefore roughly constant but it depends upon the value of η and also on $\log N$ in contrast to the case when the average kinetic energy in $u(r)$ converges. For small η (or $N\eta$)

$$\Delta E = -2\eta^2 / 3\pi E_0.$$

Certain general features of the theory here presented and of the simpler theory formerly discussed have been seen to be the same. One significant difference lies in the fact that the average value of the kinetic energy in the special electron states, ψ_A and ψ_B, is not sufficient in the case here discussed to determine the average kinetic energy of the electron-positron field in first approximation. This is true even for the case of large η. Then the proper states of the Hamiltonian are in first approximation the proper states of J. The latter are spherically symmetrical functions $u(x)$ and are also proper states of ρ_3. This means that they are linear superpositions of $S_{\frac{1}{2}}$ waves of positive kinetic energy and $P_{\frac{1}{2}}$ waves of negative kinetic energy for one proper value, $-\eta$, and superpositions of $S_{\frac{1}{2}}$, negative, with $P_{\frac{1}{2}}$ positive for $+\eta$. In fact

the absolute values of the coefficients of the normalized $S_{\frac{1}{2}}$ and $P_{\frac{1}{2}}$ waves of high kinetic energy must be equal in order to cancel out angular dependence in the result. Orthogonal linear combinations of the same $S_{\frac{1}{2}}$ and $P_{\frac{1}{2}}$ waves (for which the spherically symmetrical part of the wave is cancelled out) belong to the value zero. In taking into account the kinetic energy of the light particle field it would be necessary to calculate the effect of coupling between these orthogonal states and higher kinetic energy levels which would introduce corrections of the order of E_{kin} itself. Formerly, under the simplified treatment of spherically symmetrical functions alone, such couplings led to corrections of the order of E_{kin}^2/η and were negligible.

In this paragraph it will be understood that all wave-functions concerned are doublets and the subscript $\frac{1}{2}$ will not be used. Subscripts will rather be used to designate the sign of the kinetic energy: 1 for positive kinetic energy, 2 for negative. S_1 is, for example, an $S_{\frac{1}{2}}$ function of positive kinetic energy, S_2 of negative kinetic energy. With this notation and disregarding spin in the lowest state of the operator J the state S_1-P_2 must be filled and S_2+P_1 empty. If at the same time S_1+P_2 is empty the physical picture of the state is that in which pairs are produced and reabsorbed, electrons in S states and positrons in P states. On the other hand, if S_1+P_2 is also filled, the picture is simply that of an electron in an S state. Similarly, if S_2-P_1 is filled there will be pair-production in the lowest state but if it is empty there is simply a positron present in an S state. If η be replaced by $-\eta$ the physical description is changed so that in the lowest state there may be either pair-emission and reabsorption or electrons and positrons present in P states.

According to the mathematical solution given above the pair-emission mechanism will be still more involved. In fact, if we assume for the moment that S_1+P_2 is empty, then the kinetic energy will cause transitions of electrons in the negative sea into the S_1+P_2 state, thus causing a new kind of pair-production. Subsequently the kinetic energy will cause a transition from the S_1+P_2 state into a state of positive kinetic energy. In this way one heavy particle may be associated with pairs the number of which has no definite upper limit.

This pair-production in the neighborhood of a heavy particle might lead to an accumulation of charge near the position of the heavy particle. It will be shown, however, that no charge is to be expected in the present theory. The proposed Hamiltonian for one electron may be written

$$H=-\rho_1(\sigma, cp)-\rho_3[mc^2+H'(q, q')], \quad (22)$$

where H' is the potential due to a heavy particle located at the origin of coordinates. Disregarding the mutual interaction of electrons, (22) is also the complete Hamiltonian which operates on the antisymmetrical functional of all electrons. In the lowest state all negative levels of H are filled. If the proper functions, ψ, are now transformed by the matrix ρ_2 to $\psi'=\rho_2\psi$ all states of negative energy become states of positive energy because H anticommutes with ρ_2, $\rho_2 H\rho_2=-H$. On the other hand the charge density operator commutes with ρ_2 and thus remains unchanged. The charge density when all negative levels of H are filled is the same as that when all positive levels of H are filled. Thus the charge density when all levels (positive and negative) are filled is double that when all negative levels of (22) are filled. Filling all positive and negative levels, however, leads to a uniform charge distribution from which it follows that there is no accumulation of charge about the heavy particle under the assumed interaction. This shows, in fact, that any addition to the Hamiltonian which anticommutes with ρ_2 will not lead to difficulties with a surplus of electric charge in the vicinity of a heavy particle. Since no accumulation of charge near the heavy particle seems to be a desirable feature of the theory it seems that operators anticommuting with ρ_2 should be first considered if an interaction of heavy particles with the light particle field is introduced.

Although many arbitrary features remain in the theory of nuclear forces proposed in the above discussion this arbitrariness is reduced to some extent by the requirements which have been pointed out. Among these probably the arguments on symmetry and on the absence of charge accumulation are most important.

Spin-Dependence in the Electron-Positron Theory of Nuclear Forces

CHARLES L. CRITCHFIELD*
George Washington University, Washington, D. C.

(Received July 31, 1939)

An interaction between heavy particles and electrons is considered which includes a dependence upon relative spin orientation. The anomalous magnetic moments of neutron and proton can be accounted for by an adjustment of constants. Correct spin-dependence in the interaction of two heavy particles can be obtained only through an angular dependence of forces. An estimate of the angular dependence in this theory indicates that it is of sufficient magnitude for this purpose and of the right sign to give a "cigar-shaped" deuteron.

INTRODUCTION

PROGRESSIVE stages of an electron-positron field theory of nuclear forces have been presented from time to time.[1-3] It is the purpose of this paper to extend the most recent of these considerations (this issue of *Physical Review*) to account for spin-dependent phenomena. Definite experimental results correlating properties of nuclear particles with their spins are: (1) the magnetic moments of proton and neutron; (2) the greater binding experienced by a neutron and a proton with parallel spins (triplet deuteron) than between heavy particles with opposite spins; and (3) the electrical quadrupole moment of the deuteron. Simple explanations of these properties of one- and two-body systems are sought under the assumption that the neutron and proton interact strongly (compared with Coulomb interactions at nuclear distances) with the electron-positron field.

In the preceding formulation[3] of the spin-independent theory it was found convenient to adopt an interaction between heavy particles and electron which is proportional to the scalar spin-operator, ρ_3. Let V' represent the dependence of the interaction on coordinates and momentum of the electron. Then, neglecting the small components of the heavy particle wave function, the Dirac equation for an electron in the presence of a heavy particle may be written:

$$[E+\rho_1(\sigma, cp)+\rho_3(mc^2-V')]\psi=0. \quad (1)$$

Since in this approximation (nonrelativistic for heavy particles) the heavy particle state is not changed the calculations are simplified; also, no spin-dependent phenomena are to be expected to result from them. Relativistic invariance was abandoned in another respect, namely: functions of finite radius, $u(x)$, were used to replace delta-functions, $\delta(x)$, in the invariant form of interaction (see Eqs. (2) and (3) of reference 3). The average value of ρ_3V' used in the spin-independent theory may be written

$$\int\bar{\psi}\rho_3V'\psi dx=$$

$$-\eta\int dx\int dx'\rho_{ik}{}^3\psi_i(x)^\dagger\psi_k(x')u(x)u(x')^*. \quad (2)$$

η is the proportionality constant for the energy when normalized ψ and u-functions are used. The function $u(x)$ is centered about the heavy particle. It is clear that the radius of $u(x)$ is substantially the range of force between heavy particle and electron. This range of force may be expected to be comparable to that found between nuclear particles, $\sim e^2/mc^2$, so that the average kinetic energy in the state $u(x)$ would be of the order of $c\hbar/(e^2/mc^2)=137mc^2$. Electron states for which the integral (2) is relatively important have, therefore, kinetic energies large compared with mc^2. It was assumed that interactions between electrons could be neglected and that the kinetic energy of every free electron state could be written as $E_{\text{kin}}=cp$. The influence of ρ_3V' on each electron state was calculated under these assumptions. Summing up the

* Research Fellow in Theoretical Physics. This paper is based on the doctoral thesis on file at the George Washington University.

[1] G. Gamow and E. Teller, Phys. Rev. **51**, 289 (1937).
[2] C. Critchfield and E. Teller, Phys. Rev. **53**, 812 (1938).
[3] E. Wigner, C. Critchfield and E. Teller, Phys. Rev. this issue.

changes in energy caused by $\rho_3 V'$ (associated with one heavy particle) over all negative energy levels led to Eq. (21) of reference 3. We shall write this result as

$$\Delta E = 2\int_{-\infty}^{0} F(\eta, E)dE \tag{3}$$

with

$$F(\eta, E) = -\frac{1}{\pi}\,\mathrm{arctg}\,\frac{(4\pi^2/c^3)E^2v(E/c)^2f(E)}{1/\eta^2 - f(E)^2 + (4\pi^4/c^6)E^4v(E/c)^4},$$

$$f(E) = 4\pi\int_0^\infty \frac{p^2v(p)^2 - (E^2/c^2)v(E/c)^2}{E^2 - c^2p^2}Edp,$$

$$v(p) = (2\pi\hbar)^{-\frac{1}{2}}\int_0^\infty u(x)\exp i(p, x)/\hbar dx.$$

The argument of the arctangent is constrained by the boundary conditions to lie in the first or second quadrants.

A study of limiting cases for $\Delta E(\eta)$ has shown that for small η, $\Delta E \sim -\eta^2/E_{\mathrm{kin}}$ and for large η, $\Delta E \sim -|\eta|$. Since, with a simple form for $u(x)$, $\Delta E(\eta)$ should be a simple function of η, $\eta\partial\Delta E/\partial\eta$ is negative for all values of η. The quantity $\partial^2\Delta E/\partial\eta^2$ is negative for small η and zero for large so that in most simple examples it would be negative everywhere. These estimates of sign will be useful when spin-dependence is taken into account, for we shall direct particular attention to those cases in which the spin interaction may be considered as a perturbation and the perturbed expression for ΔE expanded in a series.

Spin-Dependent Interaction

Consider one heavy particle in the presence of all electrons in negative states. The electron states may be divided into two classes: those forming singlets with the heavy particle and those forming triplets. This classification is invariant to rotations in space and also time independent if there are no spin-orbit interactions (as here assumed). We shall, therefore, introduce spin-dependence by assuming that the interaction constant, η, is different when heavy and light particles form a singlet than when they form a triplet. In terms of the five invariants discussed in the previous work such a modification of the interaction is equivalent to adding the tensor-tensor product to the already assumed scalar-scalar product. The approximate form of the new interaction, corresponding to Eq. (2), then becomes

$$\bar{V} = -\eta\int dx\int dx'\rho_{is}{}^3[\delta_{mn}\delta_{sk} + \lambda(\sigma_{mn}, \sigma_{sk})]$$
$$\times\Psi_m{}^\dagger\Psi_n\psi_i(x)^\dagger\psi_k(x')u(x)u(x')^*, \tag{4}$$

where λ is a new constant and Ψ_m, $\Psi_m{}^\dagger$ are the (quantized) amplitudes of the heavy particle wave. Heavy particle functions must now be considered since the spin of the heavy particle may change as a consequence of the interaction.

Of the five invariant forms mentioned above it is also true that the product of pseudovectors would lead to spin-dependence without involving the negative states of heavy particles; but this operator will not be considered since it commutes with the operator on electron states, ρ_2, and may therefore modify the electric charge density in the lowest state of a heavy particle. The interaction (4) which we have chosen for further discussion anticommutes with ρ_2 and thus, according to the argument given in the former work, will present no difficulty with charge density. By the same argument it can be proved that, assuming (4), no contribution to the angular momentum of the lowest state of a heavy particle system will arise in the electron-positron field. It is thus assured that the multiplicity of the complete system of heavy particle and electrons in the lowest state is the same as for the heavy particle alone. The proof is as follows. The Hamiltonian,

$$H = -\rho_1(\sigma, cp) - \rho_3[mc^2 - V(p, q, \sigma)],$$

anticommutes with ρ_2; hence, $\rho_2 H\rho_2 = -H$, and the transformation ρ_2 changes all negative levels into positive levels and vice versa. On the other hand, the spin operator of the light particles, σ, commutes with ρ_2; the total spin when all positive energy levels are filled and all negative levels empty is then the same as when all negative levels are filled and all positive ones empty. But if all positive and negative energy levels were filled at the same time the total spin would be zero; hence, the electron spin in the lowest state of H vanishes also.

The indicated operator on spin-indices in (4) may be written in the notation of Dirac as

$$O_s=1+\lambda(\sigma, \sigma^h), \tag{5}$$

where σ^h is the heavy particle spin and σ the light particle spin. Proper states of O_s are, of course, proper states of (σ, σ^h), i.e., the triplet belonging to $+1$ and the singlet belonging to -3. Proper values of O_s are therefore $1+\lambda$ in the triplet and $1-3\lambda$ in the singlet. Interaction (4) may then be described as two interactions analogous to (2) with η replaced by $\eta(1+\lambda)$ when the heavy particle and the electron form a triplet and by $\eta(1-3\lambda)$ for singlet systems. A sum of energy changes in the electron levels taken over all possible spin configurations then leads to*

$$3\int F(\eta+\lambda\eta, E)dE+\int F(\eta-3\lambda\eta, E)dE. \tag{6}$$

In obtaining (6) heavy particle states of both spins are taken into account. Since the light particle field does not contribute to the angular momentum, (6) is the sum over two members of a doublet system. No difference in energy is to be expected between these states so that the change in energy caused by a single heavy particle is half of (6):

$$\Delta E_1=\tfrac{3}{2}\int F(\eta+\lambda\eta, E)dE+\tfrac{1}{2}\int F(\eta-3\lambda\eta, E)dE. \tag{7}$$

Expression (7) therefore replaces (3) when a spin-dependent interaction (4) is considered for one heavy particle.

Magnetic Moments of Proton and Neutron

It is well known that the observed magnetic moments of neutron and proton are not what would result from a relativistic theory of heavy particles analogous to the Dirac theory of the electron. One should suppose the magnetic moment of the neutron to be zero and that of the proton to be 1/1840 as much as the positron magnetic moment. Experiment shows, however, that the proton has about 1.8 nuclear magnetons more moment than would be expected on this basis and the neutron approximately as much less, i.e., the neutron apparently has a magnetic moment of the same sign as the electron and between one and two magnetons in magnitude. In order to explain these discrepancies it was proposed by Wick[4] that an interaction between heavy particles and a light particle field which would explain nuclear forces might also give rise to an anomalous magnetic moment. We shall, therefore, choose the spin-dependent interaction of neutron and of proton with the electron field in such a way as to account for their magnetic moments and then investigate the consequences of the choice on the forces between two heavy particles.

Let the electron which is governed by Eq. (1) be subject also to a small magnetic field represented by the vector potential, A. The change in proper energy may then be determined by a perturbation calculation. From the average value of the addition, $e\rho_1(\sigma, A)$, to the Hamiltonian we can obtain an expression for the operator of the magnetic moment of the electron

$$E'=-\int\bar{\psi}e\rho_1(\sigma, A)\psi dx$$

$$=\frac{-e}{2E}\int\bar{\psi}[H\rho_1(\sigma, A)+\rho_1(\sigma, A)H]\psi dx. \tag{8}$$

$\rho_1(\sigma, A)$ does not anticommute with ρ_3V' but the result is proportional to ρ_2 and its average value in the state ψ which is a proper state of a combination of ρ_1 and ρ_3 must vanish.

$$(\sigma, cp)(\sigma, A)+(\sigma, A)(\sigma, cp)=\hbar c(\sigma, \text{curl } A)-i\hbar \text{ div } A+2(A, p). \tag{9}$$

The part of the perturbing energy which is due to the action of the magnetic field, curl A, on the spin is then

$$E_\mu=-e\hbar c(\sigma, \text{curl } A)/2E \tag{10}$$

from which we conclude that the magnetic moment of the electron is $-e\hbar c\sigma/2E$, where E is the unperturbed energy.

We shall consider a heavy particle with upward spin. Let ax_1 and ax_1' be the average dis-

* Integrals over E will be understood to extend from $-\infty$ to zero.

[4] G. C. Wick, Accad. Lincei Atti **21**, 170 (1935).

placements of energy levels, E, of electrons with upward spin and let ax_2 and ax_2' be the average displacement when the spin is down. If the light and heavy particle spins are both up they certainly form a triplet so that expressions for x_1 and x_1' as functions of E are the same as formerly found for x (Eqs. (18) and (19), reference 3) except that η is replaced by $\eta+\lambda\eta$. If the electron spin is down the state is equally mixed from singlet and triplet states (i.e., a superposition of two states, one even, one odd under a reversal of spins) and thus an average over x and x' expressions in which η has been replaced by $\eta+\lambda\eta$ and by $\eta-3\lambda\eta$ must be taken. The magnetic moment arising from a given level, of energy E, is then

$$\begin{aligned} M_E = &-\tfrac{1}{2}e\hbar c\{(E+ax_1)^{-1}+(E+ax_1')^{-1} \\ &-(E+ax_2)^{-1}-(E+ax_2')^{-1}\} \\ &\cong(e\hbar c/2E^2)a(x_1+x_1'-x_2-x_2'). \end{aligned} \tag{11}$$

Summing over all negative energy levels the total magnetic moment due to the electron-positron field is

$$M=\tfrac{1}{4}\sigma_z{}^h e\hbar c\left\{\int F(\eta+\lambda\eta, E)\frac{dE}{E^2} - \int F(\eta-3\lambda\eta, E)\frac{dE}{E^2}\right\}. \tag{12}$$

In the special case that $|\lambda|\eta\ll\eta$, (12) may be expanded in a series of powers of λ:

$$M\cong\sigma_z{}^h e\hbar c\lambda\eta\int\frac{\partial F(\eta, E)}{\partial\eta}\frac{dE}{E^2} \tag{13}$$

from which it is apparent that the sign of the magnetic moment depends upon the sign of λ. From the former considerations[3] concerning the integration of ΔE one would conclude that

$$\eta\int\frac{\partial F(\eta, E)}{\partial\eta}\frac{dE}{E^2}\sim\begin{cases}-\eta^2/E_0{}^3 & \eta\ll E_0\\ -1/|\eta| & \eta\gg E_0\end{cases}, \tag{14}$$

where E_0 is the absolute value of the kinetic energy characteristic of the spatial extent of the wave functions $u(x)$. Now with $E_0\sim 137mc^2$, $e\hbar c/E_0\sim 30$ nuclear magnetons. Hence to account for the anomalous magnetic moment of the proton $-\lambda\eta^2/E_0{}^2\cong 1.8/30\cong\frac{1}{16}$ if η is small and $-\lambda E_0/|\eta|=\frac{1}{16}$ for large η. It is quite probable that with $\frac{1}{16}<|\lambda|<1$ the anomalous magnetic moment of the proton can be accounted for by assuming an interaction of the form (4) and with a negative "λ," $O_s{}^p=1-\lambda(\sigma, \sigma^h)$. The magnetic moment of the neutron would then be obtained by introducing a λ of the same absolute value but of positive sign, $O_s{}^n=1+\lambda(\sigma, \sigma^h)$.

Two Heavy Particles

When two heavy particles are considered two special configurations are readily treated. In one case the heavy particles are so widely separated that the $u(x)$ associated with one particle may be considered to vanish in the region in which the $u(x)$ centered on the other particle is appreciable. Then the V' operators commute and the influence of the heavy particles on the energy of the light particle field is simply additive. ΔE for two neutrons, two protons or proton and neutron at infinite separation is thus obtained by taking the corresponding sum of ΔE^n and ΔE^p. The superscripts refer to neutron and proton, respectively. Assuming $\frac{1}{16}<\lambda<1$ the results obtained for magnetic moments lead to the following expressions:

$$\begin{aligned} \Delta E^p &= \tfrac{3}{2}\int F(\eta-\lambda\eta, E)dE \\ &\quad +\tfrac{1}{2}\int F(\eta+3\lambda\eta, E)dE, \\ \Delta E^n &= \tfrac{3}{2}\int F(\eta+\lambda\eta, E)dE \\ &\quad +\tfrac{1}{2}\int F(\eta-3\lambda\eta, E)dE. \end{aligned} \tag{15}$$

The other special configuration occurs when two heavy particles occupy the same point in space. Two neutrons or two protons in a singlet state at a certain point form a spherically symmetrical system so that the spin coupling with the electron field vanishes. We shall use the subscript S on ΔE to denote a singlet state and double superscripts pp, nn, np in case of two particles at coincidence. Then

$$\Delta E_S{}^{nn}=\Delta E_S{}^{pp}=2\int F(2\eta, E)dE. \tag{16}$$

A proton and a neutron at the same point in space present a problem similar to that of a single particle. Consider one electron in a spherical state centered on the same point. The eight possible spin-states may be represented as one quartet and two doublets, i.e., proper states of $Q \equiv \lambda(\sigma, \sigma^n - \sigma^p)$. Taking the square and fourth power of Q

$$Q^4 = 12\lambda^2 Q^2, \tag{17}$$

from which we gather that the quartet belongs to zero and the doublets to $2\lambda\sqrt{3}$ and $-2\lambda\sqrt{3}$. The changes in energy of all electrons in negative states summed over all possible spin configurations of the heavy particles are then

$$\begin{aligned}\sum \Delta E^{np} = 4\int F(2\eta, E)dE \\ +2\int F(2\eta + 2\lambda\sqrt{3}\eta, E)dE \\ +2\int F(2\eta - 2\lambda\sqrt{3}\eta, E)dE.\end{aligned} \tag{18}$$

There are four spin configurations for two heavy particles: three members of a triplet and one singlet. The triplets are symmetric to an interchange of heavy particles so that they alone are affected by the quartet states in (18). Since the operator Q is antisymmetric to an interchange of neutron and proton the doublets are equally mixed of antisymmetric and symmetric functions. The terms in (18) which depend explicitly on λ are therefore half-singlets and half-triplets. From these considerations we obtain

$$\begin{aligned}\Delta E_T^{np} = \tfrac{4}{3}\int F(2\eta, E)dE \\ +\tfrac{1}{3}\int F(2\eta + 2\lambda\sqrt{3}\eta, E)dE \\ +\tfrac{1}{3}\int F(2\eta - 2\lambda\sqrt{3}\eta, E)dE,\end{aligned} \tag{19}$$

$$\begin{aligned}\Delta E_S^{np} = \int F(2\eta + 2\lambda\sqrt{3}\eta, E)dE \\ +\int F(2\eta - 2\lambda\sqrt{3}\eta, E)dE.\end{aligned}$$

The expressions (19) may be expanded in series and the following approximate energies for two coincident particles obtained:

$$\Delta E_S^{nn} = \Delta E_S^{pp} = 2\int F(2\eta, E)dE,$$

$$\begin{aligned}\Delta E_S^{np} = 2\int F(2\eta, E)dE \\ +6\lambda^2\eta^2\int \frac{\partial^2 F(2\eta, E)}{4\partial\eta^2}dE,\end{aligned} \tag{20}$$

$$\begin{aligned}\Delta E_T^{np} = 2\int F(2\eta, E)dE \\ +4\lambda^2\eta^2\int \frac{\partial^2 F(2\eta, E)}{4\partial\eta^2}dE.\end{aligned}$$

In consequence of the general conclusion that the second derivative of ΔE is negative we see from (20) that the lowest state in this approximation is the singlet deuteron, the next lowest the triplet deuteron and highest the singlet like-particle states. Experimental results[5] of scattering protons by protons and neutrons by protons indicate that the depths of the singlet wells should be the same for like and unlike particles. Relations (20) therefore force the conclusion that

$$\lambda^2\eta^2\int \frac{\partial^2 F(2\eta, E)}{\partial\eta^2}dE$$

be negligible compared with the maximum binding potential, $\equiv D$. Under this condition all the ΔE's in (20) become practically the same and the value of D is independent of λ:

$$\begin{aligned}D = 2\int F(2\eta, E)dE - 4\int F(\eta, E)dE \\ \left|\lambda^2\eta^2\int \frac{\partial^2 F(2\eta, E)}{\partial\eta^2}dE\right| \ll |D.|\end{aligned} \tag{21}$$

Relations (21) lead to an apparently unsatisfactory result in that the depth of potential wells for singlet and triplet deuteron should be

[5] M. Tuve, N. Heydenburg, L. Hafstad, Phys. Rev. **50**, 806 (1936); **53**, 239 (1938); G. Breit, E. Condon and R. Present, *ibid.* **50**, 825 (1936).

the same. Calculations with arbitrary, spherical, short range potentials have led to the result that the depth of the triplet well should be from 30 to 100 percent deeper than the singlet well. This apparent disagreement of our theory with experience might be rectified by dropping the assumption that λ is small and finding two values of the order unity which, when substituted in (12), would give the correct magnetic moments for neutron and proton. Whether such an assumption would lead also to satisfactory results with regard to forces in the two-particle systems cannot be determined, in general, without adopting a particular form for $u(x)$. There is one positive indication that $\lambda\eta \gg \eta$ would not be satisfactory because repulsions of the order of $\lambda\eta$ should arise as two heavy particles are brought together. These repulsions are due to the fact that, in general, the lowest proper states of individual heavy particles cannot be filled simultaneously when the heavy particles are close together. It is not within the scope of the present paper to investigate particular forms for $u(x)$, so that the possibility of using larger values of λ will be considered only for cases satisfying (21) with $\frac{1}{16} < \lambda < 1$.

It is not necessary that the potential well be deeper for the triplet than for the singlet deuteron if there is an angular dependence in the forces between neutron and proton. Forces of this type have been discussed by several authors in connection with nuclear forces and the electrical quadrupole moment of the deuteron.[6] It is proposed in these discussions that the forces between neutron and proton contain a part analogous to the interaction of electric or magnetic dipoles. Under such forces the lowest state of the two-particle system would not be spherical but would be elongated or flattened according to the sign of the interaction energy. The lowest state is then a superposition of spherical harmonics of higher order on the spherically symmetrical state than has been customarily assumed. A neutron and a proton in a spherical state with parallel spins can make a transition into a D state without violating the conservation of angular momentum but an analogous transition for particles with opposite spin (singlet) is impossible. The lowest triplet state of the deuteron may then be expected to lie lower than the singlet although the maximum depth of the potential wells is the same. In fact, Bethe has shown[6] for the neutral meson theory that the entire difference in binding for triplet and singlet deuteron can be ascribed to such an angular dependence. We propose, therefore, that the greater binding in the triplet is due alone to the angular dependence of the forces and thus is not in contradiction with the assumption $\frac{1}{16} < \lambda < 1$. It will not be possible to demonstrate quantitatively that the correct relation of triplet to singlet binding can be obtained without assuming a particular form for $u(x)$ and extending the calculation considerably. It will be shown, however, that an angular dependence in the potential which is of importance compared with the potential itself may be expected in the electron-positron field theory presented here.

Angular Dependence and Quadrupole Moment

An angular dependence in forces between neutron and proton would also account for the observed electrical quadrupole moment of the deuteron.[7] Present indications are that the lowest state of the triplet deuteron is prolate.[6] A potential which favors the prolate configuration may be written as a function of the unit vector, X, joining the two particles and of the distance, r, between particles:

$$V'' = -(\sigma^n, X)(\sigma^p, X)\, V''(r), \qquad (22)$$

where $V''(r)$ is assumed to be positive. We now assume, as before, a spin interaction constant, λ, for the neutron and $-\lambda$ for the proton. It is not proposed to find an exact solution of the two-body problem similar to (3); we shall rather consider a neutron and a proton not quite at the same point but sufficiently close that a description of electron states in spherical coordinates referred to the center of mass is adequate. If, at such small distances, a potential of the form (22) obtains it might be expected that the consequences discussed above will hold qualitatively for the type of interaction assumed and

[6] See H. A. Bethe, Phys. Rev. **55**, 1261 (1939).

[7] J. M. B. Kellogg, I. I. Rabi, N. F. Ramsey and J. R. Zacharias, Phys. Rev. **55**, 318 (1939).

quadrupole moment as well as binding energy could be correctly accounted for.

When two heavy particles are considered the state $v(p)$ with its interaction constant 2η applies only at coincidence. At finite separation it is convenient to set up orthogonal superpositions of $v_1(p)$ centered at one heavy particle and $v_2(p)$ at the other. Such an orthogonal set is, of course, the sum and difference. If two particles are close together and joined by a vector having the direction of the unit vector, X, the difference $v_1(p)-v_2(p)$ is approximated by the directional derivative of $v(p)$ and the sum $v_1(p)+v_2(p)$ by $v(p)$ itself. In the normalized form, therefore, we shall consider the function $v(p)$ centered on the center of mass and having the interaction constant $(\eta-\epsilon)$ and the function $(X,w)\sqrt{3}v(p)$ having the interaction constant ϵ. Here, $w=p/|p|$. The wave equation of an electron in this field then becomes

$$\begin{aligned}&(E-\rho_3E_p)\varphi'(p)+(\eta-\epsilon)v(p)\\&\quad\times\int T(p)\rho_3[1+\lambda(\sigma,\sigma^n-\sigma^p)]T^{-1}(p')\\&\quad\times v(p')^*\varphi(p')dp'+3\epsilon(w,X)v(p)\\&\quad\times\int T(p)\rho_3[1+\lambda(\sigma,\sigma^n-\sigma^p)]\\&\quad\times T^{-1}(p')(w',X)v(p')^*\varphi'(p')dp'=0\end{aligned}\tag{23}$$

with $T=1/\sqrt{2}[1+\rho_3\rho_1(\sigma,w)]$. We shall consider only very small values of ϵ, $\epsilon\ll\eta$. Then the functions $\varphi'(p)$ for which the influence of the interaction with the heavy particle is different from zero must contain a spherically symmetrical part. Following the steps of the previous treatment we accordingly choose $\varphi'(p)$ of the form $S(p)+(\sigma,w)P(p)$ where $S(p)$ and $P(p)$ are functions of the absolute value of p and also of heavy and light particle spins. Thus each $S(p)$ and $P(p)$ has sixteen components. Define

$$\xi_S=4\pi\int_0^\infty S(p)v(p)^*p^2dp$$

and

$$\xi_P=4\pi\int_0^\infty P(p)v(p)^*p^2dp.$$

Then if $\epsilon=0$, (23) becomes

$$\begin{aligned}&(E-\rho_3E_p)[S(p)+(\sigma,w)P(p)]\\&\qquad+\tfrac{1}{2}\eta v(p)\rho_3[1+\rho_1\rho_3(\sigma,w)]\\&\quad\times[1+\lambda(\sigma,\sigma^n-\sigma^p)][\xi_S+\rho_1\rho_3\xi_P]=0.\end{aligned}\tag{24}$$

Let $\xi=\xi_S+\rho_1\rho_3\xi_P$.

$$\begin{aligned}\varphi'(p)&=S(p)+(\sigma,w)P(p)\\&=-\tfrac{1}{2}\eta\frac{E\rho_3+E_p}{E^2-E_p{}^2}v(p)[1+\rho_1\rho_3(\sigma,w)]\\&\qquad\times[1+\lambda(\sigma,\sigma^n-\sigma^p)]\xi.\end{aligned}\tag{25}$$

The proper values, E, in (23) can be approximated by adding the average value in the state $\varphi'(p)$ of the term proportional to ϵ to the energy in that state. The perturbing energy is thus:

$$\begin{aligned}P=\epsilon&\int\varphi'(p)^\dagger v(p)T(p)\rho_3\\&\times\int[1+\lambda(\sigma,\sigma^n-\sigma^p)]\\&\times T^{-1}(p')v(p')^*\varphi'(p')dpdp'\\&-3\epsilon\int\varphi(p)^\dagger(w,X)v(p)T(p)dp\rho_3\\&\times\int[1+\lambda(\sigma,\sigma^n-\sigma^p)]\\&\times T^{-1}(p')(w',X)v(p')^*\varphi'(p')dp'.\end{aligned}\tag{26}$$

Integrating over $|p|$ and the angles:

$$\begin{aligned}P=&\tfrac{1}{2}\epsilon\xi\rho_3[1+\lambda(\sigma,\sigma^n-\sigma^p)]^3\xi\\&+\tfrac{2}{3}\epsilon\beta^2\xi\rho_3\{1+3\lambda(\sigma,X)(\sigma^n,X)\\&-3\lambda(\sigma,X)(\sigma^p,X)+6\lambda^2\\&-6\lambda^2(\sigma^n,X)(\sigma^p,X)+3\lambda^3(\sigma,X)(\sigma^n,X)\\&-3\lambda^3(\sigma,X)(\sigma^p,X)-\lambda^3(\sigma,\sigma^p)+\lambda^3(\sigma,\sigma^n)\},\end{aligned}\tag{27}$$

where

$$\beta=2\pi\eta\int_0^\infty\frac{E_pv(p)^2p^2dp}{E^2-E_p{}^2}.$$

The angularly dependent part of P is therefore

$$P_a(E)=-4\epsilon\beta(E)^2\xi\rho_3\lambda^2(\sigma^n,X)(\sigma^p,X)\xi.\tag{28}$$

The effect of P_a on the electron levels may be summed over all filled levels in an approximate way, sufficient for an order of magnitude estimate. If the perturbation had been simply a change in the interaction constant $\eta\to\eta-\epsilon$ only the first term in (27) would have been obtained. A sum over the first term is, therefore, prac-

tically equal to

$$-2\epsilon\int\frac{\partial F(\eta, E)}{\partial\eta}dE.$$

The same sum modified by multiplication with $2\beta^2$ occurs as a factor in (28). β^2 can be estimated from its relation to the solutions of the secular equations derived from (24) (see Eqs. (14) and (15) of reference 3).

$$2\pi\eta\int_0^\infty\frac{Ev(p)^2p^2dp}{E^2-E_p^2}=\pm\tfrac{1}{2}$$

whence $2\beta^2\sim\frac{1}{2}E_0^2/E^2$. Thus

$$\sum P_a\cong 4\epsilon\lambda^2(\sigma^n, X)(\sigma^p, X)E_0^2\times\int\frac{\partial F(\eta, E)}{\partial\eta}\frac{dE}{E^2}. \quad (29)$$

According to the considerations of magnetic moments, Eq. (13) and the subsequent discussion

$$\lambda\eta\int\frac{\partial F(\eta, E)}{\partial\eta}\frac{dE}{E^2}=\frac{-1}{16E_0},\quad \lambda>0,$$

whence

$$\sum P_a\cong-\tfrac{1}{4}\epsilon\lambda\frac{E_0}{\eta}(\sigma^n, X)(\sigma^p, X). \quad (30)$$

$\epsilon E_0/\eta$ in most cases should be of the order of magnitude of the change in total potential experienced by two particles as they are slightly separated. The angular part of the change in interaction between neutron and proton is, therefore, related to the total change in interaction by the fraction $\frac{1}{4}\lambda$. This estimate is very rough and applies only for small separations but it appears within the range of possibility that the angular dependence over the whole range of force is quite sufficient to give the desired nonspherical character to the potential well in the deuteron.

It is further satisfactory that when the heavy particles are separated in a direction parallel to their spins the energy perturbation (30) is negative. This means that the lowest state of the deuteron should be prolate, in agreement with indications from the quadrupole moment.

Conclusion

One would conclude that a satisfactory theory of nuclear forces may be built upon an interaction of neutrons and protons with the electron-positron field. This is apparent from the above work for such functions $\Delta E(\eta, \lambda)$ for which an expansion in a series of powers of λ is valid. The value of λ has been found from magnetic moment requirements to be larger than $\frac{1}{16}$. To obtain a significant angular dependence, however, λ may not be very much less than unity. The expansions in series are valid, therefore, only for those $\Delta E(\eta, \lambda)$ which are very nearly linear functions of η. The functions $\Delta E(\eta)$ become nearly straight lines for values of η larger than E_0. According to the above considerations a satisfactory theory would require: (1) $\eta\gg E_0$, (2) $\lambda E_0/\eta\cong\frac{1}{16}$, (3) λ comparable to, but less than, unity. These conditions are self-consistent.

Acknowledgment

The author wishes to take this opportunity to express his thanks to Professor Teller of The George Washington University and to Professor Wigner of Princeton University for the inspiration and assistance received from them during this study of nuclear forces and spin-dependence.

The Energies Released in the Reactions $Li^7(p, \alpha)He^4$ and $Li^6(d, \alpha)He^4$, and the Masses of the Light Atoms

NICHOLAS M. SMITH, JR.
Ryerson Physical Laboratory, University of Chicago, Chicago, Illinois

(Received July 17, 1939)

The energies of the alpha-particles arising from the reactions $Li^7(p, \alpha)He^4$ and $Li^6(d, \alpha)He^4$ have been measured by stopping the particles in a calibrated, variable pressure, air-filled absorption cell. The use of collodion windows on the cell instead of mica, the use of thin instead of thick targets, and the prevention of the formation of oil films on the targets, were improvements in technique over the older determinations of Oliphant, Kempton, and Rutherford. The energy release in the Li^7 disintegration was found to be 17.28 ± 0.03 Mev; that for the Li^6, 22.20 ± 0.04 Mev. These new values are used, together with the energies of the beryllium-proton disintegrations measured with the electrostatic analyzer, to set up masses for the light atoms concerned. The following values are obtained: Li^6, 6.01682 ± 0.00011, Li^7, 7.01784 ± 0.00009, Be^8, 8.00766 ± 0.00015, Be^9, 9.01486 ± 0.00013.

INTRODUCTION

IN a recent paper Allison[1] set up a provisional table of masses of the light atoms from disintegration data. The energies of some of the reactions used in his paper are not known with an accuracy comparable to that of the others, which were obtained in this laboratory by electrostatic deflection of the disintegration particles: Inasmuch as it is the absolute and not the percentage error which is important in mass determinations, it is necessary to know all large Q values to high precision. The present paper is a report of experiments to determine more accurately the energy released in the reactions $Li^7(p, \alpha)He^4$ and $Li^6(d, \alpha)He^4$. This was done by a comparison of the α-particle ranges with that of natural particles in an absorption cell. The most accurate measurement of these energies made previously was by Oliphant, Kempton, and Rutherford,[2] whose experiment is, in essence, duplicated here. They obtained a Q value of $22.06 \pm .07$ Mev for the Li^6 reaction which Livingston and Bethe[3] corrected to $22.07 \pm .07$, and $17.06 \pm .06$ Mev for the Li^7 reaction, similarly corrected to $17.13 \pm .06$. As in their experiment, the ranges here were compared with that of the shorter particles from Th C′.

[1] S. K. Allison, Phys. Rev. **55**, 624 (1939).
[2] M. L. E. Oliphant, A. E. Kempton, and Lord Rutherford, Proc. Roy. Soc. London **A149**, 406 (1935).
[3] M. S. Livingston and H. A. Bethe, Rev. Mod. Phys. **9**, 309, 318 (1937).

APPARATUS

The high voltage apparatus used was the Cockcroft-Walton circuit previously described by Hatch.[4] Positive ions were pulled by a tungsten probe from a low voltage capillary arc, so constructed that the ions had a path of only a few inches to traverse before receiving their first large acceleration. Magnetically separated beams of the order of ten microamperes of protons or deuterons were recorded as coming through the $\frac{1}{4}$-inch collimating apertures.

Thin targets were prepared by heating a bead of lithium fluoride on a nickel wire in a flame and holding a polished nickel target button for two or three seconds in the red flame above the bead. A faint cloud of the fluoride could be observed on the button after evaporation. Also a thin target of Li^6 separated in a mass spectrograph by L. H. Rumbaugh was used, and the agreement of mean range as calculated from it with that from the fluoride targets furnished proof of the thinness of the latter. Thin Th C′ sources were made by collecting the active emanation from radiothorium on a charged nickel button. After each run with the lithium target, the Th C′ source was quickly substituted and a run taken immediately afterward. The intensity of the Th C′ source was such that about 750 counts per minute were obtained on the flat part of the number-pressure curve. The curve

[4] G. T. Hatch, Phys. Rev. **54**, 165 (1938).

was taken with the pressure decreasing, and then repeated with the pressure increasing. The entire run could be completed in about 30 minutes, and during this time corrections for the decay of the source (effective half-life about 11 hours) were negligible. The Th C′ source was heated in the target chamber to prevent any oil film developing on it from the diffusion pumps. The same heating technique[4] was applied to the lithium fluoride and separated Li^6 targets. Targets of lithium fluoride, or other alkali halides, will discolor under ionic bombardment. This discoloration, however, is not due to carbonization of oil films, but represents a change in the halide itself, which may be similar to the effect produced by x-rays on the halides. Clean metallic targets, bombarded in the same way as the halide targets, show no brown deposit provided they are heated up from our filaments before bombardment begins.

Figure 1 is a drawing to scale of the absorption cell, target, and ionization chamber. The disintegration products were observed at 90° from the bombarding beam. Aperture C was circular and 0.636 cm in diameter. Apertures A and B were 0.953 cm in diameter. The brass plates containing A and B were seated accurately against shoulders on the cylindrical body of the absorption cell. They were held in place by collars and sealed by packing glands. The method of construction insures that the length of the cell is independent of the tightness with which the screws are drawn up to make the seal. The length of the cell was so chosen that the working pressure was always greater than atmospheric. Perforated copper screens[5] of transmission ratio 0.315 (ratio of open area to total area) covered apertures A and B as shown, and thin collodion films, of about 0.35 cm stopping power each, were placed on the high pressure sides of the screens. The low pressure side of the screen over B acted as the front plate of the ionization chamber. The rigid assembly consisting of the back plate and guard ring of the ionization chamber and first stage of the amplifier fitted snugly into the back of the cell as shown, and was held in firm mechanical contact by stretched rubber bands. It was found that this

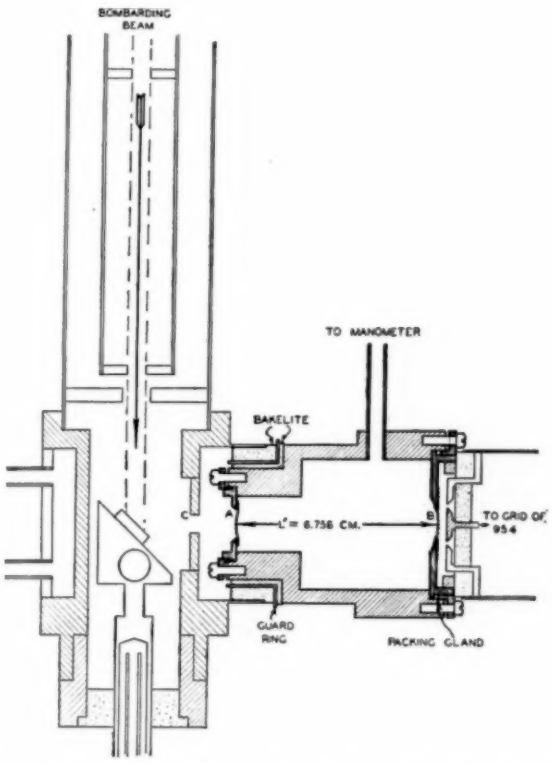

FIG. 1. The absorption cell, together with the target assembly and the ionization chamber.

was important to cut down amplifier noise arising from vibration. The depth of the chamber was 0.3 cm.

Air was admitted into the cell through a copper tube soldered into the side. The air was freed of moisture and carbon dioxide by passage through tubes of calcium chloride and sodium hydroxide. Its temperature was measured by a thermometer whose bulb rested on the cell. The pressure was measured in an open tube mercury manometer. A correction was made for the temperature of the mercury. A volume of several liters was placed on the line to stabilize the pressure. An accurate aneroid barometer measured atmospheric pressure. This was of use only for noting variations in pressure during a run. Such variations turned out to be negligible for most of the data.

In order to apply a voltage to the front plate of the ionization chamber, the entire absorption cell was raised to a potential of 216 volts by means of dry cells. The guard ring shown in the drawing served to keep leakage current from

[5] R. B. Bowersox, Phys. Rev. **55**, 323 (1939).

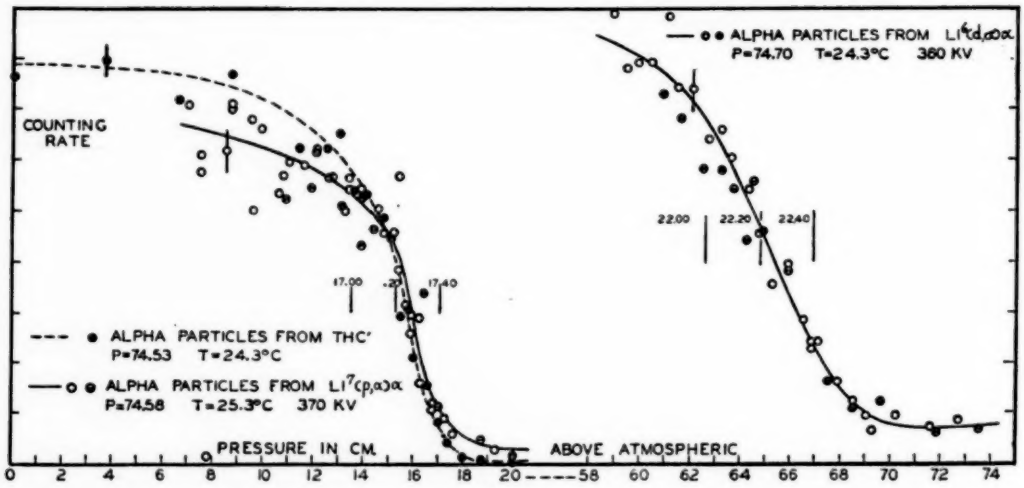

FIG. 2. A sample number-pressure curve for the natural α-particles from Th C′ and the artificial α-particles from each of the reactions: ${}_3Li^7(p, \alpha){}_2He^4$ and ${}_3Li^6(d, \alpha){}_2He^4$. The excess pressure corresponding to mean range for the Th C′ data was found by differentiation to be 15.7 cm Hg, for the Li^7 reaction 16.0 cm Hg, and for the Li^6 reaction 65.0 cm Hg. The vertical lines labeled 17.00, .20, 17.40 and those marked 22.00, 22.20, etc., refer to points where the maximum slope of the artificial α-particle curves should appear in order to give the indicated Q for the respective reactions.

being read by the beam galvanometer. The first stage of the amplifier was an RCA 954 Acorn type pentode. The tube is of small size, is not microphonic, and has a low input capacitance. The latter was further minimized by placing the tube in close proximity to the ionization chamber. A potential of about five volts was used on the heater and 22½ and 45 volts on screen and plate, respectively. The signal-to-noise ratio of the amplifier for alpha-particles was about 50 as measured on the oscilloscope, while the ratio of the biases on the scaling circuit which would just count alpha-particles to that which would just count background was 5. The scaling circuit was operated at a bias somewhat more negative than that at which background could be counted. The author estimates that it would count alpha-particles of residual range greater than 0.2 mm. This conclusion is based on an examination of the specific ionization curves of Holloway and Livingston.[6] At this bias the protons from deuterons on Li^6 were counted with the alpha-particles. Because of the long range of the protons, however, their presence made no difference in the shape of the alpha-particle curve. The bias for each lithium run was the same as for its Th C′ comparison. Sample curves are shown in Fig. 2.

THE COMPARISON OF RANGES WITH THE ABSORPTION CELL

The alpha-particle range *vs.* energy curves of Livingston and Bethe[3] apply to a pressure of 760 mm and a temperature of 15°C. We have therefore adopted these conditions as standard and reduced our readings to them. With this in mind, the action of the absorption cell in stopping a group of alpha-particles may be represented as follows:

$$R = L\frac{p+P}{76}\frac{288}{T} + C. \qquad (1)$$

In this expression R is the mean range in centimeters of the particles at 76 cm Hg pressure and 15°C; L is the length of path in the air of the absorption cell; p is the critical excess pressure in cm Hg corresponding to the mean range; P is the atmospheric pressure; T is the temperature in °K at which p was determined; and C is a constant of the absorption cell.

The constant C includes the air equivalent of the windows and the necessary penetration into the ionization chamber for registration as an alpha-particle. Since only light atoms occurred

[6] M. G. Holloway and M. S. Livingston, Phys. Rev. **54**, 18 (1938).

in the collodion of the films on the windows, the effect of the change of stopping power relative to that of air with energy of the alpha-particles is negligible. The air equivalent of C was approximately 0.8 cm.

The abscissa of the number *vs.* pressure curve at which the slope was a maximum was used for the computation of the relative mean range.

The absolute temperature T at which a curve was taken on artificial alpha-particles was usually the same as that of the comparison run on the Th C′ particles (taken immediately afterward). In the few cases in which a significant temperature change occurred between a run and its comparison, $\Delta(p+P)$ has been corrected before entry in the tables. We can thus assume T a constant for a run and its natural alpha-particle comparison. If ΔR is the difference between the mean ranges of two different homogeneous groups of alpha-particles, we can write

$$\Delta R=\frac{L}{T}\frac{288}{76}\Delta(p+P). \tag{2}$$

where $\Delta(p+P)$ is the increase in the total pressure in the absorption cell required to stop the artificial group.

The $Li^7(p, \alpha)He^4$ Reaction

Since the energy of the alpha-particles released in the artificial disintegration of Li^7 is almost exactly equal to that of the natural Th C′ particles, we may write

$$E_\alpha=E_n+\Delta R(dE/dR), \tag{3}$$

where E_α is the energy of the artificial particles, E_n that of the Th C′ particles, and dE/dR the slope of the range-energy curve in the region of 8.7 Mev. This slope is 0.64 Mev/cm. For the above reaction the energy release Q is given (at 90° to the bombarding beam of protons) by

$$Q=2E_\alpha-E_p(M_\alpha-M_p)/M_\alpha,$$

where the subscripts α and p refer to alpha-particles and protons, respectively, M's are masses, and E's, energies. On substitution of numerical values, and using Eqs. (2) and (3), we obtain

$$Q=2E_n-0.748E_p+k\Delta(p+P), \tag{4}$$

where

$$k=2(dE/dR)\frac{L}{T}\frac{288}{76}.$$

The $Li^6(d, \alpha)He^4$ Reaction

The disintegration particles from the Li^6-deuteron reaction, on the other hand, are so widely different in energy from those of Th C′ that one cannot assume the range-energy relation to be linear in the region. It is necessary to calculate the range of the artificial particles explicitly and then take the energy corresponding to this range as determined from the range-energy curves of Livingston and Bethe.[3] We may write

$$R_\alpha=R_n+k'\Delta(p+P), \tag{5}$$

where $k'=(L/T)(288/76)$.

The energy release Q in this reaction at 90° to the deuteron beam is given by

$$Q=2E_\alpha-0.4968E_d. \tag{6}$$

Corrections

Corrections for various sources of error must be estimated and applied.

(a) Window bulge

The pressure of the air in the absorption cell caused the thin copper screens in A and B to bulge outward slightly. The sagittae of the bulges of the windows were measured by means of a dial indicator. The position of contact with the copper screen of the movable ball point of the indicator was determined electrically. It was first shown that the bulges were fully developed at the pressure required to stop Th C′ particles; that is, no significant further bulge occurred when the pressure was raised to the critical point for the Li^6 particles. The absolute bulge, S_a, of window A was 0.063 cm, and S_b was 0.051 cm. The extreme distance in the cell between the tips of the bulges was 6.813 cm. Assuming that the bulges were in the form of spherical caps, a mean bulge was calculated such that half the particles traversed paths longer than this mean, and half shorter. From the sagitta formula it is easily shown that this mean is just half the total bulge. Therefore the

effective length is $6.813-\frac{1}{2}(S_a+S_b)$ or 6.756 ± 0.001 cm, and this value was used in the formulae.

(b) Temperature of the mercury manometer

The correction of the density of the mercury in the open end manometer was significant in the Li^6 reaction. It resulted in lowering $\Delta(p+P)$ by about 0.5 percent. The correction has been applied to k' in Table II.

(c) Obliquity

The geometrical effect due to finite size of the apertures limiting the alpha-particle beam results in a shortening of the observed ranges. This is a correction to be made to $\Delta(p+P)$, and is 0.13 percent as calculated from the formula of Livingston and Bethe.[7]

(d) Variation of bombarding voltage

During some runs the bombarding voltage varied by as much as 5 percent. In such cases, the observed number of particles was corrected for a change of yield with voltage. In the Li^7 reaction, the data of Haworth and King[8] were used for this purpose. However on the runs requiring correction for this effect, the scattering of the points was usually great for other reasons, and the runs were given low weight in averaging for the final result.

(e) Deviation of air from Boyle's law

The deviation from Boyle's law at the pressure of the Li^6 cut-off was computed from van der Waals' equation to require a correction of 0.10 percent. This correction is in the same direction as the obliquity correction, and both were applied to k' in Table II.

(f) Straggling

The most convenient aspect of the number-pressure curves to use in discussing the straggling is s, the difference between mean and extrapolated range, expressed in cm and reduced to 76 cm and 15°C. The three principal sources of straggling in these experiments were (1) range straggling s_1, due to the statistical nature of the loss of energy by the alpha-particle, (2) noise straggling s_2, due to the fact that the alpha-particle pulses coming from the amplifier were superimposed on a variable noise background, and (3) angle straggling s_3, due to the fact that the energy of alpha-particles from artificial disintegrations is a function of the angle of emission with respect to the bombarding beam.

The Th C′ curve of Fig. 2 should contain only range and noise straggling. The value of $\Delta(p+P)$ corresponding to the difference between mean and extrapolated ranges on this curve is $16.8-15.7=1.1$ cm, which, reduced by Eq. (2), gives $s_{12}(\text{obs.})=0.095$ cm. Other investigators have found[9] that for Th C′ alpha-particles s_1 is 1.08 percent of the 8.53 cm mean range or 0.092 cm. The agreement is good and shows that the noise straggling for the run was small compared to the range straggling.

If the aperture is sufficiently small, the angle straggling, present in the artificial disintegration curves, may be considered as superimposing a further Gaussian distribution of ranges on the range and noise straggling. The following considerations show that the aperture was sufficiently small for this method of considering the angle straggling.

From Fig. 1, it may be shown that the maximum angle that any alpha-particle can make with the axis of the absorption cell and be registered in the ionization chamber is about 4° 30′. Livingston and Bethe define the aperture angle of two circular openings of radius a, situated b cm apart, as a/b. This is half the maximum possible angular deviation; therefore in their sense our aperture angle was 2° 15′. A disintegration particle making an angle less than 90° with the bombarding beam will have energy greater than a particle leaving at exactly 90°, but must traverse more absorbing material to reach the ionization chamber. Thus there is a certain angle δ_0, measured from the forward direction of the bombarding beam, at which the projection of the range on the axis of the absorption cell

[7] M. S. Livingston and H. A. Bethe, reference 3, Eq. (778a), p. 280.
[8] L. J. Haworth and L. D. P. King, Phys. Rev. **54**, 38 (1938).
[9] M. S. Livingston and H. A. Bethe, reference 3, Fig. 37, p. 285.

is a maximum. Livingston and Bethe[10] show that δ_0 is given by

$$\cos \delta_0 = n \frac{(M_1 M_2)^{\frac{1}{2}}}{M} \left(\frac{E_1}{E_2}\right)^{\frac{1}{2}},$$

where n is the effective exponent of the velocity in the range *vs.* velocity curve at the energy of the emitted particle at 90°; M_1, M_2, M are the masses of the bombarding particle, disintegration particle, and intermediate nucleus, respectively; E_1, E_2 are the energies of the bombarding and disintegration particles.

For the Li^7 reaction we use $n=3.26$, $E_1=0.35$ Mev, $E_2=8.7$ Mev, and obtain $\cos \delta_0=0.16$, $\delta_0=80°$. For the Li^6 reaction, $n=3.33$, $E_1=0.36$ Mev, $E_2=11.1$ Mev, so that $\delta_0=77°$. These represent deviations from the axis of the absorption cell of 10° and 13°, respectively. Since our aperture is small compared to this, the geometry is "good."

The combined straggling s_{13}, due to range and angle straggling, may be found from

$$s_{13}=(s_1^2+\gamma^2)^{\frac{1}{2}}.$$

γ may be found[11] as a fraction of the mean range from

$$\frac{\gamma}{R}=\frac{a}{b} n \frac{(M_1 M_2)^{\frac{1}{2}}}{M} \left(\frac{E_1}{E_2}\right)^{\frac{1}{2}},$$

where a/b is the aperture angle in radians and the other symbols have their previous significance. a/b for our experiments is taken as 0.05. For the Li^7 reaction we get $\gamma/R=0.8$ percent, while for the Li^6 reaction γ/R is 1.0 percent. Since s_1 for the Li^6 reaction is 1.05 percent of the mean range, we obtain

$s_{13}=1.4$ percent which corresponds to 0.115 cm for Li^7

$s_{13}=1.5$ percent which corresponds to 0.191 cm for Li^6

with 12.8 cm as the mean range of the latter reaction.

The observed curve for the Li^7 disintegration particles in Fig. 2 shows an s value very close to that of the Th C′ comparison curve, and thus the observed s is slightly smaller than the predicted s_{13}. Agreement is, however, probably within experimental error.

The observed curve for the Li^6 disintegration in Fig. 2 shows $s_{13}(\text{obs.})=69.0-65.0=4.0$ cm pressure, which reduced by Eq. (2) gives 0.34 cm linear difference. This value is much larger than the s_{13} of 0.19 cm predicted above. The various curves for Li^6 obtained in the course of the work do not all agree with that of Fig. 2 in this respect, however. In the curve taken for trial 4 of Table II, the slope was steeper and from this curve we obtained $s=0.17$ cm, in agreement with the predicted s_{13}. *It is important to note that this change of observed s was not accompanied by any change in the excess pressure for maximum slope, that is, the mean range pressure.* The critical value of p for trial 2 of Table II was 65.0 cm; that of trial 4 was 64.8 cm.

We may attribute this change in observed s to the varying contribution from noise straggling. In general, the noise was more pronounced in the artificial disintegration experiments than in the Th C′ runs. This was due to the vibration from the belt-driven generator supplying power for the low voltage arc, from ripple in the high voltage coming down the bombarding beam and being picked up, etc. We may assume that conditions were fairly quiet in the Li^7 run of Fig. 2 and the Li^6 run of trial 4, Table II, and relatively noisy in the Li^6 curve of Fig. 2.

In conclusion, we may state that the amounts of straggling observed on our curves are not incompatible with those to be expected, and the straggling is of a symmetrical nature that will not change the location of the mean range pressure.

(g) Thickness of target

We have not made any correction for target thickness, but have assumed our targets to be thin. There is evidence for this in our experiments, aside from the method of preparation. The target of Li^6, made by Rumbaugh in a mass spectrograph, must certainly be considered as thin. The agreement of the mean range pressure observed from this target (trial 1 in Table II) with that from our volatilized LiF targets is strong evidence for the thinness of the latter.

[10] M. S. Livingston and H. A. Bethe, reference 3, Eq. (772), p. 278.
[11] M. S. Livingston and H. A. Bethe, reference 3, Eq. (777), p. 280.

The agreement in slope between the Li^7 and Th C′ curves of Fig. 2 is auxiliary, but not so conclusive, evidence, since the slopes may be affected by varying amplifier noise.

The Energy of the Th C′ Alpha-Particles

Briggs' latest value for the energy of the principal group of alpha-particles from Th C′ was used. He obtained $E_n = 8.7759 \pm 0.0009$ Mev.[12] The quantity $8.776 \pm .001$ Mev used in these calculations is unaffected by correction for new values of e/M for helium. According to Holloway and Livingston[5] this energy corresponds to a mean range of $8.570 \pm .007$ cm. On the range-energy curve published by Livingston and Bethe in 1937, on the other hand, this corresponds to a mean range of 8.530 cm. (The 1938 curve contains only values below 8.00 Mev.) However, one is concerned here only with an energy difference corresponding to a given range difference, so that if the whole range curve is displaced slightly, no error results. The value of dE/dR obtained from this curve for the Li^7 reaction was 0.064 Mev/mm.

Results

One set of data for each of the two reactions is plotted in Fig. 2. On these curves the excess pressure corresponding to the mean range for the Th C′ data was found by differentiation to be 15.7 cm Hg, for the Li^7 reaction 16.0 cm, and for the Li^6 reaction 65.0 cm Hg. The point just above the 8-cm mark on the abscissae is a point taken during a run on Li^7 when the bombarding beam of protons was thrown off the target by reversing the magnetic field. This experiment showed that the target holder was not contaminated with natural radioactivity from Th C′ targets which had frequently been attached to it, and thus that all the alpha-particles being counted actually came from the disintegration of Li^7. On both artificial disintegration curves the points in which the circle is traversed with a bar were taken after the target had been bombarded continuously by the beam for over an hour. They show that the LiF was not driven off the target by the action of the beam. The vertical lines labeled 17.00, .20, 17.40, and those marked 22.00, etc., refer to points where the maximum slope of the artificial alpha-particle curves should appear in order to give the indicated Q for the respective reactions. The data for the Li^7 reaction are summarized in Table I, and for the Li^6 reaction in Table II. The discrepancies given are average deviations. The vertical lines through points on the curves of Fig. 2 have a length $2M^{\frac{1}{2}}$ where M is the actual number of counts.

Table I. *The* $Li^7(p, \alpha)He^4$ *reaction. Calculation according to Eq. (4).*

Trial	k (Mev)/(cm Hg)	$\Delta(p+P)$ cm Hg	E_p Mev	Q Mev	Weight
1	0.1114	−0.69	0.325	17.23	2
2	0.1109	0.00	0.348	17.25	8
(Fig. 2)					
3	0.1100	0.22	0.365	17.31	1
4	0.1100	0.35	0.372	17.30	10
		Weighted Average		17.28±0.03 Mev.	
		Equivalent Milli-Mass Units		18.55±0.03	

These results may be used, in connection with the energies evolved in the beryllium-proton reactions,[13] to compute the masses of Li^6, Li^7, Be^8, Be^9 in terms of H^1, D^2, He^4. We take the following masses and reaction energies as basic to our calculations.

$H^1 = 1.00813 \pm 0.00002$,
$D^2 = 2.01473 \pm 0.00006$,
$He^4 = 4.00386 \pm 0.00006$.

$Li^6(d, \alpha)He^4$ $Q = 22.20 \pm 0.04$ Mev or 23.83 ± 0.04 mMU,

$Li^7(p, \alpha)He^4$ $Q = 17.28 \pm 0.03$ Mev or 18.55 ± 0.03 mMU,

$Be^9(p, \alpha)Li^6$ $Q = 2.152 \pm 0.04$ Mev or 2.311 ± 0.04 mMU,

$Be^9(p, d)Be^8$ $Q = 0.557 \pm 0.006$ Mev or 0.598 ± 0.006 mMU.

Using these values, we obtain

Li^6 6.01682±0.00011,
Li^7 7.01814±0.00009,
Be^8 8.00766±0.00015,
Be^9 9.01486±0.00013.

It is believed that these masses are the most reliable values available at present.

[12] G. H. Briggs, Proc. Roy. Soc. **A157**, 183 (1936).

[13] S. K. Allison, L. S. Skaggs, and N. M. Smith, Jr., Phys. Rev. **54**, 171 (1938). L. S. Skaggs, Phys. Rev. **56**, 24 (1939).

TABLE II. *The* $Li^6(d, \alpha)He^4$ *reaction. Calculation according to Eqs. (5) and (6). Range of* Th C′ *alpha-particle 8.530 cm.*

Trial	Target	k' corrected	$\Delta(p+P)$ (cm)	$k'\Delta(p+P)$ (cm)	R_α (cm)	E_α (Mev)	E_p (Mev)	Q (Mev)	Weight
1	Separated Li^6	0.0856	49.8	4.26	12.79	11.21	.350	22.24	3
2 (Fig. 2)	Thin LiF	0.0856	49.7	4.25	12.78	11.20	.358	22.23	10
3	Thin LiF	0.0849	48.8	4.14	12.68	11.14	.322	22.12	1
4	Thin LiF	0.0856	49.1	4.20	12.73	11.17	.324	22.18	10
					Weighted Average			22.20±0.04 Mev.	
					Equivalent Milli-Mass Units			23.83±0.04	

DISCUSSION

The Q values obtained in this work for the disintegrations of the lithium isotopes are both higher than the previous values found by Oliphant, Kempton, and Rutherford (17.28 *vs.* 17.06 and 22.20 *vs.* 22.06). Perhaps the most significant difference between the present work and that of the Cavendish investigators was the use of thin targets with precautions to prevent films forming over them. Both of these precautions, if they produced any effects at all, would tend to give higher mean ranges such as we have observed.

Barkas[14] has recently published a set of masses of the lighter elements in which the masses comparable with our list were communicated to him by Professor H. A. Bethe. The masses to be compared with ours are:

H^1 1.00812±0.00002,
D^2 2.01472±0.00002,
He^4 4.00388±0.00007,
Li^6 6.01690±0.00020,
Li^7 7.01804±0.00020,
Be^8 8.00777±0.00020,
Be^9 9.01497±0.00025.

This set agrees with ours within the uncertainties listed. Bethe* has re-interpreted the old result of Oliphant, Kempton, and Rutherford on the energy release in the reaction $Li^6(d, \alpha)He^4$ and raised their value of 22.06 Mev to 22.21 Mev. This revision receives a remarkable confirmation in our result of 22.20 Mev. The set of values recently published by Allison[1] were greatly dependent on the energy release assumed for this reaction, and were based on the 22.06 Mev value, which now seems definitely too low. The adoption of the higher value raises the mass of Be^8 until the uncertainty assigned to it overlaps twice the mass of the alpha-particle. Thus the question of the stability or instability of Be^8 is left undecided by the table. In a previous publication from our laboratory[15] we stated that Be^8 is stable by as much as 300,000 volts. With the revised values of the data used to supplement our results with the electrostatic analyzer, it is now seen that no such definite statement is compatible with the present accuracy of the mass values.

ACKNOWLEDGMENTS

This research was conducted under the supervision and with the help of Professor S. K. Allison. The author is indebted to Mr. L. S. Skaggs for the design of the absorption cell and to Professor W. D. Harkins and Professor J. B. Hoag for their generous loans of radiothorium and mesothorium. Thanks are also due the group headed by Dr. M. A. Tuve at the Carnegie Institution of Washington for their prompt and generous loan of the separated Li^6 targets prepared by Dr. L. H. Rumbaugh. Appreciation is expressed to Mr. G. J. Perlow and Mrs. E. R. Graves for assistance in taking data. Progress of the work was greatly aided by a grant from the American Philosophical Society to Professor Allison.

[14] W. H. Barkas, Phys. Rev. **55**, 691 (1939).
* H. A. Bethe, private communication.

[15] S. K. Allison, E. R. Graves, L. S. Skaggs, N. M. Smith, Jr., Phys. Rev. **55**, 107 (1939).

A Simple Picture of the Binding Energies of H^3 and He^5

KATHARINE WAY*
Bryn Mawr College, Bryn Mawr, Pennsylvania
(Received June 28, 1939)

It is shown that an approximate application of Wheeler's method of resonating groups to the nuclei, H^3 and He^5, makes it possible to evaluate the magnitude of different contributions to the total energy. The energy expressions are separated into terms representing the internal energy of a favorable sub-group, the kinetic energy of a particle outside the sub-group, and its "ordinary" and "velocity dependent" interaction with the sub-group. For H^3 the sub-group is the deuteron and for He^5 the α-particle. The results indicate considerable polarization of the deuteron and little polarization of the α-particle. The total energies found were $E(H^3)=-6.58$ mMU and $E(He^5)=-19.51$ mMU (for the most reasonable value of one parameter since no true minimum was found for He^5). These results are compared with those of other methods. The current two-body exchange forces were used (see Table I). The approximate method is quick and easy to handle. Application of the complete resonating group method to H^3, however, proved to be very laborious and difficult to make accurate. By this procedure $E(H^3)$ came out -6.68 mMU. The smallness of the improvement over the approximate method is attributed to the fact that the complete method does not take polarization into account. The calculated ground state energy for He^3 was -5.88 mMU by the approximate method and -5.94 mMU by the complete method. No bound excited state was found.

1. INTRODUCTION

IN the solution of the problem of atomic energies it is possible to evaluate the separate contributions to the total energy coming from the interaction of the different electrons with the nucleus and with each other. In contrast to the atomic results, calculations of nuclear binding energies do not, in general, yield a similar simple interpretation. This is to be expected for heavy nuclei for which the liquid drop model is a good approximation. In the lightest nuclei, however, there should be some evidence of simple structure, or tendency of particles to collect into sub-groups, which it should be possible to bring to light in the calculation of their binding energies. Such evidence should give some insight into the general situation in these nuclei. This would be especially desirable since the comparison of the light nuclei calculations with experiment will probably be a critical test for nuclear forces proposed in the future.

It is shown in this paper how the method of resonating group structure developed by Wheeler[1] makes it possible to give a simple interpretation to nuclear interactions in H^3 and He^5. The current two-body exchange force is used (see Table I for V_{ij}). It now seems clear that this force cannot account for many of the facts about light nuclei; nevertheless it seems reasonable to suppose that the evidence of structure will depend more on the wave function and the state of motion than on the exact nature of the interaction between nuclear particles.

The only important sub-group in H^3 would seem to be the deuteron, and in He^5 the α-particle. From stability considerations the grouping $2n+p$ in H^3 and either H^2+He^3 or He^2+H^3 in He^5 should be relatively unimportant. In the simple case of only one grouping the method of resonating group structure starts out with a wave function, Ψ, for the system written as the product of the internal wave function, φ, of the particles in the sub-group, and a function, F, which depends on the position of the outside particle with respect to the centroid of the sub-group. When Ψ is normalized and made properly antisymmetrical with respect to neutrons and protons[2] and inserted in the expression

$$E=\int \Psi^* H\Psi d\tau \Big/ \int \Psi^*\Psi d\tau, \qquad (1)$$

the result is

$$E=E_0+\frac{\hbar^2}{2\mu}\int \nabla F(\mathbf{X})\cdot\nabla F(\mathbf{X})d\mathbf{X}+\int V(\mathbf{X})F^2(\mathbf{X})d\mathbf{X}$$
$$+\int\int F(\mathbf{X})[J(\mathbf{X},\xi)-EI(\mathbf{X},\xi)]F(\xi)d\mathbf{X}d\xi. \qquad (2)$$

* Helen Schaeffer Huff Research Fellow. Now at University of Tennessee, Knoxville, Tennessee.

[1] J. A. Wheeler, Phys. Rev. **52**, 1083 and 1107 (1937).

[2] See appendix for complete resonating group wave functions for H^3 and He^5.

TABLE I. *Form of interaction, force constants, and approximate forms of F and ϕ used in calculation of binding energies of H^3 and He^5 by the resonating group method.*

$$V_{ij}=-B\exp(-br_{ij}^2)(1-g-g_1-g_2)P_{ij}^M+gP_{ij}^H+g_1\mathbf{1}+g_2P_{ij}^B$$

where P^M, P^H, and P^B are the Majorana, Heisenberg, and Bartlett operators, respectively.

$B=39.45$ mMU $\quad b=1.566(mc^2/e^2)^2 \quad g+g_2=0.22$
$=36.72$ Mev $\quad b^{-1}=2.25\times10^{-13}$ cm^2

FUNCTION	H^3 (1 AND 2 NEUTRONS)	He^5 (1, 2, AND 3 NEUTRONS)
$\mathbf{X}$	$\mathbf{r}_1-(\mathbf{r}_2+\mathbf{r}_3)/2$	$\mathbf{r}_1-(\mathbf{r}_2+\mathbf{r}_3+\mathbf{r}_4+\mathbf{r}_5)/4$
$F(\mathbf{X})(L=0)$	$\exp(-\beta X^2)$	$\exp(-\beta X^2)$
$F(X)(L=1)$		$\lvert X\rvert\cos\theta\exp(-\beta X^2)$
φ	$\exp(-\alpha r_{23}^2)$	$\exp[-\alpha(r_{23}^2+r_{24}^2+r_{25}^2+r_{34}^2+r_{35}^2+r_{45}^2)]$

μ is the reduced mass of the sub-group and the outside particle. $\mathbf{X}$ is the vector between the outside particle and the centroid of the sub-group and ξ is a similar vector when an exchange of particles has been made. $V(\mathbf{X})$, $J(\mathbf{X},\xi)$ and $I(\mathbf{X},\xi)$ can be found when φ is known and the integrations in (1) are carried out over the coordinates other than $\mathbf{X}$ and ξ and the coordinate of the centroid of the system.

The first term in (2), E_0, represents the internal energy of the sub-group; the second term the kinetic energy of the outside particle; and the third and fourth terms the interaction of the outside particle with the sub-group.

$$\int V(\mathbf{X})F^2(\mathbf{X})d\mathbf{X}$$

may be thought of as an "ordinary" potential energy and

$$\int\int F(\mathbf{X})[J(\mathbf{X},\xi)-EI(\mathbf{X},\xi)]F(\xi)d\mathbf{X}d\xi$$

as an effective velocity-dependent potential arising from the exchange of the outside particle with similar particles in the sub-group.

The resonating group method then makes use of the variation principle and proceeds to find the function, F, which makes E a minimum. Without going through this complicated procedure, however, interesting results can be obtained by using an approximate form for F in (2). The forms chosen for F and φ for both H^3 and He^5 are listed in Table I. The force constants used are also given there.

2. RESULTS FOR H^3 AND He^5 WITH APPROXIMATE RESONATING GROUP WAVE FUNCTIONS

The energies of H^3 and He^5 obtained with these resonating group wave functions depend on the parameters α and β in φ and F and, in the case of He^5, on the combination[3] $G_3=1+g-5g_1-3g_2$. G_3 is a factor of the V term which turns out to be positive, indicating a repulsive "ordinary" force. The requirement that heavy nuclear shall not have large spins leads however to the condition[4] $G_3\geqslant 0$. The value $G_3=0$ will therefore lead to the greatest binding.

For H^3, the minimum with respect to α and β is easily found. For He^5 there is a minimum with respect to the α-particle parameter, α, at $\alpha=0.505$. ($(1/\alpha)^{\frac{1}{2}}$ is proportional to the radius of the α-particle.) But for this value of α and for $G_3=0$, the only minimum with respect to β ($(1/\beta)^{\frac{1}{2}}$ is proportional to the mean separation of the neutron) is at $\beta=0$, a value which represents the outside neutron as being at an infinite distance from the α-particle group. Curves $RG(L=0)$ and $RG(L=1)$ of Fig. 1 show the resonating group results for states of He^5 of angular momenta $L=0$ and $L=1$. The state for $L=1$ is clearly lower than that for $L=0$. The point of inflection on the $L=1$ curve at about $\beta=1$ may be an indication of the existence of a virtual level.

For $L=1, \beta=1$, the contributions to the energy of He^5 from the different terms in (2) are listed in Table II and compared with similar terms for the values of the parameters which make $E(H^3)_{L=0}$ a minimum.

[3] In the notation of G. Breit and E. Wigner, Phys. Rev. **53**, 998 (1938), $G_3=-c_1=-(4V-M-2H+2B)$.
[4] N. Kemmer, Nature **140**, 192 (1937).

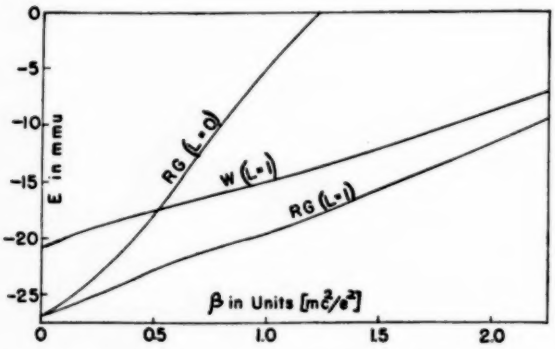

FIG. 1. Energy of He^5 as a function of the "outside" neutron parameter, β, for approximate resonating group wave functions, $RG(L=0)$ and $RG(L=1)$, and for the determinantal wave function of Watanabe, $W(L=1)$.

The values of E_0 in the tabulation show that neither the deuteron nor α-particle sub-group wave function has been very well chosen. For He^5 the value -26.94 mMU is the lowest which can be obtained for any value of α. For H^3, $\alpha=0.54$ gives a minimum for E_0 of -1.17 mMU, but this value of α gives a higher total energy for H^3. This can be interpreted as meaning that there is considerable polarization of the deuteron by the neutron in H^3 and very little polarization of the α-particle by the neutron in He^5.

The values of the kinetic energy of the neutron outside the sub-group are nearly the same in both cases and approximately equal to the average kinetic energy of a particle in the He^4 nucleus, 11 mMU.[5] This is approximately the same value found by Watanabe[5] for the p neutron after second-order perturbation corrections were applied to the regular Hartree function.

The "ordinary" potential is attractive in the H^3 case and zero for He^5 since G_3 was taken equal to zero. The "velocity dependent" potential is greater than the kinetic energy for H^3 but smaller for He^5. Coulomb terms which would still further increase the potential energy have not been included for He^5.

The breakdown of the total energy by this approximate method shows then that the interaction of Table I binds a neutron tightly to a deuteron group and not at all to an α-particle group.

For He^3 the grouping is H^2+p. The He^3 binding energy can be obtained from the H^3 value by merely adding the proper Coulomb terms. The result is -5.88 mMU. (Exp. value $=-8.1$ mMU.)

3. Comparison of Approximate Results with Results Using Other Functions

The results for the total energy by the resonating group method using the above approximate wave functions are compared with results for other simple wave functions in Table III.

For He^5, Watanabe[5] has tried a determinantal wave function involving two parameters similar to the α and β of the resonating group method. His calculations assume $g+g_2=0.25$. When the other values of the constants used here are substituted in his equation (15) and after this expression has been minimized with respect to α the curve in Fig. 1 marked $W(L=1)$ is found. It gives less binding than the resonating group $L=1$ curve for all values of β and thus, according to the variation principle, indicates that the determinantal function is less accurate than the resonating group function.

More complicated methods yield, of course,

[5] S. Watanabe, Zeits. f. Physik **112**, 159 (1939).

TABLE II. *Contributions of different terms in (2) to the total binding energies of* H^3 *and* He^5 *for approximate resonating group wave functions.*

TERM*	H^3 $L=0$ $S=\frac{1}{2}$ $\alpha=0.8$ $\beta=0.8$	He^5 $L=1$ $S=\frac{1}{2}$ $\alpha=0.54$ $\beta=1.00$ $G_3=0$
E_0	-0.67 mMU (Exp. val. $=-2.33$)	-26.94 mMU (Exp. val. $=-30.23$)
$\hbar^2/2\mu\int\nabla F(\mathbf{X})\cdot\nabla F(\mathbf{X})d\mathbf{X}$	$+10.12$	$+11.25$
$\int V(\mathbf{X})F^2(\mathbf{X})d\mathbf{X}$	-2.02	0.00
$\int\int F(\mathbf{X})[J(\mathbf{X},\xi)-EI(\mathbf{X},\xi)]F(\xi)d\mathbf{X}d\xi$	-14.01	-3.82
E (Total)	-6.58 mMU (Exp. val. $=-8.94$)	-19.51 mMU (Exp. val. $=-29.3$**)

* For algebraic expressions for all terms see appendix. Coulomb terms not included for He^5.
** Value of Williams *et al.* See discussion below.

TABLE III. *Comparison of approximate resonating group results with those for other simple functions.*

WAVE FUNCTION*	E (H^3) $L=0$ $S=\frac{1}{2}$	E (He^5) $L=1$ $S=\frac{1}{2}$
Resonating group	−6.58 mMU	−19.51 mMU ($\beta=1$)
Variation	−6.34**	
Hartree	−6.31**	−10.6***

* See appendix for forms of these functions.
** Above constants used. The difference of the resonating group and variation values from the ones given by Wheeler is due to use of slightly different constants.
*** Above constants used except $g+g_2=0.25$. Coulomb terms not included for either He^5 result.

better results. Margenau and Warren[6] using a variation function with twelve terms find $E(H^3) = -7.74$ mMU. By perturbation method Tyrrell, Carroll, and Margenau[7]* find $E(He^5) = -22$ mMU. Also using perturbation method Watanabe[5] finds $E(He^5) = -16.6$ mMU. The constants used by these authors differ slightly from each other and from the ones used here.

The present experimental data on He^5 may be summed up as follows. Investigation of the α-particles[8] and neutrons[9] from the reaction

$$D^2+Li^7 \rightarrow He^4+He^5,$$
$$He^5 \rightarrow He^4+n$$

seems to point clearly to a virtual level of He^5 0.84 Mev above the energy of a free neutron and α-particle, and a binding energy therefore of 29.3 mMU. Experiments[10] on the scattering of neutrons by α-particles agree with this result and indicate the level is a p state. From the bombardment of deuterons by low energy α-particles Joliot[11] finds evidence for a stable He^5 with binding energy 32.4 mMU. His experiments have not yet been repeated by other workers.

4. RIGOROUS APPLICATION OF RESONATING GROUP METHOD TO H^3 AND He^3

In the three-body problem, instead of the approximate functions for F and φ used above in the resonating group wave function, one can use a numerical function for φ, which is an exact solution of the deuteron wave equation, and then proceed to find the form of F which makes the energy a minimum. The complete method puts at one's disposal the adjustable function, F, rather than a number of adjustable parameters. Wheeler[2] shows that the radial equation for F can be written

$$f_L(r)+\int S_L(r,\rho)f_L(\rho)d\rho=0,$$

where S_L depends on V, J_L, I_L, and the energy E. The requirement that the Fredholm determinant of this equation vanish gives the eigenvalue of E. When this is known, $f_L(r)$ is easily found. The corresponding F is then the "best" function in the sense of the variation principle.

The results of carrying out this complicated procedure are $E(H^3) = -6.68$ mMU and $E(He^3) = -5.94$ mMU, very little improvement over the minima (−6.58 mMU and −5.88 mMU) obtained with the approximate functions. The complete method gives E_0, the deuteron binding energy, its full value of 2.33 mMU and does not therefore allow for any polarization. Its results are thus more strictly comparable with the approximate results when the E_0 there is required to have its minimum value of −1.17 mMU instead of the value −0.67 mMU which makes the total energy a minimum, that is when again no polarization is allowed. If this requirement is

[6] H. Margenau and B. E. Warren, Phys. Rev. **52**, 790 (1937).
[7] Tyrrell, Carroll, and Margenau, Phys. Rev. **55**, 790 (1939). Value given estimated from graph.
* *Note added in proof.*—W. A. Tyrrell, in a more recent detailed paper on He^5 (Phys. Rev. **56**, 250 (1939)), finds −20 Mev as the probable lower bound of the ^2P state. In addition the ^2S state is found to have practically the same energy. The two-parameter determinantal wave function for the state $L=1$ gives a curve very similar to that calculated from the equation of Watanabe since the values of the constants used differ only slightly. This curve is therefore quite similar to *RG* ($L=1$) curve. A two-parameter determinantal function for the state $L=0$, however, gives a curve not at all like the *RG* ($L=0$) curve but one which shows a distinct minimum at about −17 Mev for a finite value of the α-particle-neutron separation. This indicates superiority of the determinantal over the resonating group wave function in this case.
[8] Williams, Shepherd, and Haxby, Phys. Rev. **51**, 889 (1937).
[9] H. Staub and W. E. Stephens, Phys. Rev. **55**, 845 (1939).
[10] H. Staub and W. E. Stephens, Phys. Rev. **55**, 131 (1939).
[11] F. Joliot, J. de phys. et rad. **9**, 403 (1939).

imposed, the approximate functions give $E(H^3) = -5.84$ and $E(He^3) = -5.20$ mMU. The complete procedure thus gives an improvement over the approximate one of about 0.8 mMU. If polarization effects, or the dependence of φ on F, were taken into account, the results of the complete method might be considerably improved. The fact that in the case of He^5 the approximate resonating group method gives results which are comparable to those of much more complicated methods seems attributable to the small polarization of the α-particle. Watanabe[5] finds some evidences of polarization from a corrected Hartree wave function.

The complete procedure is very laborious on account of the large number of numerical integrations involved, many of which would be necessary even if an analytic expression for φ were used. It is also difficult to know when the size of the steps used in the numerical integrations has been made sufficiently small. Indeed, in the work leading to the above results energy values were obtained with large steps which were better than those presented. Increasing the number of steps must ultimately lead to an increase in accuracy but doubling the number of steps, for instance, increases the work fourfold. Also in an investigation of the $L=0$, $S=\frac{3}{2}$ state of H^3 a very queer result was obtained which was finally shown to be spurious and due to having taken the size of the steps too large.[12]

The resonating group method also presents in some cases another type of difficulty which can, however, be removed. The solution of the integral equation (3) proves in certain problems to be unstable with respect to small errors in the calculations. This is due to the singular nature of the numerator and denominator of the fraction (1). On choosing $F=e^{-\beta x^2}$ both numerator and denominator may vanish identically for a certain value of β, say β_0. This arises from the fact that the entire resonating group wave function itself, in the cases in question, vanishes identically for this choice of the intergroup wave function. The difficulty may be avoided in either of two ways. One can multiply the wave function by a suitably chosen power of $1/(\beta-\beta_0)$ and go to the limit $\beta=\beta_0$, where the wave function is finite (equivalent to calculating the limit of the fraction (1)). This procedure was actually followed in the He^5 calculations above for the case $L=0$, $\beta=5\alpha$. Or one may remove the difficulty by introducing a new function $\bar{F}$ connected with F by an operator equation $F=S\bar{F}$, chosen in such a way that neither numerator nor denominator of the fraction (1) vanishes for any nonzero choice of $\bar{F}$. This method is developed and applied in an unpublished paper by J. A. Wheeler on the interaction between two α-particles.

[12] Results for this state obtained with a Hartree function and very kindly sent by Dr. Tyrrell of Yale University were helpful in finding the source of the difficulty.

5. Excited State of He^3

Inspection of the p state functions J_1, I_1, and V as calculated by the complete method indicated that they would not lead to a bound state for He^3. An exact calculation for the state $L=0$, $S=\frac{3}{2}$ of this nucleus also showed that it could not be bound for any value of the combination, $1-3g_1-3g_2$, allowed by stability requirements of heavy nuclei.

6. Conclusions

If it turns out to be true that the quantum mechanics is strictly applicable to nuclear problems, a knowledge of the reliability and ease of handling different quantum-mechanical approximation methods will be important for trying out new ideas about forces. With regard to the resonating group method the above results lead to the following conclusions.

1. The use of the resonating group wave function with approximate analytic expressions for F and φ leads quickly and easily to energy values lower than those obtained with other simple functions. This is especially true when there is small polarization of the sub-groups.

2. The method permits a separation of the contributions to the total energy in such a way that one can see approximately what is going on in the nucleus.

3. The complete method, which uses the "best" form for F rather than an analytical approximation, is laborious and somewhat difficult to make accurate on account of the necessity for numerical integrations.

The writer is very much indebted to Professor John A. Wheeler of Princeton University

for many helpful discussions and to Miss Martha Cox and Miss Selma Blazer of Bryn Mawr College for assistance in checking some of the calculations.

Appendix 1

Resonating group wave functions:

H^3. Particles 1 and 2 neutrons.

$$\Psi=S_1F[1-(2+3)/2]\varphi(2\ 3)-S_2F[2-(1+3)/2]\varphi(1\ 3),$$
$$S_1=12^{-\frac{1}{2}}[\alpha(1)\alpha(2)\beta(3)+\alpha(1)\beta(2)\alpha(3)-2\beta(1)\alpha(2)\alpha(3)],$$
$$S=12^{-\frac{1}{2}}[\alpha(2)\alpha(1)\beta(3)+\alpha(2)\beta(1)\alpha(3)-2\beta(2)\alpha(1)\alpha(3)].$$

He^5. Particles 1, 2, and 3 neutrons.

$$\Psi=S_1F[1-(2+3+4+5)/4]\varphi(2345)+S_2F[2-(1+3+4+5)/4]\varphi(3145)+S_3F[3-(1+2+4+5)/4]\varphi(1245),$$
$$S_1=2^{-1}\alpha(1)[\alpha(2)\beta(3)-\beta(2)\alpha(3)]\times[\alpha(4)\beta(5)-\alpha(5)\beta(4)],$$
$$S_2=2^{-1}\alpha(2)[\alpha(3)\beta(1)-\beta(3)\alpha(1)]\times[\alpha(4)\beta(5)-\alpha(5)\beta(4)],$$
$$S_3=2^{-1}\alpha(3)[\alpha(1)\beta(2)-\beta(1)\alpha(2)]\times[\alpha(4)\beta(5)-\alpha(5)\beta(4)].$$

Variation wave function. H^3.

$$\Psi=2^{-\frac{1}{2}}\alpha(3)[\alpha(2)\beta(1)-\beta(2)\alpha(1)]\times\exp\left[-\tfrac{1}{2}\nu[r_{23}^2+r_{13}^2]-\tfrac{1}{2}\mu r_{12}^2\right].$$

Hartree wave function.

H^3. $\Psi=(3!)^{-\frac{1}{2}}|s\eta_1\cdot s\eta_2\cdot s\eta_3|$.

He^5. $\Psi=(5!)^{-\frac{1}{2}}|s\eta_1\cdot s\eta_2\cdot s\eta_3\cdot s\eta_4\cdot p\eta_1|$.

$\eta_1=\delta(s_z,\frac{1}{2})\delta(\tau_\xi,-\frac{1}{2})$, $\eta_3=\delta(s_z,\frac{1}{2})\delta(\tau_\xi,\frac{1}{2})$,
$\eta_2=\delta(s_z,-\frac{1}{2})\delta(\tau_\xi,-\frac{1}{2})$, $\eta_4=\delta(s_z,-\frac{1}{2})\delta(\tau_\xi,\frac{1}{2})$,

where τ_ξ is the isotopic spin quantum number

$$s=(\alpha/\pi)^{3/4}\exp(-\alpha r^2/2),$$
$$p=(\alpha/\pi)^{3/4}\sqrt{2\alpha}z\exp(-\alpha r^2/2).$$

For the He^5 two parameter determinantal wave function of Watanabe, the α in p is set equal to β.

Appendix 2

Resonating group energy expressions for $H^3(L=0, S=\frac{1}{2})$ and $He^5(L=1, S=\frac{1}{2})$ with the approximate wave functions of Table I.

H^3.

$$E_0=3\hbar^2\alpha/M-B/(1+b/2\alpha)^{\frac{1}{2}},$$

$$\hbar^2/2\mu\int\nabla F(\mathbf{X})\cdot\nabla F(\mathbf{X})d\mathbf{X}=9\hbar^2\beta/4M,$$

$$\int V(\mathbf{X})F^2(\mathbf{X})d\mathbf{X}=64B(\alpha\beta)^{\frac{1}{2}}\times(-\tfrac{1}{2}+\tfrac{3}{2}g-\tfrac{3}{2}g_1+\tfrac{3}{2}g_2)/(16\alpha\beta+2b\beta+8\alpha b)^{\frac{1}{2}},$$

$$\int\int F(\mathbf{X})I(\mathbf{X},\xi)F(\xi)d\mathbf{X}d\xi=256(\alpha\beta)^{\frac{1}{2}}/[(4\alpha+\beta)(4\alpha+9\beta)]^{\frac{1}{2}},$$

$$\int\int F(\mathbf{X})J(\mathbf{X},\xi)F(\xi)d\mathbf{X}d\xi=\hbar^2 3\times64^2(4\alpha+3\beta)(\alpha\beta)^{5/2}/M[(4\alpha+\beta)(4\alpha+9\beta)]^{5/2}-512B(\alpha\beta)^{\frac{1}{2}}\{(2-3g-\tfrac{3}{2}g_1-3g_2)/[(4\alpha+\beta)(4\alpha+9\beta+8b)]^{\frac{1}{2}}+1/[(4\alpha+\beta)(4\alpha+9\beta)+16\alpha b+20b\beta]^{\frac{1}{2}}\}.$$

He^5. $G=1-g-g_2$,

$$E_0=18\hbar^2\alpha/M-6GB/(1+b/4\alpha)^{\frac{1}{2}},$$

$$\hbar^2/2\mu\int\nabla F(\mathbf{X})\cdot\nabla F(\mathbf{X})d\mathbf{X}=2\hbar^2\beta/M,$$

$$\int V(\mathbf{X})F^2(\mathbf{X})d\mathbf{X}=G_3B2^{10}(\alpha\beta)^{5/2}\times(32+3b/\alpha)/[64\alpha\beta+2b(25\alpha+3\beta)]^{5/2},$$

$$\int\int F(\mathbf{X})I(\mathbf{X},\xi)F(\xi)d\mathbf{X}d\xi=2^{13}(\alpha\beta)^{5/2}/[(3\alpha+\beta)(25\alpha+3\beta)]^{5/2},$$

$$\int\int F(\mathbf{X})J(\mathbf{X},\xi)F(\xi)d\mathbf{X}d\xi=2^{13}(\alpha\beta)^{5/2}\times\{[188\hbar^2\alpha/5M-3GB/(1+b/4\alpha)^{\frac{1}{2}}]/[(3\alpha+\beta)(25\alpha+3\beta)]^{5/2}-4\hbar^2\alpha[2775\alpha^2+458\alpha\beta-49\beta^2]/5M[(3\alpha+\beta)(25\alpha+3\beta)]^{7/2}-B(6b-16\alpha)(3G+G_3)/16\alpha[(3\alpha+\beta)(25\alpha+3\beta)+50\alpha\beta+9b\beta]^{5/2}-B6G(4\alpha)^{\frac{1}{2}}(4\alpha+b)/[25\alpha^2(12\alpha+5b)+34\alpha\beta(4\alpha+b)+\beta^2(12\alpha+b)]^{5/2}\}.$$

Theory of Secondary Emission

D. E. WOOLDRIDGE
Bell Telephone Laboratories, New York, New York

(Received June 9, 1939)

The production of secondary emission by the interaction of bombarding electrons with the valence electrons of a metal target is quantum-mechanically treated. When the results are modified by considerations having to do with the relative rates of absorption of the primary and secondary particles, yield-*vs.*-bombarding energy curves are obtained which approximate the results of experiment. The primary voltage required for maximum yield, the effect of work function on the emission, and the energy range of the secondary particles are semi-quantitatively derived in terms of the properties of the target material.

IN Fröhlich's[1] theory of secondary emission there are errors which seriously affect the nature of the conclusions reached.[2] When these errors are removed, the result is a prediction that the rate of production of secondaries is independent of the energy of the bombarding primaries, rather than proportional to the square root of this energy, as Fröhlich concluded. But such a result does not appear to resemble the results of measurements. It develops that the shape of the secondary yield *vs.* primary energy curve may be a result of the fact that, in a distance less than the mean free path of the secondaries, the primary electrons may lose so much energy that they can produce no more secondaries. This conclusion will be reached as one of the products of the theory of secondary emission which is developed in the following pages.

At the beginning of Fröhlich's treatment, certain assumptions are made as to the nature of the fields inside the metal, which effectively make the theory a one-dimensional one. For example, one could not obtain any information about the distribution in direction of the secondaries from a theory of this sort. Furthermore, these assumptions make it impossible to estimate the relative importance of the neglected terms in the final result. In this paper a development is presented in which these assumptions are not made. It has been found possible to set up the quantum-mechanical problem in such a way as to lead to a solution which is more general than that given by Fröhlich.

For the convenience of the reader, this paper is divided into two sections. In the first section the fundamental problem of the interaction between the primary and the metal electrons is treated quantum-mechanically. In the second section the results of this quantum-mechanical treatment are so manipulated as to lead to explicit conclusions concerning the nature of secondary emission which can be compared with experiment.

I. QUANTUM-MECHANICAL DEVELOPMENT

The general nature of the problem has been stated by Fröhlich and may be repeated here very simply. A beam of electrons is caused to bombard a metal target. After penetrating the surface, these "primary" electrons move in a region in which they must occasionally approach some of the valence (or "lattice") electrons which are thought of as traveling around in the metal. Because of the repulsive forces thus set up, some of the lattice electrons may be given high enough energies that they can escape from the target and be observed as "secondary" electrons. In treating any problem of this nature one generally commences by neglecting the fields in the metal. But, as Fröhlich has pointed out, the usual type of secondary emission, in which electrons are ejected from the bombarded surface of the target, cannot be accounted for by this "free electron" approximation. Obviously, energy and momentum could not be conserved. Hence

[1] H. Fröhlich, Ann. d. Physik 5, **13**, 229 (1932).

[2] For example, in the equation at the top of p. 240 of Fröhlich's paper, the important term $-K_x(\pm k_x+2\pi n/a)$ has been omitted. In addition, the integration of Eq. (19″), p. 238, through which Fröhlich concluded that the secondary yield should reach a maximum and then decrease with increasing primary energy, has been extended into a region of values which can be shown to be excluded by conservation of energy considerations.

it is necessary for the theory to take account of the fact that the valence electrons are not free, but are acted upon by forces which make it possible for them to "bounce" out of the bombarded surface, the net momentum change of the process being absorbed by the metal lattice.

Although it is necessary to take into account the binding of the valence electrons to the lattice, it is nevertheless a good approximation to neglect binding terms as far as the primary electrons are concerned—for we are interested only in the forces exerted by the primary electrons and these forces will not be greatly influenced by the small restraints acting on the primaries.

The problem will then be set up as follows. Initially a beam of primary electrons, each of kinetic energy $\hbar^2K^2/2m$ and of momentum $\hbar\mathbf{K}$, is traveling through the metal lattice. Inside the lattice there is a single electron, which initially occupies one of the quantum states permitted by the particular periodicity of the lattice fields. Because of the interaction between these two electrons, there is a calculable rate at which the initial state, as above defined, varies into other states, some of which lead to secondary emission. It is this rate of change which is to be computed.

In this computation the "primary" and "lattice" or "metal" electrons (as in Fröhlich's development) will be treated like distinguishable particles. The exclusion principle will finally be taken account of in two ways—first, by the use of Fermi statistics in summing the results of the above-outlined calculations over all the lattice electrons; second, by ruling out all transitions which leave an electron in an already occupied state.

The lattice will be assumed to have a simple cubic structure throughout this calculation. It will be shown that the results obtained can be applied to other crystalline types without serious error, however. In a simple cubic lattice, the unperturbed eigenfunctions[3] are of the form given by Bloch

$$u_{\mathbf{k}}(\mathbf{r})\exp[i(\mathbf{k}\cdot\mathbf{r})],$$

where $u_{\mathbf{k}}(\mathbf{r})$ has the periodicity of the lattice. For most metals $u_{\mathbf{k}}(\mathbf{r})$ differs only slightly from unity ($\mathbf{k}$ is *not* the "reduced" wave vector) so that $\hbar\mathbf{k}$ is very nearly the momentum of the electron and $\hbar^2k^2/2m$ is very nearly its kinetic energy. As the unperturbed probability amplitude of our system of two particles we take

$$\psi_{\mathbf{k},\,\mathbf{K}}=\frac{1}{\Omega}u_{\mathbf{k}}(\mathbf{r})\exp[i(\mathbf{K}\cdot\mathbf{R})+i(\mathbf{k}\cdot\mathbf{r})],$$

where, of course, $\psi\psi^*d\tau_{\mathbf{R}}d\tau_{\mathbf{r}}$ is the probability of finding a primary electron in the volume element $d\tau_{\mathbf{R}}=dXdYdZ$ at the position $\mathbf{R}$ and a lattice electron in the volume element $d\tau_{\mathbf{r}}=dxdydz$ at the position $\mathbf{r}$. ψ has here been normalized so as to require the existence of one primary electron and one lattice electron somewhere within the volume Ω, and $u_{\mathbf{k}}$ is assumed to have been normalized so that

$$(u_{\mathbf{k}}^*u_{\mathbf{k}})_{\Omega}=1. \tag{1}$$

For this problem the perturbation potential is simply the Coulombian repulsion energy

$$U=e^2/|\mathbf{R}-\mathbf{r}|.$$

From the usual treatment of the method of variation of constants[4] we can write

$$|a_{\mathbf{k}',\,\mathbf{K}'}|^2=\frac{1}{\hbar^2}|U_{\mathbf{k},\,\mathbf{K};\,\mathbf{k}',\,\mathbf{K}'}|^2\cdot\frac{2(1-\cos\epsilon t)}{\epsilon^2}, \tag{2}$$

where

$$U_{\mathbf{k},\,\mathbf{K};\,\mathbf{k}',\,\mathbf{K}'}\equiv\frac{1}{\Omega^2}\int\frac{e^2}{|\mathbf{R}-\mathbf{r}|}u_{\mathbf{k}}(\mathbf{r})u_{\mathbf{k}'}^*(\mathbf{r})\times\exp[i(\mathbf{K}-\mathbf{K}')\cdot\mathbf{R}+i(\mathbf{k}-\mathbf{k}')\cdot\mathbf{r}]d\tau_{\mathbf{r}}d\tau_{\mathbf{R}}$$

and

$$\epsilon\equiv(E_{\mathbf{k}',\,\mathbf{K}'}-E_{\mathbf{k},\,\mathbf{K}})/\hbar. \tag{3}$$

In the usual way $|a_{\mathbf{k}',\,\mathbf{K}'}|^2$ is interpreted as representing the probability that, at the time t, the system will be in the state specified by the vectors $\mathbf{k}'$ and $\mathbf{K}'$ when, at $t=0$, the system was started in the state $\mathbf{k}, \mathbf{K}$. As Fröhlich has pointed out, the restrictions imposed by the Born approximation can be shown to be unimportant down to primary energies lower than those with which we shall be concerned.

In evaluating $U_{\mathbf{k},\,\mathbf{K};\,\mathbf{k}',\,\mathbf{K}'}$ we can employ a

[3] N. F. Mott and H. Jones, *Properties of Metals and Alloys* (Oxford, 1936), p. 57.

[4] Reference 3, p. 250.

result given by Bethe,[5] who showed that

$$\int \frac{\exp[i(\mathbf{K}-\mathbf{K}')\cdot\mathbf{R}]}{|\mathbf{R}-\mathbf{r}|}d\tau_{\mathbf{R}}=\frac{4\pi\exp[i(\mathbf{K}-\mathbf{K}')\cdot\mathbf{r}]}{|\mathbf{K}-\mathbf{K}'|^2}. \tag{4}$$

Hence

$$U_{\mathbf{k},\,\mathbf{K};\,\mathbf{k}',\,\mathbf{K}'}=\frac{1}{\Omega^2}\cdot\frac{4\pi e^2}{S^2}\int u_{\mathbf{k}}(\mathbf{r})u_{\mathbf{k}'}{}^*(\mathbf{r})\times\exp(i\mathbf{S}\cdot\mathbf{r}+i\mathbf{s}\cdot\mathbf{r})d\tau_{\mathbf{r}}, \tag{5}$$

where

$$\mathbf{S}\equiv\mathbf{K}-\mathbf{K}';\qquad \mathbf{s}\equiv\mathbf{k}-\mathbf{k}'.$$

We may expand

$$u_{\mathbf{k}}(\mathbf{r})=\sum_{\mathbf{m}}a_{\mathbf{m}}(\mathbf{k})\exp[2\pi i(\mathbf{m}\cdot\mathbf{r})/a].$$

"a" is the lattice spacing and $\mathbf{m}$ is a vector for which each component is a positive or negative integer. The summation extends over all values of $\mathbf{m}$ which this single restriction permits. The normalization condition (1) requires that

$$\sum_{\mathbf{m}}a_{\mathbf{m}}a_{\mathbf{m}}{}^*=1.$$

With the above expansion, Eq. (5) becomes

$$U_{\mathbf{k},\,\mathbf{K};\,\mathbf{k}',\,\mathbf{K}'}=\frac{1}{\Omega^2}\frac{4\pi e^2}{S^2}\sum_{\mathbf{m},\,\mathbf{n}}\int a_{\mathbf{m}}(\mathbf{k})a_{\mathbf{n}}{}^*(\mathbf{k}')\times\exp[i(\mathbf{S}+\mathbf{s}+2\pi\boldsymbol{\varrho}_{mn}/a)\cdot\mathbf{r}]d\tau_{\mathbf{r}},$$

where

$$\boldsymbol{\varrho}_{mn}\equiv\mathbf{m}-\mathbf{n}.$$

This may also be expressed as

$$U_{\mathbf{k},\,\mathbf{K};\,\mathbf{k}',\,\mathbf{K}'}=\frac{1}{\Omega^2}\frac{4\pi e^2}{S^2}\sum_{\boldsymbol{\varrho}}\left([\sum_{\mathbf{m}}a_{\boldsymbol{\varrho}+\mathbf{m}}(\mathbf{k})a_{\mathbf{m}}{}^*(\mathbf{k}')]\times\int\exp[i(\mathbf{S}+\mathbf{s}+2\pi\boldsymbol{\varrho}/a)\cdot\mathbf{r}]d\tau_{\mathbf{r}}\right), \tag{6}$$

where $\boldsymbol{\varrho}$ and $\mathbf{m}$ are to be summed independently over all vectors which have integral components.

At this point we may notice that, for $U_{\mathbf{k},\,\mathbf{K};\,\mathbf{k}',\,\mathbf{K}'}$ to have an appreciable value,

$$\mathbf{S}+\mathbf{s}+2\pi\boldsymbol{\varrho}/a\sim 0. \tag{7}$$

This is our momentum principle. In the special case of free electrons only the term $\boldsymbol{\varrho}=0,0,0$ appears in the summation and (7) reduces to the familiar conservation of momentum relation.

From (6), Eq. (2) may now be written

$$|a_{\mathbf{k}',\,\mathbf{K}'}|^2=\frac{1}{\hbar^2}\frac{1}{\Omega^4}\left(\frac{4\pi e^2}{S^2}\right)^2\left|\sum_{\boldsymbol{\varrho}}\left([\sum_{\mathbf{m}}a_{\boldsymbol{\varrho}+\mathbf{m}}(\mathbf{k})a_{\mathbf{m}}{}^*(\mathbf{k}')]\times\int\exp[i(\mathbf{S}+\mathbf{s}+2\pi\boldsymbol{\varrho}/a)\cdot\mathbf{r}]d\tau_{\mathbf{r}}\right)\right|^2\times\frac{2t^2(1-\cos\epsilon t)}{(\epsilon t)^2}. \tag{8}$$

This expression involves the product of two terms, one of which differs from zero only when, for some allowed $\boldsymbol{\varrho}$, $\mathbf{S}+\mathbf{s}+2\pi\boldsymbol{\varrho}/a\sim 0$, the other of which is appreciable only when $\epsilon t=(t/\hbar)(E_{\mathbf{k}',\,\mathbf{K}'}-E_{\mathbf{k},\,\mathbf{K}})\sim 0$. These two conditions define regions in six-dimensional $\mathbf{k}'$, $\mathbf{K}'$ space within which $|a_{\mathbf{k}',\,\mathbf{K}'}|^2$ differs appreciably from zero. Suppose we fix $\mathbf{k}'$. Then there will be discrete values of $\mathbf{K}'$ (one for each possible value of $\boldsymbol{\varrho}$) for which the integral in (8) will have an appreciable value. For any one of these allowable values of $\mathbf{K}'$, the function $(1-\cos\epsilon t)/(\epsilon t)^2$ may or may not differ appreciably from zero. If Ω is very large, then the range of $\mathbf{K}'$ around any allowed value for which the integral in (8) is of importance will be so small that $(1-\cos\epsilon t)/(\epsilon t)^2$ may be considered constant over this region. If $\mathbf{K}'_{\rho}$ is a value of $\mathbf{K}'$, for a given $\mathbf{k}$, $\mathbf{K}$ and $\mathbf{k}'$, allowed by our momentum principle, we obtain, by integrating (8)

$$|c_{\mathbf{k}',\,\mathbf{K}'_{\rho}}|^2=\frac{1}{\Omega^2}\cdot\frac{16\pi^2e^4}{\hbar^2}\frac{1}{S_{\rho}{}^4}\times|\sum_{\mathbf{m}}a_{\boldsymbol{\varrho}+\mathbf{m}}(\mathbf{k})a_{\mathbf{m}}{}^*(\mathbf{k}')|^2t^2F(\epsilon_{\rho}t)$$

where we have defined

$$F(\epsilon_{\rho}t)=\frac{2(1-\cos\epsilon_{\rho}t)}{(\epsilon_{\rho}t)^2}. \tag{9}$$

Adding such results for all possible $\boldsymbol{\varrho}$, we get

$$|a_{\mathbf{k}'}|^2\equiv\sum_{\rho}|a_{\mathbf{k}',\,\mathbf{K}'_{\rho}}|^2=\frac{1}{\Omega^2}\frac{16\pi^2e^4}{\hbar^2}t^2\times\sum_{\rho}\left(\frac{1}{S_{\rho}{}^4}F(\epsilon_{\rho}t)|\sum_{\mathbf{m}}a_{\boldsymbol{\varrho}+\mathbf{m}}(\mathbf{k})a_{\mathbf{m}}{}^*(\mathbf{k}')|^2\right)$$

[5] H. Bethe, Ann. d. Physik 5, 5, 325 (1930).

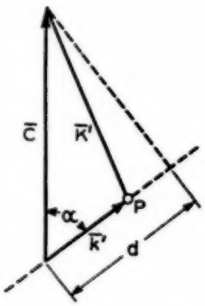

FIG. 1. Vector diagram illustrating momentum principle $\mathbf{C}=\mathbf{k}+\mathbf{K}+2\pi\boldsymbol{\varrho}/a$.

$|a_{\mathbf{k}'}|^2$ is to be interpreted as the probability, that, at the time t, a lattice electron will be found in the state $\mathbf{k}'$. In the usual way[6] the summation can be converted to an integral by multiplication by $\Omega/8\pi^3$. This gives, for the number of lattice electrons which, at time t, have their wave vectors in a range $d\tau_{\mathbf{k}'}$ around $\mathbf{k}'$,

$$dN=\frac{\Omega}{8\pi^3}\cdot\frac{1}{\Omega^2}\frac{16\pi^2e^4}{\hbar^2}t^2 \times\sum_{\rho}\left(\frac{1}{S_\rho{}^4}F(\epsilon_\rho t)\left|\sum_{\mathbf{m}}a_{\rho+\mathbf{m}}(\mathbf{k})a_{\mathbf{m}}{}^*(\mathbf{k}')\right|^2\right)d\tau_{\mathbf{k}'}. \quad (10)$$

This result was derived for the case wherein Ω contained only one primary and one lattice electron. Let N_p and $N_l(\mathbf{k})$ represent the actual numbers of primary and lattice electrons, respectively, present in the volume Ω, and let ρ_p and $\rho_l(\mathbf{k})$ denote N_p/Ω and $N_l(\mathbf{k})/\Omega$. If the primary current density is J_p (electrons cm^{-2} sec.$^{-1}$) and if the velocity of the primary electrons is V, then

$$\rho_p=J_p/V.$$

But
$$V=\hbar K/m; \quad (11)$$

$$\therefore \quad \rho_p=J_pm/K\hbar.$$

When Eq. (10) is multiplied by $N_l=\rho_l\Omega$ and by $N_p=J_pm\Omega/K\hbar$, it becomes

$$dN=\sum_{\rho}dN_\rho,$$

where

$$dN_\rho=J_p\Omega t^2\cdot\frac{2me^4}{\pi\hbar^3}\rho_l(\mathbf{k})\frac{1}{K}\left(\frac{1}{S_\rho{}^4}F(\epsilon_\rho t) \times\left|\sum_{\mathbf{m}}a_{\rho+\mathbf{m}}(\mathbf{k})a_{\mathbf{m}}{}^*(\mathbf{k}')\right|^2\right)d\tau_{\mathbf{k}'}. \quad (12)$$

[6] Reference 3, p. 56.

Thus the problem reduces to a consideration of dN_ρ, for a given value of $\boldsymbol{\varrho}$. The following considerations will apply to such a case—where $\boldsymbol{\varrho}$ is fixed. Under these circumstances the momentum condition (7) has shown that the only final states which can appear are those for which

$$\mathbf{S}+\mathbf{s}+2\pi\boldsymbol{\varrho}/a=0$$

or
$$\mathbf{K}'+\mathbf{k}'=\mathbf{K}+\mathbf{k}+2\pi\boldsymbol{\varrho}/a. \quad (13)$$

Let us now see what additional restrictions are imposed by virtue of the fact that $F(\epsilon_\rho t)$, in (12), has appreciable values only in the vicinity of $\epsilon_\rho=0$. This, of course, is the "conservation of energy" principle. We will assume that t is sufficiently large that $F(\epsilon_\rho t)$ is a much more rapidly varying function than any others remaining in the problem. Now for energy considerations, it is a good enough approximation to write

$$E_{\mathbf{k},\mathbf{K}}=\hbar^2(k^2+K^2)/2m.$$

The condition $\epsilon_\rho=0$ then becomes, simply,

$$k'^2+K'^2=k^2+K^2. \quad (14)$$

The values of $\mathbf{k}'$, $\mathbf{K}'$ which correspond to final states are those which simultaneously satisfy Eqs. (13) and (14). In Fig. 1 the vector diagram corresponding to Eq. (13) is shown. In terms of the distances and angles shown in this figure, it is easy to demonstrate that, for a given α (always measured so as to be $<\pi/2$), Eq. (14) is satisfied only by the two magnitudes of k' given by the equation

$$k'=\frac{d}{2}\left[1\pm\left(1-\frac{D^2}{d^2}\right)^{\frac{1}{2}}\right], \quad (15)$$

where it has been convenient to define

$$\mathbf{C}\equiv\mathbf{K}+\mathbf{k}+2\pi\boldsymbol{\varrho}/a \quad (16)$$

and
$$D^2\equiv 2(C^2-k^2-K^2). \quad (17)$$

Evidently, from Fig. 1,

$$d=C\cos\alpha.$$

In Eq. (15), k' is considered positive if its direction makes an angle of $<\pi/2$ with that of $\mathbf{C}$, negative otherwise.

The result given by Eq. (15) may be expressed in a convenient geometrical way. If a sphere of radius

$$R=[\tfrac{1}{4}(C^2-D^2)]^{\frac{1}{2}} \quad (18)$$

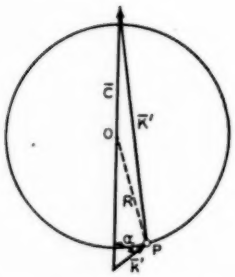

FIG. 2. Diagram illustrating effect of simultaneous operation of momentum and energy principles. The only probable transitions are those for which P lies on the sphere of radius

$$R=\tfrac{1}{2}[K^2-2\mathbf{K}\cdot(\mathbf{k}+2\pi\mathbf{\varrho}/a)+k^2-(2\pi\mathbf{\varrho}/a)^2-2\mathbf{k}\cdot(2\pi\mathbf{\varrho}/a)]^{\frac{1}{2}}.$$

is constructed with its center at the midpoint of the vector $\mathbf{C}$, Eq. (15) may be shown to be equivalent to the statement that the point P (Fig. 1) must lie on the surface of the sphere. A cross section of this geometrical construction is shown in Fig. 2. R may be $\gtrless C$ but if R becomes imaginary (Eq. (18)) there can occur no transitions.

To evaluate N_ρ (Eq. (12)) we have yet to perform an integration over $\mathbf{k}'$. Fig. 2 suggests that this integration be split into spherical components by the substitution

$$d\tau_{\mathbf{k}'}=dRd\sigma,$$

where $d\sigma$ is a spherical surface element. Let us now perform the integration with respect to R. Since $F(\epsilon_\rho t)$ is a much more rapidly varying function than any other term in Eq. (12), we may consider the other terms to be constant for this integration. Thus we wish to evaluate

$$\int F(\epsilon t)dR=\int\frac{F(\epsilon t)d(\epsilon t)}{d(\epsilon t)/dR}.$$

From Fig. 2

$$k'^2+K'^2=2R^2+\tfrac{1}{2}C^2=2mE_{\mathbf{k}',\,\mathbf{K}'}/\hbar^2 \qquad (19)$$

or, from (3),

$$2R^2+\tfrac{1}{2}C^2=(\hbar\epsilon+E_{\mathbf{k},\,\mathbf{K}})\cdot 2m/\hbar^2;$$

$$\therefore\quad d(\epsilon t)/dR=2R\cdot\hbar t/m.$$

Hence we may write

$$\int F(\epsilon t)dR=\frac{m}{2\hbar t}\cdot\frac{1}{R}\int F(\epsilon t)d(\epsilon t), \qquad (20)$$

where, from (9),

$$\int F(\epsilon t)d(\epsilon t)=\int_{-\infty}^{+\infty}\frac{2(1-\cos x)}{x^2}dx=2\pi;$$

therefore, from Eq. (20),

$$\int F(\epsilon t)dR=\frac{1}{t}\cdot\frac{\pi m}{\hbar}\cdot\frac{1}{R}.$$

Thus the first integration of Eq. (12) yields

$$dN_\rho=J_p\Omega t\cdot\frac{2m^2e^4}{\hbar^4}\rho_l(\mathbf{k})\frac{1}{R}\frac{1}{K}$$

$$\times\left(\frac{1}{S_\rho^4}\left|\sum_{\mathbf{m}}a_{\rho+\mathbf{m}}(\mathbf{k})a_{\mathbf{m}}^*(k')\right|^2\right)d\sigma. \qquad (21)$$

Consider the variable part of Eq. (21)—i.e., the expression within the brackets. The summation of the Fourier components of the unperturbed lattice eigenfunctions is a term which would not be expected to exhibit any very pronounced dependence on $\mathbf{k}'$. $1/S^4$, on the other hand, turns out to have values differing importantly from zero over only a small fraction of the surface of our sphere. This may be seen from the following considerations.

In Fig. 3 the vector $\mathbf{C}$ is shown resolved into its components $\mathbf{k}+2\pi\mathbf{\varrho}/a$ and $\mathbf{K}$. If we define

$$\mathbf{A}=\tfrac{1}{2}\mathbf{C}-(\mathbf{k}+2\pi\mathbf{\varrho}/a)$$
$$=\tfrac{1}{2}(\mathbf{K}+\mathbf{k}+2\pi\mathbf{\varrho}/a)-(\mathbf{k}+2\pi\mathbf{\varrho}/a),$$

then

$$A^2=\tfrac{1}{4}[K^2-2\mathbf{K}\cdot(\mathbf{k}+2\pi\mathbf{\varrho}/a)+(\mathbf{k}+2\pi\mathbf{\varrho}/a)^2]. \qquad (22)$$

Now, from Eqs. (16), (17) and (18),

$$R^2=\tfrac{1}{4}[K^2-2\mathbf{K}\cdot(\mathbf{k}+2\pi\mathbf{\varrho}/a)+k^2$$
$$-(2\pi\mathbf{\varrho}/a)^2-2\mathbf{k}\cdot 2\pi\mathbf{\varrho}/a]. \qquad (23)$$

From Eqs. (22) and (23)

$$A^2=R^2+\tfrac{1}{2}\cdot 2\pi\mathbf{\varrho}/a\cdot[2\pi\mathbf{\varrho}/a+2\mathbf{k}]. \qquad (24)$$

Now S is the length of the vector which joins the point Q (Fig. 3) to a point P on the sphere. Evidently the minimum possible value of S is

$$S_{\min}=A-R. \qquad (25)$$

If the primary electrons are of high energy (this assumption will be examined shortly) so that $2\pi\mathbf{\varrho}/a\ll K$ and $k\ll K$, then $R\sim\frac{1}{2}K$ and Eq. (24)

may be expanded to give

$$A\sim R+\left(\frac{1}{4}\frac{2\pi\varrho/a\cdot[2\pi\varrho/a+2\mathbf{k}]}{R^2}\right)R \quad (26)$$

or

$$S_{\min}\sim\left(\frac{1}{4}\frac{2\pi\varrho/a\cdot[2\pi\varrho/a+2\mathbf{k}]}{R^2}\right)R. \quad (27)$$

Since $2\pi\rho/a\ll R$,

$$S_{\min}\ll R.$$

Inasmuch as $1/S^4$ appears in Eq. (21), it is clear that the right side of the equation will have large values over only a small fraction of the surface of our sphere—i.e., when PP' (See Fig. 3) $\lesssim(2\pi\varrho/a)\cdot[2\pi\varrho/a+2\mathbf{k}]/K$. This conclusion is of considerable physical importance. It means that, for a given $\mathbf{k}$, $\mathbf{K}$ and ϱ, transitions are probable only to final states for which $\mathbf{k}'\sim\mathbf{O'P'}$ (See Fig. 3), where $\mathbf{O'P'}$ differs from the vector $\mathbf{k}+2\pi\varrho/a$ only by terms very much smaller than this vector. When, at the end of the present manipulations, we sum our results over all possible values of ϱ, this will mean that, when primary electrons of wave number $\mathbf{K}$ interact with lattice electrons of wave number $\mathbf{k}$, the lattice electrons are finally left in discrete groups, one group belonging to each of the possible values of ϱ.

An immediate consequence of the conclusion that $1/S^4$ has important values over only a small region of our sphere is that, in integrating Eq. (21), we can safely treat the Fourier terms as constants. We are left with $\int d\sigma/S^4$ to evaluate. This can easily be integrated over the surface of the sphere. The result is

$$\int\frac{d\sigma}{S^4}=\frac{4\pi R^2}{(A^2-R^2)^2}. \quad (28)$$

Or, from Eq. (24),

$$\int\frac{d\sigma}{S^4}=\frac{16\pi R^2}{[(2\pi\varrho/a)\cdot(2\pi\varrho/a+2\mathbf{k})]^2}.$$

Thus the integration of Eq. (21) has given

$$\frac{1}{\Omega}\frac{dN_\rho}{dt}=\frac{16\pi m^2e^4}{\hbar^4}\rho_l(\mathbf{k})\frac{J_p[2R/K]_\rho}{[(2\pi\varrho/a)\cdot(2\pi\varrho/a+2\mathbf{k})]^2}\times|\sum_{\mathbf{m}}a_{\rho+\mathbf{m}}(\mathbf{k})a_{\mathbf{m}}^*(\mathbf{k}+2\pi\varrho/a)|^2, \quad (29)$$

where N_ρ/t has been replaced by dN_ρ/dt, to indicate that our result really expresses the time rate at which lattice electrons are being knocked into new states. For large K, $2R/K=1$, and Eq. (29) does not involve the energy of the bombarding primaries.

The complete solution of our problem is obtained by summing Eq. (29) over all possible values of ϱ. But now the work of Morse[7] indicates that the coefficients $a_{\mathbf{n}}$ of the Fourier expansion of the lattice eigenfunctions diminish rapidly with increasing $|n|$ and that, even for $|n|=1$, $a_{\mathbf{n}}a_{\mathbf{n}}^*\sim10^{-2}$, as compared with $a_{000}a^*_{000}\sim1$. This means that

$$\begin{aligned}&|\sum_{\mathbf{m}}a_{\rho+\mathbf{m}}(\mathbf{k})a_{\mathbf{m}}^*(\mathbf{k}+2\pi\varrho/a)|^2\\&\sim|a_\rho(\mathbf{k})a_{000}^*(\mathbf{k}+2\pi\varrho/a)+a_{000}(\mathbf{k})a_\rho^*(\mathbf{k}+2\pi\varrho/a)|^2\\&\sim|a_\rho(\mathbf{k})+a_{-\rho}^*(\mathbf{k}+2\pi\varrho/a)|^2\equiv|b_\rho(\mathbf{k})|^2. \quad (30)\end{aligned}$$

Evidently, further, $|b_\rho(\mathbf{k})|^2$ diminishes with increasing $|\varrho|$. In addition, the denominator in (29) increases rapidly with increasing $|\rho|$. Hence a pretty good first approximation to the solution of our problem should be afforded by a consideration of only the values

$$\begin{aligned}\varrho&=0,\ 0,\ \pm1,\\ \varrho&=0,\ \pm1,\ 0,\\ \varrho&=\pm1,\ 0,\ 0.\end{aligned}$$

A great deal of the following discussion will be based upon this approximation.

In deriving Eq. (29) K has been assumed to be large, compared with $2\pi/a$ and k. Let us now examine this restriction on the range of applicability of our result.

For the usually observed secondaries, $\mathbf{k}'$ and $\mathbf{K}$ point approximately in opposite directions. Since we have seen that $\mathbf{k}'\sim\mathbf{k}+2\pi\varrho/a$, this

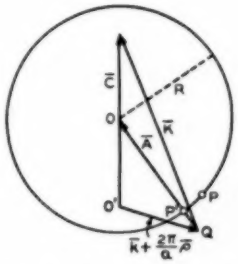

FIG. 3. Diagram showing how $S_{\min}$ is determined.

[7] P. M. Morse, Phys. Rev. **35**, 1311 (1930).

means that $R \lesssim \frac{1}{2}K$, as given by Eq. (23), as long as $|\mathbf{K}| > |\mathbf{k}+2\pi\boldsymbol{\varrho}/a|$. For these considerations we may set $\mathbf{k}=0$, not merely because $k<2\pi/a$, but also because $\mathbf{k}\cdot\boldsymbol{\varrho}$ is as often positive as negative and therefore has an average value of zero. Thus we may conclude that the expansion of Eq. (26) is valid as long as

$$\frac{(2\pi\varrho/a)^2}{K^2} \ll 1.$$

If this fraction is, say, $\sim\frac{1}{4}$, the conclusion that $1/S^4$ has a large value over only a small fraction of our sphere will be a pretty good one and the consequent neglect of the variation of the Fourier components in the integration, as well as the conclusion that $\mathbf{k}'=\mathbf{k}+2\pi\boldsymbol{\varrho}/a$, will be good enough for our purposes. For silver, for example, $(\hbar^2/2m)(2\pi/a)^2 \sim 25$ ev. This means that, for the calculation corresponding to $|\rho|=1$, our results should be good down to a primary energy of, say, 100 ev. For the calculations corresponding to $|\rho|>1$, the results become accurate only for higher values of primary voltage. However we have seen that the cases for which $|\rho|>1$ are of only secondary importance and for a first approximation can be neglected.

A more detailed investigation shows that, even when $|\mathbf{k}+2\pi\boldsymbol{\varrho}/a| \sim K$, and when $\mathbf{k}'$ and $\mathbf{K}$ do not point in opposite directions, the important region for $1/S^4$ is still sufficiently small that the neglect of the variation of the Fourier components in the integration, as well as the conclusion that $\mathbf{k}' \sim \mathbf{k}+2\pi\boldsymbol{\varrho}/a$, are fair approximations (as far as the use to which they will be put is concerned). For this range the factor $[2R/K]_\rho$ in Eq. (29) expresses the dependence on K of the results of the bombardment. Eq. (23) provides an explicit expression of this dependence. Since we will be concerned only with bombarding energies considerably greater than the Fermi energy of the electrons, we may neglect k^2/K^2 compared to one, in which case Eq. (23) may be written

$$F_\rho(\mathbf{k},\mathbf{K}) \equiv \left[\frac{2R}{K}\right]_\rho = \left[1-\frac{(\mathbf{k}+2\pi\boldsymbol{\varrho}/a)^2}{K^2}-\frac{2\mathbf{K}\cdot(\mathbf{k}+2\pi\boldsymbol{\varrho}/a)}{K^2}\right]^{\frac{1}{2}}. \quad (31)$$

In terms of Eqs. (30) and (31), Eq. (29) now becomes

$$\frac{1}{\Omega}\frac{dN_\rho}{dt} = \frac{16\pi m^2 e^4}{\hbar^4}\rho_l(\mathbf{k})J_p \times \frac{|b_\rho(\mathbf{k})|^2}{[(2\pi\boldsymbol{\varrho}/a)\cdot(2\pi\boldsymbol{\varrho}/a+2\mathbf{k})]^2}F_\rho(\mathbf{k},\mathbf{K}). \quad (32)$$

This equation should be reasonably valid down to the lowest bombarding energies we shall need to consider. The dependence of dN_ρ/dt on K is small and not at all of the right form to account for the observed shape of secondary yield *vs.* bombarding voltage curves.

At this point the effect of the exclusion principle may be disposed of. Besides requiring the use of Fermi statistics in summing the results over all the lattice electrons, the exclusion principle, as Fröhlich pointed out, forbids any final state for which either k' or K' is less than $k_{\max}$, the value of k corresponding to the top of the Fermi distribution in the metal. This is equivalent to the requirement that $(\hbar^2/2m)k'^2$ and $(\hbar^2/2m)K'^2$ must each exceed $E_{\max} \equiv (\hbar^2/2m)(k_{\max})^2$. Since, for the final states of interest, $\mathbf{k}'=\mathbf{k}+2\pi\boldsymbol{\varrho}/a$, where $|\rho|=1$, a lattice electron, on the average, absorbs energy of amount (very nearly).

$$E_0 \equiv (\hbar^2/2m)(2\pi/a)^2$$

from the primary electron which collides with it. Thus the exclusion principle requires that the production of secondaries fall off rapidly when

$$E_p \gtrsim E_0 + E_{\max}.$$

For silver, $E_0 \sim 25$ ev and $E_{\max} \sim 5$ ev. We should therefore expect the secondary emission to drop rapidly to zero when the bombarding energy E_p (measured *inside* the target) drops below 25 or 30 ev.

Free electron approximation

Before proceeding with the development it is necessary to examine the free electron approximation in the light of the foregoing results. If we start with Eq. (21) and carry out the appropriate computation, assuming $|\mathbf{k}| \ll |\mathbf{K}|$, we

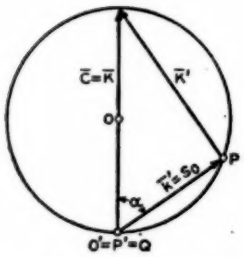

FIG. 4. Special case of momentum principle for which $\rho=0$.

obtain

$$\frac{1}{\rho_1 J_p}\frac{1}{\Omega t}(dN_0)_{tot} = \frac{e^4}{m^2V^4}(\sec^4\alpha+\csc^4\alpha)4\cos\alpha d\omega. \quad (33)$$

This is the familiar Rutherford scattering formula, which is precisely the result which one must get when, as here, the Born approximation is used and the exclusion principle is neglected.[8]

While Eq. (33) can tell us nothing about the usual type of backward secondary emission, it is of importance in any attempt to predict the production of forward secondaries, which might be observed by the use of thin foils as targets. Eq. (33) divides the scattered electrons into two almost distinct groups—(a) electrons which, after collision, differ only slightly in energy and direction from the primary beam and (b) electrons which are knocked into states of much lower energy and which move away from the primary beam at angles $>45°$. If we consider the first group of electrons to be left exactly, rather than approximately, in the primary beam after the collision, and calculate the rate at which electrons are produced in the second group with energies and directions which make it possible for them to escape from the back side of the target, we should arrive at a rough estimate of the importance of the free electron approximation in the production of forward secondaries. For normal incidence such a calculation merely involves the integration[9] of Eq. (33) between the limits $\alpha=\pi/4$ and $\alpha=\alpha_{max}$, where α_{max} is the angle for which the component of the energy of the electron normal to the target surface (parallel to $\mathbf{K}$) is just equal to the energy W_a necessary for escape from the surface. From Fig. 4 it is clear that the energy of an electron scattered into the angle α is $E_p\cos^2\alpha$, where E_p is the primary energy. Hence

$$(E_p\cos^2\alpha_{max})\cos^2\alpha_{max}=W_a$$

or

$$\cos^2\alpha_{max}=(W_a/E_p)^{\frac{1}{2}}.$$

For the rate of production of electrons which can escape from the back of the target if not further scattered, Eq. (33) gives (setting $m^2V^4=4E_p^2$)

$$\frac{1}{\rho_1 J_p}\frac{1}{\Omega t}\int(dN_0)_{tot} = \frac{e^4}{E_p^2}\int_{\alpha=\pi/4}^{\alpha_{max}}(\sec^4\alpha+\csc^4\alpha)\cos\alpha d\omega \sim \frac{\pi e^4}{E_p^2}\left[\left(\frac{E_p}{W_a}\right)^{\frac{1}{2}}-1\right]. \quad (34)$$

To obtain (34) the approximation $W_a \ll E_p$ has been employed.

From Eq. (32), the corresponding rate of production of forward electrons due to the "bound" term for which $|\rho|=1$ and $\boldsymbol{\rho}$ and $\mathbf{K}$ coincide in direction (assuming $\mathbf{K}$ to be directed along one of the axes of our simple cubic lattice) is

$$\frac{1}{\rho_1 J_p}\frac{1}{\Omega t}(N_1)\sim\frac{16\pi m^2e^4}{\hbar^4}\frac{|b_1(\mathbf{k})|^2}{(2\pi/a)^4}. \quad (35)$$

This equation also assumes E_p to be large. $|b_1(\mathbf{k})|^2$ is to be thought of as an average $|b_1|^2$ over all the lattice electrons. If we replace $\hbar^4/m^2$ by $4E_p^2/K^4$, Eq. (35) becomes

$$\frac{1}{\rho_1 J_p}\frac{1}{\Omega t}(N_1)\sim\frac{4\pi e^4}{E_p^2}\frac{|b_1(\mathbf{k})|^2}{(2\pi/aK)^4}.$$

Or, since

$$(2\pi/aK)^4=(E_0/E_p)^2,$$

$$\frac{1}{\rho_1 J_p}\frac{1}{\Omega t}(N_1)\sim\frac{4\pi e^4}{E_p^2}\frac{|b_1(\mathbf{k})|^2}{(E_0/E_p)^2}. \quad (36)$$

[8] N. E. Mott and H. S. W. Massey, *The Theory of Atomic Collisions* (Oxford, 1933), p. 76.

[9] The neglect of the exclusion principle does not produce a serious error in such an integration. See, for example, N. E. Mott and H. S. W. Massey, reference 8, pp. 73–74.

Dividing Eq. (36) by (34) gives

$$\frac{N_1}{N_0}=\frac{4|b_1(\mathbf{k})|^2(E_p/E_0)^2}{[(E_p/W_a)^{\frac{1}{2}}-1]}.$$

For silver bombarded by 400-volt primaries, the ratio becomes

$$N_1/N_0\sim 500|b_1(\mathbf{k})|^2. \tag{37}$$

From the work of Morse[7] we would guess that $|b_1(\mathbf{k})|^2\sim 10^{-2}$ and from some of the results reached later in this paper we will find reason to believe that $|b_1(\mathbf{k})|^2$ may be somewhat larger than this value. Eq. (37), from the nature of its calculation, can by no means be considered a precise result, but it is probably accurate enough to justify the conclusion that, even in the production of forward secondary electrons, in spite of the smallness of the higher Fourier components, the free electron term may not be of much importance.

This conclusion leads one to suspect that perhaps even the rate of loss of energy of the primaries might be determined principally by the terms in our expansion for which $\rho\neq 0$. If a calculation is made, similar to the above, on the rate at which the primary beam loses energy by "free electron" scattering, one finds indeed that the mean free path of electrons of a few hundred volts energy so predicted is much higher than that which is observed. In such a calculation, however, the inaccuracies are so great that the result cannot be taken too seriously. Fortunately there exists much more convincing evidence on this point.

Consider again, for example, the case of silver. When it is bombarded by 400-volt electrons the backward yield of secondaries is 1.5[10]—i.e., for every primary electron which strikes the surface, 1.5 secondaries are observed. We have seen that each secondary, on the average, absorbs about 25 ev of energy from the primary electron which creates it. Since the mean Fermi energy is only $\sim$3 ev, the secondaries will be created with a mean energy of $\sim$25–30 ev. Those which can escape have their directions confined within a rather small solid angle around the normal to the surface. For silver, this solid angle $\sim 4\pi/5$. Thus, for every secondary electron observed, four more (assuming random orientation of the crystallites), are produced which cannot escape, even if no absorption occurs. This means that, within a distance from the surface of the target approximately equal to the reciprocal of the absorption coefficient of the 25-volt secondaries, $5\times 1.5\sim 8$ secondaries are created by every primary electron. The energy required is $8\times 25=200$ ev. *This means that a 400-volt primary would have an absorption coefficient about one-half as large as that of a 25-volt secondary*, due to this cause alone. But a calculation of the relative absorption coefficients from the "free electron" formula, Eq. (33), would yield a ratio of $\sim$1 : 100, instead of 1 : 2. Although Eq. (33) is not accurate for a calculation of this type, it seems unlikely that a correct calculation based on the free electron approximation could predict a rate of loss of energy of the primaries of this order. Hence it seems safe to conclude that, when electrons of a few hundred volts energy travel through a metal, they lose energy principally by the production of secondaries[11] (corresponding to $\rho\neq 0$), until their energy becomes too small to produce any further secondaries (for Ag, $\sim$25 ev). For the remainder of their path, probably the rate of loss of energy is determined by "free electron" scattering.

Limitations on the applicability of the results

In attempting to apply Eq. (32) to an interpretation of experimental data, one would like to commence with some sort of averaging process over all the lattice electrons which would make it unnecessary to deal further with a function of $\mathbf{k}$. But, for a chosen direction of $\boldsymbol{\varrho}$, there may exist a few electrons having momenta of such directions and magnitudes that $(2\pi\boldsymbol{\varrho}/a)\cdot(2\pi\boldsymbol{\varrho}/a+2\mathbf{k})=0$. (For such electrons evidently $\mathbf{k}$ lies on the surface of a Brillouin zone.) Eq. (32) would appear to assign to these electrons an infinite probability of being knocked into the new state $\mathbf{k}'\sim\mathbf{k}+2\pi\boldsymbol{\varrho}/a$. It is easy to establish, however, that such a selectivity effect does not occur. We have employed an approximation which is not valid in this case. The integration of Eq. (4) breaks down when S becomes too small and, for the electrons in question, $S_{\min}\rightarrow 0$. A detailed consideration of

[10] H. Bruining and J. H. de Boer, Physica **5**, 17 (1938).

[11] From this point on we will speak of the bundles of electrons corresponding to $\boldsymbol{\varrho}\neq 0$ as secondary electrons. Those which escape from the target will be referred to as "observed" or "emitted" secondary electrons.

this matter removes from the picture any likelihood that the secondaries are produced mainly from the lattice electrons whose $\mathbf{k}$ vector lies on the surface of a Brillouin zone. In fact, it will be a good enough approximation for most of the following development if we treat the problem as if $\mathbf{k}\cdot\boldsymbol{\varrho}=0$. Then Eq. (32) becomes (for $\rho=1$)

$$\frac{1}{\Omega}\frac{dN_\rho}{dt}=\frac{16\pi m^2e^4}{\hbar^4}\rho_l J_p\frac{|b_\rho|^2}{(2\pi/a)^4}F_\rho(\mathbf{K}), \quad (38)$$

where now it will be accurate enough to write

$$F_\rho(\mathbf{K})\equiv\left[1-\frac{(2\pi/a)^2+2mE_F/\hbar^2}{K^2}-\frac{2\mathbf{K}\cdot(2\pi\boldsymbol{\varrho}/a)}{K^2}\right]^{\frac{1}{2}}. \quad (39)$$

Eq. (38) is to be interpreted as follows. A current of primary electrons of number J_p per cm^2 per sec. and of momentum $\hbar\mathbf{K}$, travels through a simple cubic lattice, of principal axes (1, 0, 0), (0, 1, 0), and (0, 0, 1). Corresponding to each of the six directions $\boldsymbol{\varrho}=(1, 00)$, $(-1, 0, 0)$, etc. a group of secondary electrons is produced, at a rate given by Eq. (38). On the average, the energy of a secondary electron is $E_F+(\hbar^2/2m)(2\pi/a)^2$, where E_F is the mean Fermi energy of the lattice electrons and $(\hbar^2/2m)(2\pi/a)^2$ is the average energy lost by a primary electron in producing one secondary. For a given $\boldsymbol{\varrho}$, the secondaries have their directions bunched around the direction of $\boldsymbol{\varrho}$. If $2\pi/a\gg k_{\max}$, the spread in energies and directions will be small. In the case of silver, $k_{\max}\sim\frac{1}{2}\cdot 2\pi/a$, so we must expect each group to contain secondaries of energies up to

$$\frac{\hbar^2}{2m}\left(\frac{1}{2}\cdot\frac{2\pi}{a}+\frac{2\pi}{a}\right)^2\sim 2\times\frac{\hbar^2}{2m}\left(\frac{2\pi}{a}\right)^2.$$

Thus, each group of secondaries contains a few electrons of energies up to 40 or 50 ev.

In Eq. (38), ρ_l now represents the total electron density, while $|b_\rho|^2$ is to be thought of as the value of $|b_\rho(\mathbf{k})|^2$ averaged over all the lattice electrons.

One other effect of our approximations must be mentioned. Eq. (4) was found to be inapplicable when $S_{\min}\to 0$. But, even though $\mathbf{k}\cdot\boldsymbol{\varrho}=0$, $S_{\min}$ becomes very small when K becomes very large (Eq. 27). Consequently, for large K our calculations will not hold. It is possible to predict that the secondary yield will fall off for high primary energies, from qualitative considerations. Semi-quantitative calculations of some length can be carried out which predict that, for silver, this falling off should commence for $E_p\sim 1000$ ev, but such calculations cannot be regarded as accurate.

II. Application of the Results

For this development we shall employ the following results of the foregoing treatment:

(1) Eqs. (38) and (39) with the interpretation written below them.

(2) The conclusion that, when electrons of energies up to a few hundred volts travel through a metal, they lose energy principally by the production of secondaries according to Eq. (38), until their energy becomes $\sim(\hbar^2/2m)(2\pi/a)^2(\sim 25$ ev, for silver).

In addition we shall assume that the target is composed of many crystallites, or grains, of random orientation, so that the vector $\boldsymbol{\varrho}=(1,0,0)$, for example, has equal probabilities of pointing in all directions relative to the target surface. The fraction of all the crystallites which have one of their six directions for $|\rho|=1$ within the solid angle $d\omega$, making an angle θ with the normal to the target surface, is $6d\omega/4\pi$. Thus, on the average, a volume element $d\Omega$, in time dt, emits a number of secondaries dN of directions included within the solid angle $d\omega$ at an angle θ with the normal to the target surface where, from Eq. (38)

$$dN=\frac{16\pi m^2e^4}{\hbar^4}J_p\rho_l\frac{|b_1|^2}{(2\pi/a)^4}F_1(K,\theta)6\frac{d\omega}{4\pi}d\Omega dt \quad (40)$$

$|b_1|^2$, of course, represents $|b_{1,0,0}|^2=|b_{0,1,0}|^2$, etc. For normal incidence, from Eq. (39)

$$F_1(K,\theta)=\left[1-\frac{(2\pi/a)^2+2mE_F/\hbar^2}{K^2}+\frac{2}{K}\frac{2\pi}{a}\cos\theta\right]^{\frac{1}{2}}. \quad (41)$$

We are now ready to derive an expression for the observed secondary yield as a function of the bombarding voltage. We are here concerned with the fraction of the dN of Eq. (40) which actually escape from the bombarded surface. If $d\Omega$ lies directly in the surface of the target, then the secondaries which can escape are those emitted so that their directions make angles of less than $\theta_{\max}$ with the normal to the surface, where

$$(E_0+E_F)\cos^2\theta_{\max}=W_a.$$

W_a is the normal component of energy with which an electron must approach the surface in order to escape (W_a = max. Fermi Energy $E_{\max}$ plus work function χ), E_F is the mean Fermi energy, while E_0 is the average energy given by the primary electron to a secondary:

$$E_0=(\hbar^2/2m)(2\pi/a)^2.$$

The fraction of the secondaries which can escape is, from Eq. (40)

$$f=\frac{\int_{\theta=0}^{\theta_{\max}}F_1(K,\theta)\frac{d\omega}{4\pi}}{\int_0^{\pi}F_1(K,\theta)\frac{d\omega}{4\pi}}. \tag{42}$$

With the help of Eq. (41), this can be evaluated. The result may be expanded as

$$f=\frac{1}{2}\left\{1-\left(\frac{W_a}{E_0+E_F}\right)^{\frac{1}{2}}\right\}+\frac{1}{4}\frac{2\pi}{aK}\left\{1-\frac{W_a}{E_0+E_F}\right\}+0\left|\left(\frac{2\pi}{aK}\right)^2\right|. \tag{43}$$

The two terms given will be adequate for our purposes. In the same way it can be shown that

$$\int_0^{\pi}F_1(K,\theta)\frac{d\omega}{4\pi}=1+0\left|\left(\frac{2\pi}{aK}\right)^2\right|. \tag{44}$$

In the absence of knowledge of the exact form of the scattering or absorption law for the secondary electrons, it should not be far wrong to assume an exponential relation. If we do so we may write, for the fraction of the secondaries emitted in the volume element $d\Omega$, located a distance x beneath the target surface, which escape from the target,

$$g(x)=f(x)e^{-\gamma_s x}, \tag{45}$$

where $f(x)$ is obtained from Eq. (43) by assigning to K the value left to the primary particles after they have penetrated to a depth x.[12]

From Eqs. (40), (42), (44) and (45) we obtain an expression for the observed secondary emission coefficient δ (number of secondaries per primary):

$$\delta=\frac{96\pi m^2e^4}{\hbar^4}\rho_l\frac{|b_1|^2}{(2\pi/a)^4}\int_0^{l(E_p)}f(x)e^{-\gamma_s x}dx. \tag{46}$$

$l(E_p)$ is the distance the primary electrons, which enter the target with energy E_p (measured just *under* the surface), travel before they become too slow to produce secondaries—i.e., when their energy $\rightarrow E_0$.

When the bombarding voltage is high,

$$f(x)\rightarrow\tfrac{1}{2}\left\{1-\left(\frac{W_a}{E_0+E_F}\right)^{\frac{1}{2}}\right\}$$

and we get

$$\delta_\infty=\frac{96\pi m^2e^4}{\hbar^4}\rho_l\frac{|b_1|^2}{(2\pi/a)^4}\frac{\frac{1}{2}\{1-(W_a/(E_0+E_F)^{\frac{1}{2}}\}}{\gamma_s}. \tag{47}$$

For silver we may take the approximate values: $W_a=10$ ev; $a=3\times10^{-8}$ cm; $E_0=25$ ev. From Becker's measurements[13] we may conclude that $\gamma_s\sim2\times10^6$ cm^{-1}. For ρ_l we must take $1/a^3$, corresponding to one valence electron per unit cell. The result is

$$\delta_\infty\sim20|b_1|^2.$$

Since, for silver, $\delta_\infty\sim1.5$, we require that $|b_1|^2\sim0.07$. From Eq. (30) it is evident that $|b_1|^2$ may be as high as $4|a_1|^2$ where, from the work of Morse, we expect that $|a_1|^2\sim10^{-2}$. The value required here appears therefore to be a reasonable one.

Let us return now to Eqs. (46) and (47).

[12] We are not assuming here that the secondary electrons reach the surface with their initial energies and directions, or that the absorption coefficient is the same for all secondaries. Our assumption is simply that, on the average, the probability that a secondary electron escapes depends on the depth at which it originated through an exponential relation, modified by the behavior of $f(x)$.

[13] A. Becker, Ann. d. Physik 5, 2, 249 (1929).

Dividing them, we obtain

$$\frac{\delta}{\delta_\infty}=\gamma_s\frac{\int_0^{l(E_p)}f(x)e^{-\gamma_s z}dx}{\frac{1}{2}\{1-(W_a/(E_0+E_F)\}^{\frac{1}{2}}}.$$

From Eq. (43) this may be written

$$\frac{\delta}{\delta_\infty}=\{1-\exp[-1\gamma_s l(E_p)]\}+\frac{1}{2}\left\{1+\left(\frac{W_a}{E_0+E_F}\right)^{\frac{1}{2}}\right\}\times\int_0^{l(E_p)}\frac{2\pi}{aK(x)}\exp(-\gamma_s x)\gamma_s dx. \quad (48)$$

To determine $l(E_p)$ and $E(x)$ we proceed as follows. The number of secondaries produced by a primary electron in traveling the distance dx in the target may be gotten from Eqs. (40) and (44). It is

$$dn=\frac{96\pi m^2e^4}{\hbar^4}\rho_I\frac{|b_1|^2}{(2\pi/a)^4}dx.$$

The energy thus lost by the primary is

$$-dE=E_0dn$$

or

$$-dE=E_0\cdot\frac{96\pi m^2e^4}{\hbar^4}\rho_I\frac{|b_1|^2}{(2\pi/a)^4}dx. \quad (49)$$

When the primary electron has traveled a distance

$$l(E_p)=\frac{E_p-E_0}{-dE/dx}, \quad (50)$$

its energy is only E_0 and it produces no more secondaries. From (49), (50) and (47),

$$l(E_p)=\frac{\frac{1}{2}\{1-(W_a/(E_0+E_F))^{\frac{1}{2}}\}}{\gamma_s\delta_\infty}\left\{\frac{E_p}{E_0}-1\right\}. \quad (51)$$

This is the required expression for l. For $E(x)$, Eqs. (49) and (47) give

$$E(x)=E_p-x\cdot E_0\frac{\gamma_s\delta_\infty}{\frac{1}{2}\{1-(W_a/(E_0+E_F))^{\frac{1}{2}}\}}$$

or

$$\frac{E(x)}{E_0}=\frac{E_p}{E_0}-\frac{\delta_\infty(\gamma_s x)}{\frac{1}{2}\{1-(W_a/(E_0+E_F))^{\frac{1}{2}}\}}. \quad (52)$$

Equations (48), (51) and (52) may now be combined to give

$$\frac{\delta}{\delta_\infty}=\left\{1-\exp\left[-\frac{\frac{1}{2}\{1-(W_a/(E_0+E_F))^{\frac{1}{2}}\}}{\delta_\infty}\left(\frac{E_p}{E_0}-1\right)\right]\right\}+\frac{1}{2}\left\{1+\left(\frac{W_a}{E_0+E_F}\right)^{\frac{1}{2}}\right\}\int_0^{\frac{\frac{1}{2}\{1-(W_a/(E_0+E_F))^{\frac{1}{2}}\}}{\delta_\infty}\left(\frac{E_p}{E_0}-1\right)}\frac{e^{-v}dv}{\left[\frac{E_p}{E_0}-\frac{\delta_\infty v}{\frac{1}{2}\{1-(W_a/(E_0+E_F))^{\frac{1}{2}}\}}\right]^{\frac{1}{2}}}, \quad (53)$$

where $aK(x)/2\pi$ has been written as $[E(x)/E_0]^{\frac{1}{2}}$. From this equation, if we know δ_∞, we can plot the δ *vs.* E_p curve to show how the observed secondary emission coefficient depends on the bombarding voltage.

Now Eq. (53) has been derived on the assumption that the target possesses a simple cubic lattice structure. However, most of the materials of interest possess either a face-centered or a body-centered cubic structure. When the problem is considered in terms of the proper set of (nonorthogonal) coordinates which must be employed it develops that, for both the face- and body-centered cubic structures, the foregoing result should apply if "a" is assigned a value approximately ten percent less than the cube root of the atomic volume.[14] For the calculations to be made let us therefore define

$$a_0\equiv 0.9a,$$

where, in Eq. (53)

$$E_0=(\hbar^2/2m)(2\pi/a_0)^2$$

but a^3 is the volume per atom of the target material.

δ *vs.* E_p curves

1. Silver.—Let us employ somewhat more accurate data than used heretofore. From

[14] This treatment applies also to the close-packed hexagonal lattice.

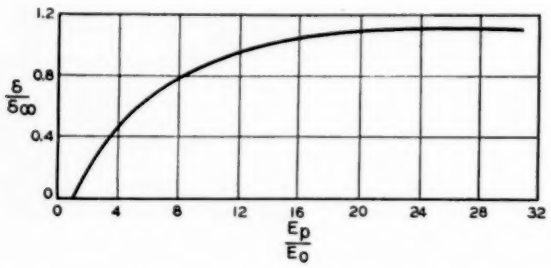

FIG. 5. First approximation to the δ/δ_∞ *vs.* E_p/E_0 curve for silver.

Mott and Jones[15] we obtain $a=2.56\times10^{-8}$ cm $\therefore$ $a_0=2.30\times10^{-8}$ cm and $E_0=28.2$ ev. For W_a we add $\chi=4.7$ ev.[16] and $E_{\max}=5.5$ ev.[17] $\therefore$ $E_F=\frac{3}{5}E_{\max}$[18] $=3.3$ ev.

In addition to these constants we require δ_∞. This must be obtained from experiment. However δ_∞ cannot be read directly from the experimental δ *vs.* E_p curve because, as has been shown earlier, we cannot expect our equations to hold when E_p becomes very large. Fortunately, however, we can evade this difficulty as follows. First assume a reasonable value of δ_∞ (say 1.5, for Ag) and plot the resulting δ *vs.* E_p curve from Eq. (53). This curve will rise to a maximum $\delta=\delta_{\max}$ which is somewhat greater than δ_∞. Compare this value of $\delta_{\max}$ with the experimentally observed value. Then multiply δ_∞ by the ratio $(\delta_{\max})_{\text{exp}}/(\delta_{\max})_{\text{theoret}}$ and plot the corresponding curve, etc. The functions are such that adequate agreement of $(\delta_{\max})_{\text{exp}}$ and $(\delta_{\max})_{\text{theoret}}$ can generally be secured on the first or second attempt. By this method of successive approximations the theoretically derived curve is adjusted from experimental data only through the one parameter $\delta_{\max}$. There is no such adjustment of either the shape of the curve or the abscissa scale.

If, as suggested, we first try $\delta_\infty=1.5$, Eq. (53) becomes

$$\frac{\delta}{\delta_\infty}=1-\exp\left[-0.145(E_p/28\text{ev}-1)\right]+0.78\int_0^{0.145(E_p/28\text{ev}-1)}\frac{e^{-v}dv}{[E_p/28\text{ev}-6.9v]^{\frac{1}{2}}}.$$

The last term can be treated graphically. The result is plotted as Fig. 5. From this curve $\delta_{\max}=1.13\delta_\infty=1.70$. Experimentally,[10] $\delta_{\max}=1.57$. Let us therefore take $\delta_\infty=(1.57/1.70)\times1.5=1.39$. The resulting curve requires only a very small further correction of δ_∞. The final result is plotted as the solid curve of Fig. 6. The experimental points are taken from the measurements of Bruining and de Boer[10] on evaporated silver.[19] The agreement is probably better than the accuracy of the theoretical derivation. It is important to observe that the *only* quantity taken from experimental secondary emission data for plotting the theoretical curve is $\delta_{\max}$. Presumably even $\delta_{\max}$ could be evaluated theoretically if accurate data were available on the lattice fields in the target.

In Figs. (7) to (13), inclusive, are shown similar comparisons of theory with the other data given by Bruining and de Boer for evaporated targets of pure metals. The constants used in these calculations are collected in Table I.

Except for the cases of caesium and barium (to be discussed below), the agreement between experiment and theory is as good as could be expected. It is probably significant that the agreement is best for copper and silver, which exhibit a practically constant δ over a wide range of values of E_p. For the other metals treated (except Cs and Ba) the theoretical curve always rises appreciably below the experimental data. This is probably partly due to the fact that the

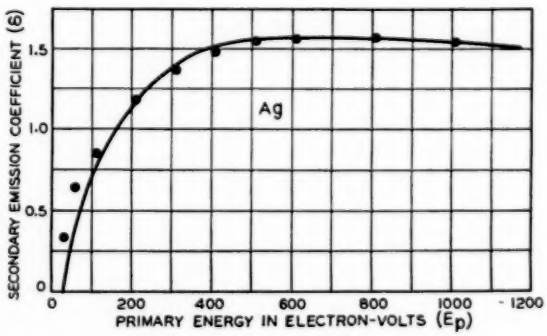

FIG. 6. Secondary yield *vs.* primary energy curve for silver. Experimental points taken from Bruining and de Boer.

[15] Reference 3, p. 318.
[16] A. L. Reimann, *Thermionic Emission* (John Wiley and Sons, 1934), p. 99.
[17] Reference 3, p. 54.
[18] Reference 3, p. 55.

[19] In this, as in all succeeding plots, the abscissa values of the experimental points have been increased by the amount W_a, since in these plots E_p represents the primary energy just *under* the surface rather than just before impact, as measured experimentally.

calculations do not contain means of including the degradation of δ which has been shown to set in at large values of E_p. In addition, the experimental data should be corrected for the elastic reflection of the primaries which becomes important at low E_p for weakly emitting targets. Such reflection modifies the yield curve so that δ does not approach zero as E_p diminishes. This effect is exhibited particularly clearly by the experimental data for Be, Cs and Ba. The inclusion of these effects in the calculations would tend to close the gap between theory and experiment.

The discrepancy between theory and experiment is too large in the cases of caesium and barium to be accounted for by elastic reflection or by the expected degradation of δ for large E_p. It seems possible that the theory breaks down in these cases through invalidation of the assumption that the primary electrons lose energy principally by the production of secondaries. The loss of energy by Rutherford scattering is probably not entirely negligible in any case; examination of theory shows that this factor should become increasingly important as the atomic volume increases. The very large atomic volumes of caesium and barium, together with their low secondary yields, may account for the discrepancy between theory and experiment.

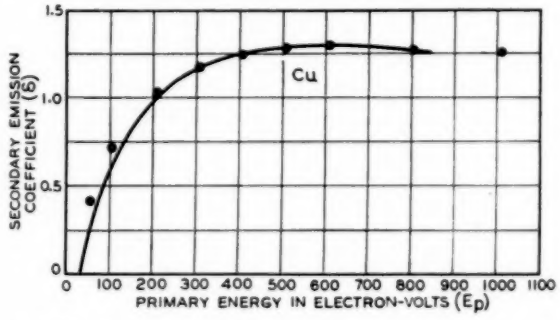

FIG. 7. Secondary yield *vs.* primary energy curve for copper. Experimental points taken from Bruining and de Boer.

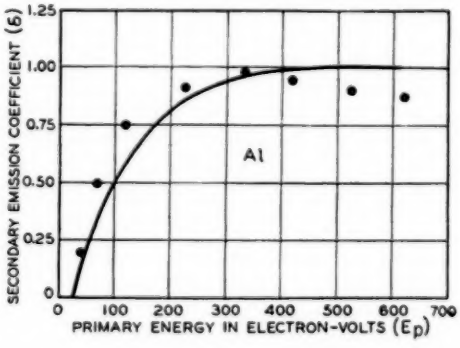

FIG. 8. Secondary yield *vs.* primary energy curve for aluminum. Experimental points taken from Bruining and de Boer.

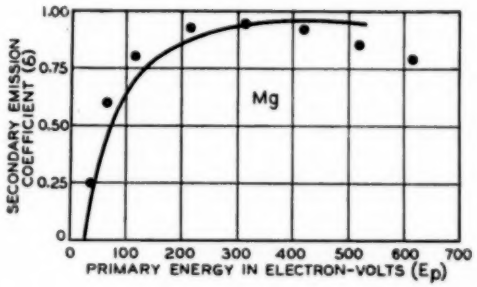

FIG. 9. Secondary yield *vs.* primary energy curve for magnesium. Experimental points taken from Bruining and de Boer.

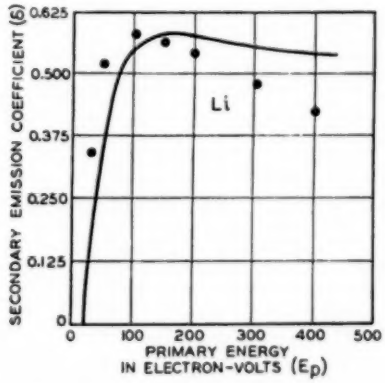

FIG. 10. Secondary yield *vs.* primary energy curve for lithium. Experimental points taken from Bruining and de Boer.

The theory set forth in this paper has been derived only for the case of targets in which the electrons are nearly free. For many pure metals this should be a good assumption, but caution must be observed in attempting to apply this theory to complex or nonmetallic surfaces. There may be many such surfaces in which the electrons behave sufficiently like free electrons to justify this extension, but in the absence of definite information such a treatment must be viewed with suspicion. Probably it is safe to conclude, however, that a complex caesium or barium surface, for example, can exhibit a very high δ for $E_p \lesssim 400$ ev only because the lattice spacing is large and E_0 is correspondingly small. Naturally, if the energy absorbed per secondary is small

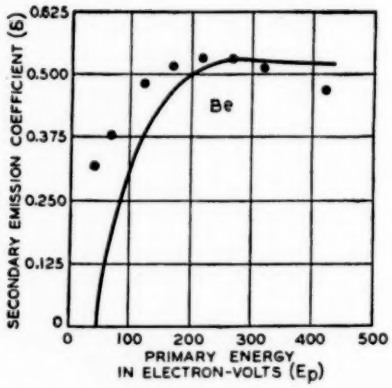

FIG. 11. Secondary yield *vs.* primary energy curve for beryllium. No correction made for elastic reflections at low energies. Experimental points taken from Bruining and de Boer.

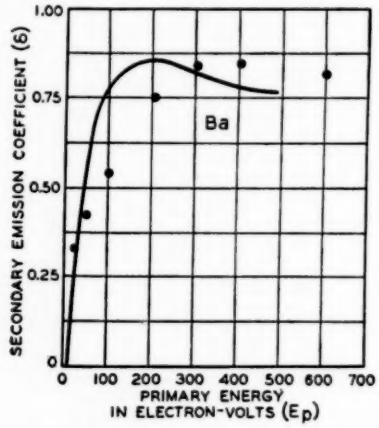

FIG. 12. Secondary yield *vs.* primary energy curve for barium. No correction made for elastic reflections at low energies. Experimental points taken from Bruining and de Boer.

enough, δ may be very large for comparatively low values of E_p. It is probably not mere coincidence that the theory here outlined predicts

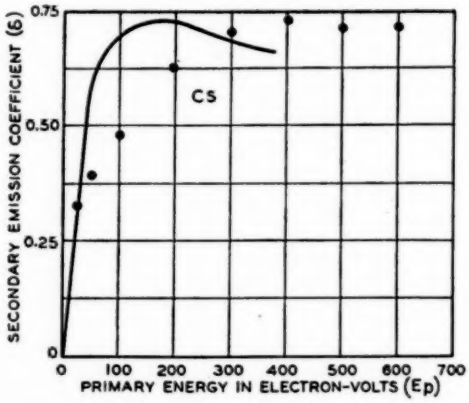

FIG. 13. Secondary yield *vs.* primary energy curve for caesium. No correction made for elastic reflections at low energies. Experimental points taken from Bruining and de Boer.

δ *vs.* E_p curves for Cs_2O and BaO surfaces which are in more than qualitative agreement with experiment, when lattice constants appropriate to the targets are employed and (in the absence of any exact information) values of E_{max} and E_F appropriate to the pure metal are used. In Fig. (14) the case of BaO is illustrated. The data employed were

$$a = 5.53 \times 10^{-8} \text{ cm}^{24} \text{ (cubic structure)};$$
$$\therefore a_0 = a \text{ and } E_0 = 5.0 \text{ ev};$$
$$\chi = 1 \text{ ev};^{25}$$
$$E_{max} = 3.6 \text{ ev};^{22}$$
$$\therefore E_F = 2.2 \text{ ev}.$$

Other properties of secondary emission

The approximations which have been used in deriving the foregoing curves are of such a nature as to lead to pretty good results when calculations of the total yield are made, but we would not

TABLE I.

METAL	a[15]	E_0	χ	E_{max}	$E_F = \frac{3}{5}E_{max}$
Aluminum	2.54×10^{-8} cm	28.4 ev	3 ev[20]	16 ev[21]	9.6 ev
Barium	3.98 "	11.6 "	2.1 "[16]	3.6 "[22]	2.2 "
Beryllium	2.00 "	45.9 "	3 "	13.5 "[21]	8.1 "
Caesium	4.89 "	7.6 "	1.9 "[16]	1.5 "[17]	0.9 "
Copper	2.27 "	35.8 "	4.4 "[23]	7.1 "[17]	4.3 "
Lithium	2.77 "	23.8 "	2.3 "[16]	4.2 "[21]	2.5 "
Magnesium	2.84 "	22.8 "	2.4 "[16]	9.0 "[21]	5.4 "
Silver	2.56 "	28.2 "	4.7 "[16]	5.5 "[17]	3.3 "

[20] P. S. Epstein, *Textbook of Thermodynamics* (Wiley, 1937), p. 280.

[21] H. M. O'Bryan and H. W. B. Skinner, Phys. Rev. **45**, 370 (1934).

[22] Calculated on the assumption of two free electrons per atom. For the method of calculation see, for example, N. F. Mott and H. Jones, reference 3, p. 54.

[23] A. L. Hughes and L. A. DuBridge, *Photoelectric Phenomena* (McGraw Hill Co., 1932), p. 75.

[24] W. G. Burgess, Zeits. f. Physik **80**, 352 (1933).

[25] W. G. Dow, *Fundamentals of Engineering Electronics* (Wiley, 1937), p. 537.

expect the same degree of accuracy to obtain for calculations of the energy distribution of the emitted secondaries, for example. For such a calculation it is not sufficient for us to know that the *average* energy given to a secondary is E_0 and that the *average* absorption coefficient of the secondaries is γ_s; instead, we require explicit information as to the distribution in energy of the produced secondaries and the exact absorption or scattering processes for each energy. The theory is capable of giving us a definite expression for the first, but the specific processes whereby the secondaries lose energy and change direction are outside the scope of this treatment. Consequently we can only observe that the theory predicts a spread in the energies of the emitted secondaries of about the value measured and that, neglecting the effects of absorption and scattering, we would expect a maximum in the observed energy distribution at around $(E_0+E_F)-W_a$ volts. This value is considerably greater than the experimentally determined voltage. (For silver, for example, $E_0+E_F-W_a=21$ ev, whereas the maximum yield occurs for a secondary energy of only about 6 ev),[26] but of course the effect of scattering, etc., would be in this direction.

The same factors limit the accuracy of predictions as to the manner in which δ should be affected by changes in the work function. To be sure, from Eq. (47) we are justified in writing, for such a case

$$\delta_x \propto \frac{1-(W_a/(E_0+E_F))^{\frac{1}{2}}}{\gamma_s}.$$

Or, nearly enough

$$\delta_{\max} \propto \frac{1-(W_a/(E_0+E_F))^{\frac{1}{2}}}{\gamma_s}.$$

Since $W_a=E_{\max}+\chi$,

$$-\frac{d}{d\chi}\log_e \delta_{\max}=\frac{d}{d\chi}\log_e \gamma_s + \frac{1}{2(E_0+E_F)(W_a/(E_0+E_F))^{\frac{1}{2}} \times\{1-(W_a/(E_0+E_F))^{\frac{1}{2}}\}}. \quad (54)$$

[26] E. Rudberg, Proc. Roy. Soc. **127**, 111 (1930).

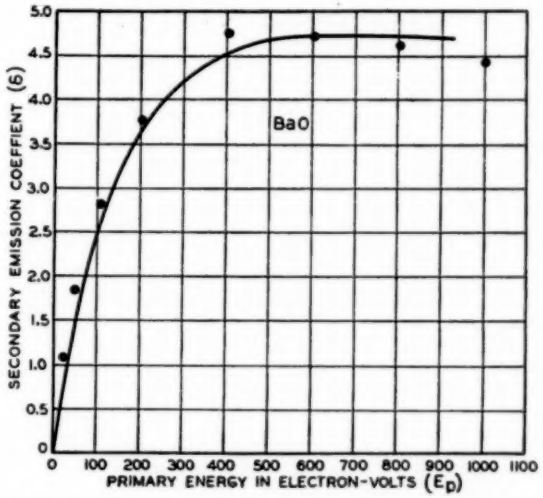

FIG. 14. Secondary yield *vs.* primary energy curve for barium oxide. Experimental points taken from Bruining and de Boer.

The second term of this expression can be evaluated, but again the first term has to do with the detailed behavior of secondaries of different energies. The average "absorption coefficient" will necessarily depend on the amount of energy a secondary must lose or the deflection it must suffer to be prevented from escaping and this, in turn, depends on χ in a manner which we cannot now predict. We can only estimate that γ_s will increase with χ at a rate whose order of magnitude should be given by some such relation as the following:

$$\gamma_s \propto \frac{1}{E_0+E_F-W_a}.$$

That is, the greater the energy that can be taken from the "average" secondary without preventing its escape, the less the "absorption coefficient." Therefore,

$$\frac{d}{d\chi}\log_e \gamma_s \sim \frac{1}{E_0+E_F-W_a}. \quad (55)$$

Now Treloar[27] has reported measurements wherein the work functions of tungsten and molybdenum were decreased by evaporating small amounts of barium or thorium on to the targets. By simultaneous measurements of χ and $\delta_{\max}$, Treloar was able to establish a linear

[27] L. R. G. Treloar, Proc. Phys. Soc. **49**, 392 (1937).

relation between $\log \delta_{max}$ and χ, provided the amount of the contaminant was kept small (less than one atomic layer). For such tiny surface deposits it seems not unreasonable to accept Treloar's assumption that the only significant change was in the work function. If so, Eq. (54) should be applicable. For either tungsten or molybdenum the value of E_0 should be ~ 28 ev. E_{max} is not known in either case, but it will be accurate enough for this calculation to assume the value corresponding to one free electron per atom. Then, in either case, $E_{max} \sim 5$ ev, $E_F \sim 3$ ev, while $\chi \sim 3$ ev for the targets measured. For these values, Eq. (55) gives

$$\frac{d}{d\chi} \log_e \gamma_s \sim 0.04 \text{ ev}^{-1}.$$

And therefore, from Eq. (54)

$$-\frac{d}{d\chi} \log_e \delta_{max} \sim 0.04 \text{ ev}^{-1} + 0.07 \text{ ev}^{-1} = 0.11 \text{ ev}^{-1}.$$

Treloar's values were 0.12 ev^{-1} for tungsten and 0.14 ev^{-1} for molybdenum. The good agreement is probably fortuitous.[28]

Summary

In this paper a quantum-mechanical treatment has been given, in three dimensions, of the interaction between primary electrons and the lattice electrons of a bombarded metal target. A certain dependence of the results of this calculation on the primary energy was found to exist, but not at all of the form exhibited by observed yield *vs.* bombarding energy curves. The shapes of the observed curves are attributed to the more or less demonstrable fact that the primary electrons lose so much of their energy that they can produce no more secondaries, in a distance which may be *less* than the mean free path of the much lower energy secondaries. An approximate method of calculating the δ *vs.* E_p curves is developed and shown to give reasonable agreement with experiment. The dependence of the yield on the work function of the target is also shown to be susceptible of rough calculation. The calculated dependence is small and is also in satisfactory agreement with experiment.

In general, the theory predicts that a large secondary emission coefficient ($\delta > 2$ or 3, say) can be obtained for moderate (400–800-ev) primary energies only from targets having a large lattice constant and a small Fermi energy. Caesium, for example, satisfies these conditions but in the pure state, (largely on *account* of its great atomic volume), its valence electrons must be so nearly free that the binding terms, on which secondary emission principally depends, are too small to permit appreciable yields. A complex caesium surface, on the other hand, retains a large lattice spacing and (probably) a low Fermi energy and at the same time possesses a lattice potential which deviates much more from constancy than that of the pure metal. Thus it is easy to understand why the pure alkali metals are such poor secondary emitters while complex alkali surfaces are very good emitters.

The absolute magnitude of the secondary emission coefficient cannot be closely predicted without further information concerning the lattice fields. Similarly, the energy distribution of the emitted secondaries cannot be accurately predicted without a detailed knowledge of the scattering and absorption processes which affect the low energy secondaries. In each case, however, the partial prediction given by the theory is about what one would expect to need to fit the experimental results.

In conclusion, it should be pointed out that this theory treats only secondary emission which is due to the interaction of the bombarding particles with the *valence* electrons of the target material. It is probably not possible, without further investigation, to say for sure that the contribution of the closed shells is entirely negligible. The extent of the agreement between the present theory and experimental results is good enough, however, to lend support to the view that the emission of secondary electrons is primarily due to the valence electrons, in some cases at least.

[28] It should be mentioned that Treloar's results have not been confirmed in some work reported since this paper was written (Edward A. Coomes, Phys. Rev. **55**, 519 (1939)).

Practice and Theory of the Modulation of Geiger Counters

JOHN N. SHIVE
Rowland Physical Laboratory, Johns Hopkins University, Baltimore, Maryland

(Received July 7, 1939)

Experiments are described in which the behavior of Geiger-Müller counters under conditions of low frequency and high frequency modulation was studied. The modulation was obtained by the superposition of an a.c. voltage wave upon the d.c. counting threshold. It was found that for frequencies up to about 500 kc such modulation could be successfully carried out. An analysis of the results of these experiments shows that for some counters the breakdown process can be ascribed to the liberation of electrons from the cathode by positive ion impact, while for other counters the photoelectric liberation of electrons from the cathode is predominant in the mechanism of the breakdown. Counters have been constructed for which there is evidence that both of these processes occur in the same counter. The theory of high frequency modulation of counters is discussed.

INTRODUCTION

OF the neutron speed experiments to date, those of Dunning, Pegram, and co-workers,[1] and of Alvarez[2] have given satisfactory results in the region of thermal velocities. Both of these methods, however, are at a disadvantage when it comes to the measurement of the speeds of neutrons with energies greater than a fraction of a volt. In the rotating disk method of Dunning it is the limitation of the speed with which the disks can be rotated which imposes this restriction. In Alvarez' work the modulation of the receiver was accomplished by alternately blocking and unblocking the amplifier which passed the pulses from the ionization chamber to the recorder. It is probable that the upper limit of the applicability of this method would be reached at such a modulation frequency that the period of the modulation cycle becomes comparable with the breakdown time of the ionization chamber.

The work reported here was undertaken for the purpose of establishing whether the direct electrical modulation of Geiger counters is possible at high frequencies. This was done with a particular view to the use of such counters as modulated receivers in neutron speed measurements beyond the limits of the methods already mentioned. From an analysis of the various theories[3, 4] of mechanisms in gas discharges it seems plausible to expect that high frequency modulation should be possible.

In modulation work the counter is maintained at a steady d.c. voltage equal to the counting threshold. Upon this is superposed an a.c. voltage wave in such a way that the counter is swung alternately up onto the plateau and down below the threshold into the insensitive voltage region.

EXPERIMENTS WITH LOW FREQUENCY MODULATION OF SOURCE AND COUNTER

As a preliminary to the investigation of counter behavior at high frequencies, the response of counters to low frequency modulation was studied in the range from 250 to 600 cycles per second. Even at the highest of these frequencies the breakdown time of the counter was less than the half-period of the modulation cycle, so that the breakdowns which occurred usually went to completion in the same half-cycle as their beginning.

An arrangement was devised for the simultaneous modulation of source and counter with variable phase. A square wave of 100 volts amplitude was obtained by means of a rotating commutator, and was impressed capacitatively onto the anode of the counter. The modulation of the source consisted of the covering and uncovering of an old radon tube by the passage of the teeth of a rotating sector disk on the same motor shaft with the commutator, so that the source was alternately shielded from and exposed to the counter.

The results of this experiment are shown in

[1] Dunning, Pegram, Fink, Mitchell, Segrè, Phys. Rev. **48**, 704 (1935).
[2] L. Alvarez, Phys. Rev. **54**, 609 (1938).
[3] K. T. Compton and I. Langmuir, Rev. Mod. Phys. **2**, 123 (1930).
[4] L. Loeb, Rev. Mod. Phys. **8**, 267 (1936).

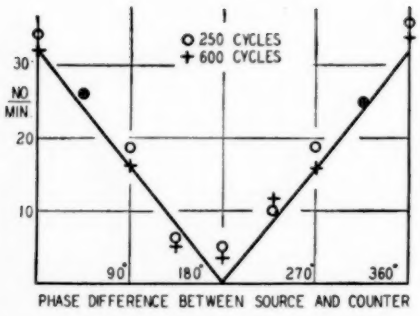

FIG. 1. Results of experiments on low frequency modulation of a typical counter and source, showing variation of counting rate with phase difference between source and counter.

Fig. 1, where the counting rates are given for two different frequencies as a function of the difference in phase between the passing of the counter voltage above the threshold and the uncovering of the source. These data have been corrected for the background and for the fraction of the rays which penetrated the teeth of the wheel. The figure shows graphically the dependence of the counting rate upon the phase difference between source and counter. The full line gives the counting rates expected from the value of the unmodulated d.c. rate with the source exposed. The results show that the low frequency modulation of Geiger counters has been accomplished.

Experiments with High Frequency Modulation of Counter Alone

Suppose the normal d.c. plateau counting rate of a Geiger counter is determined with the supply voltage maintained at some value on the plateau, and with a steady source of radiation at some convenient distance. If now the d.c. voltage is made equal to the threshold and the counter is modulated with an a.c. voltage wave, the new counting rate determined should be about one-half the d.c. plateau rate, one-half because with modulation the counter voltage is on the plateau for about half the total time, and below the threshold for the other half. This halving of the normal d.c. counting rate is thus an expected consequence of successful modulation, and can accordingly be used to trace the behavior of counters in their response to modulation of this sort. In the experiments to be reported now the counters to be tested were modulated as described, and this halving of the plateau counting rate was looked for. The apparatus used in this work is illustrated schematically in Fig. 2.

In order to include as wide a frequency range as possible, two complete variable frequency oscillators were constructed. One, for frequencies from 500 cycles to 50 kc per second, was built with a two-stage amplifier in the same unit. The other, for frequencies from 50 kc to 10 mc per second, gave sufficient voltage to use directly without amplification. Both were of the regular Hartley type. The sweep frequencies of a cathode-ray oscillograph were calibrated by the Lissajous figure method, and were used whenever needed for the determination of oscillator frequencies. The d.c. voltage for the counter was supplied by a conventional power pack and filter circuit operated from a constant-voltage motor-generator. In the determination of counting rates, the breakdowns of the counter were observed in an Edelmann string electrometer.

In order that an oscillograph analysis[5, 6, 7] of the breakdown phenomena could be made, a single-stage amplifier unit was used, as indicated in the figure. The discharge current of the counter, flowing through the grid resistance of the amplifier tube, gave the voltage pulses to the grid. In the case of a.c. modulation of the counter, the charging current through the capacity of the counter was sufficient to cause a trace of the modulation wave to appear on the screen of the oscillograph. Thus it was possible to observe not only the breakdowns themselves,

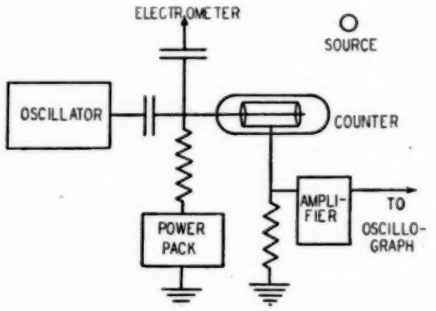

FIG. 2. Schematic arrangement of apparatus in experiments on high frequency modulation of counters.

[5] W. E. Ramsey and M. R. Lipman, Rev. Sci. Inst. **6**, 121 (1935).
[6] W. E. Danforth, Phys. Rev. **46**, 1026 (1934).
[7] P. B. Moon, J. Sci. Inst. **14**, 189 (1937), bibliography.

but the time of their occurrence during the cycle as well.

In the course of this investigation a great many counters were constructed and tested. A description will now be given of one of the most successful of these, to be hereafter referred to as counter *A*, followed by a report of its behavior at various modulation frequencies. Fig. 3 shows the details of its construction. The cathode was a brass cylinder 20 mm long and 11 mm inside diameter. A 12-mil tungsten wire 20 mm long between the bead and the end of the glass holder, served as the anode. Before the final filling, the cathode surface was oxidized by heating in air. The counter was filled with tank argon with an estimated admixture of from ½ percent to 1 percent of air to a total pressure of 6 cm. The d.c. counting rate characteristic showed a nearly flat plateau of about 150 volts' width. In modulation work a wave amplitude of 100 volts' peak from the axis was used: this was sufficient to carry the counter well up onto the plateau during the peak half-cycle. For the various frequencies the counting rates C, in counts per minute, along with the oscillograph observations, are given below, each figure representing the counting of at least 200 breakdowns. The d.c. plateau counting rate under the conditions of this experiment was 47 counts per minute.

500 cycles: $C=18$. All counts came during the peak half-cycle on the counter. Breakdowns starting late in the half-cycle were "choked off" before they could run to their normal completion.

2700 cycles: $C=17$. At this frequency all breakdowns were more or less choked off, depending on whether they started early or late in the peak half-cycle.

10 kc: $C=15$. The choking off was very pronounced at this frequency. Electrometer "kicks" were too small to observe with much reliability in counting.

25 kc: Electrometer kicks were too small to observe. All breakdowns observed in the oscillograph came during the peak half-cycle on the counter. The "tails" of the breakdown traces extended beyond the point where the counter voltage went below the threshold.

50 kc: Breakdowns began to carry over into succeeding cycles. They always started, however, during a peak half-cycle on the counter. Electrometer kicks were still very small: discharges apparently did not go to completion even though they did carry over a few cycles.

150 kc: $C=26$. 550 kc: $C=28$. 1 mc: $C=29$. 5 mc: $C=35$. The envelope of all the breakdown humps on the oscillograph screen for one discharge resembled closely a normal breakdown pulse. All breakdowns were of normal size. All breakdowns went to completion.

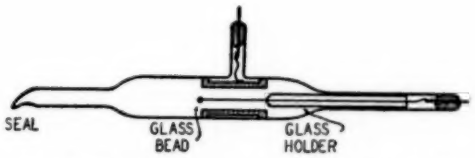

FIG. 3. Details of construction of counter *A*.

Among the counters studied in this way there were others whose reactions were so strikingly different in many ways from those of counter *A* that a detailed report of the observations made upon a typical one of these others, to be referred to hereafter as counter *B*, seems justified. Because it was intended for use later in soft x-ray work, this counter was one of several made with a thin glass window at one end. The anode wire of 20-mil unoxidized tungsten, supported at one end by a glass holder, extended for a short distance axially along the center of the cathode cylinder. This latter was of copper, 20 mm long, and of 9 mm inside diameter. The cathode surface was prepared according to a treatment described by Neher.[8] The filling gas was a mixture of 98 percent tank argon and 2 percent air at a pressure of 6 cm prepared and admitted to the counter by means of an apparatus designed for the purpose.

In preliminary experiments with this counter unmodulated a very striking phenomenon was observed, which appeared also in several of the other counters studied. As the d.c. voltage was raised above the threshold the voltage drop at each breakdown, as observed by the amplitude of the kicks in the electrometer, increased, being of a magnitude approximately proportional to the difference between the operating voltage and the threshold. At a particular point on the counting plateau, however, a very well-defined voltage was reached above which all the electrometer kicks were very much larger than expected, and where the breakdown time of the counter suddenly changed from the order of 10^{-3} sec. to the order of 10^{-4} sec. The counting rate remained practically unaltered as the voltage was raised across this "transition" value,

[8] L. Strong, *Procedures in Experimental Physics* (Prentice-Hall, 1938), Chapter 7.

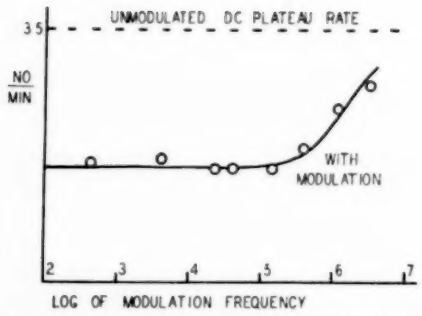

FIG. 4. Results of experiments on high frequency modulation of counter A, showing halving of the d.c. plateau counting rate for frequencies up to about a million cycles per second.

which in counter B came about 60 volts above the ordinary threshold. In modulation experiments where the wave amplitude did not exceed 60 volts, this counter in all points of behavior resembled closely counter A. For modulation wave amplitudes of around 150 volts' peak from the axis, however, the counter was above the transition voltage during most of the peak half-cycle, and it is for this condition that the following report is given. The normal unmodulated d.c. plateau counting rate under the conditions of this experiment was 35 counts per minute.

500 cycles: $C=16$. Breakdowns always occurred during the peak half-cycle on the counter.

6400 cycles: $C=17$. Tails of the breakdown traces extended beyond the point where the counter voltage passed below the threshold. No choking off of the breakdowns was observed.

22 kc: $C=15$. Breakdowns carried over one reverse half-cycle into the next following peak half-cycle. There was no apparent growth of the discharge, however, beyond the peak half-cycle it started in. The first half-cycle hump was always the larger.

45 kc: $C=15$. At this frequency the breakdowns carried over several cycles, but always began during a peak half-cycle on the counter. As before, for a given discharge, the first breakdown hump was always the largest, suggesting that the discharge was completed during the peak half-cycle in which it started, and that the collection of the positive ions was responsible for the rest of the humps.

150 kc: $C=15$. 550 kc: $C=19$. $1\frac{1}{2}$ mc: $C=24$. 5 mc: $C=27$. The envelope of all the half-cycle humps for a single breakdown resembled a normal d.c. breakdown pulse. Still no choking off of the magnitude of the breakdowns was observed.

The modulation behavior of counter B is summed up in the graph of Fig. 4, where the counting rates are plotted against the logarithm of the modulation frequency. It is seen that in this counter the halving of the unmodulated d.c. plateau rate is present up to about a million cycles per second.

Among the various counters investigated there were two others, similar in construction and cathode treatment to counter B, and filled with mixtures of 1 percent and 5 percent, respectively, of ethyl alcohol vapor in tank argon, for which the transition voltages appeared to coincide with the threshold. In these counters the magnitude of the voltage jump at each breakdown as soon as the threshold had been exceeded was about 250 volts. The modulation results on these counters showed the halving of the d.c. plateau counting rate at all frequencies below 300 kc. There was no significant difference in the behavior of the two which could be traced to the difference in alcohol concentration.

EXPERIMENTS WITH HIGH FREQUENCY MODULATION OF SOURCE AND COUNTER

In order that the modulation behavior of counters might be tested under conditions similar to those of an actual particle speed experiment, a low voltage grid-controlled x-ray tube was designed for use as a modulated source of radiation for the high frequency testing of counters. The counting rates of modulated Geiger counters were then determined for the two cases, when the counters were in phase coincidence with, and in opposition to, the emission from the x-ray tube.

The construction of the x-ray tube is shown in Fig. 5. The filament of 12-mil tungsten wire

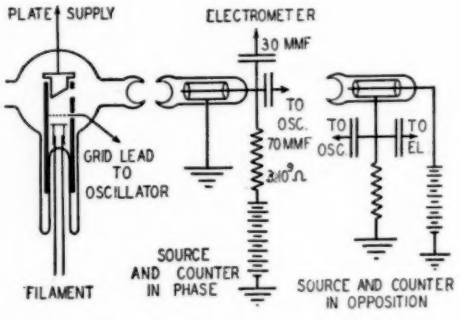

FIG. 5. Details of construction of x-ray tube, and connections in the counter circuit for in-phase and out-of-phase modulation of the counter.

was wound in a flat spiral just below the grid, which was of 40-mesh nickel gauze. A radiation-cooled piece of copper served as the anode. The whole assembly was surrounded by a metal sleeve which was grounded to the center tap of the filament winding. Because of the comparative ease with which grid control of the emission could be secured for low anode voltages, a power supply was designed which made use of a 6000-volt transformer. Thin glass windows were consequently required on the x-ray tube and Geiger counters to permit the passage of the soft rays thus obtained. In the operation of the x-ray tube it was found that more satisfactory modulation, especially at the higher frequencies, could be secured if the grid was so biased that the emission in each cycle was confined to a very short interval just at the middle of the positive half-cycle on the grid. For this purpose negative grid biases in the neighborhood of 20 volts smaller than the wave amplitudes were used.

The counter used in this experiment was similar to counter *B* with the one exception that the anode wire was much longer than the cathode and extended for some distance unshielded out of each end of the cylinder. The treatment of the cathode surface was the same as that already referred to.[8] The filling gas was a mixture of 1 percent tank oxygen in 99 percent tank argon at a pressure of 7 cm.

Figure 5 shows also the connections in the counter circuit for the cases when it was desired to have the counter in phase with, and in opposition to, the emission. In order to make sure that there was nothing inherent in the difference between the two circuit arrangements themselves which could affect the counting rate, the oscillator lead was grounded, and the unmodulated d.c. counting rate was taken for both cases. It was found to be the same. Throughout this experiment modulation waves of about 150 volts' amplitude were used.

The graph of Fig. 6 shows the relationship of the in-phase and out-of-phase counting rates for the different modulation frequencies. The ordinate represents the percent ratio of the out-of-phase to the in-phase rate. An inspection of the figure indicates that this Geiger counter could be used as a modulated receiver in a particle speed experiment at a frequency perhaps as high as 500 kc.

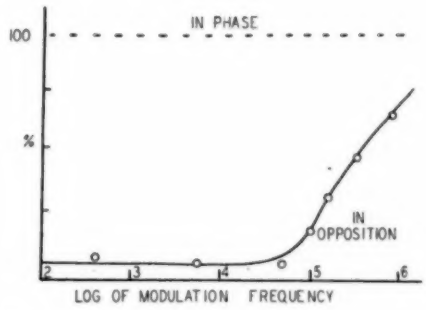

FIG. 6. Results of experiments on high frequency modulation of counter *B* with modulated x-rays.

DISCUSSION

The experiments show that the high frequency modulation of Geiger counters is practicable. If, as is suggested in the last section, a counter modulated at 500 kc is used as a receiver in a particle speed experiment at a distance of 1 meter from a modulated source, and in phase quadrature with it, the speed of a proton or neutron of about 10,000 electron-volts energy could be measured. The energy range over which this method should be useful is thus seen to be of an enormously greater extent than the range of from a few hundredths to a few tenths of a volt to which the methods (1) and (2) are restricted because of the limitations discussed.

Also, from a study of the results for counters *A* and *B*, several suggestions concerning the mechanism of the counter breakdown itself can be inferred. Of the various mechanisms which have been proposed in attempts to account for the operation of a counter, the ones which appear to be most favored by the evidence of these experiments are the positive ion process[9] and the photoelectric process.[10, 11] In the first of these the positive ions from the discharge migrate to the counter cathode and liberate electrons from it which cause further Townsend avalanches in the gas, leading to the continuation of the discharge. In the photoelectric mechanism some of the molecules involved in collisions with electrons in the avalanches are raised to spectro-

[9] A. von Hippel, Zeits. f. Physik **97**, 455 (1936).
[10] E. Greiner, Zeits. f. Physik **81**, 543 (1933).
[11] S. Werner, Zeits. f. Physik **90**, 384 (1934).

scopic levels short of complete ionization. In their radiative return to the ground state, light is emitted which by photoelectric absorption at the cathode ejects more avalanche-producing electrons which keep the discharge going.

The Positive Ion Mechanism

On the assumption of the positive ion process the explanation of high frequency modulation of counters is as follows. If an ionizing particle enters the counter during the half-cycle when the voltage is above the threshold, an ionization avalanche will occur in which enough positive ions are created to insure the liberation of several new electrons from the cathode when all the positive ions have been collected. Some of these will be liberated during the peak half-cycles of the succeeding modulation cycles when they in turn will produce more ionization and thus lead to the complete breakdown of the counter. On the other hand, an ionizing particle arriving during the half-cycle when the voltage is below the threshold will cause an avalanche in which too few positive ions will be created to insure the ejection of new electrons from the cathode, so that the discharge will probably proceed no farther than the first avalanche.

It appears from an argument based on several lines of evidence that the positive ion process is predominantly responsible for the breakdown mechanism of counter *A*. In the first place, under conditions of low frequency modulation a breakdown starting late in a peak half-cycle may yet be in progress when the counter voltage is carried below the threshold by the next alternation of the modulation wave. It is to be expected that such a breakdown will be choked off immediately. This choking off was actually observed for 500-cycle modulation of counter *A*: and it became more and more pronounced in its effect on the size of the breakdowns as the frequency was increased. On the assumption of the positive ion process, when the half-period of the modulation cycle becomes of the same order as the positive ion transport time, statistically only one avalanche should occur. As can easily be calculated[12] for a counter of this general description, the positive ion transport time from the region of the anode, where the ionization is heaviest, to the cathode surface is about 3.10^{-5} sec. The observed vanishing of the size of the breakdowns in the modulation experiments occurred somewhere between 25 kc and 50 kc, a frequency at least of the right order of magnitude to lend considerable support to the assumption of the positive ion process.

In the 25-kc oscillograph analysis it was seen that the tails of the breakdown traces extended over into the half-cycle when the voltage was below the threshold. This suggests that, even though the breakdowns were choked off when the counter voltage passed down through the threshold, the collection of the positive ions already present continued for a time which agrees in order of magnitude with the theoretically calculated transport time. It should be expected that if the frequency is increased still more, so that the half-period becomes somewhat shorter than the positive ion collection time, then the tails of the breakdowns will extend over into the next following peak half-cycle where any new electrons liberated from the cathode will cause the breakdown to continue. That this expectation is fulfilled at 50 kc, a frequency in qualitative agreement with that calculated theoretically, lends further support to the conviction that the positive ion process must predominate in this counter.

The normal breakdown time was observed for counter *A* to be about 1/1000 second, or about 30 positive ion transport times. In the normal breakdown of a counter, if the voltage is well up on the plateau, the various avalanches will begin to overlap, so that very soon after the initiation of a breakdown there may be several hundred avalanches in progress all at once. Because of this growth of the discharge the voltage across the counter falls far more rapidly than if the avalanches followed each other one at a time. The total breakdown time of this counter of about thirty positive ion transport times seems quite reasonable for a counter for whose action the positive ion process is responsible.

The Photoelectric Mechanism

In the case of the predominance of the photoelectric mechanism the discharge of the counter

[12] J. Thomson, *Conduction of Electricity Through Gases* (Cambridge, 1928), Vol. I, p. 100.

should be very rapid. There is here practically no delay between one avalanche and the liberation of electrons from the cathode to start the next, so that the *actual* breakdown of the counter should be completed in a time of the order of 50 or 100 electron transit times, either by the discharging effect of the avalanche electrons themselves, or more probably by space charge formation within the counter. The further discharging effect of the collection of the positive ions out of the field will then occur, drawing out the *apparent* breakdown time to the order of a single positive ion transport time. If this process is predominant in a counter, then successful modulation should certainly be possible up to frequencies whose half-periods are comparable with the *actual* breakdown time of the counter, which may be as short as 10^{-5} or 10^{-6} second. At successively higher frequencies the choking off of the discharges might be expected to occur, until an ultimate limit for modulation is reached when the half-period becomes of the order of the transit time of an electron.

The behavior of counter *B* above its transition voltage seems to indicate the predominance of the photoelectric process. In modulation work there was no choking off of the breakdowns observed at any frequency. All the electrometer kicks were of the same size. It must be concluded that the mechanism responsible for the breakdown here is one which does its work and is finished in an extremely short time. Again, by the use of the oscillograph, the apparent breakdown time of this counter was found to be about 1/6000 second, even when the counter was discharging the parallel coupling capacity of 70 mmf at every breakdown, while the growth of the discharge to maximum current was too rapid to be timed at all by this method. It is difficult to see how so short a breakdown time could be explained on the assumption of the positive ion process. In the 45-kc oscillograph analysis, and even in that for 150 kc, there was no apparent growth of the discharge after the first half-cycle hump. This suggests that the discharge, insofar as the electron avalanches were concerned, was all completed in the half-cycle of its inception, and that the rest of the humps were due merely to the effect of the more leisurely collection of the positive ions. This behavior is just what might be expected on the assumption of the photoelectric process.

In the light of these results it is possible to make a speculation concerning the processes involved in bringing about the transition voltage in such a counter as this. Since at voltages below the transition voltage the magnitude and duration of the breakdowns occurring indicate the operation of the positive ion process, it is logical to conclude that the transition voltage is that at which the photoelectric process becomes predominant in the mechanism of the breakdown. This would explain the shortening of the breakdown time as the transition voltage is exceeded. On this view the transition voltage would be the threshold of the counter if the photoelectric process predominated at all voltages, as is apparently the case for the two alcohol-filled counters where the threshold and transition voltages are coincident. An explanation of the sudden increase in the magnitude of the voltage drop at each breakdown as the transition voltage is exceeded is suggested by some experiments of Werner[8] on gas-filled tubes of the Geiger counter form. In a circuit containing a discharge tube and variable voltage supply, Werner found that as the d.c. voltage across the tube is raised above the value at which a self-sustaining discharge occurs, which is the same as the threshold in a Geiger counter, the strength of the corona current increases very rapidly, and that as soon as a certain critical current is reached, the corona passes over into a glow discharge. In a circuit which includes a current-limiting resistance, this change is marked by a sudden decrease in the voltage across the tube itself to a value which corresponds to the normal cathode fall of the glow discharge, and which can be very much lower than the starting voltage of the corona. In a Geiger counter circuit, then, as the transition voltage is exceeded, the rapidity with which a breakdown proceeds under the photoelectric process may give a current of sufficient magnitude to cause the discharge to pass from the corona to the glow form. On this view the sudden increase in the size of the breakdowns is to be expected, for before a breakdown can be finished, the counter voltage must fall below the value which characterizes the glow.

In conclusion the author wishes to acknowledge his indebtedness to Professor J. A. Bearden, under whose direction this work was done, for his continued interest and many valuable suggestions, to Professor James Franck for the original suggestion of the problem, and to Dr. D. R. Inglis for advice in the preparation of this manuscript.

SEPTEMBER 15, 1939 PHYSICAL REVIEW VOLUME 56

A Method for Improved Calculation of Energies of Two-Electron Configurations from Hartree Functions

Application to $2p^2$ Terms in O III

A. F. STEVENSON
Department of Applied Mathematics, University of Toronto, Toronto, Canada

(Received June 23, 1939)

A generalization of the method of the self-consistent field for two-electron configurations previously given by the author has now been simplified and improved in two ways. Firstly, it is now assumed that the radial functions are identical with the Hartree functions (or with simpler approximations to these), so that a considerable saving in labor results. Secondly, the core electrons are taken account of more accurately than in the original method. The final results are in general only valid if the valence electrons are equivalent or if the difference in their azimuthal quantum numbers exceeds two; they do not involve a great deal of computation once the Hartree functions are known. Numerical calculations have been made for the normal state of helium (as a test of the method) and for the $2p^2$ terms of O III. The improvement obtained with the present method, while not great, is significant; in particular, the separation ratio for the O III terms is markedly improved.

1. INTRODUCTION

IN a recent paper,[1] a generalization of the method of the self-consistent field (s.c.f.) was given, applicable to the case of two-electron configurations in Russell-Saunders coupling, the core electrons being taken into account through a possible screening of the Coulomb field acting on the valence electrons.[2]

The generalization consists essentially in assuming for the wave function the form

$$\psi = \psi_0 \cdot X(x), \tag{1}$$

where ψ_0 is a function of the form usually assumed in the s.c.f. method when the correct symmetry properties of the wave function are taken into account, and contains the two radial functions, while $X(x)$ is an adjustable function of $x = \cos(\mathbf{r}_1, \mathbf{r}_2)$. The variational method is then applied, and yields differential equations for the two radial functions analogous to those of the s.c.f., together with a third equation for the function X. The assumption (1) is perhaps the most general one that can be made without introducing complications which would make the calculations intractable in many cases.

As developed in I, however, the method has two disadvantages. In the first place, the labor involved in carrying through numerical calculations would be considerable, particularly when exchange terms are taken into account. Secondly —and this is the more serious objection—the wave function (1) does not automatically satisfy the condition of being orthogonal to the wave functions of lower levels which have the same symmetry characteristics.[3] Since the effect of the

[1] A. F. Stevenson, Proc. Roy. Soc. **A160**, 588 (1937), referred to hereafter as I. The following correction may be noted: in Eq. (2), the sign in front of each of the square brackets should be $-$ instead of $+$. What is really a special case of the method had been previously used by Breit, Phys. Rev. **36**, 383 (1930).

[2] The extension to the case where the core electrons are taken more accurately into account was also briefly indicated, but was not worked through in any detail.

[3] The orthogonality condition is automatically satisfied for levels with different symmetry characteristics on account of the transformation properties of the wave functions. The same nonorthogonality situation may arise in the s.c.f. method (with any number of electrons) if there are lower levels for which the electrons have the same azimuthal quantum numbers as in the configuration considered, since the corresponding radial functions will

core electrons is replaced by a given central field acting on the valence electrons, there will often be a number of lower "virtual" levels of the same symmetry characteristics in which the valence electrons are in lower orbits, even though such configurations would violate the Pauli principle if the core electrons were more properly taken into account. Consequently, the method would lead to very misleading results in some cases.

As regards the first disadvantage, a considerable simplification results if the radial functions are not regarded as being arbitrary as in I, but are assumed to be identical with the s.c.f. functions,[4] and it is probable that the resulting loss in accuracy is slight. Such a simplification is made in the present paper. Further, an extension of the method is given which takes proper account of the core electrons, so that the orthogonality difficulty mentioned above does not arise—at least so long as there are no lower states, with the same symmetry characteristics, of the atom as a whole.

It will be found that if the valence electrons are equivalent (the most important case), or if the difference in their azimuthal quantum numbers exceeds two, the final form of the results is comparatively simple, and requires (in addition to some straightforward algebraical work) only the calculation of certain integrals involving the s.c.f. radial functions, so that, when once these functions are known, the labor required is not very great. The method may thus be regarded as one for making more accurate calculations of energies from the s.c.f. functions than are provided by the usual method.

Numerical calculations have been carried through for the normal state of helium (as a try-out of the method), and for the $2p^2$ terms of O III, for which the s.c.f. (without exchange) has been worked out by Hartree and Black.[5] While the improvement obtained over the s.c.f. result is not great, it is nevertheless significant, and appears to be roughly of the same order of magnitude as the improvement obtained by including exchange terms in the s.c.f. equations.

2. The "Two-Electron" Method

We shall first work out the case where the same assumption is made as in I regarding the core electrons—i.e., we take them into account only by a modification of the central field—but where the radial functions are regarded as being already known. We may refer to this as the "two-electron" method. Although, as discussed above, this may lead to erroneous results, it may nevertheless be valid in certain cases, and the results form, as we shall see, a check on the more complicated calculations of Section 4.

We denote the configuration quantum numbers of the two electrons by (n_1l_1) and (n_2l_2) and their radial functions by $P_1(r)$, $P_2(r)$.[6] We make the assumption (1), where ψ_0 takes proper account of exchange, etc. The energy, to be minimized, is

$$E=\int\psi^*H\psi d\tau \Big/ \int|\psi|^2d\tau.$$

The method of handling such integrals (coordinate system to be adopted, etc.) has been fully discussed in I, and we shall here give only the final result. Although the general case can be handled without difficulty, the results simplify considerably if we assume *either* (1) $l_1=l_2$, *or* (2) $|l_1-l_2|>2$ and $X=$linear function of x. These include the cases considered in the more complete theory of Section 4.

We then find, measuring the energy in atomic units (instead of rydbergs as in I),

$$E=C+\int XL(X)dx \Big/ \int f(x)X^2dx, \qquad (2)$$

where

$$L(X)=-A\frac{d}{dx}\left[(1-x^2)f(x)\frac{dX}{dx}\right]+\phi(x)X. \qquad (3)$$

The integrals with respect to x are taken, in (2) and throughout this section, from -1 to $+1$. C is

not be accurately orthogonal on account of the difference in central fields. For instance, some of the calculations of Wilson and Lindsay on doubly excited states of helium (Phys. Rev. **47**, 681; **48**, 536 (1935)) would seem to be subject to doubt for this reason.

[4] It is immaterial for our purpose whether these functions are obtained by a strict application of the s.c.f. method (with or without exchange), or in some simpler manner. Naturally, the more accurate the functions are, the better.

[5] D. R. Hartree and M. M. Black, Proc. Roy. Soc. **A139**, 311 (1933). The coupling for this case appears to be sufficiently near to Russell-Saunders, though the interval rule is not very well satisfied for the ^3P multiplet.

[6] We follow Hartree in writing $P(r)/r$ for the radial part of the wave function. We suppose these functions normalized.

a constant depending only on the radial functions, and need not be given explicitly, while

$$A=(1/2)\int_0^\infty (P_1^2+P_2^2)/r^2dr. \tag{4}$$

Further,

$$\phi(x)=f(x)\sum_{n=0}^{\infty} F_nP_n(x)+g(x)\sum_{n=0}^{\infty} G_nP_n(x), \tag{5}$$

where F_n, G_n are Slater's integrals,[7]

$$\begin{aligned} F_n&=\int\int_0^\infty [P_1(r_1)P_2(r_2)]^2 r_<^n/r_>^{n+1}dr_1dr_2,\\ G_n&=\int\int_0^\infty P_1(r_1)P_2(r_2)P_2(r_1)\\ &\qquad\times P_1(r_2)r_<^n/r_>^{n+1}dr_1dr_2, \end{aligned} \tag{6}$$

and $f(x)$, $g(x)$ are certain polynomials (of which $f(x)$ is always even, while $g(x)$ can be put equal to zero for equivalent electrons), whose explicit form need not be given for the moment.

Now if X be put equal to a constant, the energy must reduce to the s.c.f. energy E_0. Hence, from (2),

$$E_0=C+E',\quad E'=\int\phi(x)dx\Big/\int f(x)dx. \tag{7}$$

E' gives the part of E_0 containing the Coulomb and exchange integrals F, G of (6). Thus from (2) and (7) we have $E=E_0+\Delta E$, where ΔE, the correction to the s.c.f. energy, is given by

$$\Delta E=\int XL(X)dx\Big/\int f(x)X^2dx-E'. \tag{8}$$

The polynomials $f(x)$, $g(x)$ may be found most simply as follows: let

$$f(x)=\sum_n f_nP_n(x),\quad g(x)=\sum_n g_nP_n(x), \tag{9}$$

where the f's and g's are constants, of which we may arbitrarily put $f_0=1$ since $f(x)$ is undetermined to a constant factor. Then from (7), (5), (9),

$$E'=\sum_n (f_nF_n+g_nG_n)/(2n+1). \tag{10}$$

[7] E. U. Condon and G. H. Shortley, *Theory of Atomic Spectra* (Cambridge, 1935), 177. These integrals are there denoted by F^n, G^n. We shall refer to this book as "C.S."

Comparing (10) with the expression for E' in terms of the F's and G's as found by the usual methods,[8] we then immediately have the values of the constants f_n, g_n, and hence, from (9), the polynomials $f(x)$, $g(x)$.

On varying the function X and minimizing E, we see from (2) that X (provided it is not restricted to be a linear function) satisfies the differential equation

$$[L-\lambda f(x)]X=0,$$

where $\lambda=\Delta E+E'$. However, it is not necessary to actually solve this equation, for X will be a slowly-varying function which will be well approximated by a polynomial, say

$$X=\sum_i a_ix^i \tag{11}$$

and we may then use the Ritz method. This leads to the determinantal equation

$$|L_{ij}-\lambda f_{ij}|=0 \tag{12}$$

for λ, where

$$L_{ij}=\int x^iL(x^i)dx,\quad f_{ij}=\int x^{i+j}f(x)dx.$$

Quite a small number of terms will suffice in (11), and it then becomes necessary to calculate only a few of the F, G integrals of (6). In fact, we shall confine ourselves later on to the case where X is a *linear* function of x. It can then be shown that (12) becomes (in a notation used for subsequent convenience)

$$\begin{vmatrix} -\Delta E & H_{01}\\ H_{01} & H_{11}'-N_{11}\Delta E\end{vmatrix}=0, \tag{13}$$

where

$$\begin{aligned} H_{01}&=\int x\phi(x)dx/f(x)dx,\\ N_{11}&=\int x^2f(x)dx\Big/\int f(x)dx,\\ H_{11}'&=A\int(1-x^2)f(x)dr\Big/\int f(x)dx. \end{aligned} \tag{14}$$

In H_{11}' certain comparatively small terms depending on the F's and G's have been neglected;

[8] C.S., Chapter 7.

this is justifiable since ΔE is small, so that it is only necessary to have an approximate value of H_{11}'. If ΔE^2 is neglected, (13) gives simply

$$\Delta E = -H_{01}^2/H_{11}'. \tag{15}$$

3. Application to Normal State of Helium

As a test of the efficacy of the method of the preceding section, we consider the simplest possible case, namely the normal state of helium, for which (8) or (12) are valid without restricting X to be a linear function. It will not, of course, be expected that results comparable in accuracy with those of Hylleraas in his well-known work on helium will be reached. We have in this case

$$f(x)=1, \quad \phi(x)=\sum_{n=0}^{\infty} F_n P_n(x), \quad E'=F_0.$$

Using (12), and confining ourselves to three terms of (11), we find

$$L_{00}=2F_0, \quad L_{01}=\frac{2}{3}F_1, \quad L_{02}=\frac{2}{3}F_0+\frac{4}{15}F_2,$$

$$L_{11}=\frac{4}{3}A+L_{02}, \quad L_{12}=\frac{2}{5}F_1+\frac{4}{35}F_3,$$

$$L_{22}=\frac{16}{15}A+\frac{2}{3}F_0+\frac{8}{35}F_2+\frac{16}{315}F_4,$$

$$f_{00}=2, \quad f_{01}=f_{12}=0, \quad f_{11}=f_{02}=\frac{2}{3}, \quad f_{22}=\frac{2}{5}.$$

Since we are here only interested in the order of magnitude of the results, we simplify the calculation of the radial integrals by using the approximate (un-normalized) function

$$P(r)=re^{-(27/16)r}$$

rather than the accurate s.c.f. function; the results will not differ much. We then find

$$A=8/27, \quad F_0=5/8, \quad F_1=3/8,$$
$$F_2=0.2605, \quad F_3=0.1973, \quad F_4=0.1580.$$

Application of (12) then gives (atomic units):

with 2-term function for X: $\Delta E=-0.0115$,
with 3-term function for X: $\Delta E=-0.0125$.

Taking the 3-term value for ΔE, we then have the following values for the ionization potential of helium in rydbergs:

s.c.f. = 1.723, corrected = 1.748,
experimental = 1.807.

The correction thus accounts for rather less than one-third of the discrepancy between the s.c.f. and experimental values. It is seen that very little improvement is obtained by taking a 3-term rather than a 2-term function for X.

4. The Generalized Method

We now generalize the method of Section 2 so as to take account more properly of the core electrons, but confine ourselves to the case where X is a linear function of x. We denote the valence electrons by 1, 2 and the core electrons by $3, \cdots, N$, and use the usual notation for quantum numbers, etc. In the "two-electron" method, our assumption (1) is now equivalent to

$$\psi=\psi_0+c\psi_1, \tag{16}$$

where $\psi_0(1, 2)$ is the s.c.f. function (more strictly, one of a *set* of such functions belonging to the given level), c is an adjustable constant, and

$$\psi_1(1, 2)=\cos(\mathbf{r}_1, \mathbf{r}_2)\psi_0(1, 2).$$

Let now U_0 denote the s.c.f. function for the whole atom. Then we know that U_0 is a linear combination of determinantal wave functions u_0 of the form

$$u_0=\frac{1}{N!}\begin{vmatrix} u(\alpha_1, 1) & \cdots & u(\alpha_N, 1) \\ \cdot & \cdot & \cdot \\ u(\alpha_1, N) & \cdots & u(\alpha_N, N) \end{vmatrix} \tag{17}$$

in which α_1 stands for the four quantum numbers $(n_1 l_1 m_1 s_1)$ etc., and where, in the usual notation

$$u(\alpha, \mathbf{r})=\frac{1}{r}P_{nl}(r)\,Y_{lm}(\theta, \phi)\delta(s, \sigma). \tag{18}$$

(s, σ denote, respectively, spin quantum number and spin variable, Y_{lm} a surface harmonic; we suppose all functions normalized.)

Consider now the function

$$u_1=u_1'+u_1''+u_1''', \tag{19}$$

where

$$u_1'=\frac{1}{N!}\begin{vmatrix} u(\alpha_1,1)\cos\theta_1 & u(\alpha_2,1)\cos\theta_1 & u(\alpha_3,1) & \cdots & u(\alpha_N,1) \\ \cdots & \cdots & \cdots & \cdots & \cdots \\ u(\alpha_1,N)\cos\theta_N & u(\alpha_2,N)\cos\theta_N & u(\alpha_3,N) & \cdots & u(\alpha_N,N) \end{vmatrix}$$

$$u_1''=\frac{1}{N!}\begin{vmatrix} u(\alpha_1,1)\sin\theta_1\cos\phi_1 & u(\alpha_2,1)\sin\theta_1\cos\phi_1 & u(\alpha_3,1) & \cdots & u(\alpha_N,1) \\ \cdots & \cdots & \cdots & \cdots & \cdots \\ u(\alpha_1,N)\sin\theta_N\cos\phi_N & u(\alpha_2,N)\sin\theta_N\cos\phi_N & u(\alpha_3,N) & \cdots & u(\alpha_N,N) \end{vmatrix} \tag{20}$$

$$u_1'''=\frac{1}{N!}\begin{vmatrix} u(\alpha_1,1)\sin\theta_1\sin\phi_1 & u(\alpha_2,1)\sin\theta_1\sin\phi_1 & u(\alpha_3,1) & \cdots & u(\alpha_N,1) \\ \cdots & \cdots & \cdots & \cdots & \cdots \\ u(\alpha_1,N)\sin\theta_N\sin\phi_N & u(\alpha_2,N)\sin\theta_N\sin\phi_N & u(\alpha_3,N) & \cdots & u(\alpha_N,N) \end{vmatrix}$$

and let U_1 denote the *same* linear combination of the functions u_1 of (19) that U_0 is of the functions u_0 of (17). Then a suitable assumption for the wave function is, analogously to (16),

$$\psi=U_0+cU_1. \tag{16'}$$

For, since

$$\cos(\mathbf{r}_1,\mathbf{r}_2)=\cos\theta_1\cos\theta_2+\sin\theta_1\cos\phi_1 \times\sin\theta_2\cos\phi_2+\sin\theta_1\sin\phi_1\sin\theta_2\sin\phi_2,$$

we see that U_1 reduces to our previous ψ_1 if $N=2$. Further, if the determinants (20) be expanded by Laplace's rule from the first two columns, it can be seen that, when the proper linear combinations for the function U_1 are taken, the set U_1 transforms in the correct way under rotations and reflections. Also evidently U_1 is antisymmetrical in all electrons. Thus (16'), with (17), (19), (20), satisfies all requirements as to symmetry properties and is the required generalization.

Minimizing the energy with respect to c with (16'), we see that E is given by

$$\begin{vmatrix} H_{00}-EN_{00} & H_{01} \\ H_{01} & H_{11}-EN_{11} \end{vmatrix}=0, \tag{21}$$

where

$$H_{ij}=\int U_i^*HU_j d\tau, \quad N_{ij}=\int U_i^*U_j d\tau.$$

To calculate H_{ij}, N_{ij} we need only find these matrix elements with respect to the functions u_0, u_1 of (17), (19), and then use the diagonal sum rule in the familiar way.[9] We shall therefore calculate

$$H_{ij}=\int u_i^*Hu_j d\tau, \quad N_{ij}=\int u_i^*u_j d\tau,$$

and understand that it is really linear combinations of such quantities which are implied. We now use the formulae[10]

$$\begin{aligned} Y_{lm}\cos\theta&=aY_{l+1,\,m}+bY_{l-1,\,m} \\ Y_{lm}\sin\theta\cos\phi&=cY_{l+1,\,m}+dY_{l+1,\,m-1} \\ &\quad +eY_{l-1,\,m+1}+fY_{l-1,\,m-1} \\ Y_{lm}\sin\theta\sin\phi&=i(-cY_{l+1,\,m+1}+dY_{l+1,\,m-1} \\ &\quad -eY_{l-1,\,m+1}+fY_{l-1,\,m-1}), \end{aligned} \tag{22}$$

where

$$\begin{aligned} a=a(l,m)&=\left[\frac{(l-m+1)(l+m+1)}{(2l+1)(2l+3)}\right]^{\frac{1}{2}}, \\ b&=\left[\frac{l^2-m^2}{4l^2-1}\right]^{\frac{1}{2}}, \\ c&=-\frac{1}{2}\left[\frac{(l+m+1)(l+m+2)}{(2l+1)(2l+3)}\right]^{\frac{1}{2}}, \\ d&=\frac{1}{2}\left[\frac{(l-m+1)(l-m+2)}{(2l+1)(2l+3)}\right]^{\frac{1}{2}}, \\ e&=\frac{1}{2}\left[\frac{(l-m)(l-m-1)}{4l^2-1}\right]^{\frac{1}{2}}, \\ f&=-\frac{1}{2}\left[\frac{(l+m)(l+m-1)}{4l^2-1}\right]^{\frac{1}{2}}. \end{aligned} \tag{23}$$

It is then possible to express u_1 as a sum of 12 determinants containing one-electron functions of the type (17). To save space, we write (17),

[9] See, e.g., C.S., 191 *et seq.* We use the term "diagonal sum rule" in a somewhat more general sense than usual, namely: if $\phi_1, \phi_2, \cdots$ and $\chi_1, \chi_2, \cdots$ are any two sets of the same number of functions, and if $\phi_1', \phi_2', \cdots$ and $\chi_1', \chi_2', \cdots$ are the sets obtained from these by the *same* unitary transformation, then

$$\Sigma_i\int\phi_i^*H\chi_i d\tau=\Sigma_i\int\phi_i'^*H\chi_i' d\tau.$$

[10] These follow at once from C.S., 53, formula (21), on using $\cos\phi=(e^{i\phi}+e^{-i\phi})/2$ etc. A particular definition of Y_{lm} for negative m is implied.

with the help of (18), as follows:

$$u_0=(l_1, m_1; l_2, m_2),$$

that is, all four quantum numbers of the core electrons and the n, s quantum numbers of the valence electrons are regarded as being always equal to those in (17), and we only allow for the possibility of the l, m quantum numbers of the valence electrons varying. With this convention, and using (20), (22), (23) we can now write (19) in the form

$$u_1=\sum_{k=1}^{12}\gamma_k u_1^{(k)}, \tag{24}$$

where

$$\begin{aligned}
&\gamma_1=a_1a_2, \quad \gamma_2=b_1b_2, \quad \gamma_3=a_1b_2,\\
&\gamma_4=a_2b_1, \quad \gamma_5=2c_1d_2, \quad \gamma_6=2c_2d_1,\\
&\gamma_7=2c_1f_2, \quad \gamma_8=2c_2f_1, \quad \gamma_9=2d_1e_2,\\
&\gamma_{10}=2d_2e_1, \quad \gamma_{11}=2e_1f_2, \quad \gamma_{12}=2e_2f_1
\end{aligned} \tag{25}$$

$$(a_1=a(l_1, m_1) \text{ etc.})$$

and

$$\begin{aligned}
u_1^{(1)}&=(l_1+1, m_1; l_2+1, m_2),\\
u_1^{(2)}&=(l_1-1, m_1; l_2-1, m_2),\\
u_1^{(3)}&=(l_1+1, m_1; l_2-1, m_2),\\
u_1^{(4)}&=(l_1-1, m_1; l_2+1, m_2),\\
u_1^{(5)}&=(l_1+1, m_1+1; l_2+1, m_2-1),\\
u_1^{(6)}&=(l_1+1, m_1-1; l_2+1, m_2+1),\\
u_1^{(7)}&=(l_1+1, m_1+1; l_2-1, m_2-1),\\
u_1^{(8)}&=(l_1-1, m_1-1; l_2+1, m_2+1),\\
u_1^{(9)}&=(l_1+1, m_1-1; l_2-1, m_2+1),\\
u_1^{(10)}&=(l_1-1, m_1+1; l_2+1, m_2-1),\\
u_1^{(11)}&=(l_1-1, m_1+1; l_2-1, m_2-1),\\
u_1^{(12)}&=(l_1-1, m_1-1; l_2-1, m_2+1).
\end{aligned} \tag{26}$$

For clarity, we give the extended form of $u_1^{(1)}$ for instance: $u_1^{(1)}$ is the same as the function u_0 of (17), except that now

$$\begin{aligned}
u(\alpha_1, \mathbf{r})&=\frac{1}{r}P_{n_1l_1}(r)\,Y_{l_1+1,\,m_1}(\theta, \phi)\delta(s_1, \sigma),\\
u(\alpha_2, \mathbf{r})&=\frac{1}{r}P_{n_2l_2}(r)\,Y_{l_2+1,\,m_2}(\theta, \phi)\delta(s_2, \sigma).
\end{aligned} \tag{27}$$

Each of the $u_1^{(k)}$ is of the usual form of determinantal wave function; but for facility in calculating matrix elements, it is necessary that the one-electron functions of which the determinant is composed be mutually orthogonal. This is not so in general, the function $P_{n_1l_1}(r)$ in (27), for instance, not being orthogonal to the other radial functions which have azimuthal quantum number (l_1+1). However, we can, without altering the value of the determinant, add to $P_{n_1l_1}(r)$ and $P_{n_2l_2}(r)$ multiples of the radial functions of quantum numbers $l_1\pm1$, $l_2\pm1$ so that all the one-electron functions are mutually orthogonal (cf., for instance, Hartree and Black).[5] We shall suppose this done, and shall write P_{nl}^{+}, P_{nl}^{-} for the radial functions which have thus been made orthogonal to all other radial functions having azimuthal quantum numbers $l+1$, $l-1$ respectively, so that in (27), e.g., we would have $P_{n_1l_1}^{+}(r)$ instead of $P_{n_1l_1}(r)$. We must remember, however, that the functions P_{nl}^{+}, P_{nl}^{-} are not normalized.

For convenient calculation it is further necessary that the one-electron functions composing a given $u_1^{(k)}$ be either orthogonal or identical with those composing u_0 and the remaining $u_1^{(k)}$. An examination of (26) shows that this is always the case *either if the electrons are equivalent or if* $|l_1-l_2|>2$. Since the calculations would be very complicated unless the orthogonality conditions are satisfied, we shall restrict ourselves to these two cases.[11] If $|l_1-l_2|>2$, the functions u_0, $u_1^{(1)}$, $\cdots$, $u_1^{(12)}$ are mutually orthogonal; but in the equivalent electron case, we must note that:[12]

(a) if $s_1=s_2$, $m_1=m_2+1$, then

$$u_1^{(1)}=-u_1^{(6)}, \quad u_1^{(2)}=-u_1^{(12)},$$
$$u_1^{(3)}=-u_1^{(8)}, \quad u_1^{(4)}=-u_1^{(9)}.$$

(b) if $s_1=s_2$, $m_1=m_2+2$, then

$$u_1^{(6)}=u_1^{(12)}=0.$$

We can now calculate our matrix elements with the formulae given in C.S., 196 *et seq.*, the only difference being that the functions P_{nl}^{+}, P_{nl}^{-} are not necessarily normalized. In calculating H_{11}

[11] The formulae to be given are still valid in certain other cases; we shall not detail these.

[12] The cases $s_1=s_2$, $m_2=m_1-1$ and $s_1=s_2$, $m_2=m_1-2$ are also exceptional, but these need not be dealt with separately, since we can always suppose $m_1\geqslant m_2$.

we shall simplify by regarding each electron as moving in the same (screened) central field and disregarding interaction: this is justifiable (cf. the discussion following (14)). The results are then as follows:

$$H_{00}=E_0,$$

$$H_{01}=\sum_{k=1}^{12}\sum_{j}\gamma_k[c^j(l_1m_1, l_1{}^km_1{}^k)c^j(l_2{}^km_2{}^k, l_2m_2)\times F_j(n_1l_1{}^k, n_2l_2{}^k)-\delta(s_1, s_2)\times c^j(l_1m_1, l_2{}^km_2{}^k)c^j(l_1{}^km_1{}^k, l_2m_2)\times G_j(n_1l_1{}^k, n_2l_2{}^k)],$$

$$H_{11}=N_{11}E_0+H_{11}',$$

where (28)

$$H_{11}'=(l_1+1)(B_1N_2{}^++B_2N_2{}^-)A(n_1l_1{}^+)-l_1(B_3N_2{}^++B_4N_2{}^-)A(n_1l_1{}^-)+(l_2+1)(B_1N_1{}^++B_3N_1{}^-)A(n_2l_2{}^+)-l_2(B_2N_1{}^++B_4N_1{}^-)A(n_2l_2{}^-),$$

$$N_{00}=1,\quad N_{01}=0,$$

$$N_{11}=B_1N_1{}^+N_2{}^++B_2N_1{}^+N_2{}^-+B_3N_1{}^-N_2{}^++B_4N_1{}^-N_2{}^-,$$

where

$$B_1=\gamma_1{}^2+\gamma_5{}^2+\gamma_6{}^2,\quad B_2=\gamma_3{}^2+\gamma_7{}^2+\gamma_9{}^2,$$

$$B_3=\gamma_4{}^2+\gamma_8{}^2+\gamma_{10}{}^2,\quad B_4=\gamma_2{}^2+\gamma_{11}{}^2+\gamma_{12}{}^2.$$

We use $l_1{}^k$ for $l_1\pm1$, etc., depending on the l, m values in the particular $u_1{}^{(k)}$ which goes with γ_k according to (24) and (26). The c^j are integrals of the product of three tesseral harmonics and are identical with the constants denoted thus in C.S., 175, formula (6). They are tabulated in C.S., 178, 179. The A, F, G are radial integrals analogous to those of (4) and (6), namely, with k denoting + or − according as $l_1{}^k=l_1\pm1$, $l_2{}^k=l_2\pm1$,

$$A(nl^k)=\int_0^\infty P_{nl}(r)P_{nl}{}^k(r)/r^2dr,$$

$$F_j(n_1l_1{}^k, n_2l_2{}^k)=\int\int_0^\infty P_{n_1l_1}(r_1)P_{n_2l_2}(r_2)\times P_{n_1l_1}{}^k(r_1)P_{n_2l_2}{}^k(r_2)r_<{}^j/r_>{}^{j+1}dr_1dr_2,$$

$$G_j(n_1l_1{}^k, n_2l_2{}^k)=\int\int_0^\infty P_{n_1l_1}(r_1)P_{n_2l_2}(r_2)\times P_{n_2l_2}{}^k(r_1)P_{n_1l_1}{}^k(r_2)r_<{}^j/r_>{}^{j+1}dr_1dr_2.$$

Finally, the N's are normalizing factors:

$$N_1{}^+=N(n_1l_1{}^+)=\int_0^\infty[P_{n_1l_1}{}^+(r)]^2dr, \text{ etc.}$$

All these formulae hold for the case of equivalent electrons (when $F_j=G_j$), except that they must be modified in the exceptional cases (a), (b) mentioned above as follows:

Case (a):—To B_1, B_4, B_2+B_3 we must add $-2\gamma_1\gamma_6$, $-2\gamma_2\gamma_{12}$, $-2(\gamma_3\gamma_8+\gamma_4\gamma_9)$, respectively (only the sum B_2+B_3 occurs in the case of equivalent electrons).

Case (b):—Put $\gamma_6=\gamma_{12}=0$.

Putting $E=E_0+\Delta E$, (21) now takes precisely the form (13), with the meanings of H_{01}, H_{11}', N_{11} given in (28). Moreover, since the final results involve only the radial functions of the valence electrons, except for the "orthogonality" modification, we see that if this modification be disregarded—i.e. if we put $P_{nl}{}^+=P_{nl}{}^-=P_{nl}$—the H_{01}, H_{11}', N_{11} of (28) must reduce precisely to those of (14) obtained by the "two-electron" method. This forms a useful check on the work, since the integrals in (14) are easily calculated.

5. Application to $2p^2$ Terms in O III

The configuration is $1s^22s^22p^2$ and the terms ^1S, ^3P, ^1D. Application of the formulae of the preceding section, together with the diagonal sum rule, leads to the following results:

$$H_{01}(^1S)=\frac{4}{15}F_1(2p, 2p)+\frac{1}{3}F_1(2p^-, 2p^-)+\frac{6}{35}F_3(2p, 2p),$$

$$H_{01}(^3P)=\frac{1}{5}F_1(2p, 2p)-\frac{3}{35}F_3(2p, 2p),$$

$$H_{01}(^1D)=\frac{7}{75}F_1(2p, 2p)+\frac{4}{15}F_1(2p, 2p^-)+\frac{3}{175}F_3(2p, 2p),$$

$$H_{11}'=[4B_1+2(B_2+B_3)N(2p^-)]A(2p)-[(B_2+B_3)+2B_4N(2p^-)]A(2p^-),$$

$$N_{11}=B_1+(B_2+B_3)N(2p^-)+B_4[N(2p^-)]^2,$$

TABLE I.

	S.C.F.	CORRECTED	OBSERVED
^3P:	−1.988	−1.992	−2.025
	0.099	0.099	0.091
^1D:	−1.889	−1.893	−1.934
	0.148	0.134	0.105
^1S:	−1.741	−1.759	−1.829
$\frac{^1S-{}^1D}{^1D-{}^3P}$:	1.5	1.35	1.15

where, for

$$^1S:\quad B_1=\frac{4}{15},\quad B_2+B_3=0,\quad B_4=\frac{1}{3},$$

$$^3P:\quad B_1=\frac{1}{5},\quad B_2+B_3=0,\quad B_4=0,$$

$$^1D:\quad B_1=\frac{7}{75},\quad B_2+B_3=\frac{4}{15},\quad B_4=0.$$

$P_{2p}^-(r)$ denotes the $2p$-function made orthogonal to both the $1s$ and $2s$ functions in the manner explained;[13] $P_{2p}^+(r)$ is identical with $P_{2p}(r)$ since there are no d electrons.

Numerical integration with the functions of Hartree and Black[5] yields the approximate values:

$$F_1(2p, 2p)=0.575,\quad F_1(2p, 2p^-)=0.002,$$
$$F_1(2p^-, 2p^-)=0.000_6,\quad F_3(2p, 2p)=0.317,$$
$$A(2p)=2.27_5,\quad A(2p^-)=-0.068,$$
$$N(2p^-)=0.005,$$

whence, for ^1S, ^3P, ^1D, respectively:

$$H_{01}=0.208,\ 0.088,\ 0.059,$$
$$H_{11}'=2.43,\ 1.82,\ 0.873_5,$$
$$N_{11}=0.267,\ 0.200,\ 0.0947.$$

Hence from (13) (or (15), which is sufficiently accurate),

$$\Delta E(^1S)=-0.018,\quad \Delta E(^3P)=-0.004,$$
$$\Delta E(^1D)=-0.004.$$

This leads to the results in Table I, with energies in atomic units and measured from the normal state of O IV as zero.

The improvement in energy values relative to the O IV ground state is small, but it must be remembered that the energy of the O IV ground state used by Hartree and Black is itself the result of an s.c.f. calculation. The results become more significant if we consider the separations between the ^3P, ^1D, ^1S terms, also shown above. It is then seen that the good agreement between the calculated (s.c.f.) and observed $^1D-{}^3P$ separation is left unaltered, while the calculated $^1S-{}^1D$ separation is noticeably improved, about $\frac{1}{3}$ of the discrepancy between theory and observation being accounted for.[14] The improvement in the separation ratio $(^1S-{}^1D)/(^1D-{}^3P)$ is of particular interest (somewhat less than one-half the discrepancy being accounted for), since the s.c.f. theory leads to a value 1.5 for this ratio for p^2 terms independently of the radial functions, this value not being in good agreement with experiment in most cases.[15]

Thus the method of this paper, where applicable, seems—judging by the results worked out here—to afford a worthwhile improvement over the ordinary s.c.f. method, and to indicate that theory would be in complete agreement with experiment if the mathematical difficulties could be surmounted.

[13] The $1s$ and $2s$ functions must also be made orthogonal to each other as explained by Hartree and Black, reference 5.

[14] Hartree and Black estimate that the probable error of their calculated results is "rather smaller" than 0.007, so that it is really only the correction for the ^1S which is significant. This does not invalidate the above comparison.

[15] C.S., 198. It may be remarked, however, that the value 1.5 would not be obtained if the s.c.f. *with exchange* were used.

A Precise Method of Measuring Heat Conductivity Applicable to Either Molten or Solid Metals. Thermal Conductivity of Zinc

CHARLES C. BIDWELL
Lehigh University, Bethlehem, Pennsylvania

(Received April 22, 1939)

A metal rod or a hollow vertical graphite cylinder containing molten metal is packed in silocel contained in an outer iron cylinder. Downward heat flow is established, and vertical gradients are measured differentially by thermojunctions in quartz tubes as are also radial temperature drops across the silocel at all levels. At low temperatures the iron cylinder is surrounded by constant temperature baths, at high temperatures by additional silocel contained in magnesia pipe lagging. The differential junction measurements were obtained by raising one junction progressively while the other was left at the bottom. High temperatures were obtained by a heater winding placed directly on the specimen or graphite cylinder but insulated electrically. For either low or high temperature arrangements the gradient down the specimen is found to change with distance at a constant rate. This means that radial temperature drops across the silocel are constant from bottom to top. This was checked experimentally. Previously published values for solid zinc are verified and extended through the melting point to 730°. The drop in conductivity at the melting point agrees with data of Konno (the only data found in the literature). The values in the liquid state decrease slightly with rise of temperature. Konno's data suggested this but did not extend far enough to prove it.

INTRODUCTION

METHODS of measuring thermal conductivity by longitudinal heat flow—the only procedure possible for liquids—are unsatisfactory in several respects. Most workers have depended upon compensation of lateral or radial heat flow and assumed perfect compensation when the gradient down the rod became constant. The author has found considerable chance for judgment as to when compensation is effected and particularly a large uncertainty as to whether the source of energy producing the heat flow is the heater coil intended for that purpose or the compensating coil. Variations as high as 20 percent may result from this uncertainty. A method which avoids these uncertainties and largely eliminates the personal judgment of the observer is here reported.

THEORY OF PRESENT METHOD

The method here employed is based upon the observation that with a downward heat flow established in a test rod packed vertically in thermal insulation, the thermal gradient in the rod, under certain easily attainable conditions, changes at a constant rate as one moves down the rod and where this is true the radial heat loss across the insulation per cm length is constant. The expression which equates the radial heat loss per cm to the difference in vertical heat flow per cm is

$$2\pi k_s \Delta T/2.30 \log R_2/R_1 = k_x A d^2T/dx^2.$$

k_s is the thermal conductivity of the silocel at the temperature in question; ΔT, the radial temperature drop across the insulation (constant for all levels); R_2 and R_1, the outer and inner radii of the silocel; k_x, the thermal conductivity of the test rod; A, its cross section area; and d^2T/dx^2, the (constant) slope of gradient-distance line. Under the circumstances the insulation at its outer radius follows the same temperature drop as does the test rod although its average temperature may be 60 or more degrees lower. This was thoroughly checked experimentally. The necessary conditions can of course only be approximated[1] but *over the length at which the gradient changes are constant, the lateral losses are constant.* This is the essential idea of the method.

EXPERIMENTAL ARRANGEMENT FOR SOLID METALS

Figure 1 shows the experimental set-up as used for molten metals. For solid metals the

[1] To attain the necessary conditions with rods 25 cm long, the top 6 cm must be disregarded. With very long rods and small heat input at the top the lateral loss toward the bottom approaches zero.

arrangement is similar except that the upper bored out part of the graphite rod is replaced by the solid metal rod. The test rod (zinc) 4 to 5 cm in diameter, 20 to 25 cm long, was mounted upon a solid graphite cylinder (heat sink) of like dimensions and centered in an iron cylinder 12 cm in diameter and 50 cm long. The space between the test rod and iron cylinder was packed with silocel. Five additional cm of silocel were packed outside the iron cylinder and contained in an outer asbestos tube. Silocel was packed above and below the specimen for about 20 cm. For low temperatures the same rods were centered in a tin cylinder, 12 cm in diameter, 50 cm long. The cylinder was closed at the bottom and the metal rod rested directly upon the tin bottom instead of on the graphite rod (sink). The top of the cylinder (above the test rod) was filled with silocel. The tin cylinder was immersed directly in constant temperature baths —cracked ice, CO_2 slush with alcohol or liquid nitrogen.

Before mounting, the specimen and the graphite cylinder upon which it rested were each wound their entire length with Nichrome ribbon insulated by a single layer of asbestos paper, the winding being put on with the asbestos paper wet. Thus the specimen could be heated quickly to any desired temperature and, since the winding on the graphite was separate, any temperature gradient in the specimen could, within limits, be eliminated by adjusting the energy input into the graphite base. Alternating current was used always in these heater windings. A small pancake type heating coil was fastened to the top of the test metal, thus permitting a known input of electrical energy at the top and establishing a heat flow down the specimen. The current in this heater will be known as direct current. The specimen was originally cast with two one-eighth-inch o.d. thin-walled quartz tubes extending clear to the bottom for the insertion of thermojunctions. Temperatures and temperature gradients were measured differentially between the two junctions, one junction being raised progressively, usually 2 cm at a time, the other left at the bottom. The differential readings were read directly as galvanometer deflections. A third junction kept in melting ice could be thrown in series with either junction

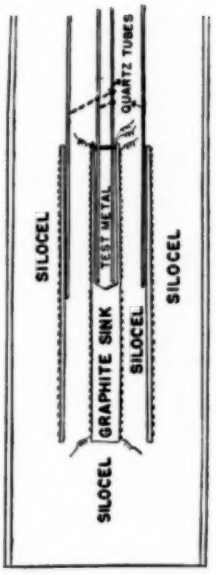

FIG. 1. Arrangement for molten metals.

and the actual temperature obtained. For this latter case a potentiometer was used. Since the bore of the quartz tubes was only about 1.5 mm and since temperatures were carried as high as 800°C, the problem of insulation for the junction wires required attention. The junction wires were of Chromel and copper and it was found that heating each to a good red heat oxidized the surfaces such that no further insulation was needed. Such wires could not be twisted together as that would fracture the oxide crust but they could be laid in contact and slipped up and down the tubes with impunity.

For reading temperatures across the insulation, two quartz tubes with thermojunctions were inserted in the silocel just inside the iron or tin cylinder. These tubes extended down to the level of the bottom of the test specimen. With either of these junctions used differentially with the stationary junction at the bottom of the specimen, the temperature drop across the silocel insulation and temperature variation up and down at the outer radius of the silocel could be read.

EXPERIMENTAL PROCEDURE

The temperature is raised to the desired region by means of the heater windings on the specimen and its graphite base, with the same current in each winding. When approximate temperature equilibrium is attained (in one or two hours),

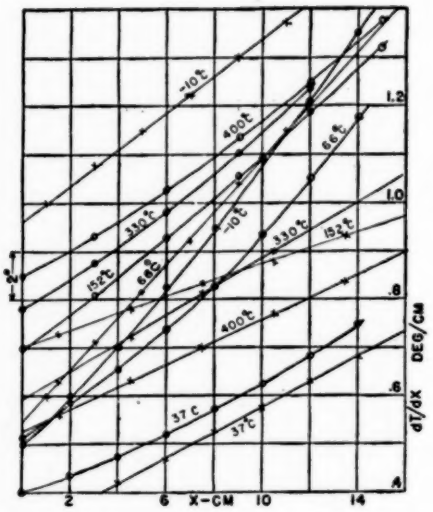

FIG. 2. Gradient data for solid zinc. T, x curves and dT/dx, x curves (straight lines).

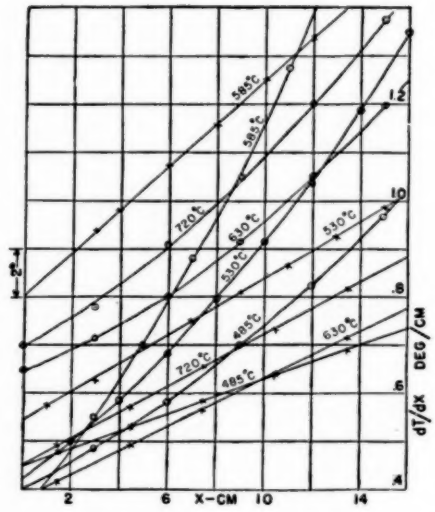

FIG. 3. Gradient data for molten zinc. T, x curves and dT/dx, x curves (straight lines).

the current in the winding on the supporting base is adjusted so as approximately to eliminate any vertical gradient in the specimen. Also at high temperatures the radial drop, ΔT, is reduced by current in a winding on the iron cylinder. After waiting again for equilibrium the residual vertical temperature gradients in the specimen and the gradients in the insulation just within the outer iron cylinder and the temperature differences across the silocel from specimen to iron cylinder at all levels are observed. Then current is sent into the d.c. heater at the top of the specimen and after approximately one hour the vertical gradients established in the specimen and those at the outer iron cylinder are read, and the radial drop across the silocel at the level of the lower fixed junctions. The radial drop at all other levels can be computed from the data. By correcting for the initial gradients, the vertical gradients down the specimen and the radial drops across the silocel *due to the heat added at the top* can be obtained. In all the above proceedings it is very necessary to continue repeating readings until they become constant.

PROCEDURE FOR MOLTEN METALS

The molten metal was contained in a graphite cylinder, 50 cm long, bored out for a depth of 25 cm, leaving walls about 4 mm thick (see Fig. 1). The lower unbored half of the graphite acted as a heat sink and contained a winding separate from that on the upper bored half. The d.c. heater consisted of a coil of Nichrome wire, B and S No. 22, wound on a $\frac{1}{8}$-inch mandril for about 3 inches and placed in a Pyrex tube. The tube was bent into the form of a circle and the ends of the tube bent upward at right angles to the plane of the circle. Thus a flat heater was obtained which was immersed in the molten metal at the top. It is always necessary that convection be eliminated by having the top slightly warmer than the bottom. This was done usually by adjusting the alternating current in the coil on the upper half of the cylinder relative to that on the lower half or by applying a small current in the d.c. heater. Temperatures and temperature gradients were measured exactly as in the case of the solid rods. In this case the two $\frac{1}{8}$-inch quartz tubes were simply lowered into the molten metal. With the molten metal one could measure the temperatures vertically up the specimen either by raising the junction in one of the quartz tubes or by raising the quartz tube itself. Careful tests gave identical results. It was more convenient to leave the tubes fixed and raise the junction.

CORRECTION FOR THE CONTAINING GRAPHITE WALLS

In determining the heat flow at the various levels down the liquid it is necessary in the case

of the molten metals to estimate and correct for the flow down the walls of the graphite containing cylinder. The correction is effected by assuming the cross-section area increased by the area of the walls and *assuming the conductivity of the walls the same as that of the test metal.*[2]

Thermal Conductivity of Zinc[3]

The plotted data for solid zinc are shown in Fig. 2 and for molten zinc in Fig. 3. The curves show temperature plotted against x (distance up the rod), and the gradients (dT/dx) plotted against x. The straight lines for the latter case clearly indicate the constancy of d^2T/dx^2. Values of thermal conductivity (k) for zinc as determined from the above plots are shown in Fig. 4. The line overlaps for 100 degrees the author's

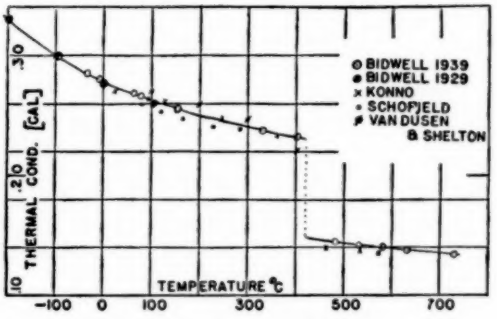

Fig. 4. Thermal conductivity of zinc.

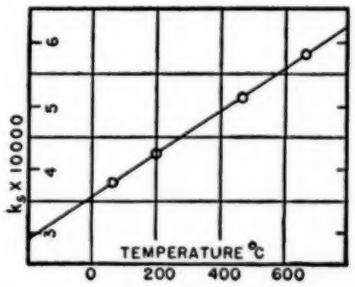

Fig. 5. Thermal conductivity of silocel.

previous line for zinc[4] and continues that line through change of state to 720°C in the molten condition. For comparison, data by Schofield,[5] Konno,[6] and Van Dusen and Shelton[7] are shown. Konno's points for both solid and molten zinc are in excellent agreement with those here shown. His data also agree in indicating a slight decrease in thermal conductivity with temperature for the molten metal.

Sample computations for k for two temperatures are shown herewith. When constant temperature baths were used the ΔT across the insulation at top (20 cm level) as observed was about 10 percent higher than at the bottom (0 level). The test rod in this case was 20 cm long and if computations are confined to the lower 14 cm, the ΔT's are sensibly the same and the equation holds. The variation in such case was not over 2 percent and the average ΔT was taken. At high temperatures, where additional silocel was used outside the iron cylinder, no variation was found in ΔT if one disregarded the top 4 cm.

Sample Data

At -37°C, $A=13.89$[8] cm², $R_2=5$ cm, $R_1=2.12$ cm, $k_s=0.000345$ cal., $d^2T/dx^2=0.050$, $\Delta T=41°$, watts input at top $=12.70$. $k_z=0.285$ cal.

At 630°C, $A=15.5$, $A_{gr}=4.14$, $R_2=11.5$, $R_1=2.5$, $k_s=0.00057$, $d^2T/dx^2=0.050$, $\Delta T=58°$, watts $=30.4$. $k=0.138$.

In conclusion the author ventures the opinion that the method here described is so superior to

[2] To check this wall correction a special test was made with mercury as test material at room temperature, (1) contained in the graphite cylinder, (2) contained in a glass cylinder of approximately same internal diameter. Other conditions were as in the tests on zinc except that no heat sink was used at the bottom. 10 watts were used in the d.c. heater in each case. With the graphite cylinder, the effective cross-section area is $(A_{Hg}+A_{gr}-a)$, where $A_{Hg}=13.84$ cm², $A_{gr}=4.14$ cm², a, the correction for the cross section of the two quartz tubes, $=0.20$ cm², $R_2=6.2$ cm, $R_1=2.7$ cm, $k_s=0.00038$ cal., ΔT (observed) $=36°$, d^2T/dx^2 (observed) $=0.035$. This gives $k_{Hg}=0.016$ cal. at 70°C. With the glass cylinder the heat flow down the glass is negligible compared with that flowing down the mercury and the effective cross section is $(A_{Hg}-a)$, $a=0.20$, $R_2=6.2$, $R_1=2.10$, $k_s=0.00038$, ΔT (observed) $=7.5°$, $A_{Hg}=13.2$, and d^2T/dx^2 (observed) $=0.075$. This gives $k_{Hg}=0.016$ at 50°C. (The large ΔT observed in the first case was due to a shorter length graphite tube [24 cm of mercury as compared with 32 for glass], resulting in a small heat capacity and consequent higher temperature.)

[3] To obtain a satisfactory rod of zinc, i.e., a casting free from blow holes and "piping," the metal was melted in a graphite cylinder 5 cm in cross section, bored out to a 25-cm depth, leaving walls about 5 mm thick. This cylinder containing the melt was slowly lowered by clockwork through the furnace at the rate of about 1 inch per hour. This slow freezing from the bottom up always gave rods free from blow holes and in some cases single crystals although this report does not deal with the latter.

[4] C. C. Bidwell and E. J. Lewis, Phys. Rev. **33**, 249 (1929).

[5] F. H. Schofield, Proc. Roy. Soc. London **A107**, 206 (1925).

[6] S. Konno, Phil. Mag. **40**, 542 (1920).

[7] M. S. Van Dusen and S. M. Shelton, Nat. Bur. Stand. J. Research **12**, 429 (1934).

[8] Corrected for the area of the quartz tubes 0.20 cm.

any hitherto reported, at least where values over a wide temperature range are desired, that it should become standard.

Note on the Thermal Conductivity of Silocel

The method above described required an exact knowledge of the conductivity of the silocel insulation at all temperatures and, since this presumably depended upon the looseness of packing, a special determination was made for this material. A copper tube 4-cm o.d. and 20 cm long with an inner bore of 1-cm diameter was centered in the large iron tube above used and the intervening space packed with silocel. The iron cylinder was surrounded by about 5 cm of additional thermal insulation. A Nichrome winding on the iron cylinder allowed the cylinder and its contents to be heated to any desired temperature. A Nichrome heating coil was centered exactly in the hole drilled through the copper cylinder. This was for direct heating current. The iron cylinder was about three times the length of the copper tube, the latter centered in it and packed above and below with silocel. Thermojunctions were placed in grooves in the iron cylinder and in the walls of the copper tube. The d.c. energy input into the central third of the copper cylinder was measured as was the temperature drop across the silocel. Thus the conductivity could be determined. The silocel was tamped firmly but the degree of tamping had no observable effect on the conductivity. The value at room temperature, 0.00038, is slightly higher than the handbook value, 0.00034. The increase with temperature was found to be linear (Fig. 5).

SEPTEMBER 15, 1939 PHYSICAL REVIEW VOLUME 56

The Effect of High Pressure on the Order-Disorder Transformation in Alloys*

Thomas C. Wilson
Yale University, New Haven, Connecticut

(Received July 17, 1939)

With electrical resistance as an index of degree of order, the behavior of the order-disorder transformation under high hydrostatic pressure has been investigated with the three alloys, CuAu, Cu_3Au and CuZn. Measurements were made under pressures up to 10,000 kg/cm² and over the temperature range 50°C to 426°C. For temperatures below the critical point the course of the transition under pressure may be predicted from reported thermal expansion data and deductions from the Bragg-Williams' theory. The observed behavior of the alloys seems to be consistent with these predictions. Measurements made near the critical temperature with the alloys CuAu and Cu_3Au show that the critical point is raised by pressure in both cases. One alloy, alpha brass (Cu_3Zn), not hitherto included in the class of the three alloys above mentioned has been examined. The conclusion is reached that a slight ordering of the constituents of the alloy occurs under high pressure.

Introduction

THE only prior work relating to this subject is apparently that of P. W. Bridgman,[1] who gave a report of the compressibilities and pressure coefficients of resistance of eighteen intermetallic compounds measured at 30°C and 75°C. Some of these compounds are capable of the order-disorder transition. The irregularity of results in all cases as compared with results for other substances was noticed and emphasized by the investigator. Sudden changes in the shape of curves, and hysteresis effects, were attributed to a shifting under pressure of the conditions of internal equilibrium, possibly to a change in the complicated type of superstructure characteristic of some of these compounds (e.g., Sn_8Cu_{31} (?) with 416 atoms in the unit cell).

If the ordering process is considered simply as a rearrangement in which atoms or ions of small diameter are fitted in the interstices between those of larger diameter so that the volume of the resulting structure is a minimum, one would expect high hydrostatic pressure to accentuate the volume differences and promote an ordered structure. With this view, the shifting of the conditions of internal equilibrium, above men-

* Part of a dissertation presented to the Faculty of the Graduate School of Yale University in candidacy for the degree of Doctor of Philosophy.

[1] P. W. Bridgman, Proc. Am. Acad. Sci. **70**, 285 (1935).

tioned, might be interpreted as due simply to changes in degree of order rather than to change in the type of structure. This seems particularly probable in the cases of compounds, such as CuZn, having a simple type of superstructure.

From the theory of the order-disorder transition and from experimental values of thermal expansion coefficients, it is, in fact, possible to predict such a change in degree of order under pressure, and to obtain a quantitative estimate of the changes to be expected. In the following, the predictions of the theory have been examined for pressures up to 10,000 kg/cm² and temperatures up to 426°C with the three alloys CuAu, Cu_3Au, and CuZn. Results of investigation of a fourth alloy, alpha brass (Cu_3Zn), are also included.

Theoretical

From the fundamental law of thermodynamics the change of entropy per unit volume $(d\phi/V)$ is defined as

$$d\phi/V=(dU+pdV)/TV. \tag{1}$$

If the usual assumption in thermodynamic treatments of the order-disorder process is made that the quantities in (1) may each be separated into two independent parts, one part due to the thermal vibrations of the atoms of the solid, the other a configurational part (hereafter indicated by a subscript c), we may write the average change in the configurational entropy per unit change of pressure at constant temperature as

$$\frac{1}{V}\frac{\Delta\phi_c}{\Delta p}=\frac{1}{TV\Delta p}\int_0^p dU_c+\frac{1}{TV\Delta p}\int_0^p pdV_c. \tag{2}$$

The left-hand side of (2) is from Maxwell's fourth relation

$$(\partial\phi/\partial p)_T=-(\partial V/\partial T)_p \tag{3}$$

equal to the negative of the configurational part of the thermal expansion coefficient to within the approximation involved in substituting an average for an instantaneous coefficient. The first term on the right of (2) may be expressed in terms of changes in the short range order σ or in the long range order S. The latter definition is here chosen because it is more easily correlated with the electrical resistance, the index of order used in this investigation. The relation between configurational energy and long range order is from the Bragg-Williams theory[2, 3]

$$U_c=U_{0c}(1-S^2), \tag{4}$$

where U_{0c} is the total energy required to destroy superlattice order. Therefore

$$dU_c=-U_{0c}d(S^2)+(1-S^2)dU_{0c} \tag{5}$$

and from (2), (3) and (5) we have

$$\frac{1}{V}\frac{\Delta V_c}{\Delta T}=\frac{U_{0c}}{TV}\frac{\Delta(S^2)}{\Delta p}-\delta, \tag{6}$$

where

$$\delta\equiv\frac{1}{TV\Delta p}\left[\Delta U_{0c}(1-S^2)+\int_0^p pdV_c\right].$$

Here $\Delta(S^2)$ and ΔU_{0c} refer to integrated changes in S^2 and U_{0c} due to the change of pressure Δp from 0 to p.

The value of the correction term δ may be estimated from experimental data later described. If we assume with the alloy CuAu, for example, that ΔU_{0c} is given by the change in the critical temperature with a pressure of 10,000 kg/cm², the value of $\Delta U_{0c}(1-S^2)$ for one gram-atom varies from about $0.1(10)^8$ erg at 200°C to $5.3(10)^8$ ergs at 400°C. The term $\int_0^p pdV_c$ cannot be evaluated without compressibility measurements but a reasonable guess would place its value somewhat lower in absolute magnitude than $\Delta U_{0c}(1-S^2)$ in the same temperature range, and negative, so that the two terms partly cancel. The value of $U_{0c}\Delta(S^2)$, on the other hand, varies between $1.1(10)^8$ ergs and $80(10)^8$ ergs between 200°C and 400°C, respectively, and for the same pressure. The description of δ as a correction term seems justified. It should be noted that (6) is inexact to the extent that it involves implicitly the approximation of Bragg and Williams that the ordering energy varies linearly with degree of order.

A derivation of (6) without such an assumption can be made by calculating the entropy through its statistical definition and expressing it in terms

[2] W. L. Bragg and E. J. Williams, Proc. Roy. Soc. **145**, 699 (1934).
[3] W. L. Bragg and E. J. Williams, Proc. Roy. Soc. **151**, 540 (1935).

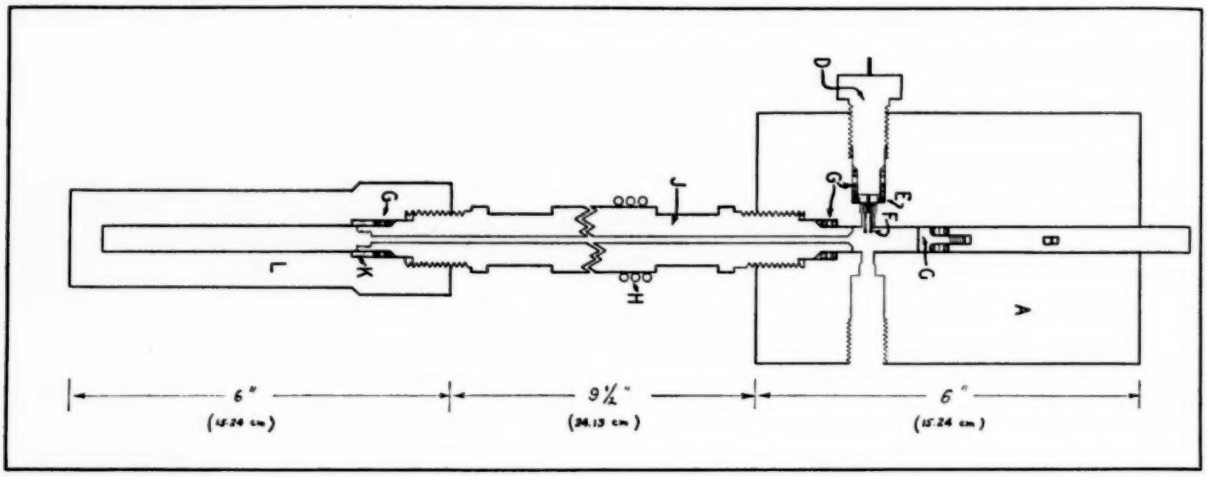

FIG. 1. High pressure unit.

of the long range order. The result for an AB alloy (the only case where a simple relation exists) is

$$d\phi_c = -\frac{kN}{2}\left\{\log\frac{1+S}{1-S}\right\}dS$$

$$= -\frac{kN}{2}d(S^2)[1+\tfrac{1}{3}S^2+\tfrac{1}{5}S^4\cdots],$$

so that the analogy to (6) becomes

$$\frac{1}{V}\frac{\Delta V_c}{\Delta T} = \frac{kN}{2V}\frac{\Delta(S^2)}{\Delta p}[1+\tfrac{1}{3}S^2\cdots]. \qquad (7)$$

For comparison purposes (6) may be rewritten for the AB case as

$$\frac{1}{V}\frac{\Delta V_c}{\Delta T} = \frac{kN}{2V}\left(\frac{T_c}{T}\right)\frac{\Delta(S^2)}{\Delta p} - \delta \qquad (6_{AB})$$

by means of the relation

$$U_{0c} = \tfrac{1}{2}NkT_c,$$

where T_c is the critical temperature.

The difference between (6_{AB}) and (7) is not large, and since (6) is applicable for all compositions, it is used hereafter. In the following, approximate values of the right side of the equation derived from measurements of electrical resistance of the alloys CuAu and CuZn under pressure are compared with reported values of the left side.

The considerations above are applicable to observations made below the critical point. At or above the critical point, the resistance measurements are of little use in evaluating the quantities of Eq. (6). However, observations made in this region may be analyzed in two ways, depending upon whether the transition occurring at the critical point is considered, in Ehrenfest's terminology, to be of the first kind or of the second kind. If it is of the first kind (a definite phase change involving a definite latent heat), then Clapeyron's equation

$$dT_c/dp = T\Delta V/L \qquad (8)$$

is applicable. An observed shift of the critical point with pressure predicts at the critical point an abrupt volume change proportional to the latent heat. If, on the other hand, the transformation is of the second kind (characterized by no latent heat) one may consider the appropriate equations to be

$$\frac{dT_c}{dp} = T\frac{\Delta(\partial V/\partial T)_p}{\Delta C_p} = -\frac{\Delta(\partial V/\partial p)_T}{\Delta(\partial V/\partial T)_p}. \qquad (9)$$

(It should be mentioned that the validity of these equations has been questioned by several authors.*) In the section giving the observations on the alloys Cu_3Au and CuAu, deductions are made from these equations.

* See for example the discussion in Epstein's *Thermodynamics*.

Apparatus

The technique for attaining high pressures was, as closely as possible, that described by P. W. Bridgman.[4] I wish to acknowledge also his personal advice on the general design of the high pressure unit of the apparatus and his generous loan to the Sloane Physics Laboratory of the hydraulic press and hand pump used in this investigation.

The high pressure unit, illustrated in Fig. 1, is in most respects of standard design. Because of the high temperatures used, the insulating plugs *D* carrying the electrical leads are introduced in the upper cylinder *A*, kept cool by the coil *H* on the connecting tube *J*. The lower specimen chamber *L* is of unusually small inner diameter, $\frac{3}{8}$ in. (0.953 cm), for two reasons, (a) the fluid capacity is small and heats of compression on change of pressure therefore small; a great convenience in making readings involving change of pressure at constant temperatures—(b) the wall thickness of the chamber may be kept to a minimum 0.6 in. (1.52 cm) and temperature equilibrium between the heating bath and the specimen readily established; a desirable feature for readings at constant pressure and changing temperatures.

All parts of the unit, except the piston *B* (which was of tool steel), were machined from Simplex forging steel, a product of the Crucible Steel Company of America and furnished through their generosity. (Special thanks are due to Mr. F. J. Dawless of their local office.) The machined parts were subjected to the heat treatment recommended for maximum hardness. For the majority of the work the steel proved eminently satisfactory. On occasion, however, experimental conditions required that the specimen chamber *L* be held at high pressure for several hours at temperatures between 350°C and 426°C, well over its recommended annealing temperature. These conditions invariably caused slow leak, because of a gradual distortion of the recess in the specimen chamber which retains the washers *G*. The recess was rebored on such occasions and new washers fitted. For convenience in removing washers, a sleeve *K* was placed at the bottom of the recess. This could be withdrawn with the aid of a pronged tool fitting into holes in the wall of the sleeve.

Lead and mild steel packing washers were used at connections indicated by the letter *G*. At temperatures above 300°C, however, the lead washers in chamber *L* were replaced by washers of soft sheet aluminum and well-annealed copper.

The compression medium (the high pressure unit was vacuum filled) was kerosene. Ethylene glycol was tried originally because of its high boiling point but was discarded because it becomes conducting under pressure. Decomposition of the kerosene was noticed on only one run, that reaching 426°C. The products were a gas and a liquid fraction which evaporated readily.

A potentiometer method (Bridgman[5]) was used for making the resistance measurements. The three wires required to connect the steel sleeves *F* with the specimen in chamber *L* were of copper, insulated with spun glass, a product (Vitrotex magnet wire) of the Anaconda Wire and Cable Company and generously furnished by them. This insulation at low temperatures withstood the pressures applied very well, but flaked off those parts of the wire exposed to temperatures above 250°–300°C after about four or five runs, because of the necessary flexing of the wire when specimens were changed. It was considered very satisfactory to renew the wiring so infrequently, considering the conditions of its use.

In the upper cylinder *A*, the wires were soldered to the sleeves *F*, which in turn were electrically connected with the electrodes of the insulating plugs by springs. In the lower cylinder *L*, the wires were held by screw clamps to the leads on the specimen.

The resistance specimens were of narrow strip, rod, or wire, 5–7 cm in length. Short copper cross wires welded to them near the ends served as potential leads. With all alloys, the welding was assisted by first coating the copper lightly with silver solder.

The precision of the potentiometer method justifies recording resistance to $1(10)^{-6}$ ohm for the specimens used, ranging from $2(10)^{-2}$-ohm

[4] P. W. Bridgman, *Physics of High Pressure* (Macmillan, 1931).

[5] P. W. Bridgman, Proc. Am. Acad. Sci. **56**, 61 (1921).

to $1(10)^{-3}$-ohm total resistance, a fact emphasized by adjusting the size of the points on the resistance-pressure graphs for the different alloys. Deviations of the readings from a smooth curve generally occur and are attributed mostly to slight departures of the specimen from an equilibrium condition. Contributing factors of minor degree are the various parasitic e.m.f.'s. Such troubles were minimized by immersing all copper-to-iron junctions in constant temperature baths. In general, the accuracy of the measurements of changes in resistance must be judged by the scatter of the points on each curve. The scatter changes from specimen to specimen and varies with temperature.

Measurements of pressure were made by recording changes in resistance of a manganin coil, wound upon the electrode of one of the four insulating plugs in cylinder *A*, and connected in one arm of a Wheatstone bridge circuit.

While measurements of relative changes of resistance were made with high precision, absolute values of resistance are probably correct only within about 2 percent. Likewise the absolute values of pressure readings cannot be regarded as fixed to better than about 4 percent. Such absolute errors, however, affect the conclusions in only a slight degree.

The heating bath was a welded steel container of about 1.5 gallons' (6 liters) capacity, around which was wrapped a heating coil—used however only as an auxiliary for high temperatures. The whole was suitably insulated and swiveled on a forked lever so that it could be conveniently brought up to or dropped away from the specimen chamber. Most of the heat was supplied to this bath by three immersion heaters in liquid tight copper tubing. The removable Transite cover carried these heaters, a tube containing the thermocouple, a mercury thermostat, and the stirring device. Because of the temperatures used, the latter rotated in a ball bearing lubricated with graphite, being driven through flexible shafting by a motor some distance away.

The mercury thermostat was satisfactory at temperatures under 300°C (the range initially contemplated), maintaining temperatures constant to within 0.05°C. Above 300°C, temperatures were manually controlled, the temperature fluctuations noted and appropriate corrections made to the readings.

For a range of temperatures up to 200°C, Russian mineral oil was used for the thermostatic liquid. Above this point a salt bath was employed, a product of a local company, supplying baths for the heat treatment of steels. It is stated by them to be a "eutectic mixture of salts melting at about 175°C." It proved eminently satisfactory, being very fluid, odorless, and noncorrosive.

Temperatures were measured with a Chromel-Alumel thermocouple in conjunction with a Wolff potentiometer, the thermal e.m.f.-temperature relation being taken from the *International Critical Tables*. The standard cell used was recalibrated just prior to use, the whole unit being checked against the melting point of test lead. It is believed that all temperature measurements are accurate to within ±0.4°C.

TABLE I. *Values of resistivity of* CuAu.

AUTHORS	COMPOSITION ATOMIC % AU	$\rho(20)°C \times (10)^6$ ohm·cm		T_c (HEATING) °C
		ANNEALED	QUENCHED	
Haughton and Payne[6]	49.8	5	—	405
	50.2	5	—	421
	50.3*	5	—	422
Kurnakow and Ageew[10]	50.24	4.86	14.2	400–450
Johansson and Linde[a]	49.2	4.24	—	—
	50.0	3.63	14.1	—
	50.5	3.98	—	—
Grube *et al.*[12]		3.79	—	420
Wilson		4.30	14.52	415

* Oxygen-free sample.
[a] C. H. Johansson and J. O. Linde, Ann. d. Physik **5**, 1 (1936).

TABLE II. *Values of resistivity of* Cu_3Au. *All values of* $\rho \times (10)^6$ *ohm·cm.*

AUTHORS	$(\rho)_{22°}$ ORDERED	$(\rho)_{400°}$	$(\rho)_{22°}$ QUENCHED	T_c (HEATING) °C
Sachs and Weerts[a]	4.7	14.35	11.4	—
Grube *et al.*[12]	4.15	—	—	395
Haughton and Payne[6]	7	—	—	392
Sykes and Evans[7]	4.5	14.2	11.5	386
Sykes and Jones[b]	—	—	—	391*
Borelius *et al.*[c]	—	—	—	390
Wilson	4.31	14.4	11.35	391.5

* From specific heat measurements
[a] G. Sachs, and J. Weerts, Zeits. f. Physik **67**, 507 (1931).
[b] C. Sykes, and F. W. Jones, Proc. Roy. Soc. **161**, 440 (1937).
[c] G. Borelius, C. H. Johansson, and J. O. Linde, Ann. d. Physik **86**, 291 (1928).

EXPERIMENTAL METHODS AND RESULTS

CuAu alloys

Numerous investigators have shown that with both CuAu and Cu_3Au, it is extremely difficult to obtain resistivity values characteristic of an equilibrium condition when cooling a disordered alloy from above its critical point to room temperature. In cooling, values of the resistivity at any given temperature are higher than those on the heating curve of an ordered alloy, the difference being greater, the faster the cooling. On the other hand, Haughton and Payne[6] have indicated that in heating an ordered alloy resistivity values are inappreciably affected by the rate of heating. It would seem to follow that resistivity measurements may be used as a good index of order in these CuAu alloys only when the specimen is being transformed by a rise of temperature from an ordered to a disordered state. This conclusion is further supported by the fact that different resistivity investigations of Cu_3Au[6, 7] indicate from heating curves a critical temperature of about 390°C (compared with the temperature 391°C accurately determined from specific heat data[8]) while cooling curves may indicate temperatures from 10°C to 30°C lower, depending on the rate of cooling.

For these reasons all measurements of resistivity as an index of order, here reported, were made at selected temperatures during heating of initially ordered alloys.

Small ingots of the alloys CuAu and Cu_3Au (1 to 3 grams) were prepared by Handy and Harman of Bridgeport, Connecticut for the purpose of the experiment. These were prepared under charcoal and contained by synthesis the exact composition indicated by the chemical formulae. No analysis was made subsequently.

The castings of CuAu and Cu_3Au were rolled and drawn into wires 0.58 mm diameter and 0.44 mm diameter, respectively. The frequent annealings necessary were carried out in hydrogen. After drawing, the wires were further homogenized by annealing for a period of one hour at about 850°C.

Potential leads were welded on, the specimens sealed in evacuated Pyrex tubes and heat treated for ordering as follows:

CuAu: 24 hours at 450°C, gradual cooling to 210°C over a period of 150 hours, then to room temperature in 12 hours.

Cu_3Au: 50 hours at 370°C, gradual cooling to 210°C over a period of 100 hours, 50 hours at 210°C, further cooling to 135°C over a 50-hour period, then to room temperature in one hour.

The resulting values of the resistivities of the specimens used are given in the last lines of Tables I and II, together with other characteristics of the alloys. Listed in these tables for comparison are corresponding values reported by other investigators.

Table I indicates that the specimens of CuAu here used deviated slightly from the equi-atomic composition. An assumption that a few tenths of one percent of silver was present (perhaps introduced from the silvered potential leads) would explain the lowering of the critical temperature (Hultgren[9]) and might also explain the slightly high values of the resistivity in both quenched and annealed states. Two specimens

[6] J. L. Haughton and R. J. M. Payne, J. Inst. Metals **46**, 457 (1931).
[7] C. Sykes and H. Evans, J. Inst. Metals **58**, 255 (1936).
[8] C. Sykes and F. W. Jones, Proc. Roy. Soc. **157A**, 213 (1936).
[9] R. Hultgren and S. Tarnopol, Metals Technology (January, 1938).

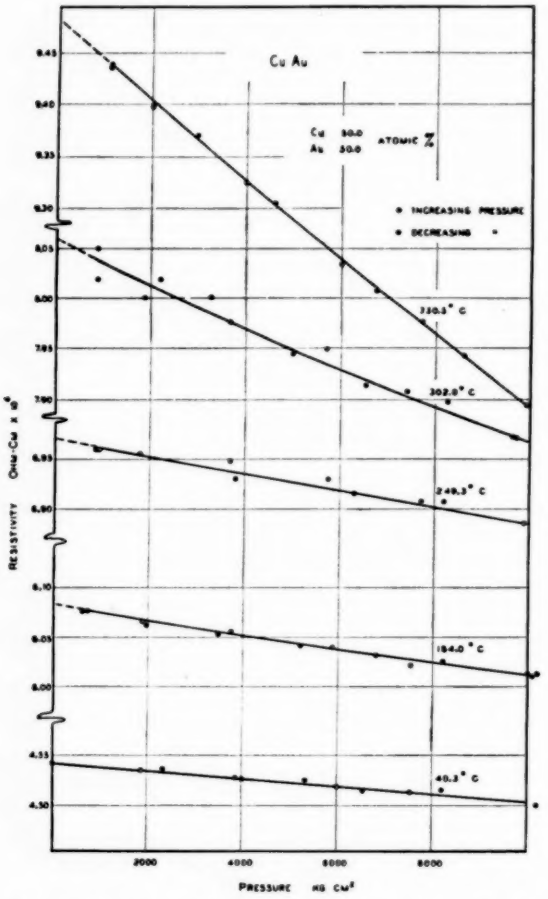

FIG. 2. Variation with pressure of resistivity of CuAu at various temperatures. The identification of the ordinate should read "Pressure, kg/cm²."

of Cu_3Au were used, their resistivities coinciding within the limits set by the measurements of dimensions. Table II indicates a fair agreement of the values obtained with those reported by other workers.

CuAu—results.—Pressure runs at constant temperature were made successively on one specimen at the temperatures indicated in Fig. 2, with the results there shown. With the exception of the runs at 249.3°C and 302.0°C the points taken on increasing and decreasing pressure fall fairly well on single smooth curves, the sample not exhibiting irregularities (to be expected in samples not seasoned under pressure) on the first run at 40.3°C.

It should be noted that the values of ρ, the resistivity, shown in this graph are uncorrected for the change in volume of the specimen, so that the ordinates are proportional to what may be called atomic resistivity. This statement applies to all other data (or to calculations where they are used) in this investigation.

The average pressure coefficients of resistance measured to 10,000 kg/cm² as derived from the curves of Fig. 2 are given in Table III and are plotted against temperature in Fig. 3.

A further constant temperature-pressure run was attempted at 390°C, after completion of the run at 350.5°C, but was abandoned after the first increase in pressure due to the slow drift of the readings of resistance; caused either by the impossibility of holding the temperature absolutely constant (it was manually controlled) or by the well-known sluggishness of the reaction n CuAu near the critical point. The pressure iwas accordingly then increased to 8700 kg/cm² (the increase being accompanied by an immediate drop in resistivity of $0.4\times(10)^{-6}$ ohm·cm) and the temperature slowly raised. The course of the resistivity under these conditions is shown in Fig. 4 by the upper part of the dashed curve. Just below point *A*, the rate of heating was greatly reduced. At *A* (427°C) the pressure had dropped to 8200 kg/cm². There seemed to be no change in the resistance of the specimen at this point which could not be attributed to a small decrease in the pressure due to slow leak,

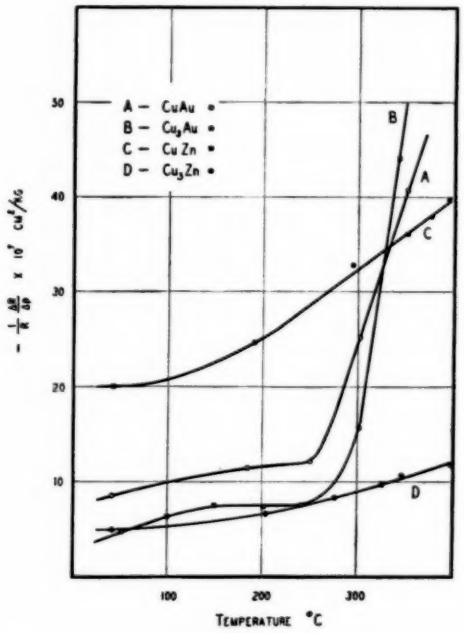

FIG. 3. Average pressure coefficients of resistance.

indicating that equilibrium conditions were closely approached. On release of pressure to 5000 kg/cm² the resistivity changed immediately to point *B*, and on a further release to about 1000 kg/cm², it moved more gradually to *C*. The rise in temperature between *A* and *C* was of the order of 1°C.

In view of the resistance-*vs.*-temperature readings later made on the same specimen at atmospheric pressure (full line, Fig. 4) it would appear that the critical point of the CuAu alloy was raised by about 1.7°C per 1000 kg/cm² pressure.

Analysis of data on CuAu.—Data taken below the critical temperature allow a comparison to be made of the ordering effect of pressure with the experimentally reported values of the thermal expansion coefficient, by means of Eq. (6).

To make such a comparison, the factor $\Delta(S^2)$ must first be evaluated from the resistivity measurements by finding S, the degree of order, and ΔS the change in order under pressure. (Calculations of the latter quantity are made for an arbitrary pressure change Δp of 10,000 kg/cm².) The only useful theory relating resistivities to degree of order is that of Bragg and Williams.[2] They assume that the resistivity of an ordered alloy behaves like that of a pure metal, while the resistivity of the disordered phase of the same alloy behaves like that of an impure metal, or that a portion of its resistivity, $\rho_{0\ \text{disorder}}$, is temperature independent. Referring to Fig. 4 where ρ_0, the resistivity of the disordered phase, and ρ_1, the resistivity of the ordered phase, are plotted against temperature it follows from their assumptions that the degree of order at a temperature of 330°C is given by

$$S=(\rho_0-\rho)/(\rho_0-\rho_1)=DE/DG.$$

The change in the degree of order (ΔS) due to 10,000 kg/cm² pressure is obtained in an analogous fashion. At any given temperature there is a total change $\Delta\rho_T$ in the resistivity due to a pressure of 10,000 kg/cm². Part of this change $\Delta\rho_N$ is a normal change, being due simply to a decrease in the amplitude of the atomic thermal vibrations. This is subtracted from $\Delta\rho_T$ giving $\Delta\rho_{\text{order}}$, the portion of the total change in resistivity due to the ordering effect. As above

$$\Delta S=\frac{\Delta\rho_{\text{order}}}{\rho_0-\rho_1}$$

The seemingly arbitrary choice of the normal decrease in resistivity should actually be governed by the behavior of pure metals under pressure, in view of the above assumptions. The variations of the average coefficients with temperature of the three pure metals concerned in

TABLE III. *Average pressure coefficient of resistance of* CuAu.

TEMPERATURE °C	$\frac{1}{R}\left(\frac{\Delta R}{\Delta p}\right)_{10,000}$ CM²/KG.
40.3	$-8.45(10)^{-7}$
184.0	−11.4
249.3	−12.1
302.0	−25.1
350.5	−40.6

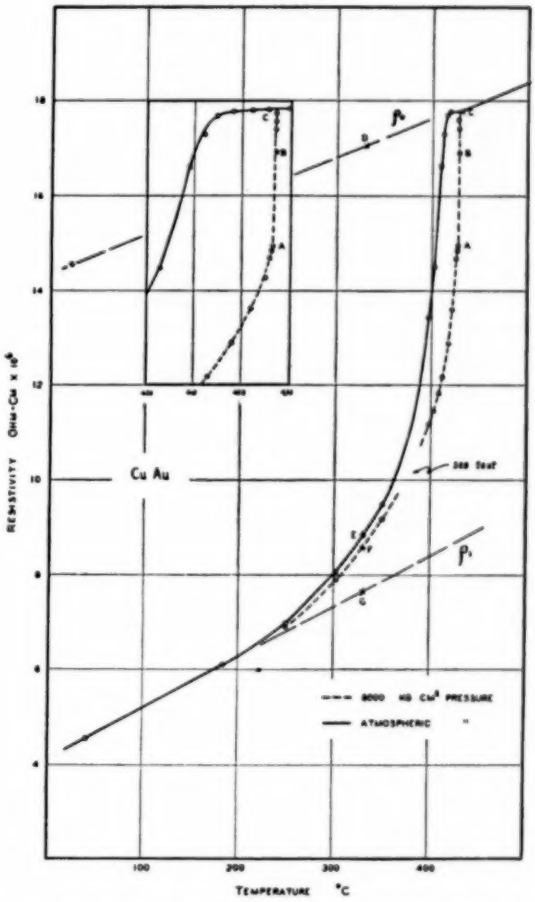

FIG. 4. Variation of the ordered and disordered resistivity of CuAu with temperature.

this investigation, as derived from Bridgman's results are given below.

Values of $(1/R)(\Delta R/\Delta p)_{12,000}$.

	0°C	100°C
Au	$-2.87(10)^{-6}$	$-2.92(10)^{-6}$
Cu	-1.83	-1.77
Zn	-4.70	-4.50

One would conclude that changes in the pressure coefficients with temperature are small, a conclusion which Bridgman generalizes to apply to most metals.

The assumption has therefore been made that the average pressure coefficient of resistance of an ordered alloy, measured at 50°C (where the ordering effect of pressure must be very small) defines its normal decrease of resistance under pressure. The value of $(1/R)(\Delta R/\Delta p)$ at 50°C is therefore subtracted from the values of the pressure coefficients at higher temperatures and the remainder used to calculate $\Delta\rho_{\text{order}}$ from the resistivity ρ appropriate to these higher temperatures.

From the resulting values of S and ΔS, with U_{0c} equal to $\frac{1}{2}RT_c$, $T_c=420$°C, and with $V=8.71$ cm³ (Hultgren[9]), the left side of Eq. (6) may be evaluated to within the factor δ. The results, for seven different temperatures, are given in Table IV together with values of the thermal expansion coefficients for CuAu determined from the heating curve of Kurnakow and Ageew.[10]

Considering the approximations used in evaluating the quantities appearing in the third column of Table IV, and the approximate character of the thermal expansion data, it is considered that the quantitative agreement between the third and fifth columns is sufficiently close to confirm the deductions made from the Bragg-Williams theory.

TABLE IV. *Values of* $\Delta S^2/\Delta p$ *and of the thermal expansion coefficient of* CuAu *alloy.*

TEMP. °C	$\frac{\Delta(S^2)}{\Delta p}$ CM²/DYNE	$\frac{1}{V}\frac{\Delta V_c}{\Delta T}$	$\left(\frac{1}{V}\frac{dV}{dT}\right)_{EXP}$	$\left(\frac{1}{V}\frac{dV_c}{dT}\right)^*_{EXP}$
50	0	0	$48(10)^{-6}$	0
200	$0.38(10)^{-12}$	$2.6(10)^{-6}$	48	0
250	0.51	3.2	50	$2(10)^{-6}$
300	0.71	4.1	58	10
350	5.4	29.	66	18
375	13.	66.	74	26
400	28.	138.	105–135	57–87

* $\frac{1}{V}\frac{dV_c}{dT}$ is taken to be $\frac{1}{V}\left(\frac{dV}{dT}\right)_T-\frac{1}{V}\left(\frac{dV}{dT}\right)_{50°}$.

The observed shift of the critical point of CuAu with pressure is about $1.7(10)^{-9}$°C·cm²·dyne^{-1}. With $T_c=420$°C(693°K), we may conclude that if a latent heat exists, there is an abrupt volume change given by Eq. (8) as

$$\Delta V=2.5(10)^{-12}L.$$

If no latent heat exists, then from Eq. (9) the relation between the change of the specific heat and the change of the thermal expansion coefficient is

$$\Delta(\partial V/\partial T)_p=2.5(10)^{-12}\Delta C_p.$$

Experimental evidence is insufficient for a choice to be made between these two expressions. Theoretical considerations due to A. H. Wilson[11] point to a definite latent heat and therefore to the first expression. Theories of Bragg-Williams, Bethe, Peierls, and Shockley predict zero latent heat and therefore require the second expression. In particular the theory of Bragg-Williams predicts a value for $\Delta C_p=1.5R$ erg·g atom^{-1}·degree^{-1} $(1.43(10)^7$ c.g.s. units). The predicted change in the thermal expansion coefficient is therefore

$$\frac{1}{V}\Delta\left(\frac{\partial V_c}{\partial T}\right)_p=36(10)^{-6}\text{°C}^{-1}.$$

The rather rough thermal expansion data on CuAu[10, 12] indicate values much higher than this for the actual change in the thermal expansion coefficient, in fact more than three times the predicted change. The discrepancy may lie in either the predicted value of ΔC_p or in defects of Eq. (9). Inasmuch, however, as the Bragg-Williams prediction on ΔC_p is known to be in error by a factor of about three in the case of beta brass, the evidence points to the applicability and the validity of Eq. (9).

Cu_3Au results.—The results of the pressure runs made at successively higher constant temperatures on the initially ordered specimens are plotted in Fig. 5. The irregularities of the readings on the first two runs, at 51.0°C and at 99.0°C, are quite noticeable, being so marked at

[10] N. S. Kurnakow and N. W. Ageew, J. Inst. Metals **46**, 481 (1931).

[11] A. H. Wilson, Proc. Camb. Phil. Soc. **34**, 81 (1938).

[12] G. Grube, G. Schonmann, F. Vaupel, W. Weber, Zeits. f. anorg. Chemie **201**, 41 (1931).

51.0°C that only points taken on decreasing pressure are plotted. These irregularities are attributed to the process of seasoning which most metals undergo on initial applications of pressure. On the successively higher runs at 149.4°C, 201.1°C and 240.8°C, equilibrium conditions seemed to be fairly well maintained, points taken on increase and decrease of pressure falling on the same smooth curve. At 301.5°C, however, the curves for increasing and decreasing pressure form a well marked hysteresis loop. The sluggish nature of the reaction indicated by this behavior was expected to be even more marked at 342.0°C. The run at that temperature was therefore conducted by increasing the pressure immediately to 8200 kg/cm² and holding it constant there for one-half hour. Strangely enough the resistivity did not change during this period from the value obtained at the end of the first six minutes by an amount greater than that ascribable to small temperature fluctuations. Subsequent readings on decreasing pressure fell fairly well on the curve drawn.

The average pressure coefficients of resistance measured to 10,000 kg/cm² as derived from the curves of Fig. 5 are given in Table V and are plotted against temperature in Fig. 3.

At temperatures above 350.5°C two runs were made, the specimens being kept under high pressure and the temperature alternately raised and lowered. During the first run, leaks were troublesome, the pressure initially being 8400 kg/cm² at 355°C but falling to 6800 kg/cm² as the transition point was crossed. This occurred between 397°C and 405°C, the exact point being uncertain. On subsequent cooling the pressure held at a constant value of 3400 kg/cm², the transition point on cooling at a rate of 100°/hr. being at 382°C and on heating at a rate of 50°/hr. at 394°C.

During the second run (not immediately after the first) the transition point on heating the specimen, held at 7600 kg/cm², came at 400.5°C. The pressure was then allowed to fall to 600 kg/cm², the critical points being at 375.8°C on cooling and 392.4°C on heating under these conditions. The suggested course of the resistivity on heating at 8000 kg/cm² pressure is plotted in Fig. 6 as the dashed curve. The full line shows the resistivity on heating at atmospheric pressure, the points thereon having been taken from Fig. 5; the critical point from an extrapolation of the observations just described (from 600 kg/cm² to zero). No significance should be attached to the shape of the resistivity curve near the critical point. The only accurate resistance readings were made on the first run and are those plotted in Fig. 6. Attention thereafter was concentrated on the more accurate determination of the transition temperatures.

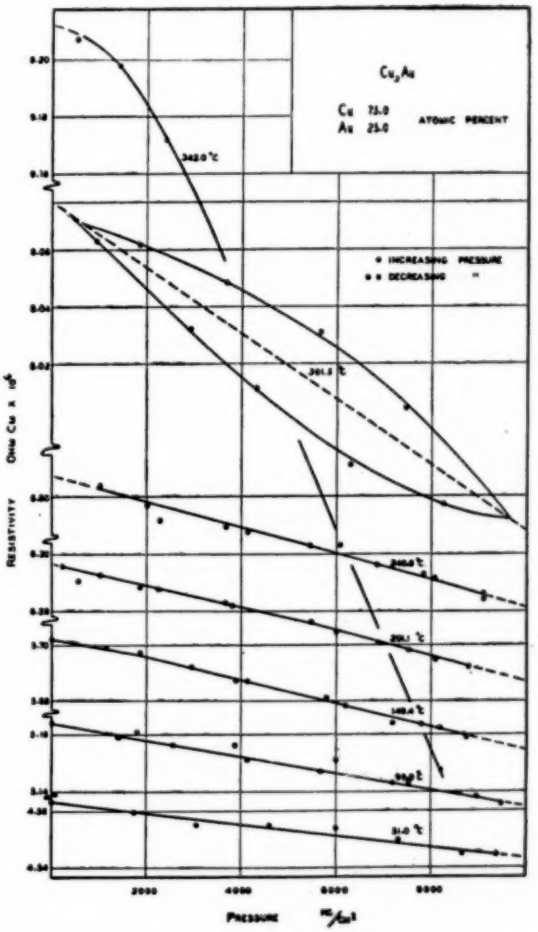

FIG. 5. Variation with pressure of resistivity of Cu_3Au at various temperatures.

Several observations were made on quenched specimens. Early pressure runs at 50°C (on an impure sample, however) had indicated that no substantial change in degree of order as measured by resistivity was to be expected at this low temperature. Although slight permanent decreases in resistance were noted after applying pressure to these specimens, further decreases

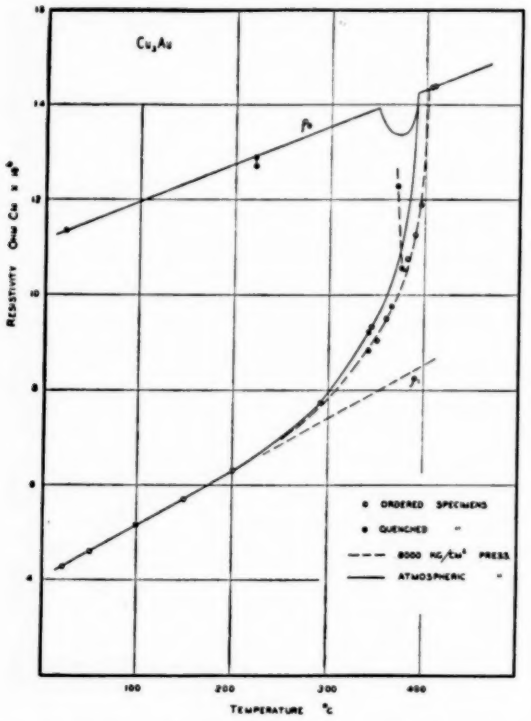

FIG. 6. Variation of the ordered and disordered resistivity of Cu_3Au with temperature.

were not observed in repeated runs and the initial changes were therefore attributed to seasoning effects.

A pressure run was later made (on a pure specimen) at 222°C. The results were very irregular and only significant because the resistivity declined permanently from a value of $12.81(10)^{-6}$ ohm·cm before the run to $12.71(10)^{-6}$ ohm·cm after. Following this run the specimen was heated to 370°C and a pressure of 9000 kg/cm² then applied, the temperature being slowly raised. The resistivity declined from an initial value of about $13(10)^{-6}$ at 370°C to $10.57(10)^{-6}$ at 376°C and thereafter followed the same course as that of an initially ordered alloy (Fig. 6).

Analysis of data on Cu_3Au.—An analysis of the data taken below the critical temperature may be made in the same manner as with CuAu. The values of the configurational part of the thermal expansion coefficient derived from these data through Eq. (6) are given in Table VI. Here the experimentally determined value of 5.5 cal./g $(2.81\ (10)^9$ ergs/cm³ (reference *b*, Table II)) is taken for the quantity U_{0c} in Eq. (6).

The reported values of $(1/V)(dV/dT)$ for Cu_3Au are not sufficiently precise to compare with these results.

From the data summarized above, one would infer that the shift of the critical point with pressure for Cu_3Au is about 1.2°C per 1000 kg/cm² or in c.g.s. units $1.2(10)^{-9}$.

Sykes and Jones[8] have investigated the behavior of Cu_3Au by thermal means and have concluded that the latent heat at the critical point is 1.26 cal./g $(0.64(10)^9$ ergs/cm³). Eq. (8) then indicates that an abrupt volume change occurs at the critical point given by $\Delta V/V = 0.0012$ whereas the total volume change in going from a completely disordered to an ordered structure is known to be $\Delta V/V = 0.0041$. From the curves of Sykes and Jones relating size of nuclei to changes of volume of the alloy Cu_3Au the abrupt volume change above is consistent with a change in size of nuclei from about 10A to a negligibly small value.

It should be noted that the thermal measurements of Sykes and Jones upon an alloy previously cooled at 30°/hour did not show a latent heat at the critical point but instead a change in the specific heat of finite amount 1.92 cal. $g^{-1}°C^{-1}$

TABLE V. *Average pressure coefficients of resistivity of* Cu_3Au.

TEMP. °C.	$\frac{1}{R}\left(\frac{\Delta R}{\Delta p}\right)$ CM²/KG × (10)⁷
51.0	−4.73
99.0	−6.31
149.4	−7.52
201.1	−7.26
240.8	−7.48
301.5	−15.75
342.0	−44

TABLE VI. *Values of $\Delta S^2/\Delta p$ and of the thermal expansion coefficients of* Cu_3Au.

TEMP. °C.	$\frac{\Delta(S^2)}{\Delta p}$ CM⁴/DYNE	$\frac{1}{V}\frac{\Delta V_c}{\Delta T}$
50	0	0
100	$0.24(10)^{-12}$	$1.8(10)^{-6}$
150	.48	3.2
200	.54	3.2
250	.71	3.8
300	2.60	13
350	11.1	50
360	12.9	57
380	14.8	64

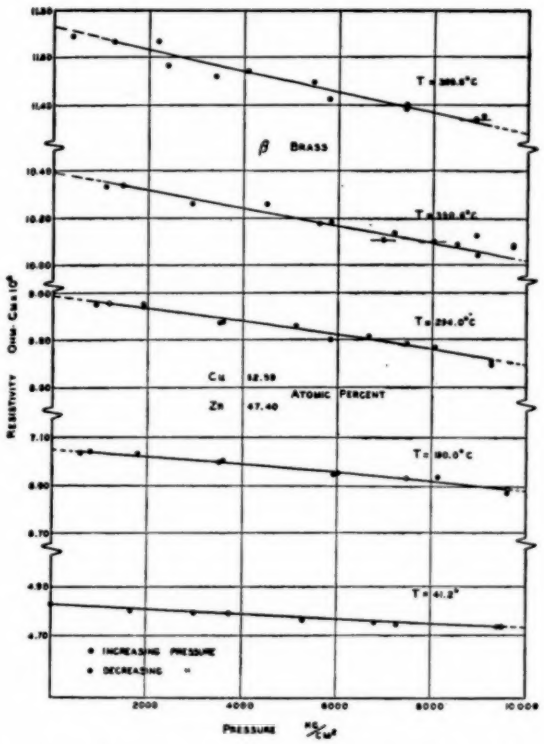

FIG. 7. Variation with pressure of the resistivity of beta brass at various temperatures.

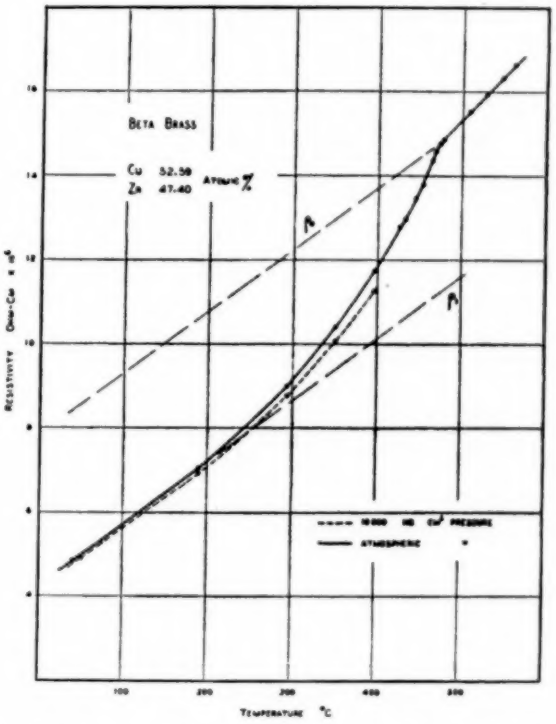

FIG. 8. Variation of the ordered and disordered resistivity of beta brass with temperature.

$(98(10)^7$ erg cm^{-3}°C$^{-1})$. This was attributed to presence of anti-phase nuclei. For such a case, Eq. (9) gives a finite change in the thermal expansion of

$$\frac{1}{V}\Delta\left(\frac{\partial V}{\partial T}\right)_p = 1770(10)^{-6}\text{°C}^{-1}.$$

It would be of interest to have accurate thermal expansion data to compare with the results above.

Copper-zinc alloys.—Alloys of both alpha and beta brass were supplied through the courtesy of the American Brass Company, Waterbury, Connecticut. Special thanks are due Dr. Cyril S. Smith, Research Metallurgist, under whose direction they were prepared.

TABLE VII. *Average pressure coefficients of resistance for beta brass.*

TEMP. °C.	$\frac{1}{R}\left(\frac{\Delta R}{\Delta p}\right)_{10,000}$ CM²/KG
41.2	$-2.00(10)^{-6}$
190.0	−2.46
294.0	−3.27
350.6	−3.60
395.6	−3.96

Beta brass—CuZn.—The samples were of hot rolled rod $\frac{1}{8}$" (0.317 cm) diameter. The analysis furnished was, in atomic percent, copper 52.59, zinc 47.40, lead 0.001, iron 0.01. Resistance specimens were prepared by grinding the rolled rod to a square form with 0.0153 cm² cross-sectional area. On sections of this rod about 5 cm in length silvered potential leads were attached by welding. The specimens were then heated above the transformation point in hydrogen and quenched. This heat treatment apparently preserved no detectable amount of disorder at room temperature, the resulting value of the resistivity at 25°C proving to be $4.60(10)^{-6}$ ohm·cm. This is slightly higher than Webb's[13] value of $4.5(10)^{-6}$ ohm·cm for annealed single crystals of this composition but lower than that of Haughton and Griffiths[14] who reported $4.62(10)^{-6}$ ohm·cm (room temperature). Subsequently, the samples under pressure

[13] W. Webb, Phys. Rev. **55**, 300 (1939).
[14] J. S. Haughton and W. T. Griffiths, J. Inst. Metals **34**, 245 (1925).

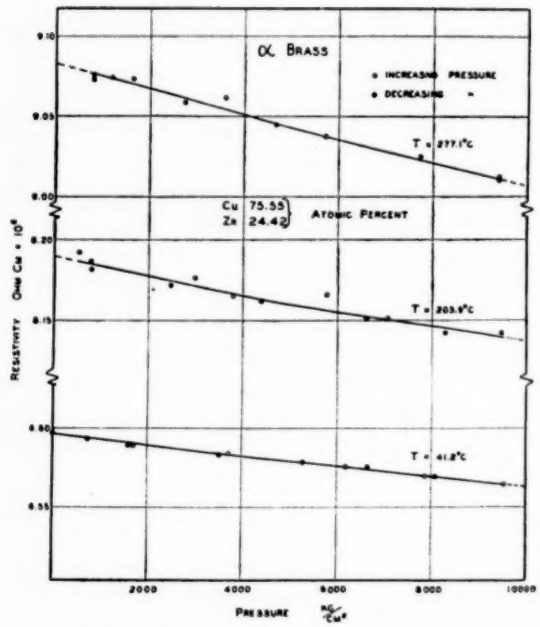

FIG. 9. Variation with pressure of resistivity of alpha brass at various temperatures.

showed no irregularities aside from those due to initial seasoning effects. They were therefore considered to be in an ordered state requiring no further heat treatment.

The five runs made at various temperatures up to 395.6°C are plotted in Fig. 7. Bridgman[1] has measured the pressure coefficient of resistance of CuZn (exact composition not stated). From his data we derive the following values

Temp.	$\frac{1}{R}\left(\frac{\Delta R}{\Delta p}\right)_{10,000}$ cm²/kg
30°C	$-2.06(10)^{-6}$
75°C	$-2.03(10)^{-6}$

The first run here made, at 41.2°C gives in the same units $-2.00(10)^{-6}$, affording a check upon the method of measurement.

The average pressure coefficients of resistance derived from the curves of Fig. 7 are given in Table VII and plotted in Fig. 3 against temperature. Values of the thermal expansion coefficient due to the configurational changes may be calculated from the values of the pressure coefficients given in Fig. 3. A difficulty arises, however, in that the line representing the behavior of the resistivity of the disordered alloy cannot be drawn on the resistivity-temperature graph (Fig. 8) below the critical point with any degree of confidence. Beta brass, unlike the CuAu alloys, cannot be retained in a disordered state below the critical temperature, and ρ_0 is not therefore defined by experimental points in this region. The policy, adopted by Webb,[13] of extrapolating the resistivity-temperature curve above the critical point linearly to temperatures below the critical point is not justifiable. If such extrapolation is made, the formula above derived relating resistivity to degree of order actually gives negative values of $\rho_{0\ \text{disorder}}$ in the equation $\rho_0=\rho_{0\ \text{disorder}}+\alpha_0 T$. It will be remembered that $\rho_{0\ \text{disorder}}$ is assumed to represent the contribution of the disordered state to the resistivity at 0°K, so that it cannot be negative. Moreover, such an assumed curve actually crosses the curve ρ_1 for the resistivity of the ordered phase. Obviously, at the intersection, and for lower temperatures, the relation between degree of order and resistivity

$$S=(\rho_0-\rho)/(\rho_0-\rho_1)$$

becomes meaningless.

In this dilemma it has been here assumed that the line ρ_0 is parallel to ρ_1 below the critical point, as drawn in Fig. 8. This involves the assumption that $\rho_{0\ \text{disorder}}$ may be equated to the value $\rho_0-\rho_1$ at the critical point.

With this assumption, values of S and ΔS may be calculated for various temperatures.

With $U_{0c}=8.7$ cal./g [$3.02(10)^9$ ergs/cm³] from experimental measurements of Sykes and Wilkinson[15] for the composition used, calculated values of the left side of Eq. (6) are given in Table VIII. Given also are the thermal expansion coefficients reported by Merica and Schad[16] and

TABLE VIII. *Values of $\Delta S^2/\Delta p$ and of the thermal expansion coefficient of beta brass.*

TEMP. °C	$\frac{\Delta(S^2)}{\Delta p}$ CM²/DYNE	$\frac{1}{V}\frac{\Delta V_c}{\Delta T}$	$\frac{1}{V}\frac{dV}{dT}$	$\frac{1}{V}\frac{dV_c}{dT}$
50	0	0	$5.8(10)^{-5}$	0
200	$2.0(10)^{-12}$	$1.7(10)^{-5}$	6.6	$.8(10)^{-5}$
250	3.6	2.7	7.1	1.3
300	5.2	3.6	7.6	1.8
350	6.6	4.2	8.4	2.6
400	7.1	4.2	9.4	3.6

[15] C. Sykes and H. Wilkinson, J. Inst. Metals **61**, 223 (1937).

[16] P. D. Merica and L. W. Schad, Nat. Bur. Stand. Sci. Pap. 14, 1918.

the estimated values of $(1/V)(dV_c/dT)$ derived from these measurements.*

Alpha brass.—The samples were a hot rolled rod $\frac{1}{8}''$ (0.317 cm) diameter, the analysis made by the American Brass Company being in atomic percent, copper 75.55, zinc 24.42, lead 0, and iron 0.03.

Resistance specimens were prepared by rolling the samples to ribbon 0.107 mm thick, and cutting the ribbon into strips about 6 cm long and 1 to 2 mm wide. After attaching potential leads, the specimens were heated to between 500°C and 600°C, and quenched. No undue irregularities were noted on the six constant temperature-pressure runs subsequently made. The results of these runs are plotted in Figs. 9 and 10; the derived pressure coefficients of resistance are shown in Table IX and plotted against temperature in Fig. 3.

In going from 40°C to 400°C there is an increase in the absolute magnitude of the pressure coefficient of alpha brass which is about one-third the increase in beta brass for the same temperature range. The relative increase is, however, somewhat greater than that of beta brass.

If the interpretation which has been attached throughout this analysis to an increase with temperature of the pressure coefficient of resistance is correct, the conclusion must be drawn that an ordered phase in alpha brass is promoted by pressure.

In this connection, it should be pointed out

TABLE IX. *Values of the pressure coefficients of resistance for alpha brass.*

TEMP. °C	$\frac{1}{R}\frac{\Delta R}{\Delta p}$ CM²/KG.
41.2	$4.95(10)^{-7}$
203.9	6.52
277.1	8.30
325.5	9.68
347.2	10.52
398.2	11.70

* The values of $(1/V)(dV/dT$ reported by Merica and Schad are averages for the temperature ranges 0–100°C, 100–200°C, etc. These have been plotted as points at 50°C, 150°C, etc., and the values on the smooth line joining these points are given in Table VIII.

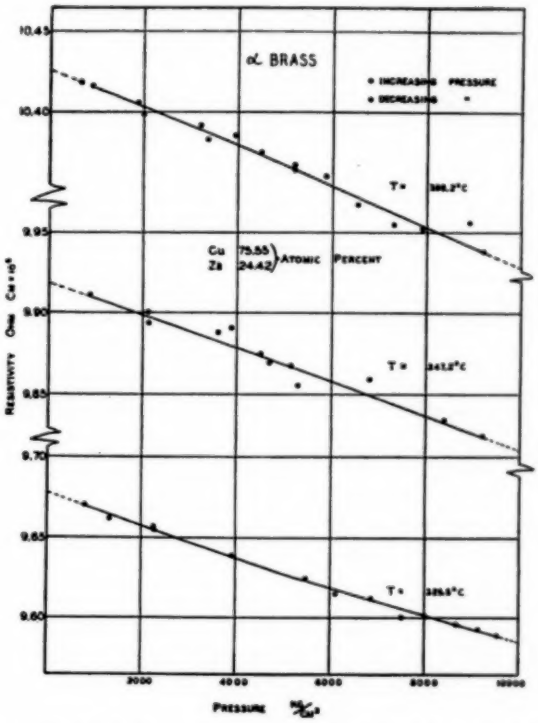

FIG. 10. Variation with pressure of resistivity of alpha brass at various temperatures.

that a specific heat measurement by Sykes and Wilkinson on a sample of alpha brass containing 36 percent Zn by weight showed an anomalous behavior below 210°C. The indication is that a slight degree of order exists in alpha brass at room temperature, which gradually vanishes on heating. The effect of pressure is apparently to enhance the ordering tendency.

The writer takes pleasure in acknowledging his indebtedness to Professor L. W. McKeehan under whose guidance this work was carried out. His stimulating and keen advice was invaluable throughout the course of the investigation.

Mention has already been made in the text of the material aid afforded to this research from many sources. Especially, it will be recalled that the technical difficulties were greatly simplified by the generous loan of part of the pressure equipment by Professor P. W. Bridgman of Harvard.

LETTERS TO THE EDITOR

Prompt publication of brief reports of important discoveries in physics may be secured by addressing them to this department. Closing dates for this department are, for the first issue of the month, the eighteenth of the preceding month, for the second issue, the third of the month. Because of the late closing dates for the section no proof can be shown to authors. The Board of Editors does not hold itself responsible for the opinions expressed by the correspondents.

Communications should not in general exceed 600 words in length.

β-Ray Selection Rules and the Meson Theory

The selection rules for β-decay have been discussed on the basis of Fermi's theory,[1] with the result that the only allowed transition is the one in which the angular momentum of the nucleus does not change. According to the modification of Fermi's formalism, proposed by Gamow and Teller,[2] the inversion of the spin of the heavy particle may take place in the β-emission, thus transitions in which the angular momentum of the nucleus changes by 1, are also allowed. It was shown by these authors that the new selection rule is in better agreement with the experimental evidence than the original one.

We want to discuss here the significance of these two selection rules from the point of view of the Yukawa theory of β-emission.[3] We shall consider here the two possibilities of a meson with spin 0 and 1. In this theory, the β-decay is a second-order process, consisting in the emission of a meson and its consequent disintegration into an electron and a neutrino. In order to deal with the changes of the angular momentum of the emitting nucleus, we need to consider only the first step of the β-disintegration i.e., the emission of the meson.

According to Kemmer[4] there are four possible forms of the meson theory, two of which correspond to mesons with spin 0 and the other two to mesons with spin 1. The nonrelativistic part of the interaction leading to the meson emission are:

$$H_0^{\mathrm{I}}=H_1^a=ck\int dV\{\Phi_N^*[g_a\psi^*-f_a\pi]\Phi_P \quad +\text{conjugate complex}\}$$

$$H_0^{\mathrm{II}}=H_1^d=-c\int dV\{\Phi_N^* g_d(\boldsymbol{\sigma}\ \mathrm{grad}\ \psi^*)\Phi_P+\text{conj. comp.}\}$$

$$H_1^{\mathrm{I}}=H_1^b=c\int dV\{\Phi_N^*[(\boldsymbol{\sigma}\ \mathrm{curl}\ \psi^*)-g_b\ \mathrm{div}\ \Psi^*]\Phi_P \quad +\text{conj. comp.}\}$$

$$H_1^{\mathrm{II}}=H_1^c=-ck\int dV\{\Phi_N^*[f_c(\boldsymbol{\sigma}\psi^*)+f_c(\boldsymbol{\sigma}\boldsymbol{\Pi})-g_c(\boldsymbol{\sigma}\pi)+g_c(\boldsymbol{\sigma}\Psi^*)]\Phi_P \quad +\text{conj. comp.}\}$$

$$\mathrm{div}\,\psi=\mathrm{div}\,\pi=0 \qquad \mathrm{curl}\,\Psi=\mathrm{curl}\,\boldsymbol{\Pi}=0.$$

The notations are the same as Kemmer's paper. We can observe that these interactions behave under space symmetry as a scalar or an axial vector and so they cannot lead to odd changes of the orbital part of the angular momentum of the nucleus. Thus we may consider only transitions without changes in this momentum.

The transitions due to H_0^{I} do not affect the spin of the heavy particle, as far as H_0^{I} does not contain $\boldsymbol{\sigma}$. On the other hand H_0^{II} leads to the emission of mesons with the angular momentum $l=1$ and $m=0$ or 1, with a change of 0 or 1 in the spin of the heavy particle. H_1^{I} induces emissions of transversal mesons with $l=1$ and $m=0$ or 1 and to the emission of longitudinal mesons (terms wigh g). The first correspond to a spin change of 0 or 1, whereas the second leave the spin unchanged. The analysis of the emissions due to H_1^{II} is much more complicated and will be discussed elsewhere.

Thus we come to the conclusion that *the meson theory of disintegration leads to the Gamow-Teller selection rule*, not only for the theory with spin 1 that gives correct neutron-proton forces, but even for one of the forms of the theory with 0 spin.

I thank Professors Gamow and Wataghin for the discussions and the interest they took in this paper.

MARIO SCHÖNBERG

Department of Physics,
University of São Paulo,
São Paulo, Brazil,
August 10, 1939.

[1] E. Fermi, Zeits. f. Physik **88**, 161 (1934).
[2] G. Gamow and E. Teller, Phys. Rev. **49**, 895 (1936).
[3] H. Yukawa, Proc. Phys. Math. Soc. Japan **17**, 48 (1935).
[4] N. Kemmer, Proc. Roy. Soc. **166**, 127 (1938).

The Elastic Scattering of Fast Electrons by Heavy Elements

Mott[1] has derived an exact expression for the scattering of a Dirac electron in a Coulomb field, as a series in Legendre polynomials. We have summed this series numerically for mercury, and the results should be approximately true for the nearby elements (gold, lead, thallium and bismuth).

Let θ be the angle of scattering, and $q=Zc/137v$, where v is the velocity of the incident electrons, and $Z=80$ for Hg. If we multiply our calculated scattering intensity by $(4/q^2)\sin^4\frac{1}{2}\theta$, we obtain the ratio r of our intensity to that of ordinary Rutherford scattering (with relativistic electron mass). In Table I are given the values of the ratio r, together with those of δ (polarization quantity defined by Mott), as a function of q or of $\epsilon(=E/mc^2)$.

TABLE I. *Values of r and δ.*

q	ϵ	15°	30°	45°	60°	90°	120°	150°	180°	δ
0.6	3.35	1.12	1.34	1.62	1.85	1.89	1.30	0.51	0.15	0.012
0.65	1.28	1.09	1.29	1.55	1.78	1.89	1.44	0.82	0.54	0.036
0.73	0.666	1.06	1.22	1.45	1.67	1.86	1.59	1.19	1.00	0.057
0.8	0.463	1.04	1.17	1.37	1.58	1.82	1.68	1.43	1.31	0.064
0.9	0.314	1.03	1.11	1.28	1.48	1.77	1.75	1.65	1.59	0.068
1.0	0.232	1.02	1.07	1.21	1.39	1.71	1.78	1.80	1.78	0.066
1.2	0.145	1.01	1.02	1.10	1.25	1.58	1.79	1.97	1.98	0.057
1.5	0.086					1.39	1.73	2.05	2.31	
2.0	0.046					1.19	1.58	2.04	2.35	0.027

The angular variation of r at high energies will be about the same as at $q=0.6$, and the intensity at 180° approaches zero with increasing energy. The previous approximate formula due to Mott[2] gives only the correct order of magnitude of scattering intensity for a heavy element such as mercury.

Our angular distribution agrees well with that observed by Barber and Champion,[3] the numbers in the angular ranges 20°–30°, 30°–60°, and 60°–180° being in the ratio 37 : 27 : 9 (theoretical) as against the experimental ratio 37 : 30 : 8. However, the disagreement between theory and experiment concerning absolute intensities still remains.

Our polarization values are about 10 percent less than those of Mott at the maximum, so that the theory still predicts an effect which has not yet been observed.

The angular distributions at small energies will probably be modified when shielding is taken into account.

Full details will be published later.

J. H. Bartlett
R. E. Watson

Department of Physics,
University of Illinois,
Urbana, Illinois,
August 21, 1939.

[1] N. F. Mott, Proc. Roy. Soc. **A135**, 429 (1932).
[2] N. F. Mott, Proc. Roy. Soc. **A124**, 438 (1929).
[3] A. Barber and F. C. Champion, Proc. Roy. Soc. **A168**, 159 (1938).

Helium and Hydrogen of Mass 3

We have now adjusted the shims of the 60-inch cyclotron so that it is possible to obtain a steady beam of 24-Mev He^{3++} ions.[1] We have compared the isotopic ratio He^3/He^4 of tank (gas-well) helium to that of spectroscopically pure (atmospheric) helium, and find that it is about twelve times as great for atmospheric helium as for the gas-well variety. The absolute values have been approximately determined with the aid of a thin-walled Victoreen R-meter. These ratios are 10^{-8} and 10^{-7} for the two types of helium. When the cyclotron chamber is filled with atmospheric helium, the He^3 beam has sufficient intensity to induce appreciable radioactivity in silicon. We have observed a 2.5-minute period with an initial intensity of 200 counts/minute, on a background of 30 counts per minute. The activity could be followed for four half-lives; it is probably P^{30} formed in the reaction.

$$_{14}Si^{28}+{}_2He^3\rightarrow{}_{15}P^{30}+{}_1H^1$$
$$_{15}P^{30}\rightarrow{}_{14}Si^{30}+e^+.$$

When the silicon was bombarded under identical conditions except for the substitution of tank helium for spectroscopic helium, the activity was reduced to a small value consistent with the abundance ratios given above.

Since we have shown that He^3 is stable, it seemed worth while to search for the radioactivity of H^3. We have therefore bombarded deuterium gas with deuterons, and passed the gas into an ionization chamber connected to an FP-54 amplifier. The gas showed a definite activity of long half-life. We have now shown that this gas has the properties of hydrogen by circulating it through active charcoal cooled in liquid nitrogen and allowing it to diffuse through hot palladium. The radiation emitted by this hydrogen is of very short range as was shown by the almost linear form of the intensity *vs.* pressure curve when the gas was pumped out of the chamber. When sufficient time has elapsed for us to make some statement regarding the half-life of this activity, we will submit the details of the work to this journal for publication.

We are indebted to Dr. S. Ruben for the use of his thin-walled counter and to Dr. A. Langsdorf for the loan of a d.c. amplifier. It is a pleasure to acknowledge the friendly interest of Professor E. O. Lawrence in these experiments, and to thank the Research Corporation for financial assistance.

Luis W. Alvarez
Robert Cornog

Radiation Laboratory,
Department of Physics,
University of California,
Berkeley, California,
August 29, 1939.

[1] L. W. Alvarez and R. Cornog, Phys. Rev. **56**, 379 (1939).

Intensity and Rate of Production of Mesotrons as a Function of Altitude

With the view of obtaining information on the intensity and on the rate of production of mesotrons as a function of altitude, we have performed the following free balloon experiment.

Four G-M counters were arranged with lead absorbers, as shown in Fig. 1. Counters 1, 2 and 3 constituted one threefold coincidence set and counters 2, 3 and 4 constituted the other. Since a particle which passes through either set of counters must penetrate at least 8 cm of lead, we are dealing here only with the penetrating component, i.e., mesotrons. The top set of counters can be actuated only by mesotrons which have originated outside of the equipment, whereas the lower set can be set off by either a mesotron entering from the outside or by one which is produced in the lead block L. If there is such a production of mesotrons in the lead block L, by a non-ionizing radiation, one should observe a greater number of counts in the lower set of counters than in the upper set.[1]

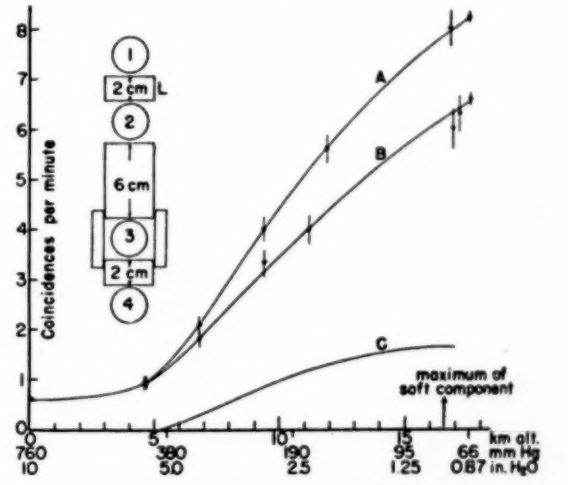

FIG. 1. Arrangement of counters and number of coincidences per minute in the lower (A) and upper (B) counters.

TABLE I. *Ratio of the number of mesotrons produced in the lead block to the intensity of the soft component as obtained by Regener.*

PRESSURE MM HG	ALTITUDE KM	Ns	Ny	Ny/Ns
66	17.6	26	1.55	0.060
100	14.7	28	1.65	0.059
150	12.1	21	1.33	0.063
200	10.2	16	1.00	0.062
250	8.7	10.5	0.70	0.066
300	7.4	8.4	0.40	0.048

The G-M counters (4″ long by 1″ in diameter) were made according to Shonka's technique.[2] A Neher-Harper[3] type of circuit was used. All the individual threefold coincidences from each set of counters were recorded photographically on a rotating drum. The pressures and temperatures were recorded by a barograph of the type used by one of us in previous flights.[4] The total weight of the equipment was about 38 lb. Fifteen balloons, each inflated to a lifting power of 3.1 lb., were used. The apparatus remained aloft for ten hours, about five hours of which were at the maximum altitude of 17.6 km (66 mm of Hg).

The results obtained are shown in Fig. 1. Curve B represents the number of threefold coincidences per minute recorded by the upper set of counters as a function of the altitude. This curve gives directly the increase with altitude of the intensity of the penetrating component, and shows that the mesotron intensity increases by a factor of 11 between sea level and 17.6 km. There is no evidence for a maximum in the mesotron intensity up to the highest altitude reached in this flight. At the position of the maximum of the total vertical intensity[5] (8 cm of Hg), our results show that 12 percent of the total vertical cosmic-ray intensity consists of penetrating particles.

The number of threefold coincidences per minute registered in the lower set of counters is shown by curve A. The fact that the counting rate corresponding to this curve increases considerably over that corresponding to curve B indicates that an appreciable production of mesotrons takes place as the altitude increases above about 7 km. The difference between the ordinates of the two curves, which gives directly the number of mesotrons produced in the lead block L at different altitudes, is represented by curve C. If photons are responsible for their creation, the intensity of the mesotrons produced in the lead should follow that of the soft component. Evidence for this is indicated in Table I. N_s represents the intensity of the soft component as obtained by Regener and Ehmert.[6] N_y gives our values of the number of mesotrons produced in the lead block L (curve C), and in the last column are tabulated the ratios N_y/N_s. The constancy of these ratios lends support to the hypothesis that mesotrons can be created by photons. On the basis of the known intensity of the soft component we can calculate a cross section for the creation of a mesotron by a photon. We obtain a value per proton in the lead nucleus of 1.7×10^{-27} cm², which is in qualitative agreement with the result obtained by Schein and Wilson[7] at 25,000 feet altitude.

The writers acknowledge with thanks the valuable suggestions given them by Professor A. H. Compton. They also wish to express their appreciation to Professor Norman Hilberry, for his generous assistance.

MARCEL SCHEIN
W. P. JESSE
E. O. WOLLAN

Ryerson Physical Laboratory,
University of Chicago,
Chicago, Illinois,
August 25, 1939.

[1] B. Rossi, Zeits. f. Physik **82**, 151 (1933); D. S. Hsiung, Phys. Rev. **46**, 653 (1934).
[2] F. R. Shonka, Phys. Rev. **55**, 24 (1939).
[3] H. V. Neher and W. W. Harper, Phys. Rev. **49**, 940 (1936).
[4] W. P. Jesse (in print).
[5] G. Pfotzer, Zeits. f. Physik **102**, 23 (1936).
[6] E. Regener and A. Ehmert, Zeits. f. Physik **111**, 501 (1939).
[7] M. Schein and V. C. Wilson, Phys. Rev. **54**, 304 (1938).

Induced Radioactivity Produced by Bombarding Aluminum with Protons

Silicon[27] has been reported as being produced by the reactions[1] $Mg^{24}(\alpha, n)Si^{27}$ and $Si^{28}(n, 2n)Si^{27}$, and having a half-life of about 6.5 minutes with a positron upper limit of 2.0 Mev. It should be possible to produce the same isotope by proton bombardment of aluminum, since the proton energies available are well above the expected threshhold (3.8 Mev) for the reaction. However, all our attempts to find such a period have been completely unsuccessful, its intensity if present being at least ten thousand times weaker than would be predicted from (p, n) cross sections for neighboring elements. We have, however, found an activity of 3.7 seconds half-life which is produced in aluminum by protons. Fig. 1 shows a decay curve for this activity. For each point a separate sample was bombarded, placed over the ionization chamber at a time after the end of bombardment given by the abscissa, and allowed to decay completely. Suitable corrections were made for longer-lived activities which got onto the target by recoil from the air. In Fig. 2 is shown an excitation curve for this activity obtained in a similar manner to the decay curve except that the samples were placed over the ionization chamber at a fixed time (7 seconds) after the end of bombardment. The energy of the bombarding particles

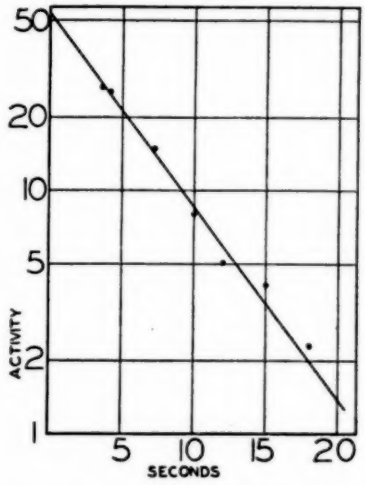

FIG. 1. Decay curve for the 3.7-second activity resulting from the bombardment of aluminum by protons.

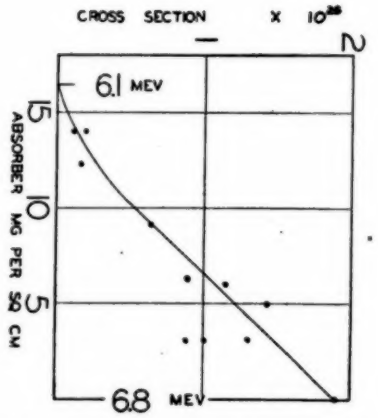

FIG. 2. Excitation curve of the 3.7-second activity resulting from the bombardment of aluminum by protons.

was reduced by interposing calibrated aluminum foils. Proton energies were obtained from the range-energy relation of Livingston and Bethe[2] with the assumption that visual range as measured with a fluorescent screen is equivalent to extrapolated range. This may make the experimental value of the threshhold, which is found to be 6.1 Mev, perhaps 0.1 Mev too high. The targets used were 0.0005-inch aluminum foil so that the excitation curve is essentially a thin-target one. To get the cross sections, we calibrated the ionization chamber with a uranium oxide source, using only the UX_2 beta-particles. It was assumed that the chamber was equally sensitive to beta-particles from the two sources.

Since a (p, n) reaction is the only type which can lead to a radioactive isotope from protons on aluminum, unless some new type such as (p, D) occurs, and since the cross sections found are too large to permit the activity to be due to an impurity, it seems unavoidable to assign it to Si^{27}. If we assume for the moment that it is Si^{27} which is just produced in its ground state at the observed threshhold, its mass comes out to be 26.9956 (with $Al^{27}=26.9989$, $n-H=0.00081$) which is to be compared with the predicted value of Barkas[3] of 26.9944. This leaves the 6.5-minute activity unaccounted for. One explanation which seems very unlikely might be that the 6.5-minute activity is the decay of an isomeric state of so much higher energy that the proton energy available (6.8 Mev) is insufficient to form it. If the particles emitted were electrons instead of positrons as has been reported, it would be possible to assign the activity to Al^{29} which could be produced by $Mg^{26}(\alpha, p)Al^{29}$ or $Si^{29}(n, p)Al^{29}$.

We wish to thank Dr. S. W. Barnes and Mr. Ralph McCreary for assistance during the observations.

G. KUERTI
S. N. VAN VOORHIS

Department of Physics,
University of Rochester,
Rochester, New York,
August 31, 1939.

[1] H. Fahlenbrach, Zeits. f. Physik **96**, 503 (1935); C. D. Ellis and W. J. Henderson, Proc. Roy. Soc. **156**, 358 (1936); Pool, Cork and Thornton, Phys. Rev. **52**, 239 (1937); W. J. Henderson and R. L. Doran, Phys. Rev. **56**, 123 (1939).
[2] M. S. Livingston and H. A. Bethe, Rev. Mod. Phys. **9**, 245 (1937).
[3] W. H. Barkas, Phys. Rev. **55**, 691 (1939).

A New Electro-Optical Effect

In two previous notes[1] one of the writers reported various anomalous electro-optical properties of bentonite colloids. Through the collaboration of Professor Hauser and Dr. Le Beau, who prepared for us a series of monodisperse sols, we have now been able to extend the investigation to cover the dependence on concentration and particle size and to study the behavior in electric fields of higher intensity and higher frequencies. Our previous results and those of Norton[2] have been confirmed for monodisperse sols. The curious behavior is therefore not caused by the presence of particles of different sizes. Contrary to a statement in our first note we find now that in the strongest fields a very slight change of the intensity of the scattered light is perceptible. Depending on whether the incident light vibrates parallel or normal to the field the scattering is increased or decreased. Whenever this effect can be observed the field also creates a small dichroism. Evidently the dichroism is caused by the difference of apparent absorption, i.e., of absorption due to scattering, of the two light components.

Of greater interest are our new results concerning the dependence of the birefringence on strength and frequency of the acting field. Fig. 1 gives a typical set of data. For high frequencies the birefringence is always positive, it varies not much with changes of frequency and increases in a normal way with increasing field strength. At low frequencies, however, the behavior is quite anomalous. The negative birefringence for small fields reaches a maximum and the Kerr effect becomes positive above a critical field strength. This behavior is analogous to that observed in the famous Majorana effect in colloidal "Bravais-Iron." We believe that we are dealing here with the electric analog to this still unexplained magneto-optical effect.

The most promising way of explaining these observations is to assume the superposition of two effects: A normal positive Kerr effect, caused by the orientation of the anisotropic micelles, and a new type of electro-optical effect which causes negative birefringence. For sufficiently high frequencies only the normal effect occurs. The data obtained with high frequency fields agree with the predictions of the orientation theory, i.e., the effect is proportional to

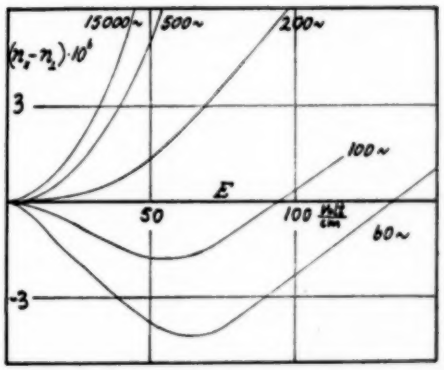

FIG. 1. The electro-optical birefringence as functions of strength and frequency of the electric field in a monodisperse bentonite sol with an average particle radius of $29\mu\mu$ and a concentration of 0.61 percent.

the sol concentration, it is independent of frequency, it tends towards saturation as should be expected for large particles, and it increases rapidly with the size of the particles. The relaxation effects, discussed in a previous note, are in excellent agreement with Tummers'[3] theory. The negative effect occurs only for low frequency fields and reaches saturation for small fields. It exists for all particle sizes, but in the case of large particles no inversion with field or frequency occurs because the normal effect is here always predominant. It is significant that this new type of effect disappears also when the concentration of the sol is reduced. This suggests that it may be caused by the interaction between the micelles. Our concentration range is close to that where thixotropy and gel formation occur and it is conceivable that an electric field can influence the interaction to produce an anisotropic distribution of the particles and give rise to a type of electro-optical effect which Havelock once suggested.

HANS MUELLER
B. W. SAKMANN

Massachusetts Institute of Technology,
Cambridge, Massachusetts,
September 1, 1939.

[1] H. Mueller, Phys. Rev. **55**, 508, 792 (1939).
[2] F. J. Norton, Phys. Rev. **55**, 668 (1939).
[3] J. H. Tummers, Diss. Utrecht, 1914.

Phase Shifts (K_1) for the Square Well

The K_1 phase shifts for the square well $D=10.5$ Mev, $r=e^2/mc^2$, which approximate[1] closely the experimental data on proton-proton scattering are calculated for the experimental energies. The phase shifts are smaller than those for the error well. Table I contains the calculated phase shifts K_1 for both the repulsive p and attractive p interactions. The Mott ratios considering the effect of K_0 and K_1 are calculated for the Gauss error and square wells for the energies 670, 776, 867 kev. The experimentally derived phase shifts (K_0) at these energies apparently do not agree with the theoretical phase shifts (K_0) for any potential so far investigated.[2] The maximum contribution to the Mott ratio due to K_1 is 0.011 at 30° for the error well at 867 kev.

TABLE I. *Phase shifts calculated for the square well.*

E in kev	670	776	867	860	1200
Repulsive p	−0.01(8)	−0.02(3)	−0.02(8)	−0.02(8)	−0.03(5)
Attractive p	0.03(0)	0.04(0)	0.04(8)	0.04(8)	0.08(5)
E in kev	1390	1830	2105	2392	
Repulsive p	−0.06(5)	−0.10(3)	−0.13(0)	−0.16(2)	
Attractive p	0.11(0)	0.17(5)	0.22(2)	0.27(3)	

A. M. MONROE
HUBERT M. THAXTON

Department of Physics,
The Agricultural and Technical College of North Carolina,
Greensboro, North Carolina,
August 28, 1939.

[1] Breit, Thaxton and Eisenbud, Phys. Rev. **55**, 1018 (1939).
[2] Unpublished calculations of K_0 by the authors for these energies for square, Gauss error, exponential and meson potentials reveal general discrepancies at these energies for all potentials. See also reference 1.

(K_1) Phase Shifts for the Error Well

The phase shifts K_1 for the attractive and repulsive p interaction in the proton-proton scattering problem have been calculated for the error well ($Ae^{-\alpha r^2}$) with $A=51.44$, $\alpha=21.59$ for the exact experimental energies.[1] The method of contiguous adjunction of interior and exterior wave functions has been applied. The formulas for the calculation of the necessary functions are found in a paper by Yost[2] and others. The adjunction formula is easily derived for any L from formula (3) of reference 2. Table I contains the results of the calculations. The phase shifts are observed to be small for all energies.

TABLE I. *Phase shifts calculated for the error well* ($Ae^{-\alpha r^2}$).

E in kev	670	776	867	860	1200
Repulsive p	−0.02(7)°	−0.03(3)°	−0.04(2)°	−0.04(2)°	−0.07(2)°
Attractive p	0.03(5)°	0.04(4)°	0.05(6)°	0.05(5)°	0.09(4)°
E in kev	1390	1830	2105	2392	
Repulsive p	−0.09(4)°	−0.15(0)°	−0.18(3)°	−0.22(8)°	
Attractive p	0.12(2)°	0.19(7)°	0.24(7)°	0.30(2)°	

HUBERT M. THAXTON
A. M. MONROE

Department of Physics,
The Agricultural and Technical College of North Carolina,
Greensboro, North Carolina,
August 28, 1939.

[1] Herb, Kerst, Parkinson and Plain, Phys. Rev. **55**, 998 (1939); Heydenburg, Hafstad and Tuve, Phys. Rev. **55**, 603(A) (1939). See also Breit, Thaxton and Eisenbud, Phys. Rev. **55**, 1018 (1939).
[2] Yost, Wheeler and Breit, J. Terr. Mag. Atmos. Elec. 443 (1935).

The Effects of Alkali Halides on the 4.7μ Water Band

The measurements of Plyler and Barr[1] of the infra-red absorption of aqueous solutions of alkali halides have been repeated with the purpose of determining the effects of these salts on the absorption coefficient of water in the region of the 4.7μ associational band. The cell thicknesses of 0.03 mm employed were controlled as carefully as possible by means of a circular aluminum washer. However, since the accurate control of the thickness of extremely thin cells by this method is difficult, relative thicknesses were determined by comparison of absorption factors in spectral regions in which the water absorption is not appreciably affected by the presence of the salts. By this method the relative absorption coefficients of the solutions could be determined to within two percent. The absorption coefficients as determined in this manner are based upon equivalent solvent thicknesses.

The results obtained are summarized in Table I in which the effects of two series of salts on the absorption coefficient at the position of maximum absorption in the associational band are indicated. The table also gives the value of the relative polarizing powers of the various ions involved. This quantity as defined by Bernal and Fowler[2] is the ratio of ionic charge to ionic radius. According to the Bernal-Fowler theory of liquid water, ions having a large polarizing power produce changes in water structure similar to those produced when the temperature of water is decreased, whereas ions of small polarizing power have effects similar

TABLE I. *Effect of various salts on the absorption coefficient of water.*

SOLUTION (3.9 NORMAL)	RELATIVE POLARIZING POWER (ELECTRONS PER ANGSTROM) ANION	CATION	CHANGE IN ABSORPTION COEFFICIENT (PERCENT)	CHANGE IN FREQUENCY (CM^{-1})
Lithium Chloride	0.55	1.47	−4.4	+ 9
Sodium Chloride	0.55	1.02	−2.6	0
Potassium Chloride	0.55	0.75	−6.8	+ 6
Rubidium Chloride	0.55	0.67	−6.9	−26
Potassium Fluoride	0.75	0.75	−0.2	+55
Potassium Chloride	0.55	0.75	−6.8	+ 6
Potassium Bromide	0.51	0.75	−6.8	−18
Potassium Iodide	0.46	0.75	−7.2	−35

to those produced when the temperature is raised. As Ganz[3] has shown, increasing the temperature of water decreases the absorption coefficients in the 4.7μ region. Therefore, according to the Bernal-Fowler theory, when the effects of salts with a common cation are studied, the absorption coefficient should decrease with decreasing polarizing power of the anion; a corresponding variation should be observed when a common anion is present with different cations.

As one may observe from Table I, the results obtained experimentally show only a rough agreement with predictions of theory. When a common anion (Cl^-) is involved, the decrease in coefficient produced by Li^+ is greater than expected, while the decreases produced by Rb^+ and K^+ are almost equal. With a common cation (K^+), the various anions produce changes which are, within the limits of experimental error, in agreement with predictions based on the Bernal-Fowler theory.

The variations in band position observed in the present study are in agreement with those reported by Plyler and Barr.[1] On account of the broadness of the associational band the position of maximum absorption could be determined only to $\pm 0.025\mu$. As indicated in Table I, the frequency of maximum absorption is decreased as the polarizing power of the anion decreases. Plyler and Barr reported their inability to detect shifts in band position in solutions containing a common anion (Cl^-) and different alkali cations. The present study confirms these results except in the case of RbCl, which was found to produce a pronounced decrease in frequency.

No clear separation of the band into two components, as reported by Ganz[3] for $MgCl_2$, was observed in the spectra of the salts studied in the present investigation, although some indications of this effect were observed in the case of KF. As the polarizing powers of K^+ and F^- are approximately equal, this separation, if real, indicates that positive and negative ions of equal polarizing power are not equally effective in producing changes in water structure.

T. N. GAUTIER
DUDLEY WILLIAMS

University of Florida,
Gainesville, Florida,
August 29, 1939.

[1] E. K. Plyler and E. S. Barr, J. Chem. Phys. **6**, 316 (1938).
[2] J. D. Bernal and R. H. Fowler, J. Chem. Phys. **1**, 515 (1933).
[3] E. Ganz, Zeits. f. physik. Chemie **33**, 163 (1936).

THE AMERICAN INSTITUTE OF PHYSICS

INCORPORATED

ADMINISTRATIVE STAFF

HENRY A. BARTON, *Director*

MADELINE M. MITCHELL, *Publications Manager*

Office: 175 Fifth Avenue, New York, New York

JOURNALS

THE PHYSICAL REVIEW

REVIEWS OF MODERN PHYSICS

JOHN T. TATE, *Editor*

J. W. BUCHTA, *Assistant Editor*

JOURNAL OF APPLIED PHYSICS

ELMER HUTCHISSON, *Editor*

THE JOURNAL OF THE OPTICAL SOCIETY OF AMERICA

THE REVIEW OF SCIENTIFIC INSTRUMENTS

F. K. RICHTMYER, *Editor*

JOURNAL OF THE ACOUSTICAL SOCIETY OF AMERICA

FLOYD A. FIRESTONE, *Editor*

THE JOURNAL OF CHEMICAL PHYSICS

HAROLD C. UREY, *Editor*

JOSEPH E. MAYER, *Assistant Editor*

THE AMERICAN PHYSICS TEACHER

DUANE ROLLER, *Editor*

GOVERNING BOARD

For The American Physical Society:

JOHN T. TATE, *Chairman*
University of Minnesota

GEORGE B. PEGRAM, *Secretary*
Columbia University

KARL T. COMPTON
Massachusetts Institute of Technology

For The Optical Society of America:

E. C. CRITTENDEN
National Bureau of Standards

A. C. HARDY
Massachusetts Institute of Technology

W. B. RAYTON
Bausch & Lomb Optical Company

For The Acoustical Society of America:

FLOYD A. FIRESTONE
University of Michigan

HARVEY FLETCHER
Bell Telephone Laboratories

WALLACE WATERFALL
The Celotex Corporation

For The Society of Rheology:

WHEELER P. DAVEY
Pennsylvania State College

MELVIN MOONEY
United States Rubber Products, Inc.

R. L. PEEK, JR.
Bell Telephone Laboratories

For The American Association of Physics Teachers:

PAUL E. KLOPSTEG
Central Scientific Company

FREDERIC PALMER, JR.
Haverford College

F. K. RICHTMYER
Cornell University

The American Institute of Physics is a membership corporation of which five societies are the founding members. These five societies are the principal national societies devoted to pure and applied physics in America. Their names, and those of their representatives who form the Governing Board of the Institute, are given above. The principal work of the Institute is the publication of journals sponsored by the societies or by itself. The names and the editors of the journals are also listed above.

The broad purpose of the Institute is to represent, in all matters of wide or common interest, the five thousand or more members and subscribers associated with the Founder Societies and the journals. It aims to advance the science and profession of physics, and to promote cooperation between pure research, the applied sciences and the industries. To achieve these aims, it is greatly in need of an endowment and is empowered by law to administer grants and funds of any kind.

UNIVERSITY OF MICHIGAN LIBRARIES

CONTENTS

PHYS. REV. 58 (1939) SEPTEMBER 15

Latitude Cosmic-Ray Effects at Sea Level . . . . . R. A. MILLIKAN, H. V. NEHER AND D. O. SMITH 487

New Evidence for a Change with Time of the Total Energy Brought into the Earth by Cosmic Rays . . . . . R. A. MILLIKAN AND H. V. NEHER 491

On the Production of the Hard Component of the Cosmic Radiation. I. The Photon Hypothesis . . . . . L. W. NORDHEIM AND M. H. HEBB 494

On the Production of the Hard Component of the Cosmic Radiation. II. Protons or Neutral Particles as Primaries . . . . . L. W. NORDHEIM 502

β-Decay and Spin of Light Nuclei . . . . . B. O. GRØNBLOM 508

Short-Lived Radioactivities Induced in Fluorine, Sodium and Magnesium by High Energy Protons . . . . . M. G. WHITE, L. A. DELSASSO, J. G. FOX AND E. C. CREUTZ 512

On the Coupling Conditions in Light Nuclei and the Lifetimes of β-Radioactivities . . . . . E. P. WIGNER 519

On the Nuclear Magnetic Moments of the Isotopes of Rubidium and Chlorine . . . . . P. KUSCH AND S. MILLMAN 527

Electron-Positron Field Theory of Nuclear Forces . . . . . EUGENE P. WIGNER, CHARLES L. CRITCHFIELD AND EDWARD TELLER 530

Spin-Dependence in the Electron-Positron Theory of Nuclear Forces . . . . . CHARLES L. CRITCHFIELD 540

Energies Released in the Reactions $Li^7(\phi, \alpha)He^4$ and $Li^6(d, \alpha)He^4$, and the Masses of the Light Atoms . . . . . NICHOLAS M. SMITH, JR. 548

Energy Picture of the Binding Energies of F^{19} and Ne^{21} . . . . . KATHARINE WAY 556

Theory of Secondary Radiation . . . . . D. E. WOOLDRIDGE 562

Function and Theory of the Modification of Geiger Counters . . . . . JOHN N. SHIVE 579

Method for Improved Calculation of Energies of Two-Electron Configurations from Hartree Eigenvalues. Application to $2p^2$ Terms in O III . . . . . A. F. SHENSTONE 586

Absolute Method of Measuring Heat Conductivity Applicable to Either Molten or Solid Metals. Thermal Conductivity of Zinc . . . . . CHARLES C. BIDWELL 594

Effect of High Pressure on the Order-Disorder Transformation in Alloys . THOMAS C. WILSON 598

Letters to the Editor:

β-Ray Selection Rules and the Meson Theory . . . . . MARIO SCHÖNBERG 612

Atomic Scattering of Fast Electrons by Heavy Elements . . . . . J. H. BARTLETT AND R. E. WATSON 613

Helium and Hydrogen of Mass 3 . . . . . LUIS W. ALVAREZ AND ROBERT CORNOG 613

Intensity and Rate of Production of Mesotrons as a Function of Altitude . . . . . MARCEL SCHEIN, W. P. JESSE AND E. O. WOLLAN 613

Induced Radioactivity Produced by Bombarding Aluminum with Protons . . . . . G. KUERTI AND S. H. VAN VOORHIS 614

New Electron-Optical Effect . . . . . HANS MOTZ AND E. W. SALZBERG 615

Plane Shifts (K_1) for the Square Well . . . . . A. M. MORRIS AND HOBART M. TRAUGOTT 615

(K_1) Phase Shifts for the Born Well . . . . . HOBART M. TRAUGOTT AND A. M. MORRIS 615

Effects of Alkali Halides on the Al_2O_3-Water Bond . . . . . T. H. GOUCHER AND DUDLEY WILLIAMS 616

LANCASTER PRESS, INC., LANCASTER, PA.